

**TXSAMC (TRANSPORT CROSS SECTIONS FROM APPLIED MONTE
CARLO): A NEW TOOL FOR GENERATING SHIELDED MULTIGROUP
NEUTRON CROSS SECTIONS**

A Thesis

by

MATTHEW TORGERSON HIATT

Submitted to the Office of Graduate Studies of
Texas A&M University
in partial fulfillment of the requirements for the degree of

MASTER OF SCIENCE

August 2007

Major Subject: Nuclear Engineering

**TXSAMC (TRANSPORT CROSS SECTIONS FROM APPLIED MONTE
CARLO): A NEW TOOL FOR GENERATING SHIELDED MULTIGROUP
NEUTRON CROSS SECTIONS**

A Thesis

by

MATTHEW TORGERSON HIATT

Submitted to the Office of Graduate Studies of
Texas A&M University
in partial fulfillment of the requirements for the degree of
MASTER OF SCIENCE

Approved by:

Chair of Committee,
Committee Members,

Department Head,

Marvin L. Adams
William Charlton
Guergana Petrova
Thomas Marcille
John Poston

August 2007

Major Subject: Nuclear Engineering

ABSTRACT

TXSAMC (Transport Cross Sections from Applied Monte Carlo): A New Tool for
Generating Shielded Multigroup Neutron Cross Sections. (August 2007)

Matthew Torgerson Hiatt, B.S., Texas A&M University

Chair of Advisory Committee: Dr. Marvin L. Adams

This thesis describes a tool called TXSAMC (Transport Cross Sections from Applied Monte Carlo) that produces shielded and homogenized multigroup cross sections for small fast reactor systems. The motivation for this tool comes from a desire to investigate reactor systems that are not characterized well by existing tools. Proper investigation usually requires the use of deterministic codes to characterize the time-dependent reactor behavior and to link reactor neutronics codes with thermal-hydraulics and/or other physics codes. Deterministic codes require an accurate set of multigroup cross section libraries. The current process for generating these libraries is time consuming. TXSAMC offers a shorter route for generating these libraries.

TXSAMC links three external codes together to create these libraries. The code creates an MCNP (Monte Carlo N-Particle) model of the reactor and calculates the zone-averaged scalar flux in various tally regions and a core-averaged scalar flux tallied by energy bin. The core-averaged scalar flux provides a weighting function for NJOY. The zone-averaged scalar flux data is used in TRANSX for homogenization and shielding. The code runs NJOY to produce multigroup cross sections that are tabulated by nuclide, temperature and background cross section in MATXS (Material-wise cross section)

format. This library is read by TRANSX which, in conjunction with the RZFLUX (Regular Zone-averaged Flux) files, shields the cross sections and homogenizes them. The result is a macroscopic cross section for the cell within the reactor from which the RZFLUX file was written.

The cross sections produced by this process have been tested in five different sample problems and have been shown to be reasonably accurate. For reactor cells containing fuel pins, the typical error in the overall fission, νsigf , $(n,2n)$, absorption and total RRD is only a few percent and is often less than one percent. It appears that the error is less for hexagonal lattices than for square lattices. A significant amount of error is associated with threshold reactions like $(n,2n)$ in the sodium coolant. For the square lattice test problems, a reduction in error occurs when smaller tally regions are selected. This reduction was not observed for hexagonal lattice reactors. Overall, the cross sections produced by TXSAMC performed very well.

DEDICATION

To my wife Lindsey, for all her support, love and friendship.

ACKNOWLEDGEMENTS

I would like to thank Marvin Adams for his extensive help on this project as my advisor. His suggestions and advice were invaluable. I greatly appreciate all of the time he took out of a busy schedule to meet with me. I would also like to express my appreciation to Tom Marcille. This research project began as a result of our discussions at Los Alamos National Lab and I am very grateful for the opportunity to contribute to this project. The support of LANL and Tom was greatly appreciated. I would also like to thank William Charlton and Guergana Petrova for serving on my committee and Pavel Tsvetkov for serving as a substitute at my defense.

This research was performed under appointment to the U.S. Department of Energy Nuclear Engineering and Health Physics Fellowship Program sponsored by the U.S. Department of Energy's Office of Nuclear Energy, Science, and Technology. I greatly appreciate the support of the DOE in funding my education and this project.

At this time, I would also like to thank all of those who made my experiences at Texas A&M so great and who have taught me so much. This includes my professors, my friends and most importantly, my wife, Lindsey. Her love and support has meant a great deal to me and has kept me going when things were tough. And above all, I would like to thank God, for without Him, none of this would have been possible.

NOMENCLATURE

| | |
|------|----------------------------------|
| LANL | Los Alamos National Laboratory |
| MGXS | Multigroup Cross section |
| SSR | Square-Simple Reactor |
| SCR | Square-Complex Reactor |
| SCRA | Square-Complex Reactor Alternate |
| HSR | Hex-Simple Reactor |
| HCR | Hex-Complex Reactor |
| RRD | Reaction Rate Density |

TABLE OF CONTENTS

| | Page |
|--|------|
| ABSTRACT | iii |
| DEDICATION | v |
| ACKNOWLEDGEMENTS | vi |
| NOMENCLATURE | vii |
| TABLE OF CONTENTS | viii |
| LIST OF FIGURES | x |
| LIST OF TABLES | xii |
| CHAPTER | |
| I INTRODUCTION | 1 |
| Background | 1 |
| Motivation | 6 |
| Process | 9 |
| II EXTERNAL CODES | 11 |
| MCNP | 11 |
| NJOY | 13 |
| TRANSX | 24 |
| III TXSAMC PROCESS | 29 |
| Overview | 29 |
| Input File | 31 |
| Output and Summay | 36 |
| IV NUMERICAL RESULTS | 38 |
| Square-Simple Reactor | 40 |
| Hex-Simple Reactor | 48 |
| Square-Complex Reactor | 54 |
| Square-Complex Reactor Alternate | 75 |

| CHAPTER | Page |
|---------------------------------|------|
| Hex-Complex Reactor | 94 |
| V SUMMARY AND CONCLUSIONS | 115 |
| REFERENCES | 120 |
| APPENDIX A | 122 |
| APPENDIX B | 131 |
| APPENDIX C | 164 |
| APPENDIX D | 165 |
| VITA | 166 |

LIST OF FIGURES

| FIGURE | Page |
|---|------|
| 1 Comparison of multigroup and continuous energy cross sections for ^{23}Na | 4 |
| 2 TXSAMC process flowchart..... | 30 |
| 3 SSR layout in x-y plane. | 42 |
| 4 "Partial" percent errors in each energy group for reaction-rate densities in SSR. | 47 |
| 5 HSR layout in x-y plane..... | 50 |
| 6 "Partial" percent errors in each energy group for reaction-rate densities in HSR..... | 54 |
| 7 SCR layout in x-y plane. | 57 |
| 8 "Partial" percent errors for reaction-rate densities in SCR tally region 1..... | 61 |
| 9 "Partial" percent errors for reaction-rate densities in SCR tally region 2..... | 64 |
| 10 Plot of total, absorption and (n,2n) cross sections for ^{23}Na | 67 |
| 11 "Partial" percent errors for reaction-rate densities in SCR tally region 3..... | 68 |
| 12 "Partial" percent errors for reaction-rate densities in SCR tally region 4..... | 71 |
| 13 "Partial" percent errors for reaction-rate densities in SCR tally region 5..... | 74 |
| 14 "Partial" percent errors for reaction-rate densities in SCRA tally region 1..... | 79 |
| 15 "Partial" percent errors for reaction-rate densities in SCRA tally region 2..... | 83 |
| 16 Plot of 187 group weighting function with sodium cross section..... | 86 |
| 17 "Partial" percent errors for reaction-rate densities in SCRA tally region 3..... | 87 |
| 18 "Partial" percent errors for reaction-rate densities in SCRA tally region 4..... | 90 |
| 19 "Partial" percent errors for reaction-rate densities in SCRA tally region 5..... | 93 |

| FIGURE | Page |
|---|------|
| 20 HCR layout in x-y plane. | 97 |
| 21 "Partial" percent errors for reaction-rate densities in HCR tally region 1. | 101 |
| 22 "Partial" percent errors for reaction-rate densities in HCR tally region 2. | 104 |
| 23 "Partial" percent errors for reaction-rate densities in HCR tally region 3. | 107 |
| 24 "Partial" percent errors for reaction-rate densities in HCR tally region 4. | 110 |
| 25 "Partial" percent errors for reaction-rate densities in HCR tally region 5. | 113 |

LIST OF TABLES

| TABLE | Page |
|-------|--|
| 1 | LANL 30 group structure..... 18 |
| 2 | EPRI 69 group structure..... 19 |
| 3 | LANL 70 group structure..... 20 |
| 4 | LANL 187 group structure..... 21 |
| 5 | Description of materials, geometry and temperatures in SSR 41 |
| 6 | 30 group MCNP scalar flux, TXSAMC cross sections and reaction rates in SSR 43 |
| 7 | 30 group MCNP reaction rates and reaction rate comparison in SSR 44 |
| 8 | Energy structure for weight function 45 |
| 9 | Description of materials, geometry and temperatures in HSR..... 49 |
| 10 | 30 group MCNP scalar flux, TXSAMC cross sections and reaction rates in HSR..... 51 |
| 11 | 30 group MCNP reaction rates and reaction rate comparison in HSR 52 |
| 12 | Description of materials, geometry and temperatures in SCR..... 56 |
| 13 | MCNP scalar flux, TXSAMC cross sections and reaction rates in SCR tally region 1 59 |
| 14 | MCNP reaction rates and reaction rate comparison in SCR tally region 1..... 59 |
| 15 | MCNP scalar flux, TXSAMC cross sections and reaction rates in SCR tally region 2 62 |
| 16 | MCNP reaction rates and reaction rate comparison in SCR tally region 2..... 63 |

| TABLE | Page |
|---|------|
| 17 MCNP scalar flux, TXSAMC cross sections and reaction rates in SCR tally region 3 | 65 |
| 18 MCNP reaction rates and reaction rate comparison in SCR tally region 3..... | 66 |
| 19 MCNP scalar flux, TXSAMC cross sections and reaction rates in SCR tally region 4 | 69 |
| 20 MCNP reaction rates and reaction rate comparison in SCR tally region 4..... | 70 |
| 21 MCNP scalar flux, TXSAMC cross sections and reaction rates in SCR tally region 5 | 72 |
| 22 MCNP reaction rates and reaction rate comparison in SCR tally region 5..... | 73 |
| 23 MCNP scalar flux, TXSAMC cross sections and reaction rates in SCRA tally region 1 | 77 |
| 24 MCNP reaction rates and reaction rate comparison in SCRA tally region 1..... | 78 |
| 25 MCNP scalar flux, TXSAMC cross sections and reaction rates in SCRA tally region 2 | 81 |
| 26 MCNP reaction rates and reaction rate comparison in SCRA tally region 2..... | 82 |
| 27 MCNP scalar flux, TXSAMC cross sections and reaction rates in SCRA tally region 3 | 84 |
| 28 MCNP reaction rates and reaction rate comparison in SCRA tally region 3 | 84 |
| 29 MCNP scalar flux, TXSAMC cross sections and reaction rates in SCRA tally region 4 | 88 |
| 30 MCNP reaction rates and reaction rate comparison in SCRA tally region 4..... | 89 |

| TABLE | Page |
|-------|---|
| 31 | MCNP scalar flux, TXSAMC cross sections and reaction rates in SCRA tally region 591 |
| 32 | MCNP reaction rates and reaction rate comparison in SCRA tally region 592 |
| 33 | Description of materials, geometry and temperatures in HCR95 |
| 34 | MCNP scalar flux, TXSAMC cross sections and reaction rates in HCR tally region 198 |
| 35 | MCNP reaction rates and reaction rate comparison in HCR tally region 199 |
| 36 | MCNP scalar flux, TXSAMC cross sections and reaction rates in HCR tally region 2 102 |
| 37 | MCNP reaction rates and reaction rate comparison in HCR tally region 2103 |
| 38 | MCNP scalar flux, TXSAMC cross sections and reaction rates in HCR tally region 3 105 |
| 39 | MCNP reaction rates and reaction rate comparison in HCR tally region 3106 |
| 40 | MCNP scalar flux, TXSAMC cross sections and reaction rates in HCR tally region 4 108 |
| 41 | MCNP reaction rates and reaction rate comparison in HCR tally region 4109 |
| 42 | MCNP scalar flux, TXSAMC cross sections and reaction rates in HCR tally region 5 111 |
| 43 | MCNP reaction rates and reaction rate comparison in HCR tally region 5112 |

CHAPTER I

INTRODUCTION

This thesis describes the creation, operation and accuracy of a new tool, Transport Cross Sections from Applied Monte Carlo (TXSAMC), for generating shielded multigroup cross sections for deterministic reactor analysis codes. TXSAMC provides a way to link the accuracy and flexibility of stochastic neutron simulation codes with the speed and time-dependent analysis capabilities of deterministic reactor physics codes. TXSAMC allows the user to create an accurate set of shielded multigroup cross sections for small fast reactors with extension to virtually any geometry that can be modeled in MCNP. Within this introductory chapter, we will discuss the background of this area of research including current methods for generating multigroup constants, the motivation for the creation of TXSAMC, existing methods of multigroup cross section generation with Monte Carlo methods and the structure of this project.

BACKGROUND

In the reactor physics community, the vast majority of the existing computer codes used for reactor design and analysis are deterministic in nature; that is, the codes operate by solving numerically either the Boltzmann Transport Equation (1) or the Diffusion Equation (2):

$$\begin{aligned} & \frac{1}{v} \frac{\partial \psi}{\partial t} + \hat{\Omega} \cdot \nabla \psi + \Sigma_t(r, E) \psi(r, E, \hat{\Omega}, t) \\ & = \int_{4\pi} d\hat{\Omega}' \int_0^\infty dE' \Sigma_s(E' \rightarrow E, \hat{\Omega}' \rightarrow \hat{\Omega}) \psi(r, E', \hat{\Omega}', t) + s(r, E, \hat{\Omega}, t) \end{aligned} \quad (1)$$

This thesis uses the style of *Nuclear Science and Engineering*.

$$\begin{aligned}
& \frac{1}{v} \frac{\partial \phi}{\partial t} - \nabla \cdot D(\underline{r}, E) \nabla \phi + \Sigma_t(\underline{r}, E) \phi(\underline{r}, E, t) \\
& = \int_0^\infty dE' \Sigma_s(E' \rightarrow E) \phi(\underline{r}, E', t) + S(\underline{r}, E, t)
\end{aligned} \tag{2}$$

where v is the neutron speed, $\psi(\underline{r}, E, \hat{\Omega}, t)$ is the space-, energy- and time- dependent angular flux, $\phi(\underline{r}, E, t)$ is the space-, energy- and time-dependent scalar flux. $\hat{\Omega}$ is a unit vector in the direction of particle travel. $\Sigma_t(\underline{r}, E)$ is the space- and energy-dependent total cross section and $\Sigma_s(E' \rightarrow E, \hat{\Omega}' \rightarrow \hat{\Omega})$ is the double-differential scattering cross section, $\Sigma_s(E' \rightarrow E)$ is the single-differential scattering cross section, $D(\underline{r}, E)$ is the space- and energy-dependent diffusion coefficient, $s(\underline{r}, E', \hat{\Omega}', t)$ is the space-, energy-, angle- and time-dependent neutron source rate, and $S(\underline{r}, E, t)$ is the energy- and time-dependent neutron source rate.¹ The source term includes neutrons emitted from fission for fissionable regions.

These solutions are accomplished by segmenting these two equations into many small pieces defined by neutron energy, spatial location, time and angle (direction), writing the equations in terms of matrices and solving the resultant system. For the solution to be accurate, the equations must be given accurate nuclear cross sections. Since the equations to be solved are divided into energy bins or “groups”, the cross section data must likewise be divided appropriately into groups. These sets of nuclear data are called multigroup cross sections (MGXS) or multigroup constants and are one of the keys to solving a reactor physics problem correctly. Equation (3) shows the Boltzmann Transport Equation in multigroup form.

$$\hat{\Omega} \cdot \nabla \psi_g + \Sigma_{t,g} \psi_g(\underline{r}, \hat{\Omega}) = \sum_{g'=1}^G \int_{4\pi} d\hat{\Omega}' \Sigma_{s,g' \rightarrow g}(\underline{r}, \hat{\Omega}' \rightarrow \hat{\Omega}) \psi_{g'}(\underline{r}, \hat{\Omega}') + s_g(\underline{r}, \hat{\Omega}) \quad (3)$$

$$g = 1, \dots, G$$

where ψ_g is the angular flux for group g , $\Sigma_{t,g}$ is the total neutron cross section in that energy group, $\Sigma_{s,g' \rightarrow g}$ is the group-to-group scattering cross section and s_g is the neutron source rate in the g -th energy group.¹ For regions with fissionable nuclides, the source term includes fission neutrons emitted into that group. Equation (4) shows the k -eigenvalue Diffusion Equation in multigroup form.

$$-\nabla \cdot D^g(r) \nabla \phi_g(r) + \Sigma_r^g(r) \phi_g(r) = \sum_{g' \neq g}^G \Sigma_s^{g' \rightarrow g}(r) \phi_{g'}(r) + \frac{1}{k} \chi^g \sum_{g'=1}^G \nu \Sigma_f^{g'}(r) \phi_{g'}(r) \quad (4)$$

$$g = 1, \dots, G$$

where $D^g(r)$ is the diffusion coefficient within group g , $\phi_g(r)$ is the scalar flux within the group, $\Sigma_r^g(r)$ is the removal cross section from that group, $\Sigma_s^{g' \rightarrow g}(r)$ is the group-to-group scattering cross section, k is the multiplication factor (eigenvalue), χ^g is the fraction of neutrons from fission emitted in group g , ν is the number of neutrons emitted per fission and $\Sigma_f^{g'}(r)$ is the fission cross section for group g' .²

Nuclear cross sections vary tremendously with energy and as result it can sometimes be very difficult to represent this data with even a rather large number of energy groups. Fig. 1 shows a plot of the continuous energy total neutron cross section of ^{23}Na as a function of energy³ along with a sample 30 group representation of the same data. Clearly, the multigroup representation does not perfectly track the continuous energy cross section, especially in the resonance regions, but if the 30 group cross

sections are properly weighted averages of the continuous data, then it is possible to obtain a very close approximation of important reactor characteristics such as reaction rate and criticality. Properly weighting the cross sections to achieve a close approximation is much easier said than done. The proper weighting function is almost always unique to the particular reactor problem for which it is used. Unless the characteristics of two problems are very similar to each other in time, geometry, temperature, material composition, etc., the weighting function for one problem will not produce accurate MGXS for another problem.

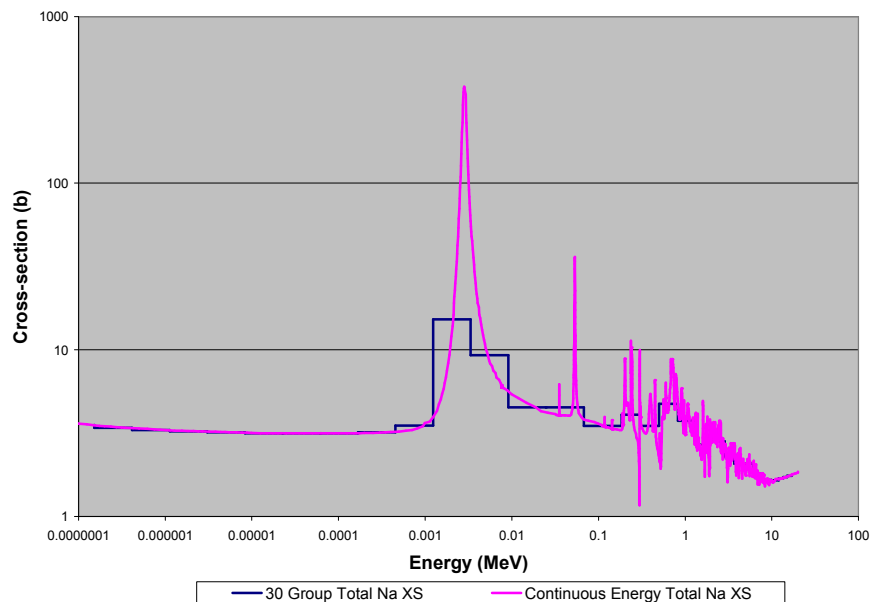


Fig. 1. Comparison of multigroup and continuous energy cross sections for ^{23}Na .

As a result, it is usually necessary to generate a new weighting function for each problem to be examined. Typically, the proper weighting function is derived from the

energy-dependent scalar flux within the system. This can present a somewhat circular problem: a weighting function is needed to generate the right cross sections to obtain the scalar flux to derive the weighting function and so on. Unless the weighting function is well-known before beginning to analyze the problem, some process must be used to determine the correct function. Generally this involves first generating a set of ultrafine group cross sections, solving the reactor problem (or a representative problem that is easier to solve) for the ultrafine group spectrum and then using this spectrum to weight coarse group cross sections. This process is based on the assumption that for very fine group structures, the within-group shape of the flux is approximated well enough by analytic expressions that can be embedded in cross section processing codes such as NJOY. For more coarse structures, the within-group shape can be more complicated which precludes direct generation of coarse cross sections except for a very small subset of reactors for which the weighting functions are well-known (commercial power reactors).

For new reactor types for which we have little experience or experimental data, the above-described process must be used. A somewhat arbitrary weighting function is chosen to weight the ultrafine cross sections and then the reactor physics problem (or a simpler representative problem) is solved. From the solution of this problem, a new weighting function is derived and the process is repeated for a coarse group structure. This approach will generally yield an accurate weighting function but it can be very time-consuming, requiring a significant amount of computer time to solve the ultrafine

reactor problem. This can be a rather unwieldy tool for investigation of new reactor designs, particularly if only a portion of the reactor physics “answer” is needed.

Further difficulties are introduced when attempting to homogenize a pin cell in the reactor; without knowledge of the flux within the cell (which comes from a solution of the reactor physics problem using the same nuclear data that needs a weight function), it is impossible to homogenize the cell accurately. This results in very detailed and tedious calculations being necessary to investigate even the simplest of problems.

MOTIVATION

In the reactor design and analysis process, there are many situations where only a portion of the solution is needed. For example, one might want to calculate an estimate of the criticality of the system at a particular point in time and power level rather than solve the complete problem and obtain criticality as a tabulated function of time, power, temperature, burn-up, etc.. Within the current machinery of deterministic reactor analysis, however, it is very difficult to get an answer to any part of the problem without going through the entire cross section generation process in all of its detail. This is especially true when doing preliminary analysis of new reactors for which we have very little experimental data. In order to do realistic and relevant design of new nuclear reactors within the existing deterministic reactor analysis world, a new method of generating multigroup cross sections is needed.

In order to meet the needs of designers, this new method of cross section generation must be accurate and extensible to a wide variety of problems. As noted previously, the key to this problem is creating an appropriate weight function which is

generally not known in advance. However, since the energy-dependent scalar flux is often a very good proxy for the weighting function, if we can calculate the scalar flux correctly for the reactor in question, it should be possible to construct an appropriate weighting function. Calculating this scalar flux accurately and non-iteratively is difficult to do within current deterministic methods, but it is possible to do it with a Monte Carlo computer code. Such a code uses stochastic methods and continuous energy neutron cross sections to simulate the behavior of neutrons in a reactor. Quantities of interest are “tallied” as particles pass through particular surfaces or volumes. Within the limits of how accurately the geometry and material composition are specified, limits on the fidelity of tabulated and interpolated cross section data and within the statistical error on the tallied quantities, the results are nearly exact solutions of the Boltzmann equation.

Given the ability of Monte Carlo codes to calculate the flux and other quantities of interest directly, it is understandable to ask why deterministic codes are used at all for reactor analysis. The answer lies in the extreme difficulty of simulating time-dependent quantities (reactor transients, startup, burn-up, etc.) and the amount of particles that need to be simulated to achieve good statistics in Monte Carlo codes. The result is that for certain classes of problems, such as small, fast reactors, Monte Carlo may be used to calculate a weighting function to generate the appropriate multigroup cross sections for use in deterministic codes. Keep in mind that due to the difficulty of simulating time-dependent quantities, the generated cross sections will probably be limited to a certain state of the reactor (and perhaps limited perturbations from that state).

Currently, a desire exists within the nuclear industry and academia to investigate small, fast reactor systems for which cross section libraries do not exist. These systems include both space reactors and burner reactors for programs such as GNEP.⁴ Since the Monte Carlo code MCNP can model these systems fairly easily and generate the weighting function needed to generate valid libraries, a significant improvement in the design process could be made if a tool was created to link an MCNP model and its output results to a cross section generation tool. In addition to the ability to weight the cross sections accurately, MCNP can also be used to obtain the scalar flux data needed to homogenize and shield the multigroup cross sections. This would then allow a designer to use the existing deterministic reactor analysis codes to investigate these new systems.

Because of the possibilities that using continuous energy Monte Carlo methods opens up, there have been several attempts to use the Monte Carlo code MCNP to generate multigroup cross sections.⁵⁻⁶ Generally, these methods have involved directly tallying the group-wise reaction rates and the group-wise scalar flux in a continuous energy MCNP model of a cell and dividing the former by the latter to calculate the macroscopic multigroup cross sections. The scattering matrices can be calculated in a number of different ways but perhaps the most common is to directly tally which group a particle is scattering from and which group it is scattering into when it undergoes a scattering reaction.⁶ While these methods are correct and will generate valid results, they do have some drawbacks. The most important of these is the computational expense of tallying all of the required quantities. Using the existing methods of generating cross

sections from MCNP would require many tallies: one for each reaction of interest plus one for the scalar flux in every area of interest (every zone in every cell of interest). In MCNP, tallies consume a great deal of the computational time needed for any given simulation. An even greater expense is the amount of computer time needed to generate quality statistics in the scattering matrices. Neglecting upscattering, a 30 group scattering matrix for a single material zone encompasses 465 bins. Assuming that all of the tallies are evenly distributed (equal number in every scattering bin), to generate the same statistical accuracy for each bin in the scattering matrix as for each bin in the other reaction types (one bin per group) would require 15 times as many particles. All of these drawbacks point to a need for a better method of applying the advantages of Monte Carlo methods to generating multigroup cross sections.

PROCESS

With this motivation, the remainder of this thesis describes the creation and evaluation of a process called TXSAMC that links MCNP-generated scalar flux data to the cross section generation tool NJOY and the homogenization, shielding and interface code TRANSX. Through this process, the user can generate properly shielded, multigroup cross sections for small, fast reactor systems. The process has the flexibility to generate these cross sections for individual pins, groupings of pins or the entire reactor. This allows the user to correct for various heterogeneities in the reactor system.

In Chapter II, we will discuss the details of each of the codes linked in this process and their key assumptions, input and outputs. In Chapter III, we will discuss the structure, assumptions and general operation of TXSAMC itself. In Chapter IV, we will

present numerical results that demonstrate the accuracy of the multigroup cross sections generated by this tool. In Chapter V, we will present a summary of our research, our conclusions and future areas of work.

CHAPTER II

EXTERNAL CODES

In this section, we describe the three codes that are incorporated into the TXSAMC process to generate shielded multigroup cross sections. These three major codes are MCNP, NJOY and TRANSX2. We summarize the basic features, limitations and assumptions inherent in each code.

MCNP

The first of the external codes used in TXSAMC is the Monte Carlo N-Particle (MCNP) code which uses stochastic methods to simulate the histories of neutrons, photons, electrons or any combination of these three particles in a system. It is capable of modeling any geometry and material configuration that can be bounded by “first- and second-degree surfaces and fourth-degree elliptical tori”.⁷⁻⁸ Through the simulation of these particles, MCNP is capable of calculating various quantities of interest including the scalar flux in a particular region of the problem or the criticality of the system. In order to calculate the criticality of the system, a KCODE card is used to specify that the k -eigenvalue problem is to be solved.⁷⁻⁸ Within the MCNP input deck, the number of “histories” or particles to be simulated in the problem is specified along with a distribution of starting points, directions, and energies. For KCODE problems, the number of histories is determined by the number of “cycles” and the number of histories per cycle. For the first cycle, the source distribution is specified by the user and the number of histories per cycle is launched from there. The starting direction and energy are determined by sampling in probability density functions. The energy is usually

sampled from a Watt's fission spectrum for the material used in the reactor. Each particle is tracked through the reactor; the distance traveled between collisions is calculated by random sampling of an exponential distribution and at each point of interaction, a reaction type is sampled from the discrete neutron cross sections for that particle's energy given the material at that location. If a fission event or other neutron production reaction occurs, the current particle's path is paused while the new particles are tracked to their deaths. A particle can die by being absorbed, dropping below certain energies, leaking from the reactor or taking too much time. When a cycle is finished, the locations of fission events from the previous cycle are used to start the new cycle's particles. Within each cycle, the criticality can be estimated by dividing neutrons produced by neutrons lost.

One of the advantages of Monte Carlo is that the solutions it produces are almost as exact as the statistics, input nuclear data, and specified geometry are. That is, few assumptions are necessary. No assumptions are needed about weighting functions for MGXS, numerical solver techniques, homogenization schemes, or other items that characterize most deterministic reactor analysis. If we use accurate continuous-energy nuclear data (readily available from the ENDF libraries) and specify the geometry accurately (generally easy to do since most things to be modeled are composed of the above-mentioned first- and second-degree surfaces), then the main limitation on accuracy is how much computer time we are willing to expend to achieve a certain level of statistical error in the answer. For some problems that are common in reactor analysis, the number of particles needed to achieve the desired level of statistical error is

extremely high. For example, successfully modeling the power deposition axially in each pin of a light water reactor core could take billions of histories and weeks of computer time. There are variance-reduction methods such as particle splitting and Russian roulette⁷⁻⁸ that can be used to reduce the number of histories needed for large, complex problems, but there are limits. In particular, variance reduction almost always improves the statistics in certain regions of phase space at the cost of degrading them in other regions. For these reasons, Monte Carlo analysis is generally limited to smaller reactors. At present it is also prohibitively expensive to use Monte Carlo for time-dependent analysis such as modeling transients or performing burnup calculations (although much work in these areas has been done in recent years). In the context of this project, neither of these drawbacks is that severe since we are interested in small, fast reactor systems and we are looking to use information from MCNP to generate data for deterministic codes that can do the time-dependent analyses. It should be noted that the results in this paper use MCNPX v.2.5 but the process should work equally well with MCNP5 or MCNP4C; none of the features used in the TXSAMC process are unique to MCNPX.

NJOY

NJOY is a computer code used to generate point-wise or multigroup cross section libraries from evaluated nuclear data (i.e. ENDF files).⁹ NJOY is composed of a set of modules, each of which performs a separate task in the cross section processing, and the NJOY program itself which runs each of the modules. Within the TXSAMC process, we will use the RECONR, BROADR, HEATR, PURR, THERMR, MODER, GROUPE and MATXS modules to produce multigroup cross sections in MATXS

format which can be read by TRANSX. We describe below each of the modules in the order in which it is used in the TXSAMC process. It should be noted that TXSAMC runs each nuclide separately up through the GROUPT module, at which point the files are all combined for the MATXS processing. Except for the MATXS file, all data tapes used in this code are in ASCII format. The particular version of NJOY used for the data in this report is NJOY99_112, although most versions of NJOY99 should work (older versions may work as well, although the PURR module may be swapped for the UNRESR module).

The RECONR module is used to reconstruct the point-wise or energy-dependent cross sections from the ENDF tapes.⁹ More specifically it reads the resonance parameters and interpolation schemes off of the ENDF tape and turns these into point-wise cross sections written to a PENDF (Point-wise Evaluated Nuclear Data File). The input file for this module includes specification of the ENDF tape number, the output PENDF tape number, the nuclide name and the resonance reconstruction parameters. By specifying the reconstruction parameters, we also end up specifying the computer time necessary and the size of the output files. For the TXAMC process, we specify that the fractional reconstruction tolerance be set to 0.1% (this parameter determines the amount of integral error in the reconstruction grids on a barns/reconstruction point) and leave all other parameters with their default values. The output is a PENDF tape for that nuclide.

The BROADR subroutine is used to perform the Doppler broadening of the point-wise cross sections for each of the temperatures specified in the problem.⁹ The input file for this module includes specification of the ENDF tape number, the PENDF

tape number from RECONR, the output PENDF tape number, the nuclide in question, the number of temperatures at which the cross sections are broadened, the values of these temperatures and the resolution to which they are broadened. In the TXSAMC process, the only resolution parameter specified is the fractional tolerance for thinning which is given a value of 0.1%. All other parameters retain their default values. The output from this module is the broadened cross sections written in PENDF form.

The HEATR module is used to generate heat-production (KERMA factors) and radiation-damage cross sections.⁹ This step is optional since many applications of TXSAMC will not need these cross sections. The input file for this module includes specification of the ENDF tape number, the “broadened” PENDF tape number, the output PENDF tape number, the nuclide, the number of temperatures and the various MT (reaction) numbers for the heating, KERMA and damage cross sections desired. The output is in PENDF form.

The PURR module is used to construct probability tables for the unresolved resonance region for each nuclide.⁹ The input file for this module includes specification of the ENDF tape number, the broadened and heated PENDF tape number, the output PENDF tape number, the nuclide, the number of temperatures, the number of background cross sections (σ_0), the value of the temperatures and the value of the background cross sections. (We describe the use of the “background” cross section in the discussion of the GROUPT module below.) The output file is in PENDF form.

The THERMR module is used to produce the cross sections that govern scattering in thermal energy ranges.⁹ Like HEATR, this module may be optional for

some uses of the TXSAMC process. When investigating fast reactors, the thermal scattering effects are often very small so this module can be neglected. The input file for this module includes specification of the PENDF tape number (from the PURR output), the output PENDF tape number, the nuclide, the number of temperatures, the type of scattering to be modeled (free gas thermal is the one most commonly used), the values of the temperatures and parameters describing the details of the thermal scattering cross sections. The output file is in PENDF form.

In the TXSAMC process, when the THERMR module is not called for, the MODER module is used to change tape numbers and maintain continuity in the process. All that the MODER module does is convert data tapes from ASCII to binary and vice versa.⁹ However, it can be used to maintain the same file type and change its tape number, which is how it is used here. The output remains a PENDF formatted file.

The GROUPT module “generates self-shielded multigroup cross sections, group-to-group scattering matrices, photon production matrices, and charged-particle cross sections from point-wise input”.⁹ This is by far the most important NJOY module as it relates to the TXSAMC process since it is the one that generates the tabulated multigroup cross sections that will later be homogenized and spatially shielded by TRANSX. The input for this file includes the ENDF tape number, the PENDF tape number (THERMR output), the GENDF (Groupwise Evaluated Nuclear Data File) tape number for the output, the nuclide, the neutron and photon group structures, the weighting function, the Legendre order of anisotropic scattering, the number of background cross sections, a temperature value and a list of the background cross

sections. Tables 1 through 4 show the energy boundaries of some of the NJOY built-in group structures.⁹ The 30 and 70 group structures are targeted more towards fast systems, the 69 group structure is targeted more towards thermal systems while the 187 group structure is broadly applicable. If the group structure or weighting function is not one that is built in to NJOY, the input file also includes the specifications for the group structure or weighting function. Choosing the appropriate weight function is critical for the GROUPT module since it heavily influences the shielding of the cross sections. The built-in weighting functions cover a fairly broad range of systems, from thermal to fast to fusion, but this may not be sufficient to accurately generate cross sections for a particular problem. In these cases, a new weight function can be generated and written to the input file. This is what TXSAMC does using MCNP-generated data. The input file also allows specification of the interpolation scheme for reconstructing the weight function from tabulated points. The most commonly used is an interpolation that is linear on a log-log scale.

TABLE 1
LANL 30 group structure

| Group | Upper Bound (MeV) |
|-------|-------------------|
| 1 | 1.520E-07 |
| 2 | 4.140E-07 |
| 3 | 1.130E-06 |
| 4 | 3.060E-06 |
| 5 | 8.320E-06 |
| 6 | 2.260E-05 |
| 7 | 6.140E-05 |
| 8 | 1.670E-04 |
| 9 | 4.540E-04 |
| 10 | 1.235E-03 |
| 11 | 3.350E-03 |
| 12 | 9.120E-03 |
| 13 | 2.480E-02 |
| 14 | 6.760E-02 |
| 15 | 1.840E-01 |
| 16 | 3.030E-01 |
| 17 | 5.000E-01 |
| 18 | 8.230E-01 |
| 19 | 1.353E+00 |
| 20 | 1.738E+00 |
| 21 | 2.232E+00 |
| 22 | 2.865E+00 |
| 23 | 3.680E+00 |
| 24 | 6.070E+00 |
| 25 | 7.790E+00 |
| 26 | 1.000E+01 |
| 27 | 1.200E+01 |
| 28 | 1.350E+01 |
| 29 | 1.500E+01 |
| 30 | 1.700E+01 |

TABLE 2
EPRI 69 group structure

| Group | Upper Bound (MeV) | Group | Upper Bound (MeV) |
|-------|-------------------|-------|-------------------|
| 1 | 5.000E-09 | 36 | 1.150E-06 |
| 2 | 1.000E-08 | 37 | 1.300E-06 |
| 3 | 1.500E-08 | 38 | 1.500E-06 |
| 4 | 2.000E-08 | 39 | 2.100E-06 |
| 5 | 2.500E-08 | 40 | 2.600E-06 |
| 6 | 3.000E-08 | 41 | 3.300E-06 |
| 7 | 3.500E-08 | 42 | 4.000E-06 |
| 8 | 4.200E-08 | 43 | 9.877E-06 |
| 9 | 5.000E-08 | 44 | 1.597E-05 |
| 10 | 5.800E-08 | 45 | 2.770E-05 |
| 11 | 6.700E-08 | 46 | 4.805E-05 |
| 12 | 8.000E-08 | 47 | 7.550E-05 |
| 13 | 1.000E-07 | 48 | 1.487E-04 |
| 14 | 1.400E-07 | 49 | 3.673E-04 |
| 15 | 1.800E-07 | 50 | 9.069E-04 |
| 16 | 2.200E-07 | 51 | 1.425E-03 |
| 17 | 2.500E-07 | 52 | 2.240E-03 |
| 18 | 2.800E-07 | 53 | 3.519E-03 |
| 19 | 3.000E-07 | 54 | 5.530E-03 |
| 20 | 3.200E-07 | 55 | 9.118E-03 |
| 21 | 3.500E-07 | 56 | 1.503E-02 |
| 22 | 4.000E-07 | 57 | 2.478E-02 |
| 23 | 5.000E-07 | 58 | 4.085E-02 |
| 24 | 6.250E-07 | 59 | 6.734E-02 |
| 25 | 7.800E-07 | 60 | 1.110E-01 |
| 26 | 8.500E-07 | 61 | 1.830E-01 |
| 27 | 9.100E-07 | 62 | 3.025E-01 |
| 28 | 9.500E-07 | 63 | 5.000E-01 |
| 29 | 9.720E-07 | 64 | 8.210E-01 |
| 30 | 9.960E-07 | 65 | 1.353E+00 |
| 31 | 1.020E-06 | 66 | 2.231E+00 |
| 32 | 1.045E-06 | 67 | 3.679E+00 |
| 33 | 1.071E-06 | 68 | 6.066E+00 |
| 34 | 1.097E-06 | 69 | 1.000E+01 |
| 35 | 1.123E-06 | | |

TABLE 3
LANL 70 group structure

| Group | Upper Bound (MeV) | Group | Upper Bound (MeV) |
|-------|-------------------|-------|-------------------|
| 1 | 6.144E-05 | 36 | 2.187E-02 |
| 2 | 1.013E-04 | 37 | 2.479E-02 |
| 3 | 1.301E-04 | 38 | 2.809E-02 |
| 4 | 1.670E-04 | 39 | 3.183E-02 |
| 5 | 2.145E-04 | 40 | 4.087E-02 |
| 6 | 2.754E-04 | 41 | 5.248E-02 |
| 7 | 3.536E-04 | 42 | 6.738E-02 |
| 8 | 4.540E-04 | 43 | 8.652E-02 |
| 9 | 5.829E-04 | 44 | 1.111E-01 |
| 10 | 7.485E-04 | 45 | 1.426E-01 |
| 11 | 9.611E-04 | 46 | 1.832E-01 |
| 12 | 1.089E-03 | 47 | 2.352E-01 |
| 13 | 1.234E-03 | 48 | 3.020E-01 |
| 14 | 1.398E-03 | 49 | 3.877E-01 |
| 15 | 1.585E-03 | 50 | 4.394E-01 |
| 16 | 1.796E-03 | 51 | 4.979E-01 |
| 17 | 2.035E-03 | 52 | 5.642E-01 |
| 18 | 2.306E-03 | 53 | 6.393E-01 |
| 19 | 2.613E-03 | 54 | 7.244E-01 |
| 20 | 2.960E-03 | 55 | 8.209E-01 |
| 21 | 3.355E-03 | 56 | 9.301E-01 |
| 22 | 3.801E-03 | 57 | 1.054E+00 |
| 23 | 4.307E-03 | 58 | 1.194E+00 |
| 24 | 4.881E-03 | 59 | 1.353E+00 |
| 25 | 5.531E-03 | 60 | 1.738E+00 |
| 26 | 6.267E-03 | 61 | 2.231E+00 |
| 27 | 7.102E-03 | 62 | 2.865E+00 |
| 28 | 8.047E-03 | 63 | 3.679E+00 |
| 29 | 9.119E-03 | 64 | 4.724E+00 |
| 30 | 1.033E-02 | 65 | 6.065E+00 |
| 31 | 1.171E-02 | 66 | 7.788E+00 |
| 32 | 1.327E-02 | 67 | 1.000E+01 |
| 33 | 1.503E-02 | 68 | 1.284E+01 |
| 34 | 1.704E-02 | 69 | 1.649E+01 |
| 35 | 1.930E-02 | 70 | 2.000E+01 |

TABLE 4
LANL 187 group structure

| Group | Upper Bound (MeV) | Group | Upper Bound (MeV) | Group | Upper Bound (MeV) |
|-------|-------------------|-------|-------------------|-------|-------------------|
| 1 | 2.540E-10 | 64 | 1.210E-05 | 127 | 2.809E-02 |
| 2 | 7.602E-10 | 65 | 1.371E-05 | 128 | 3.183E-02 |
| 3 | 2.277E-09 | 66 | 1.554E-05 | 129 | 3.607E-02 |
| 4 | 6.325E-09 | 67 | 1.760E-05 | 130 | 4.087E-02 |
| 5 | 1.240E-08 | 68 | 1.995E-05 | 131 | 4.631E-02 |
| 6 | 2.049E-08 | 69 | 2.260E-05 | 132 | 5.248E-02 |
| 7 | 2.550E-08 | 70 | 2.561E-05 | 133 | 5.946E-02 |
| 8 | 3.061E-08 | 71 | 2.902E-05 | 134 | 6.738E-02 |
| 9 | 3.550E-08 | 72 | 3.289E-05 | 135 | 7.635E-02 |
| 10 | 4.276E-08 | 73 | 3.727E-05 | 136 | 8.652E-02 |
| 11 | 5.000E-08 | 74 | 4.223E-05 | 137 | 9.804E-02 |
| 12 | 5.692E-08 | 75 | 4.785E-05 | 138 | 1.111E-01 |
| 13 | 6.700E-08 | 76 | 5.422E-05 | 139 | 1.259E-01 |
| 14 | 8.197E-08 | 77 | 6.144E-05 | 140 | 1.426E-01 |
| 15 | 1.116E-07 | 78 | 6.962E-05 | 141 | 1.616E-01 |
| 16 | 1.457E-07 | 79 | 7.889E-05 | 142 | 1.832E-01 |
| 17 | 1.523E-07 | 80 | 8.940E-05 | 143 | 2.075E-01 |
| 18 | 1.844E-07 | 81 | 1.013E-04 | 144 | 2.352E-01 |
| 19 | 2.277E-07 | 82 | 1.148E-04 | 145 | 2.665E-01 |
| 20 | 2.510E-07 | 83 | 1.301E-04 | 146 | 3.020E-01 |
| 21 | 2.705E-07 | 84 | 1.474E-04 | 147 | 3.422E-01 |
| 22 | 2.907E-07 | 85 | 1.670E-04 | 148 | 3.877E-01 |
| 23 | 3.011E-07 | 86 | 1.893E-04 | 149 | 4.394E-01 |
| 24 | 3.206E-07 | 87 | 2.145E-04 | 150 | 4.979E-01 |
| 25 | 3.577E-07 | 88 | 2.430E-04 | 151 | 5.642E-01 |
| 26 | 4.150E-07 | 89 | 2.754E-04 | 152 | 6.393E-01 |
| 27 | 5.032E-07 | 90 | 3.120E-04 | 153 | 7.244E-01 |
| 28 | 6.251E-07 | 91 | 3.536E-04 | 154 | 8.209E-01 |
| 29 | 7.821E-07 | 92 | 4.007E-04 | 155 | 9.301E-01 |
| 30 | 8.337E-07 | 93 | 4.540E-04 | 156 | 1.054E+00 |
| 31 | 8.764E-07 | 94 | 5.145E-04 | 157 | 1.194E+00 |
| 32 | 9.100E-07 | 95 | 5.830E-04 | 158 | 1.353E+00 |
| 33 | 9.507E-07 | 96 | 6.606E-04 | 159 | 1.534E+00 |
| 34 | 9.710E-07 | 97 | 7.485E-04 | 160 | 1.738E+00 |
| 35 | 9.920E-07 | 98 | 8.482E-04 | 161 | 1.969E+00 |
| 36 | 1.014E-06 | 99 | 9.611E-04 | 162 | 2.231E+00 |
| 37 | 1.043E-06 | 100 | 1.089E-03 | 163 | 2.528E+00 |
| 38 | 1.053E-06 | 101 | 1.234E-03 | 164 | 2.865E+00 |
| 39 | 1.062E-06 | 102 | 1.398E-03 | 165 | 3.247E+00 |
| 40 | 1.072E-06 | 103 | 1.585E-03 | 166 | 3.679E+00 |
| 41 | 1.099E-06 | 104 | 1.796E-03 | 167 | 4.169E+00 |
| 42 | 1.125E-06 | 105 | 2.035E-03 | 168 | 4.724E+00 |
| 43 | 1.166E-06 | 106 | 2.306E-03 | 169 | 5.353E+00 |
| 44 | 1.308E-06 | 107 | 2.613E-03 | 170 | 6.065E+00 |
| 45 | 1.457E-06 | 108 | 2.960E-03 | 171 | 6.873E+00 |
| 46 | 1.595E-06 | 109 | 3.355E-03 | 172 | 7.788E+00 |
| 47 | 1.726E-06 | 110 | 3.801E-03 | 173 | 8.825E+00 |
| 48 | 1.855E-06 | 111 | 4.307E-03 | 174 | 1.000E+01 |
| 49 | 2.102E-06 | 112 | 4.881E-03 | 175 | 1.100E+01 |
| 50 | 2.382E-06 | 113 | 5.531E-03 | 176 | 1.200E+01 |
| 51 | 2.700E-06 | 114 | 6.267E-03 | 177 | 1.300E+01 |
| 52 | 3.059E-06 | 115 | 7.102E-03 | 178 | 1.350E+01 |
| 53 | 3.466E-06 | 116 | 8.047E-03 | 179 | 1.375E+01 |
| 54 | 3.928E-06 | 117 | 9.119E-03 | 180 | 1.394E+01 |
| 55 | 4.451E-06 | 118 | 1.033E-02 | 181 | 1.420E+01 |
| 56 | 5.044E-06 | 119 | 1.171E-02 | 182 | 1.442E+01 |
| 57 | 5.715E-06 | 120 | 1.327E-02 | 183 | 1.464E+01 |
| 58 | 6.476E-06 | 121 | 1.503E-02 | 184 | 1.500E+01 |
| 59 | 6.868E-06 | 122 | 1.704E-02 | 185 | 1.600E+01 |
| 60 | 7.338E-06 | 123 | 1.931E-02 | 186 | 1.700E+01 |
| 61 | 8.315E-06 | 124 | 2.188E-02 | 187 | 2.000E+01 |
| 62 | 9.422E-06 | 125 | 2.479E-02 | | |
| 63 | 1.068E-05 | 126 | 2.606E-02 | | |

Equation (5) shows how the GROUPR module creates the needed tabulated cross sections from the existing continuous energy cross sections and the weighting function applied to the problem.

$$\sigma_{t,l,g}^i(\sigma_0, T) = \frac{\int_g \frac{\sigma_t^i(E, T)}{[\sigma_0 + \sigma_t^i]^{l+1}} C(E) dE}{\int_g \frac{1}{[\sigma_0 + \sigma_t^i]^{l+1}} C(E) dE} \quad (5)$$

where $\sigma_{t,l,g}^i(\sigma_0, T)$ is the total microscopic cross section for nuclide i , group g , and Legendre order l as a function of background cross section σ_0 and temperature T . $C(E)$ is the weighting function (note that the same weighting function is used for all Legendre orders).⁹ It should be noted that this equation requires the weighting function to not already have the influence of each of the resonances in the system to avoid shielding resonances twice. It should be a broad shaping function rather than being highly oscillatory (having a sharp dip at every resonance). This implies that the weighting function produced by MCNP in the TXSAMC process should not be produced from a group structure so fine that it resolves the resonances. It also suggests that the MCNP-produced function does not provide a significantly greater amount of information than an educated guess for the weight function since both functions only reflect broad shape. However, it may be possible to modify NJOY in such a way so as to remove the inverse relationship to the total and background cross sections in equation (5) and use a weighting function that does explicitly resolve the resonances. There are a number of

issues with using this method (such as creating problem dependent group structures) but it is a promising avenue for directly shielding the cross sections.

Finally, the input file for GROUPT contains a list of cross sections and other nuclear data to be written to the GENDF file, including any special edits such as the fission spectrum, number of delayed neutrons per fission, etc. The GROUPT module is run for each temperature desired in the problem. The result is a GENDF file for each combination of nuclide and temperature. A subsidiary utility called MERG_GENDF (written by Tom Marcille, listed in Appendix D) is used to combine all of the GENDF files into a single data file.

The final module used in NJOY is the MATXS module which “formats multigroup data for the newer MATXS material cross section interface file, which works with the TRANSX code”.⁹ The input file for this module includes specification of the tape number for the combined GENDF file, the tape number for the GAMINR module output (not used in TXSAMC), the tape number for the MATXS-formatted output file, the number of particle types (neutrons and/or gammas), the number of data types (neutron scattering, gamma scattering, gamma production, etc.), the number of nuclides and the input and output particles for each data type. The output from this module is a MATXS file which consists of multigroup cross sections that are tabulated by nuclide, energy group and background cross section.

NJOY employs many approximations in its processing of cross sections. The most important assumptions are in the weighting function used in the GROUPT module, including the expression that contains the background cross section. If this function does

not accurately represent the flux, there can be significant error in the multigroup cross sections. Accurate knowledge of this weight function is one of the biggest limitations to the NJOY processing system since it is often not known *a priori*. Another limitation on the NJOY system is the amount of computer time needed to do the various reconstructions, broadenings, etc.; it can take a significant amount of time to do the processing to the level of detail desired. However, in the TXSAMC approach, the data that comes from this one-time processing can be used for a large number of calculations.

TRANSX

TRANSX is a computer code designed to produce multigroup cross sections and scattering matrices for deterministic transport codes and diffusion codes.¹⁰ The TRANSX 2001 version of this code also contains an option to produce multigroup cross sections for MCNP. TRANSX models a particular cell geometry and uses input fluxes and the tabulated MATXS data to shield (spatial and mixture) and homogenize the cross sections, thus producing macroscopic cross sections for the cell. Within the TXSAMC framework, there are many different options in TRANSX that can be selected depending on the nature of the problem to be solved.

There are nine different output-format options for TRANSX: CARD, CLAW, FIDO, ANISN, GOXS, ISOTXS, ANISNB, ANIGIF and ACEM (MCNP multigroup format). Each of these works for a different transport, diffusion or Monte Carlo code. TRANSX can be run in either direct or adjoint mode, although only the direct mode is used by TXSAMC. If coupled particle data sets are included on the MATXS file, TRANSX is capable of creating coupled cross section data in the chosen output format.

If necessary, transport corrections can be applied to the cross sections (such as Consistent-P or Bell-Hansen-Sandmeier). One of the key features of TRANSX is the ability to collapse cross sections from a fine group structure to a coarser group structure. To do this, the number of groups on the MATXS file must match the number of fine groups specified on the input file. If a collapse is requested, the structure of the collapse (number of fine groups in each coarse group) must also be specified on the input file; the number of fine groups in each coarse group must be specified. In addition to these features, TRANSX also allows the user to specify the number of Legendre tables, the number of upscatter and thermal groups and the number of extra edits (additional non-standard cross sections).

In order to correctly homogenize cross sections, the cross sections must be weighted by both volume and flux. To do this, TRANSX is capable of calculating the flux in different cell regions in several ways depending on the user input. TRANSX can use the P0 flux off of the MATXS library (calculated by GROUPT and written there by MATXSRT) or it can use a P0 flux specified by the user on the input file. It can also read three different CCCC-IV interface files: RTFLUX (Regular Total Flux), RZMFLX (Regular Zone Moments Flux) and RZFLUX (Regular Zone-Averaged Flux).¹¹ For many cross sections the scalar flux is sufficient as a weighting function but for the higher order scattering cross sections, it may not be the best choice of a weight function. Future versions of TXSAMC may attempt to generate RZMFLX files to better weight the higher order anisotropic scattering cross sections but the current version is limited to using the scalar flux as a weighting function.

Equation (6) shows how TRANSX creates a cell-averaged macroscopic cross section from the generated flux data.

$$\Sigma_{l,g,cell} = \sum_{i \in cell} \sum_j \frac{\rho_{j,i} \sigma_{l,g,i}^j \phi_{l,g,i} v_i}{\phi_{l,g,cell} V} \quad (6)$$

where $\Sigma_{l,g,cell}$ is the homogenized macroscopic cross section for the cell for group g and Legendre order l . $\rho_{j,i}$ is the number density for material j in region i of the cell, v_i are the region volumes in the cell, $\sigma_{l,g,i}^j$ is the microscopic cross section for material j in region i , $\phi_{l,g,i}$ is the flux for group g and Legendre order l in region i and $\phi_{l,g,cell}$ is the total flux in the cell for group g and Legendre order l .¹⁰ If the higher moment fluxes are not specified, the code uses the scalar flux for all Legendre orders.

The next critical component of the TRANSX code is the region and geometry specification. TRANSX is capable of handling cylindrical cells, cylinders in hexagonal or square lattices or slab cells with a variety of boundary conditions. For each of these cell types, the code will calculate the escape cross sections for the fuel lump within the cell and apply any relevant Dancoff corrections. The code will automatically calculate mean chord lengths for resonance lumps such as fuel pins. For each region in the cell, the region volume is specified using a 1D approximation (i.e. for the cylinders in a lattice, only the cross-sectional area is specified and the radius is calculated; the length is assumed to be identical for each region in a cell) and the region temperature is specified.

Within each region, the number density (in atom/b-cm) of each component nuclide is specified. Between the region and geometry specification and the flux data, the code calculates a background cross section for each nuclide in each region and uses

that to shield the cross sections. This background cross section is calculated by equation (7):

$$\sigma_{0,g}^i = \frac{1}{N_i} \sum_{j \neq i} N_j \sigma_{t,g}^j(\sigma_{0,g}^j) + \sigma_{x,g}^i \quad (7)$$

where $\sigma_{0,g}^i$ is the background cross section for nuclide i and group g , N_i is the number density for nuclide i , N_j is the number density for nuclide j , $\sigma_{t,g}^j(\sigma_{0,g}^j)$ is the total cross section for nuclide j at the background cross section for that nuclide and $\sigma_{x,g}^i$ is the escape cross section for nuclide i .¹⁰ This is clearly an iterative process since the total cross section is dependent on the background cross section. The escape cross section is defined by equation (8):

$$\sigma_{x,g}^i = \frac{1}{N_i \bar{l}} \frac{b_1(1-C_g)}{1+(b_2-1)C_g} \quad (8)$$

where b_1 and b_2 are called Bell corrections, C_g is the Dancoff correction for group g and \bar{l} is the mean chord length of the lump of resonance material.¹⁰ For a cylinder, the appropriate values for the Bell corrections are 1.35. The TRANSX manual contains examples of how the code calculates each Dancoff factor.¹⁰ The Dancoff correction varies depending on the lattice type and the cross sections in the other regions of the cell.

There are a few major assumptions in TRANSX that must be understood when using the code. The first is that the geometries modeled in TRANSX are effectively one dimensional: all regions in a cell are assumed to have the same length and the same shape (i.e. it models rings of cladding and moderator around the fuel meat for cylinders even if the moderator in the real application occupies a non-cylindrical volume). Another

major assumption is that the escape cross sections for a fuel lump in a lattice are calculated assuming an infinite lattice of pins even if this does not reflect the reactor system. These assumptions do not necessarily result in inaccurate cross sections if the system is fairly close to these approximations or if the cross sections are not sensitive to the differences. A major advantage of using the TRANSX architecture is that it provides portability across different transport and diffusion codes. The same MATXS library can be used to generate the cross sections needed for all of these codes (assuming the geometry and flux profile haven't changed) which reduces the need to generate all new cross sections through the NJOY machinery for each different code.

CHAPTER III

TXSAMC PROCESS

OVERVIEW

The TXSAMC process is designed to create shielded and homogenized cross sections for cells in a reactor. In order to do this, the code links data about the scalar flux in a cell from MCNP; NJOY-processed multigroup cross sections; and shielding and homogenization routines from TRANSX. TXSAMC begins by reading a significant number of user-defined parameters from an input file and using this information to write the input files needed for execution of each code. It then executes each code in sequence. As necessary, it reads the output from each code to provide input for the next stage in the process. The final result is a series of cross section libraries for each selection of pin-cells in the problem. Fig. 2 shows the basic outline of this process. The initial version of TXSAMC is written in FORTRAN 95 for Windows-based machines.

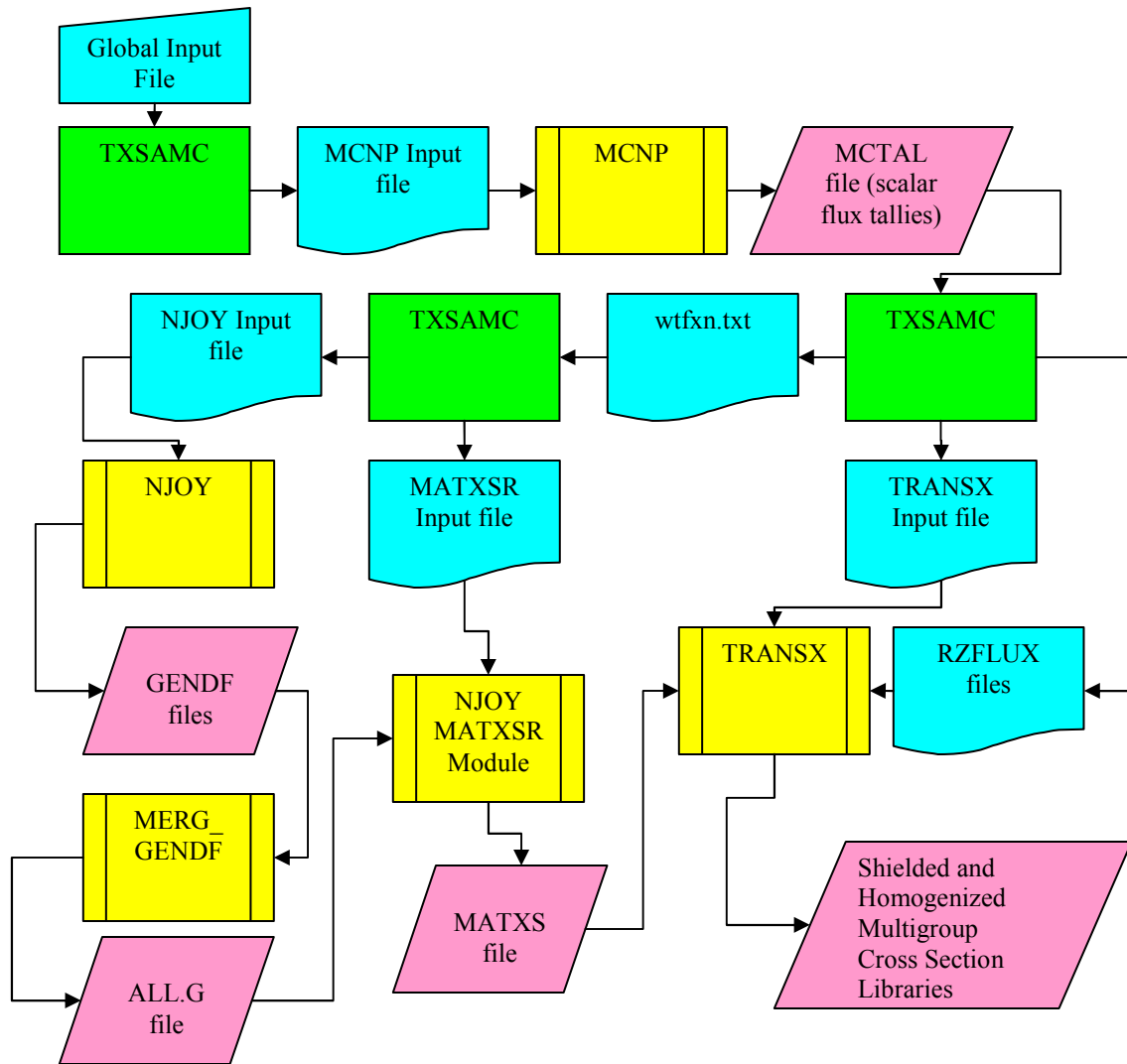


Fig. 2. TXSAMC process flowchart.

Blue denotes input files read or written by TXSAMC, green denotes processing performed by TXSAMC, yellow denotes execution of external codes and pink denotes data files output by the external codes

To summarize the process that TXSAMC implements: MCNP tallies core-averaged and region-averaged scalar fluxes by energy bin, NJOY uses the core-averaged spectrum to generate multigroup cross sections for each nuclide, and TRANSX employs

MCNP's region-averaged scalar fluxes and NJOY's cross sections to generate properly self-shielded and homogenized multigroup cross sections for each pin-cell type that was defined.

In this Chapter, we provide a general description of the input file (a detailed listing is shown in Appendix B), a description of the TXSAMC output and the code's major limitations and assumptions. (A detailed description of the code's processing is covered in Appendix A).

INPUT FILE

The TXSAMC input file is divided into four sections: a general section, an MCNP section, a NJOY section and a TRANSX section. The general section specifies the basepath variable which locates the data and executables to be used in the process. This variable currently requires the MCNP, NJOY, TRANSX and MERG_GENDF executables and the ENDF data to be located in very specific places. Future work may change this to allow these files to remain in their existing locations on the user's computer. The general section also specifies the problem title and the portions of TXSAMC that are to be used. It is possible to run each block (MCNP, NJOY and TRANSX) separately or to turn them all off so that only input files are written. Although there are certain applications for which only one block needs to be executed, this feature is mostly included for debugging; most applications of TXSAMC will require all three sections.

The MCNP section specifies everything needed to generate the MCNP input files for the problem. All length and thickness dimensions on the input file are specified in

cm. It begins with specification of the cross section directory file `xmdir` and the lattice type. The currently implemented logic allows two different lattice types: square or hexagonal but each of these can be used in either a realistic configuration (with a reactor vessel and vacuum boundaries) or a simple configuration (without a reactor vessel and with reflecting boundaries). This effectively allows the specification of four different reactor types. Following this, the input file also specifies the size of the lattice: number of pins on a side for the square lattice and number of pins tip-to-tip in a hex lattice. Currently, the code is limited to a 25x25 square lattice at its largest. This is not a fundamental limitation of MCNP but rather a limitation due to the way in which TXSAMC is able to write the MCNP input file. Future versions of TXSAMC will probably expand this. For both lattice types, only odd numbers of pins are allowed (1x1, 3x3, etc.). Again, this is a limitation due the way in which TXSAMC calculates vessel dimensions and lattice dimensions, not a fundamental MCNP limitation. The cell pitch, pin length, cladding thickness and pin diameter are specified for the base fuel pin. While the process allows as many as six different fuel pin-types, there is a base pin specified for every problem. The input file also specifies the vessel length and thickness.

We then specify the material, density and temperature of the vessel, coolant, cladding and fuel meat, respectively. While the process is flexible enough to handle almost any material that can be specified as a mixture of nuclides, there are only six materials programmed in at the current time (316L stainless steel, sodium, natural zirconium, uranium dioxide, aluminum and a silver-indium-cadmium mixture). Additional materials can be added by a quick modification of the Matter and Mixer

subroutines in TXSAMC. The next specifications on the input file are the fuel enrichment and the number of “other” cell-types. These cell-types can include coolant channels, control rods or fuel pins with different dimensions or enrichments than the base pin. For each cell-type, the input specifies the number of radial regions (not including the coolant), the MCNP “universe” number, the radius of each region, the material, density and temperature in each region, the enrichment (for fuel regions) and the number and location of this cell-type. The location is a series of x-y coordinates that are arranged according to the default layout in MCNP, as described in the manual.⁷⁻⁸

The final specifications on the MCNP input block are the number of particles per KCODE cycle, the number of active and inactive KCODE cycles and a flag to tally reaction rates in the reactor. The latter feature is not functional at this time and is an area for future work. At the bottom of the MCNP input block is a “map” of all of the lattice positions in the reactor. Because of the way MCNP defines the lattice, this map includes lattice positions that do not physically appear in the reactor or contain pin-cells. This map describes how to group the pins for the purposes of tallying the various fluxes needed for later processes. For each position in the map, there is a number 0-9; all positions with the same number are tallied together. Positions marked with a 0 are not tallied. TXSAMC is not currently capable of mixing different cell types in the same tally region; all positions marked by the same digit (other than a 0) must be of the same cell-type. This concludes the MCNP block of the input file.

The NJOY section specifies everything needed to process the cross sections. It begins with a specification of the number of nuclides in the problem, followed by a table

of nuclide names (i.e. “U235” for ^{235}U), material identification numbers (i.e. “9225” for ^{235}U), nuclide ZA’s (i.e. “92235” for ^{235}U), cross section types for each nuclide (this is based on the nuclide and controls special cross section calls in GROUPR like χ) and the ENDF tape labels for each nuclide. Also included is a marker for different regions; at the current time, this feature is not used and the marker may be omitted. Following this table, the number of temperatures for processing is specified. This is followed by a table listing each temperature, its corresponding suffix for multigroup MCNP processing and a tape number for the GROUPR output (this should begin at 44 and increase by one with each temperature). The suffix is used to distinguish the temperature of the produced cross sections. For example, the material cross section file 92235.50m has a suffix of “50” and would contain multigroup cross sections for ^{235}U at 500 K (a suffix of “80” equals 800 K and so forth).

The next part of the NJOY input is specification of the neutron group structure, number of neutron groups, photon group structure, number of photon groups and weighting function. The group structures and weight function use the standard terminology from NJOY’s GROUPR module. The next specifications on the input file are the number of Legendre tables and the number of background cross sections to be used in the process. This is followed by a list of the background cross sections. Finally, the input file specifies whether or not to run the THERMR module and the number of particle types and data types for the MATXSR module. This concludes the NJOY section of the input file.

The TRANSX section specifies all of the information needed to shield and homogenize the NJOY-processed cross sections. The block begins with specification of the output format for the cross sections, the problem type (direct or adjoint), the particle set to be processed, the order of the output (by material or energy group), any transport corrections and whether or not the cross sections will be collapsed into coarse groups. At the current time, TXSAMC does not directly support the group collapse of cross sections, so the latter option should remain turned off. Next, the source of the flux for weighting functions is specified: currently, TXSAMC only supports the library and RZFLUX options. The number of energy groups is again read in; this may seem redundant since this value has already been specified in the NJOY options section but it is needed if the group collapse option is ever implemented. The number of Legendre tables, the number of upscatter groups and the number of thermal groups are specified next. For the fast systems typically investigated by the TXSAMC process, the latter two numbers can usually be set to zero. The next item specified is the number of output mixtures. Since homogenization is desired, this number should be set to one. Following this, the number of special edit cross sections is specified along with a list of these edits and their weights. The heterogeneity option is also specified; if this number does not correspond with the lattice type in the MCNP section, TXSAMC will ask if the user wishes to overwrite it with the correct value. All of the options listed in this section use the same terminology and numbering as those listed in the TRANSX 2 manual.¹⁰ This concludes the TRANSX input block.

There is one small block at the bottom that controls the magnitude of the data written to the RZFLUX file during operation. The nominal reactor power and average v are specified here. After some testing, it was concluded that the absolute magnitude of the values on the RZFLUX file does not matter, so these options are extraneous. They are retained strictly for their potential in future areas of work with the code.

OUTPUT AND SUMMARY

The output file(s) of greatest importance from the TXSAMC process are the shielded and homogenized cross section files. Depending on the output format, these files can have different names. For ACEM formatted files, these files will be named “acemg8#” where the # is replaced by the index of the tally region. The other output files that may be of interest are the TRANSX output files (labeled “pincell8#.out” where the # is replaced by the index of the tally region), the output files for each of the NJOY runs and the MCNP output, as they collectively provide a pedigree for the cross sections in question. It is important that the user realize that the produced cross sections are not perfect. As will be shown in the next chapter, while the overall error in the cross sections may be fairly small, certain cross sections may have significant error. The cross sections should only be applied to the problem for which they were generated and as much as possible, the user should make careful choices in the options chosen for each of the underlying codes to reduce errors and assumptions. For example, the user should keep the tally regions to the minimum needed to characterize the problem well, because statistical error increases in smaller tally regions. The user should also try to avoid modeling reactors with very short pins to minimize the error in TRANSX calculations of

the Dancoff factor. Above all, the user should take care not to use the TXSAMC code to model reactors and systems for which it is ill-suited. If the structure of a real reactor is not very similar to the existing capabilities of this code, the resulting cross sections will represent the TXSAMC model, not the real reactor.

Finally, the TXSAMC code should be viewed as a prototype. There are a number of modifications that can be made to the code to increase its practical use. These include, but are not limited to: porting the code to UNIX/Linux systems, adding more material options, adding more reactor features such as a reflector or a power conversion system to the MCNP model, adding tallies to the MCNP portion so that reaction rate comparisons such as those in Chapter IV can be made more easily and allowing larger reactors. It should also be noted that there are a number of improvements that could be made in the software engineering. These include but are not limited to: modifying the section of the code that reads the MCTAL file to use formatted reads with implied DO loops, and not using a scratch file to convert from character to integer and vice versa. There are also additions that need to be made to make sure that output cross section files from TRANSX for each tally region do not overwrite each other. This has been done for ACEM formatted output but not other output types.

CHAPTER IV

NUMERICAL RESULTS

In this chapter, we present the results of the TXSAMC process on five test cases. In order to measure the accuracy of the multigroup cross sections generated by TXSAMC, we must create some method of testing the cross sections. The method used here is a comparison of five principal reaction rates within the cells of interest: fission, (n,2n), neutron emission by fission (nusigf), absorption and total interactions. These five reactions were chosen because they are the key reactions for determining neutron production and destruction in the system which drive many of the quantities of interest for reactors including criticality, leakage and energy deposition. By comparing the reaction rate that is generated by the TRANSX cross sections to that measured directly through the use of reaction-rate tallies in MCNP, we obtain an estimate of the error produced by the process and embodied in the cross sections. In order to generate reaction rates from multigroup cross sections, a scalar flux is needed. We generated the necessary scalar flux data from F4 tallies (path-length estimator of the scalar flux) in MCNP. Since both the reaction rate tallies and the scalar flux tallies in MCNP are generated from the same track-length estimator of the scalar flux and the same random number sequence, they will have the same standard deviation and implied mean (the value of the scalar flux over the same energy group). Since the reaction rate tally uses the reference continuous-energy cross sections to calculate the reaction rates, any difference between the TXSAMC reaction rate and the MCNP reaction rate comes from the TXSAMC process rather than statistical fluctuations. Given reactions whose MCNP tallies are as

statistically precise as the scalar-flux tallies, the reaction-rate difference is a quantitative indicator of the error introduced by the TXSAMC process. However, when MCNP samples a reaction more poorly than it samples the scalar flux, reaction-rate differences do not necessarily indicate errors caused by TXSAMC. This can happen with threshold reactions, for example, in the energy bin that contains the threshold. In this bin, fewer particle tracks contribute to the threshold-reaction tally than to the scalar-flux tally. Thus, for threshold reactions the MCNP reaction-rate estimate will in general have a larger standard deviation than the scalar-flux estimate. This can happen to some extent in any energy bin containing a rapidly varying cross section (as in the resonance region). This raises the possibility that the TXSAMC reaction rate could be more accurate than the MCNP rate. We should keep this in mind when comparing MCNP and TXSAMC results below.

For each test case, the TXSAMC process was used to generate multigroup cross sections for each region in the problem. For all five test cases, only 30 group cross sections were generated. In the first two test cases, the cross sections were generated for only one type of pin-cell. In the last three test cases, cross sections for multiple pin-cell types and locations were generated. This allows us to evaluate the suitability of using TXSAMC for different reactor problems and to gain some understanding of the overall limitations of the process. The fourth test case was created to test the effect of finer weighting functions in NJOY. The test cases are labeled Square-Simple Reactor (SSR), Hex-Simple Reactor (HSR), Square-Complex Reactor (SCR), Square-Complex Reactor Alternate (SCRA) and Hex-Complex Reactor (HCR), respectively.

SQUARE-SIMPLE REACTOR

This reactor is modeled as a 23x23 square lattice with each cell containing a fuel pin and sodium coolant. The pin is composed of a 10% enriched UO_2 meat and a zirconium cladding that is 29.8 cm long. The cladding is at a reduced density of 2.7 g/cc. The lattice is bounded on all six sides by a reflecting boundary which results in the reactor being almost equivalent to a square pin-cell in an infinite lattice. The difference is that just inside the reflecting reactor boundary is a thin layer of coolant which is inserted to avoid direct surface overlap between the lattice pin-cell boundaries and the reactor boundary. Without this slight adjustment, errors occur in the MCNP portion of TXSAMC. The results of this test problem are shielded and homogenized multigroup cross sections for a single pin-cell. Since all of the pin-cells are identical in composition and, thanks to the reflecting reactor boundaries, identical in location, the various tallies in MCNP are performed over all of the pin-cells and normalized by the volume of all of the pin-cells. The reactor is slightly supercritical ($k_{\text{eff}} \sim 1.06$) and is run in a warm state; the fuel temperature is 800 K. The basic dimensions, materials and temperatures for the Square-Simple Reactor (SSR) are described in Table 5. The reactor layout can be seen in Fig. 3.

TABLE 5
Description of materials, geometry and temperatures in SSR

| | |
|--------------------------------------|-------------------|
| Reactor Label | SSR |
| Lattice Type | Square |
| Matrix Size | 23x23 |
| Pitch | 2.1 cm |
| | |
| Vessel Length | N/A |
| Vessel Thickness | N/A |
| Vessel Material | N/A |
| Vessel Temperature | N/A |
| Vessel Density | N/A |
| | |
| Coolant Material | Sodium |
| Coolant Temperature | 450 K |
| Coolant Density | 2.0 g/cc |
| | |
| Pin Length | 29.8 cm |
| Pin Diameter | 2.0 cm |
| Cladding Thickness | 0.1 cm |
| Cladding Material | Natural Zirconium |
| Cladding Temperature | 600 K |
| Cladding Density | 2.7 g/cc |
| Fuel Length | 29.8 cm |
| Fuel Diameter | 1.8 cm |
| Fuel Material | Uranium Dioxide |
| Enrichment | 10% |
| Fuel Temperature | 800 K |
| Fuel Density | 10.5 g/cc |
| | |
| Number of Control Rods | 0 |
| Number of Coolant Channels | 0 |
| | |
| Number of kcode cycles | 210 |
| Number of inactive cycles | 10 |
| Number of particles per cycle | 5000 |
| Number of histories | 1000000 |
| keff | 1.06058 |

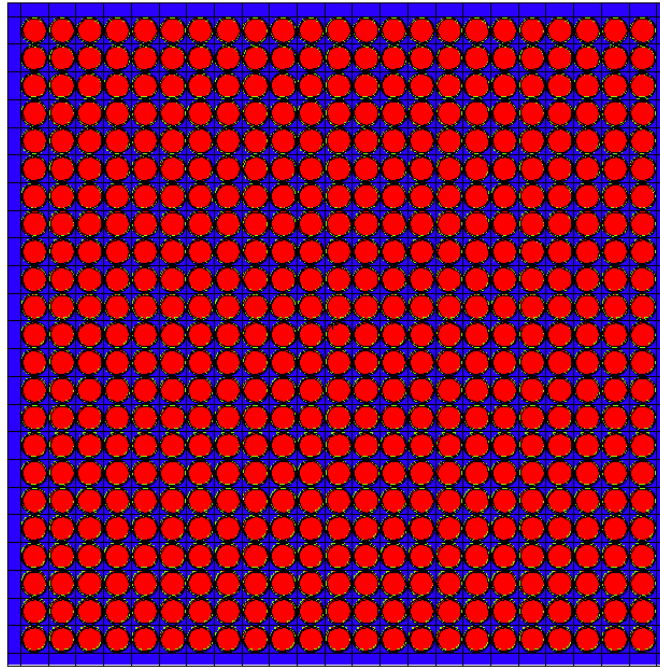


Fig. 3. SSR layout in x-y plane.
Red denotes fuel rods, blue is coolant.

For this problem, the weighting function used to weight the initial cross sections in TXSAMC (GROUPE module of NJOY) is the core-averaged scalar flux as tallied by MCNP. To finish the shielding process and homogenize the pin-cell, the scalar flux is tallied over each region within the pin-cell: fuel meat, cladding and coolant. From these three tallies, the needed RZFLUX files are derived. The multiplying flux for the TRANSX cross sections is the core-averaged scalar flux. Table 6 shows the MCNP-tallied scalar flux for the pin-cell, its relative standard deviation, the TXSAMC-generated cross sections and the TXSAMC-generated reaction rate densities for the 30 group problem. Table 7 shows the MCNP-tallied reaction rate densities, their standard deviations and the partial percent error between the TXSAMC-generated reaction rates and the MCNP-tallied reaction rates. This is calculated by equation (9):

$$\text{Partial \% Error} = \frac{(\text{TXSAMC RRD}_g - \text{MCNP RRD}_g)}{\text{MCNP RRD}_g} * 100\% * \frac{\text{MCNP RRD}_g}{\text{Total MCNP RRD}} \quad (9)$$

TABLE 6
30 group MCNP scalar flux, TXSAMC cross sections and reaction rates in SSR

| Energy Group | Scalar Flux (n/cm ² /nps) | Rel. Error (1 σ) | TXSAMC SIGMA (cm ⁻¹) | | | | | TXSAMC RRD (cm ⁻³) | | | | |
|--------------|--------------------------------------|------------------|----------------------------------|----------|----------|----------|----------|--------------------------------|----------|----------|----------|----------|
| | | | fission | nusigf | n2n | abs-fis | total | fission | nusigf | n2n | abs-fis | total |
| 1 | 0.00E+00 | 0.00% | 3.20E-01 | 7.80E-01 | 0.00E+00 | 7.48E-02 | 7.00E-01 | 0.00E+00 | 0.00E+00 | 0.00E+00 | 0.00E+00 | 0.00E+00 |
| 2 | 0.00E+00 | 0.00% | 2.29E-01 | 5.59E-01 | 0.00E+00 | 6.17E-02 | 5.94E-01 | 0.00E+00 | 0.00E+00 | 0.00E+00 | 0.00E+00 | 0.00E+00 |
| 3 | 0.00E+00 | 0.00% | 9.55E-02 | 2.33E-01 | 0.00E+00 | 2.21E-02 | 4.17E-01 | 0.00E+00 | 0.00E+00 | 0.00E+00 | 0.00E+00 | 0.00E+00 |
| 4 | 0.00E+00 | 0.00% | 2.66E-02 | 6.48E-02 | 0.00E+00 | 1.72E-02 | 3.38E-01 | 0.00E+00 | 0.00E+00 | 0.00E+00 | 0.00E+00 | 0.00E+00 |
| 5 | 0.00E+00 | 0.00% | 2.25E-02 | 5.47E-02 | 0.00E+00 | 9.03E-02 | 4.01E-01 | 0.00E+00 | 0.00E+00 | 0.00E+00 | 0.00E+00 | 0.00E+00 |
| 6 | 2.60E-10 | 42.56% | 4.33E-02 | 1.05E-01 | 0.00E+00 | 1.57E-01 | 5.42E-01 | 1.12E-11 | 2.74E-11 | 0.00E+00 | 4.09E-11 | 1.41E-10 |
| 7 | 3.01E-08 | 6.54% | 5.61E-02 | 1.36E-01 | 0.00E+00 | 2.89E-02 | 3.98E-01 | 1.69E-09 | 4.10E-09 | 0.00E+00 | 8.69E-10 | 1.20E-08 |
| 8 | 6.48E-07 | 1.59% | 2.58E-02 | 6.28E-02 | 0.00E+00 | 3.33E-02 | 3.83E-01 | 1.67E-08 | 4.07E-08 | 0.00E+00 | 2.16E-08 | 2.48E-07 |
| 9 | 6.56E-06 | 0.54% | 1.90E-02 | 4.62E-02 | 0.00E+00 | 2.11E-02 | 3.76E-01 | 1.25E-07 | 3.03E-07 | 0.00E+00 | 1.38E-07 | 2.47E-06 |
| 10 | 3.48E-05 | 0.23% | 1.28E-02 | 3.12E-02 | 0.00E+00 | 1.93E-02 | 3.65E-01 | 4.46E-07 | 1.08E-06 | 0.00E+00 | 6.72E-07 | 1.27E-05 |
| 11 | 4.35E-05 | 0.15% | 7.69E-03 | 1.87E-02 | 0.00E+00 | 1.36E-02 | 6.15E-01 | 3.34E-07 | 8.14E-07 | 0.00E+00 | 5.89E-07 | 2.67E-05 |
| 12 | 9.91E-05 | 0.10% | 4.99E-03 | 1.21E-02 | 0.00E+00 | 1.01E-02 | 4.52E-01 | 4.95E-07 | 1.20E-06 | 0.00E+00 | 1.00E-06 | 4.48E-05 |
| 13 | 2.22E-04 | 0.06% | 3.45E-03 | 8.39E-03 | 0.00E+00 | 8.05E-03 | 3.80E-01 | 7.65E-07 | 1.86E-06 | 0.00E+00 | 1.79E-06 | 8.43E-05 |
| 14 | 3.18E-04 | 0.05% | 2.59E-03 | 6.29E-03 | 0.00E+00 | 5.24E-03 | 3.69E-01 | 8.25E-07 | 2.00E-06 | 0.00E+00 | 1.67E-06 | 1.17E-04 |
| 15 | 4.02E-04 | 0.05% | 2.06E-03 | 5.01E-03 | 0.00E+00 | 2.65E-03 | 3.32E-01 | 8.26E-07 | 2.01E-06 | 0.00E+00 | 1.07E-06 | 1.33E-04 |
| 16 | 1.93E-04 | 0.08% | 1.77E-03 | 4.34E-03 | 0.00E+00 | 1.88E-03 | 3.15E-01 | 3.41E-07 | 8.36E-07 | 0.00E+00 | 3.63E-07 | 6.08E-05 |
| 17 | 1.49E-04 | 0.09% | 1.62E-03 | 4.01E-03 | 0.00E+00 | 1.66E-03 | 3.56E-01 | 2.43E-07 | 5.99E-07 | 0.00E+00 | 2.49E-07 | 5.32E-05 |
| 18 | 1.64E-04 | 0.12% | 1.54E-03 | 3.84E-03 | 0.00E+00 | 1.62E-03 | 2.82E-01 | 2.52E-07 | 6.28E-07 | 0.00E+00 | 2.66E-07 | 4.62E-05 |
| 19 | 8.78E-05 | 0.16% | 1.94E-03 | 4.94E-03 | 0.00E+00 | 1.56E-03 | 2.76E-01 | 1.71E-07 | 4.34E-07 | 0.00E+00 | 1.37E-07 | 2.43E-05 |
| 20 | 4.32E-05 | 0.24% | 5.84E-03 | 1.52E-02 | 0.00E+00 | 9.86E-04 | 2.07E-01 | 2.53E-07 | 6.57E-07 | 0.00E+00 | 4.26E-07 | 8.93E-06 |
| 21 | 3.52E-05 | 0.27% | 7.96E-03 | 2.10E-02 | 0.00E+00 | 6.99E-04 | 1.98E-01 | 2.80E-07 | 7.39E-07 | 0.00E+00 | 2.46E-07 | 6.98E-06 |
| 22 | 3.48E-05 | 0.29% | 8.27E-03 | 2.22E-02 | 0.00E+00 | 4.27E-04 | 1.80E-01 | 2.88E-07 | 7.72E-07 | 0.00E+00 | 1.49E-07 | 6.26E-06 |
| 23 | 2.16E-05 | 0.35% | 8.07E-03 | 2.23E-02 | 0.00E+00 | 2.79E-04 | 2.11E-01 | 1.74E-07 | 4.82E-07 | 0.00E+00 | 6.02E-07 | 4.55E-06 |
| 24 | 2.20E-05 | 0.38% | 8.27E-03 | 2.48E-02 | 1.10E-05 | 2.06E-03 | 1.95E-01 | 1.82E-07 | 5.46E-07 | 2.42E-10 | 4.54E-08 | 4.28E-06 |
| 25 | 3.33E-06 | 0.95% | 1.25E-02 | 4.21E-02 | 4.16E-03 | 3.18E-04 | 1.59E-01 | 4.16E-08 | 1.40E-07 | 1.38E-08 | 1.06E-09 | 5.29E-07 |
| 26 | 9.88E-07 | 1.72% | 1.47E-02 | 5.36E-02 | 1.60E-02 | 0.00E+00 | 1.53E-01 | 1.46E-08 | 5.29E-08 | 1.58E-08 | 0.00E+00 | 1.51E-07 |
| 27 | 1.73E-07 | 3.92% | 1.45E-02 | 5.74E-02 | 2.01E-02 | 0.00E+00 | 1.54E-01 | 2.51E-09 | 9.93E-09 | 3.47E-09 | 0.00E+00 | 2.66E-08 |
| 28 | 3.38E-08 | 8.58% | 1.50E-02 | 6.36E-02 | 1.92E-02 | 0.00E+00 | 1.58E-01 | 5.07E-10 | 2.15E-09 | 6.48E-10 | 0.00E+00 | 5.32E-09 |
| 29 | 9.59E-09 | 15.17% | 1.65E-02 | 7.34E-02 | 1.35E-02 | 0.00E+00 | 1.59E-01 | 1.58E-10 | 7.04E-10 | 1.30E-10 | 0.00E+00 | 1.53E-09 |
| 30 | 3.40E-09 | 28.49% | 1.78E-02 | 8.29E-02 | 1.04E-02 | 0.00E+00 | 1.61E-01 | 6.04E-11 | 2.82E-10 | 3.53E-11 | 0.00E+00 | 5.48E-10 |
| Total | 1.88E-03 | 0.03% | 1.01E+00 | 2.62E+00 | 8.33E-02 | 5.77E-01 | 9.82E+00 | 6.08E-06 | 1.52E-05 | 3.42E-08 | 8.09E-06 | 6.38E-04 |

TABLE 7
30 group MCNP reaction rates and reaction rate comparison in SSR

| Energy | MCNP RRD (cm ⁻³) | | | | | MCNP Standard Deviation | | | | | Partial Percent Error (TXSAMC-MCNP)/MCNP | | | | | |
|--------|------------------------------|----------|----------|----------|----------|-------------------------|---------|--------|--------|---------|--|---------|--------|--------|---------|--------|
| | Group | fission | nusigf | n2n | abs-fis | total | fission | nusigf | n2n | abs-fis | total | fission | nusigf | n2n | abs-fis | total |
| 1 | 0.00E+00 | 0.00E+00 | 0.00E+00 | 0.00E+00 | 0.00E+00 | 0.00E+00 | N/A | N/A | N/A | N/A | N/A | N/A | N/A | N/A | N/A | N/A |
| 2 | 0.00E+00 | 0.00E+00 | 0.00E+00 | 0.00E+00 | 0.00E+00 | 0.00E+00 | N/A | N/A | N/A | N/A | N/A | N/A | N/A | N/A | N/A | N/A |
| 3 | 0.00E+00 | 0.00E+00 | 0.00E+00 | 0.00E+00 | 0.00E+00 | 0.00E+00 | N/A | N/A | N/A | N/A | N/A | N/A | N/A | N/A | N/A | N/A |
| 4 | 0.00E+00 | 0.00E+00 | 0.00E+00 | 0.00E+00 | 0.00E+00 | 0.00E+00 | N/A | N/A | N/A | N/A | N/A | N/A | N/A | N/A | N/A | N/A |
| 5 | 0.00E+00 | 0.00E+00 | 0.00E+00 | 0.00E+00 | 0.00E+00 | 0.00E+00 | N/A | N/A | N/A | N/A | N/A | N/A | N/A | N/A | N/A | N/A |
| 6 | 1.26E-11 | 3.06E-11 | 0.00E+00 | 2.86E-11 | 1.28E-10 | 73.60% | 73.60% | N/A | 49.24% | 38.52% | 0.00% | 0.00% | N/A | 0.00% | 0.00% | 0.00% |
| 7 | 1.56E-09 | 3.80E-09 | 0.00E+00 | 1.22E-09 | 1.29E-08 | 6.37% | 6.37% | N/A | 7.83% | 5.60% | 0.00% | 0.00% | N/A | 0.00% | 0.00% | 0.00% |
| 8 | 1.73E-08 | 4.20E-08 | 0.00E+00 | 2.37E-08 | 2.56E-07 | 1.65% | 1.65% | N/A | 1.75% | 1.33% | -0.01% | -0.01% | N/A | -0.03% | 0.00% | 0.00% |
| 9 | 1.30E-07 | 3.18E-07 | 0.00E+00 | 1.53E-07 | 2.53E-06 | 0.57% | 0.57% | N/A | 0.59% | 0.45% | -0.10% | -0.09% | N/A | -0.18% | -0.01% | -0.01% |
| 10 | 4.51E-07 | 1.10E-06 | 0.00E+00 | 7.06E-07 | 1.29E-05 | 0.24% | 0.24% | N/A | 0.25% | 0.18% | -0.08% | -0.08% | N/A | -0.41% | -0.03% | -0.03% |
| 11 | 3.64E-07 | 8.87E-07 | 0.00E+00 | 6.48E-07 | 2.70E-05 | 0.16% | 0.16% | N/A | 0.17% | 0.10% | -0.49% | -0.48% | N/A | -0.71% | -0.05% | -0.05% |
| 12 | 4.83E-07 | 1.17E-06 | 0.00E+00 | 1.03E-06 | 4.60E-05 | 0.10% | 0.10% | N/A | 0.11% | 0.07% | 0.20% | 0.19% | N/A | -0.41% | -0.18% | -0.18% |
| 13 | 7.68E-07 | 1.87E-06 | 0.00E+00 | 1.81E-06 | 8.51E-05 | 0.06% | 0.06% | N/A | 0.06% | 0.05% | -0.05% | -0.05% | N/A | -0.26% | -0.14% | -0.14% |
| 14 | 8.28E-07 | 2.01E-06 | 0.00E+00 | 1.69E-06 | 1.18E-04 | 0.05% | 0.05% | N/A | 0.05% | 0.04% | -0.05% | -0.04% | N/A | -0.32% | -0.08% | -0.08% |
| 15 | 8.26E-07 | 2.01E-06 | 0.00E+00 | 1.07E-06 | 1.33E-04 | 0.05% | 0.05% | N/A | 0.05% | 0.04% | 0.01% | 0.01% | N/A | -0.03% | -0.03% | -0.03% |
| 16 | 3.40E-07 | 8.34E-07 | 0.00E+00 | 3.62E-07 | 6.06E-05 | 0.08% | 0.08% | N/A | 0.08% | 0.06% | 0.01% | 0.01% | N/A | 0.01% | 0.03% | 0.03% |
| 17 | 2.43E-07 | 5.99E-07 | 0.00E+00 | 2.49E-07 | 5.37E-05 | 0.09% | 0.09% | N/A | 0.09% | 0.07% | 0.00% | 0.00% | N/A | 0.00% | -0.08% | -0.08% |
| 18 | 2.52E-07 | 6.28E-07 | 0.00E+00 | 2.65E-07 | 4.64E-05 | 0.12% | 0.12% | N/A | 0.12% | 0.09% | 0.00% | 0.00% | N/A | 0.01% | -0.04% | -0.04% |
| 19 | 1.72E-07 | 4.37E-07 | 0.00E+00 | 1.35E-07 | 2.41E-05 | 0.16% | 0.16% | N/A | 0.16% | 0.12% | -0.02% | -0.02% | N/A | 0.02% | 0.03% | 0.03% |
| 20 | 2.51E-07 | 6.52E-07 | 0.00E+00 | 4.28E-08 | 8.94E-06 | 0.24% | 0.24% | N/A | 0.23% | 0.19% | 0.03% | 0.03% | N/A | 0.00% | 0.00% | 0.00% |
| 21 | 2.80E-07 | 7.39E-07 | 0.00E+00 | 2.46E-08 | 6.99E-06 | 0.27% | 0.27% | N/A | 0.26% | 0.21% | 0.00% | 0.00% | N/A | 0.00% | 0.00% | 0.00% |
| 22 | 2.88E-07 | 7.71E-07 | 0.00E+00 | 1.50E-08 | 6.25E-06 | 0.29% | 0.29% | N/A | 0.28% | 0.22% | 0.00% | 0.00% | N/A | 0.00% | 0.00% | 0.00% |
| 23 | 1.74E-07 | 4.82E-07 | 0.00E+00 | 6.02E-09 | 4.54E-06 | 0.35% | 0.35% | N/A | 0.33% | 0.29% | 0.00% | 0.00% | N/A | 0.00% | 0.00% | 0.00% |
| 24 | 1.82E-07 | 5.48E-07 | 2.47E-10 | 4.56E-08 | 4.27E-06 | 0.38% | 0.38% | 1.22% | 0.45% | 0.30% | 0.00% | -0.01% | -0.01% | 0.00% | 0.00% | 0.00% |
| 25 | 4.14E-08 | 1.39E-07 | 1.34E-08 | 1.47E-08 | 5.29E-07 | 0.96% | 0.96% | 1.27% | 0.89% | 0.75% | 0.00% | 0.00% | 1.22% | -0.16% | 0.00% | 0.00% |
| 26 | 1.45E-08 | 5.28E-08 | 1.58E-08 | 5.72E-09 | 1.51E-07 | 1.71% | 1.71% | 1.69% | 1.38% | 1.36% | 0.00% | 0.00% | 0.05% | -0.07% | 0.00% | 0.00% |
| 27 | 2.50E-09 | 9.90E-09 | 3.46E-09 | 1.75E-09 | 2.66E-08 | 3.93% | 3.93% | 3.72% | 3.01% | 3.13% | 0.00% | 0.00% | 0.02% | -0.02% | 0.00% | 0.00% |
| 28 | 4.99E-10 | 2.11E-09 | 6.42E-10 | 3.18E-10 | 5.28E-09 | 8.58% | 8.59% | 7.85% | 6.32% | 6.83% | 0.00% | 0.00% | 0.02% | 0.00% | 0.00% | 0.00% |
| 29 | 1.68E-10 | 7.47E-10 | 1.36E-10 | 8.53E-11 | 1.58E-09 | 15.47% | 15.49% | 13.09% | 11.56% | 12.64% | 0.00% | 0.00% | -0.02% | 0.00% | 0.00% | 0.00% |
| 30 | 6.23E-11 | 2.92E-10 | 3.56E-11 | 2.58E-11 | 5.53E-10 | 29.38% | 29.41% | 19.94% | 21.25% | 23.69% | 0.00% | 0.00% | 0.00% | 0.00% | 0.00% | 0.00% |
| Total | 6.11E-06 | 1.53E-05 | 3.37E-08 | 8.30E-06 | 6.42E-04 | 0.04% | 0.05% | 1.07% | 0.05% | 0.02% | -0.52% | -0.51% | 1.28% | -2.58% | -0.58% | -0.58% |

It should be noted that the group structures listed in the above tables are in ascending order by energy. Energy group 1 has the lowest energy; group 30 has the highest energy. The bounds of each energy group are shown in Table 8.

TABLE 8
Energy structure for weight function

| Group | Upper Bound (MeV) |
|-------|-------------------|
| 1 | 1.520E-07 |
| 2 | 4.140E-07 |
| 3 | 1.130E-06 |
| 4 | 3.060E-06 |
| 5 | 8.320E-06 |
| 6 | 2.260E-05 |
| 7 | 6.140E-05 |
| 8 | 1.670E-04 |
| 9 | 4.540E-04 |
| 10 | 1.235E-03 |
| 11 | 3.350E-03 |
| 12 | 9.120E-03 |
| 13 | 2.480E-02 |
| 14 | 6.760E-02 |
| 15 | 1.840E-01 |
| 16 | 3.030E-01 |
| 17 | 5.000E-01 |
| 18 | 8.230E-01 |
| 19 | 1.353E+00 |
| 20 | 1.738E+00 |
| 21 | 2.232E+00 |
| 22 | 2.865E+00 |
| 23 | 3.680E+00 |
| 24 | 6.070E+00 |
| 25 | 7.790E+00 |
| 26 | 1.000E+01 |
| 27 | 1.200E+01 |
| 28 | 1.350E+01 |
| 29 | 1.500E+01 |
| 30 | 1.700E+01 |

From the tallied scalar flux data in Table 6, it is clear that the SSR is a very fast system since there are no flux tallies below the 6th energy group which corresponds to the 8-22 eV range. This is expected given the very weak moderating effects of liquid sodium and the lack of any other moderator within the system.

The zeros in the TXSAMC non-fission absorption cross section at high energy do not reflect a complete lack of non-fission absorption reactions at high energies but are an artifact of the TRANSX cross section production process. Since the comparison tests

used to validate the multigroup cross sections are based on MCNP tallies, the TXSAMC/TRANSX produced cross sections were written in ACEM (MCNP readable) format. Due to the way TRANSX handles neutron balance, the non-fission absorption cross section is “corrected” to remove neutron production reactions like (n,2n) which typically occur at high energies, and thus is really a “net capture” cross section. This cross section can be negative, for example when the (n,2n) cross section is larger than the (n, γ) cross section. When it is negative, TRANSX sets it to zero¹⁰. When TXSAMC is used to generate cross sections for deterministic codes, it will employ a different TRANSX option that will not have this artifact.

The data in Table 7 suggest that the cross sections produced by TXSAMC reproduce most reaction rates in the pin cells. (Total reaction rates, summed over all energy groups, are shown in the bottom line of each table.) For the fission and nusigf reaction rate density (RRD), the code reproduces the total RRD for each reaction to within half of a percent. The greatest partial percent error in any group for any reaction is less than 10.5%. The vast majority of the groups have an error of less than one percent. As expected, the nusigf and fission RRD’s have the same percent error relative to their benchmarks. Part of the low percent error in these reaction rates is attributable to the non-threshold nature of the reactions and the very good statistics that this implies in each energy group. The total interaction RRD mirrors the fission RRD in the level of its error. This is expected given the dominant fission cross section in the system and the lack of any serious scattering reactions. Given that the overall error in the reproduction of the reaction rates is in the few-percent range, it seems reasonable to conclude that

TXSAMC is capable of appropriately shielding and homogenizing cross sections for a simple, square infinite lattice problem. The process may not provide enough fidelity to do final design work but this would seem to be a good basis for preliminary studies and for answering questions that cannot be solved on the back of an envelope.

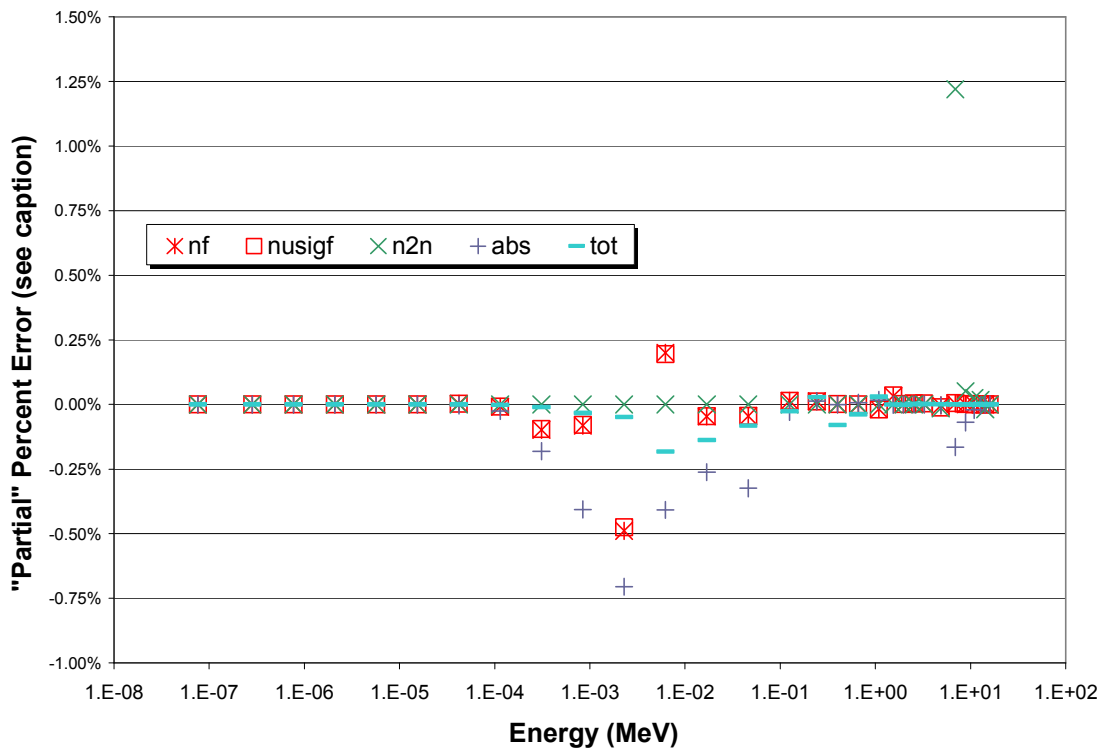


Fig. 4. "Partial" percent errors in each energy group for reaction-rate densities in SSR. Each "partial" error is plotted at the midpoint energy of its group. The percent error in a given reaction rate is the sum of the 30 partial percent errors.

In Fig. 4 we see the difference in the TXSAMC and MCNP RRD's for the reactor displayed graphically. The very low errors in the low energy range are quite obvious in this plot as well as the general accuracy of the cross sections at mid-to-high

energy range groups with the largest error in any group being less than one and a half percent. Most of the error in the mid-range is less than one half percent. Since these higher energy groups are generally more important for determining the overall RRD in the cell, this leads to a rather minimal overall error in the cell. For all of the reactions, the error appears to be very reasonable for this test case.

HEX-SIMPLE REACTOR

This reactor is modeled as a regular hexagonal lattice with 23 pins along the x-axis with each cell containing a fuel pin and sodium coolant. The pin is composed of a 10% enriched UO₂ meat and a zirconium cladding (at a reduced density of 2.7 g/cc) that is 29.8 cm long. The lattice is bounded on all eight sides (six planes perpendicular to the x-y plane and two planes perpendicular to the z-axis) by a reflecting boundary which results in the reactor being almost equivalent to a hexagonal pin-cell in an infinite lattice. The difference is that just inside the reflecting reactor boundary is a thin layer of coolant, which is inserted to avoid direct surface overlap between the lattice pin-cell boundaries and the reactor boundary. Without this slight adjustment, errors occur in the MCNP portion of TXSAMC. The results of this test problem are shielded and homogenized multigroup cross sections for a single pin-cell. The reactor is slightly supercritical ($k_{\text{eff}} \sim 1.07$). Since all of the pin-cells are identical in composition and, thanks to the reflecting reactor boundaries, identical in location, the various tallies in MCNP are performed over all of the pin-cells and normalized by the volume of all of the pin-cells. The basic dimensions, materials and temperatures for the Hex-Simple Reactor (HSR) are described in Table 9. The HSR layout can be seen in Fig. 5.

TABLE 9
Description of materials, geometry and temperatures in HSR

| | |
|--------------------------------------|-------------------|
| Reactor Label | HSR |
| Lattice Type | Hexagonal |
| Rows Along Diagonal | 23 |
| Pitch | 2.1 cm |
| Vessel Length | N/A |
| Vessel Thickness | N/A |
| Vessel Material | N/A |
| Vessel Temperature | N/A |
| Vessel Density | N/A |
| Coolant Material | Sodium |
| Coolant Temperature | 450 K |
| Coolant Density | 2.0 g/cc |
| Pin Length | 29.8 |
| Pin Diameter | 2.0 cm |
| Cladding Thickness | 0.1 cm |
| Cladding Material | Natural Zirconium |
| Cladding Temperature | 600 K |
| Cladding Density | 2.7 g/cc |
| Fuel Length | 29.8 cm |
| Fuel Diameter | 1.8 cm |
| Fuel Material | Uranium Dioxide |
| Enrichment | 10% |
| Fuel Temperature | 800 K |
| Fuel Density | 10.5 g/cc |
| Number of Control Rods | 0 |
| Number of Coolant Channels | 0 |
| Number of kcode cycles | 210 |
| Number of inactive cycles | 10 |
| Number of particles per cycle | 5000 |
| Number of histories | 1000000 |
| keff | 1.07708 |

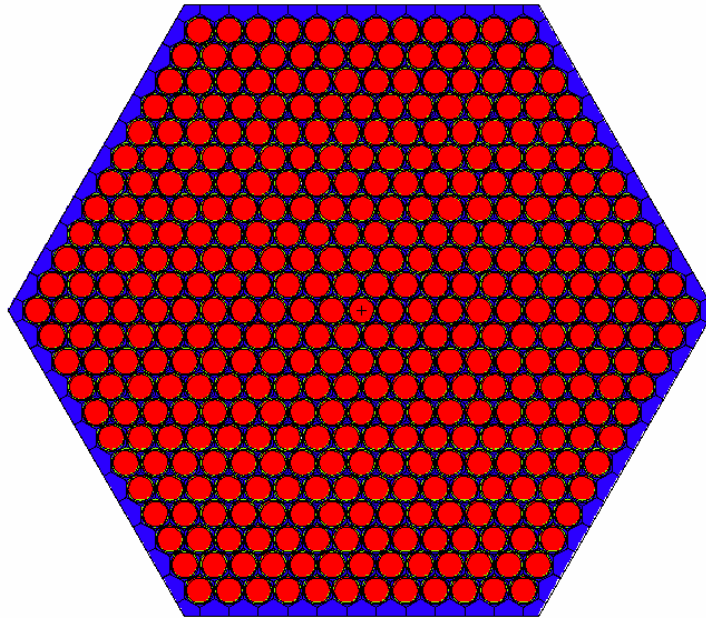


Fig. 5. HSR layout in x-y plane.
Red denotes fuel rods, blue denotes coolant.

For this problem, the weighting function used to weight the initial cross sections in TXSAMC (GROUPR module of NJOY) is the core-averaged scalar flux as tallied by MCNP. To finish the shielding process and homogenize the pin-cell, the scalar flux is tallied over each region within the pin-cell: fuel meat, cladding and coolant. From these three tallies, the needed RZFLUX files are derived. The multiplying flux for the TRANSX cross sections is the core-averaged scalar flux. Table 10 shows the MCNP-tallied scalar flux for the pin-cell, its relative standard deviation, the TXSAMC-generated cross sections and the TXSAMC-generated reaction rate densities for the 30 group HSR problem. Table 11 shows the MCNP-tallied reaction rate densities, their

standard deviations and the partial percent error between the TXSAMC-generated reaction rates and the MCNP-tallied reaction rates for the 30 group HSR problem.

TABLE 10
30 group MCNP scalar flux, TXSAMC cross sections and reaction rates in HSR

| Energy Group | Scalar Flux (n/cm ² /nps) | Rel. Error (1 σ) | TXSAMC SIGMA (cm ⁻¹) | | | | | TXSAMC RRD (cm ⁻³) | | | | |
|--------------|--------------------------------------|--------------------------|----------------------------------|----------|----------|----------|----------|--------------------------------|----------|----------|----------|----------|
| | | | fission | nusigf | n2n | abs-fis | total | fission | nusigf | n2n | abs-fis | total |
| 1 | 0.00E+00 | 0.00% | 3.70E-01 | 9.01E-01 | 0.00E+00 | 8.44E-02 | 7.80E-01 | 0.00E+00 | 0.00E+00 | 0.00E+00 | 0.00E+00 | 0.00E+00 |
| 2 | 0.00E+00 | 0.00% | 2.65E-01 | 6.45E-01 | 0.00E+00 | 6.99E-02 | 6.58E-01 | 0.00E+00 | 0.00E+00 | 0.00E+00 | 0.00E+00 | 0.00E+00 |
| 3 | 0.00E+00 | 0.00% | 1.10E-01 | 2.69E-01 | 0.00E+00 | 2.47E-02 | 4.55E-01 | 0.00E+00 | 0.00E+00 | 0.00E+00 | 0.00E+00 | 0.00E+00 |
| 4 | 0.00E+00 | 0.00% | 3.08E-02 | 7.51E-02 | 0.00E+00 | 1.94E-02 | 3.64E-01 | 0.00E+00 | 0.00E+00 | 0.00E+00 | 0.00E+00 | 0.00E+00 |
| 5 | 0.00E+00 | 0.00% | 2.61E-02 | 6.35E-02 | 0.00E+00 | 1.08E-01 | 4.42E-01 | 0.00E+00 | 0.00E+00 | 0.00E+00 | 0.00E+00 | 0.00E+00 |
| 6 | 0.00E+00 | 0.00% | 5.09E-02 | 1.24E-01 | 0.00E+00 | 1.88E-01 | 6.12E-01 | 0.00E+00 | 0.00E+00 | 0.00E+00 | 0.00E+00 | 0.00E+00 |
| 7 | 9.65E-10 | 39.62% | 6.66E-02 | 1.62E-01 | 0.00E+00 | 3.43E-02 | 4.42E-01 | 6.43E-11 | 1.56E-10 | 0.00E+00 | 3.31E-11 | 4.26E-10 |
| 8 | 2.33E-07 | 2.38% | 2.99E-02 | 7.28E-02 | 0.00E+00 | 3.94E-02 | 4.19E-01 | 6.96E-09 | 1.69E-08 | 0.00E+00 | 9.16E-09 | 9.76E-08 |
| 9 | 5.29E-06 | 0.69% | 2.20E-02 | 5.36E-02 | 0.00E+00 | 2.53E-02 | 4.12E-01 | 1.17E-07 | 2.84E-07 | 0.00E+00 | 1.34E-07 | 2.18E-06 |
| 10 | 3.36E-05 | 0.28% | 1.48E-02 | 3.60E-02 | 0.00E+00 | 2.31E-02 | 3.98E-01 | 4.98E-07 | 1.21E-06 | 0.00E+00 | 7.76E-07 | 1.34E-05 |
| 11 | 5.21E-05 | 0.18% | 8.92E-03 | 2.17E-02 | 0.00E+00 | 1.72E-02 | 6.54E-01 | 4.65E-07 | 1.13E-06 | 0.00E+00 | 8.96E-07 | 3.41E-05 |
| 12 | 1.33E-04 | 0.11% | 5.74E-03 | 1.40E-02 | 0.00E+00 | 1.19E-02 | 4.54E-01 | 7.62E-07 | 1.85E-06 | 0.00E+00 | 1.58E-06 | 6.03E-05 |
| 13 | 3.00E-04 | 0.07% | 3.99E-03 | 9.70E-03 | 0.00E+00 | 9.34E-03 | 4.06E-01 | 1.20E-06 | 2.91E-06 | 0.00E+00 | 2.80E-06 | 1.22E-04 |
| 14 | 4.50E-04 | 0.06% | 2.99E-03 | 7.26E-03 | 0.00E+00 | 6.05E-03 | 3.91E-01 | 1.35E-06 | 3.26E-06 | 0.00E+00 | 2.72E-06 | 1.76E-04 |
| 15 | 5.69E-04 | 0.05% | 2.38E-03 | 5.79E-03 | 0.00E+00 | 3.06E-03 | 3.55E-01 | 1.35E-06 | 3.29E-06 | 0.00E+00 | 1.74E-06 | 2.02E-04 |
| 16 | 2.79E-04 | 0.08% | 2.04E-03 | 5.00E-03 | 0.00E+00 | 2.16E-03 | 3.31E-01 | 5.68E-07 | 1.39E-06 | 0.00E+00 | 6.03E-07 | 9.22E-05 |
| 17 | 2.12E-04 | 0.09% | 1.87E-03 | 4.63E-03 | 0.00E+00 | 1.92E-03 | 3.83E-01 | 3.98E-07 | 9.84E-07 | 0.00E+00 | 4.08E-07 | 8.13E-05 |
| 18 | 2.47E-04 | 0.12% | 1.77E-03 | 4.43E-03 | 0.00E+00 | 1.87E-03 | 2.87E-01 | 4.38E-07 | 1.09E-06 | 0.00E+00 | 4.61E-07 | 7.07E-05 |
| 19 | 1.24E-04 | 0.16% | 2.23E-03 | 5.68E-03 | 0.00E+00 | 1.80E-03 | 2.88E-01 | 2.77E-07 | 7.04E-07 | 0.00E+00 | 2.23E-07 | 3.58E-05 |
| 20 | 5.98E-05 | 0.24% | 6.74E-03 | 1.75E-02 | 0.00E+00 | 1.14E-03 | 2.17E-01 | 4.03E-07 | 1.05E-06 | 0.00E+00 | 6.80E-08 | 1.30E-05 |
| 21 | 4.90E-05 | 0.27% | 9.20E-03 | 2.42E-02 | 0.00E+00 | 8.04E-04 | 2.06E-01 | 4.51E-07 | 1.19E-06 | 0.00E+00 | 3.94E-08 | 1.01E-05 |
| 22 | 5.15E-05 | 0.29% | 9.49E-03 | 2.54E-02 | 0.00E+00 | 4.88E-04 | 1.84E-01 | 4.89E-07 | 1.31E-06 | 0.00E+00 | 2.52E-08 | 9.50E-06 |
| 23 | 3.14E-05 | 0.35% | 9.26E-03 | 2.56E-02 | 0.00E+00 | 3.19E-04 | 2.24E-01 | 2.90E-07 | 8.04E-07 | 0.00E+00 | 1.00E-08 | 7.02E-06 |
| 24 | 3.25E-05 | 0.37% | 9.50E-03 | 2.85E-02 | 1.28E-05 | 2.34E-03 | 2.07E-01 | 3.09E-07 | 9.27E-07 | 4.18E-10 | 7.61E-08 | 6.74E-06 |
| 25 | 5.05E-06 | 0.94% | 1.43E-02 | 4.83E-02 | 4.78E-03 | 1.87E-05 | 1.68E-01 | 7.25E-08 | 2.44E-07 | 2.42E-08 | 9.44E-11 | 8.50E-07 |
| 26 | 1.41E-06 | 1.72% | 1.69E-02 | 6.14E-02 | 1.83E-02 | 0.00E+00 | 1.63E-01 | 2.37E-08 | 8.63E-08 | 2.57E-08 | 0.00E+00 | 2.28E-07 |
| 27 | 2.52E-07 | 3.92% | 1.67E-02 | 6.60E-02 | 2.31E-02 | 0.00E+00 | 1.64E-01 | 4.21E-09 | 1.66E-08 | 5.82E-09 | 0.00E+00 | 4.14E-08 |
| 28 | 4.79E-08 | 9.11% | 1.72E-02 | 7.27E-02 | 2.19E-02 | 0.00E+00 | 1.67E-01 | 8.22E-10 | 3.48E-09 | 1.05E-09 | 0.00E+00 | 8.03E-09 |
| 29 | 1.41E-08 | 16.46% | 1.91E-02 | 8.51E-02 | 1.55E-02 | 0.00E+00 | 1.71E-01 | 2.69E-10 | 1.20E-09 | 2.18E-10 | 0.00E+00 | 2.41E-09 |
| 30 | 6.04E-09 | 30.81% | 2.05E-02 | 9.58E-02 | 1.16E-02 | 0.00E+00 | 1.72E-01 | 1.24E-10 | 5.79E-10 | 7.03E-11 | 0.00E+00 | 1.04E-09 |
| Total | 2.64E-03 | 0.03% | 1.17E+00 | 3.03E+00 | 9.52E-02 | 6.78E-01 | 1.06E+01 | 9.47E-06 | 2.38E-05 | 5.74E-08 | 1.26E-05 | 9.37E-04 |

TABLE 11
30 group MCNP reaction rates and reaction rate comparison in HSR

| Energy | MCNP RRD (cm ⁻³) | | | | | MCNP Standard Deviation | | | | | Partial Percent Error (TXSAMC-MCNP)/MCNP | | | | |
|--------|------------------------------|----------|----------|----------|----------|-------------------------|--------|--------|---------|--------|--|--------|--------|---------|--------|
| | fission | nusigf | n2n | abs-fis | total | fission | nusigf | n2n | abs-fis | total | fission | nusigf | n2n | abs-fis | total |
| 1 | 0.00E+00 | 0.00E+00 | 0.00E+00 | 0.00E+00 | 0.00E+00 | N/A | N/A | N/A | N/A | N/A | N/A | N/A | N/A | N/A | N/A |
| 2 | 0.00E+00 | 0.00E+00 | 0.00E+00 | 0.00E+00 | 0.00E+00 | N/A | N/A | N/A | N/A | N/A | N/A | N/A | N/A | N/A | N/A |
| 3 | 0.00E+00 | 0.00E+00 | 0.00E+00 | 0.00E+00 | 0.00E+00 | N/A | N/A | N/A | N/A | N/A | N/A | N/A | N/A | N/A | N/A |
| 4 | 0.00E+00 | 0.00E+00 | 0.00E+00 | 0.00E+00 | 0.00E+00 | N/A | N/A | N/A | N/A | N/A | N/A | N/A | N/A | N/A | N/A |
| 5 | 0.00E+00 | 0.00E+00 | 0.00E+00 | 0.00E+00 | 0.00E+00 | N/A | N/A | N/A | N/A | N/A | N/A | N/A | N/A | N/A | N/A |
| 6 | 0.00E+00 | 0.00E+00 | 0.00E+00 | 0.00E+00 | 0.00E+00 | N/A | N/A | N/A | N/A | N/A | N/A | N/A | N/A | N/A | N/A |
| 7 | 5.32E-11 | 1.30E-10 | 0.00E+00 | 5.17E-11 | 5.10E-10 | 33.30% | 33.30% | N/A | 60.12% | 40.86% | 0.00% | 0.00% | N/A | 0.00% | 0.00% |
| 8 | 6.99E-09 | 1.70E-08 | 0.00E+00 | 9.55E-09 | 9.92E-08 | 2.52% | 2.52% | N/A | 2.98% | 2.14% | 0.00% | 0.00% | N/A | 0.00% | 0.00% |
| 9 | 1.20E-07 | 2.92E-07 | 0.00E+00 | 1.38E-07 | 2.21E-06 | 0.74% | 0.74% | N/A | 0.77% | 0.61% | -0.04% | -0.03% | N/A | -0.04% | 0.00% |
| 10 | 5.02E-07 | 1.22E-06 | 0.00E+00 | 7.81E-07 | 1.34E-05 | 0.30% | 0.30% | N/A | 0.30% | 0.25% | -0.04% | -0.04% | N/A | -0.04% | -0.01% |
| 11 | 5.02E-07 | 1.22E-06 | 0.00E+00 | 8.82E-07 | 3.12E-05 | 0.19% | 0.19% | N/A | 0.19% | 0.13% | -0.39% | -0.38% | N/A | 0.11% | 0.31% |
| 12 | 7.48E-07 | 1.82E-06 | 0.00E+00 | 1.58E-06 | 6.12E-05 | 0.11% | 0.11% | N/A | 0.12% | 0.09% | 0.15% | 0.14% | N/A | -0.06% | -0.10% |
| 13 | 1.20E-06 | 2.92E-06 | 0.00E+00 | 2.82E-06 | 1.22E-04 | 0.07% | 0.07% | N/A | 0.07% | 0.06% | -0.04% | -0.04% | N/A | -0.13% | -0.02% |
| 14 | 1.35E-06 | 3.27E-06 | 0.00E+00 | 2.76E-06 | 1.76E-04 | 0.06% | 0.06% | N/A | 0.06% | 0.05% | -0.05% | -0.05% | N/A | -0.27% | -0.05% |
| 15 | 1.35E-06 | 3.29E-06 | 0.00E+00 | 1.74E-06 | 2.02E-04 | 0.05% | 0.05% | N/A | 0.05% | 0.04% | 0.01% | 0.01% | N/A | -0.03% | -0.01% |
| 16 | 5.67E-07 | 1.39E-06 | 0.00E+00 | 6.02E-07 | 9.21E-05 | 0.08% | 0.08% | N/A | 0.08% | 0.07% | 0.01% | 0.01% | N/A | 0.01% | 0.00% |
| 17 | 3.98E-07 | 9.83E-07 | 0.00E+00 | 4.08E-07 | 8.21E-05 | 0.09% | 0.09% | N/A | 0.09% | 0.08% | 0.00% | 0.00% | N/A | 0.00% | -0.09% |
| 18 | 4.38E-07 | 1.09E-06 | 0.00E+00 | 4.61E-07 | 7.13E-05 | 0.12% | 0.12% | N/A | 0.12% | 0.10% | 0.00% | 0.00% | N/A | 0.01% | -0.06% |
| 19 | 2.78E-07 | 7.08E-07 | 0.00E+00 | 2.20E-07 | 3.54E-05 | 0.16% | 0.17% | N/A | 0.16% | 0.13% | -0.02% | -0.02% | N/A | 0.02% | 0.04% |
| 20 | 4.00E-07 | 1.04E-06 | 0.00E+00 | 6.83E-08 | 1.30E-05 | 0.25% | 0.25% | N/A | 0.23% | 0.20% | 0.03% | 0.03% | N/A | 0.00% | 0.00% |
| 21 | 4.50E-07 | 1.19E-06 | 0.00E+00 | 3.94E-08 | 1.01E-05 | 0.27% | 0.27% | N/A | 0.26% | 0.22% | 0.00% | 0.00% | N/A | 0.00% | 0.00% |
| 22 | 4.90E-07 | 1.31E-06 | 0.00E+00 | 2.54E-08 | 9.47E-06 | 0.29% | 0.29% | N/A | 0.28% | 0.24% | 0.00% | 0.00% | N/A | 0.00% | 0.00% |
| 23 | 2.90E-07 | 8.03E-07 | 0.00E+00 | 9.99E-09 | 7.01E-06 | 0.35% | 0.35% | N/A | 0.34% | 0.30% | 0.00% | 0.00% | N/A | 0.00% | 0.00% |
| 24 | 3.09E-07 | 9.30E-07 | 4.25E-10 | 7.66E-08 | 6.72E-06 | 0.37% | 0.38% | 1.21% | 0.45% | 0.32% | 0.00% | -0.01% | -0.01% | 0.00% | 0.00% |
| 25 | 7.20E-08 | 2.42E-07 | 2.33E-08 | 2.38E-08 | 8.49E-07 | 0.94% | 0.94% | 1.24% | 0.93% | 0.79% | 0.01% | 1.54% | -0.19% | 0.00% | 0.00% |
| 26 | 2.38E-08 | 8.65E-08 | 2.58E-08 | 8.17E-09 | 2.28E-07 | 1.72% | 1.72% | 1.70% | 1.52% | 1.45% | 0.00% | 0.00% | -0.19% | -0.06% | 0.00% |
| 27 | 4.18E-09 | 1.66E-08 | 5.80E-09 | 2.52E-09 | 4.13E-08 | 3.91% | 3.91% | 3.70% | 3.25% | 3.30% | 0.00% | 0.00% | 0.04% | -0.02% | 0.00% |
| 28 | 8.38E-10 | 3.56E-09 | 1.05E-09 | 4.40E-10 | 8.10E-09 | 9.13% | 9.13% | 8.45% | 7.44% | 7.81% | 0.00% | 0.00% | 0.00% | 0.00% | 0.00% |
| 29 | 2.71E-10 | 1.21E-09 | 2.19E-10 | 1.20E-10 | 2.41E-09 | 16.47% | 16.48% | 13.80% | 13.20% | 14.04% | 0.00% | 0.00% | 0.00% | 0.00% | 0.00% |
| 30 | 1.29E-10 | 6.07E-10 | 6.64E-11 | 4.20E-11 | 1.05E-09 | 30.57% | 30.65% | 21.34% | 24.01% | 26.31% | 0.00% | 0.00% | 0.01% | 0.00% | 0.00% |
| Total | 9.50E-06 | 2.39E-05 | 5.67E-08 | 1.27E-05 | 9.37E-04 | 0.04% | 0.04% | 1.06% | 0.05% | 0.02% | -0.37% | -0.36% | 1.38% | -0.70% | 0.01% |

Like the SSR, Table 10 shows the very fast nature of this system with no tallied reactions or flux in the bottom six energy groups. From the data in Table 11, we see that while there is still some modest error in the TXSAMC estimation of the reaction rates, the percent error is significantly less than that of the SSR system for all of the reaction rates. This is highlighted by the 0.01% difference in the total interaction rate between the homogenized pin-cell and its benchmark. Some of this reduced error might be due to better approximation of the Dancoff factor in TRANSX and the escape cross section but it would take further study to verify this. Given that the other major difference between the SSR and HSR is that there is less sodium in each HSR pin cell, it is possible that some of this reduction in error can be attributed to a reduction in sodium in the cell. The

mechanism for this is unclear at this time. Similar to the SSR, the partial percent error in each group is generally very good with the vast majority having a value of less than half of a percent. Again, TXSAMC appears to produce shielded cross sections that accurately reproduce a reaction rate in a homogenized pin-cell. Although TXSAMC calculates the homogenized cross sections better for the HSR than for the SSR, this cannot be extended to conclude that it works better for hexagonal lattices than for square lattices without further work.

In Fig. 6 we see the difference in the TXSAMC and MCNP RRD's for the reactor displayed graphically. The very low errors in the low energy range are quite obvious in this plot as well as the general accuracy of the cross sections at mid-to-high energy range groups with the largest error in any group being around one and a half percent. With the exception of one group in the (n,2n) reaction rate density, every other error is less than one half percent. Since the higher energy groups are generally more important for determining the overall RRD in the cell, this leads to a rather minimal overall error in the cell. For all of the reactions, the error appears to be very reasonable for this test case.

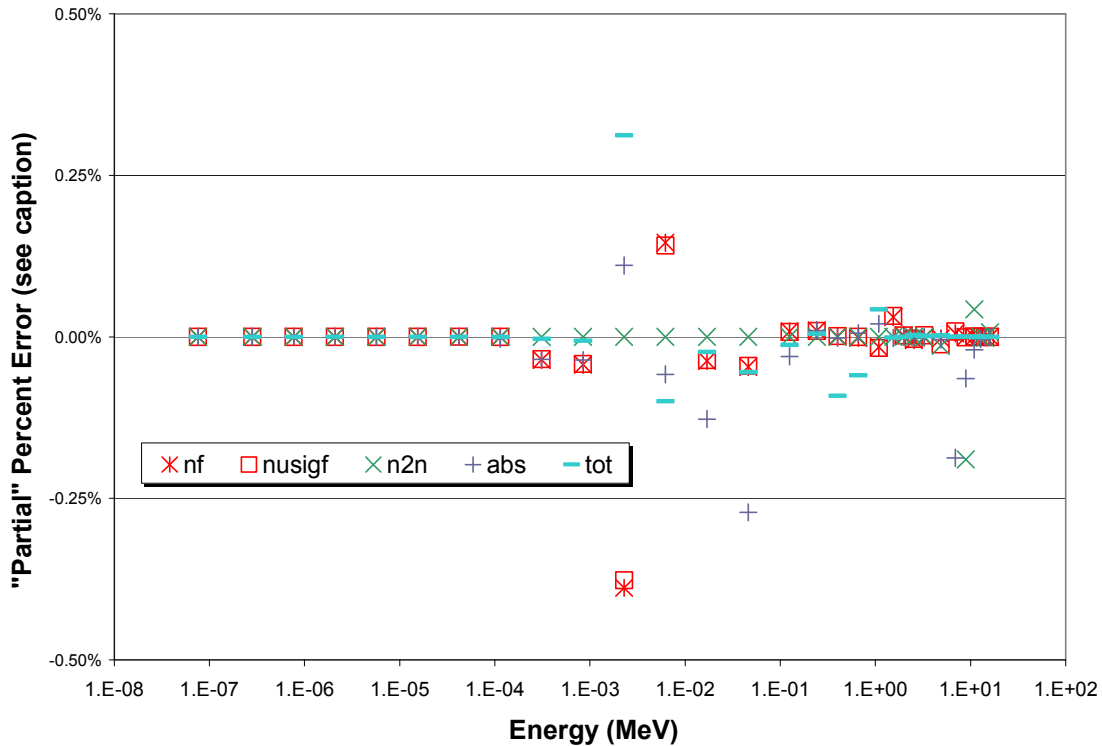


Fig. 6. "Partial" percent errors in each energy group for reaction-rate densities in HSR. Each "partial" error is plotted at the midpoint energy of its group. The percent error in a given reaction rate is the sum of the 30 partial percent errors.

SQUARE-COMPLEX REACTOR

This reactor is modeled as a regular square lattice of 23 by 23 pin-cells but unlike the SSR, it has non-fuel pin-cells and a reactor vessel. While this reactor is more complex and realistic in its layout and features than the SSR, it is by no means a high-fidelity model of an actual reactor. It is missing many of the components that are usually modeled in a reactor such as a shield, coolant inlets and outlets or the power conversion system. It is also missing some of the temperature gradients that would be associated with a real reactor; the coolant temperature is the same at every point in the reactor and

the temperature is the same in every fuel pin. It does, however, do a reasonable job of modeling some of the complexities associated with real reactor designs such as leakage and control rods. The reactor vessel is a cylindrical shell of 316L stainless steel that is 35 cm long and 1.5 cm thick. As in the SSR and HSR, the coolant is liquid sodium at 450 K and the pins retain the same radial dimensions and temperatures. Unlike the SSR and HSR, the fuel pins in this reactor are enriched to 90%, have a pin length of 30 cm and a fuel length of 29.8 cm. The higher enrichment results in a similar criticality ($k_{\text{eff}} \sim 1.13$) when compared to the SSR due to the tremendous increase in leakage in the system. This system also has two coolant channels and two control rod locations. The control rods are half the diameter of a fuel pin but the same length and are composed of an AgInCd core surrounded by a SS316L sleeve. The basic dimensions, materials and temperatures for the Square-Complex Reactor (SCR) are described in Table 12. The SCR layout can be seen in Fig. 7.

TABLE 12
Description of materials, geometry and temperatures in SCR

| | |
|-------------------------------|-----------------------|
| Reactor Label | SCR |
| Lattice Type | Square |
| Matrix Size | 23x23 |
| Pitch | 2.1 cm |
| Vessel Length | 35 cm |
| Vessel Thickness | 1.5 cm |
| Vessel Material | 316L Stainless Steel |
| Vessel Temperature | 400 K |
| Vessel Density | 5.5 g/cc |
| Coolant Material | Sodium |
| Coolant Temperature | 450 K |
| Coolant Density | 2.0 g/cc |
| Pin Length | 30.0 cm |
| Pin Diameter | 2.0 cm |
| Cladding Thickness | 0.1 cm |
| Cladding Material | Natural Zirconium |
| Cladding Temperature | 600 K |
| Cladding Density | 2.7 g/cc |
| Fuel Length | 29.8 cm |
| Fuel Diameter | 1.8 cm |
| Fuel Material | Uranium Dioxide |
| Enrichment | 90% |
| Fuel Temperature | 800 K |
| Fuel Density | 10.5 g/cc |
| Number of Control Rods | 2 |
| Control Rod Length | 30.0 cm |
| Control Rod Diameter | 1.0 cm |
| Control Rod Clad Thickness | 0.1 cm |
| Control Rod Clad Material | 316L Stainless Steel |
| Control Rod Clad Temperature | 400 K |
| Control Rod Clad Density | 5.5 g/cc |
| Control Rod Meat Length | 29.8 cm |
| Control Rod Meat Diameter | 0.8 cm |
| Control Rod Meat Material | Silver-Indium-Cadmium |
| Control Rod Meat Temperature | 500 K |
| Control Rod Meat Density | 8.5 g/cc |
| Number of Coolant Channels | 2 |
| Number of kcode cycles | 410 |
| Number of inactive cycles | 10 |
| Number of particles per cycle | 5000 |
| Number of histories | 2000000 |
| keff | 1.12926 |

To test the ability of TXSAMC to produce properly shielded cross sections for a particular region in a reactor, the lattice was broken into five tally regions. The first region is composed of fuel pin-cells and is marked by the yellow fuel rods in Fig. 7. This region represents all pins not adjacent to heterogeneities such as a coolant channel or

control rod location. The second tally region is the two control rod positions which are marked by red on the reactor layout. The third region is the two coolant channels which are the light blue squares in the interior of the core. The fourth region is composed of the eight nearest pin-cells surrounding each control rod (sixteen total cells) and is marked in purple on the reactor layout. The final region is composed of the eight nearest pin-cells surrounding the coolant channels (sixteen total cells) and is marked in brown on the reactor layout. For each of these regions, TXSAMC was used to create shielded and homogenized cross sections for the cells.

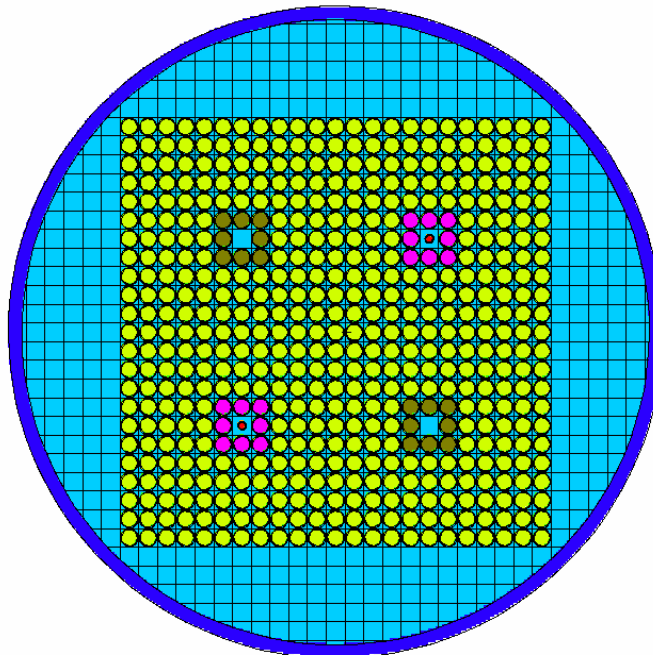


Fig. 7. SCR layout in x-y plane.

Yellow denotes tally region 1, red denotes tally region 2, light blue within core denotes tally region 3, purple denotes tally region 4 and brown denotes tally region 5. Dark blue denotes the reactor vessel.

The weighting function that is used in the NJOY module of TXSAMC is based on a core-averaged scalar flux for this reactor as tallied by MCNP using 30 energy bins. The multiplying scalar flux used to produce the TXSAMC RRD's is the cell-averaged scalar flux for the pin-cells within the specified tally region. The normalization of this scalar flux is over the combined cell volumes of the entire region. Since the TXSAMC-produced cross sections assume a one dimensional representation of the pin-cell, the MCNP-produced RRD's are adjusted to reflect this. For example, in the fuel pin-cells the MCNP RRD for each component (meat, clad, coolant) is multiplied by the cross-sectional area in the x-y plane of that component and divided by the total pin-cell cross-sectional area. The net effect of this adjustment is small as long as the pin length and vessel length are similar (i.e. not a lot of extra coolant above and below the pins) since the TXSAMC cross sections are produced by appropriately volume-normalized RZFLUX files and the MCNP RRD is also volume-normalized.

The first tally region is made up of all fuel pin-cells not adjacent to the coolant channels or control rods. In Table 13 we show the MCNP-tallied scalar flux for the pin-cell, its relative standard deviation, the TXSAMC-generated cross sections and the TXSAMC-generated reaction rate densities for the first tally region. Table 14 shows the MCNP-tallied reaction rate densities, their standard deviations and the partial percent error between the TXSAMC-generated reaction rates and the MCNP-tallied reaction rates for the first tally region.

TABLE 13
MCNP scalar flux, TXSAMC cross sections and reaction rates in SCR tally region 1

| Energy Group | Scalar Flux (n/cm ² /hps) | Rel. Error (1 σ) | TXSAMC SIGMA (cm ⁻¹) | | | | | TXSAMC RRD (cm ⁻³) | | | | |
|--------------|--------------------------------------|--------------------------|----------------------------------|----------|----------|----------|----------|--------------------------------|----------|----------|----------|----------|
| | | | fission | nusigf | n2n | abs-fis | total | fission | nusigf | n2n | abs-fis | total |
| 1 | 0.00E+00 | 0.00% | 2.89E+00 | 7.04E+00 | 0.00E+00 | 5.00E-01 | 3.76E+00 | 0.00E+00 | 0.00E+00 | 0.00E+00 | 0.00E+00 | 0.00E+00 |
| 2 | 0.00E+00 | 0.00% | 2.06E+00 | 5.03E+00 | 0.00E+00 | 4.35E-01 | 2.86E+00 | 0.00E+00 | 0.00E+00 | 0.00E+00 | 0.00E+00 | 0.00E+00 |
| 3 | 0.00E+00 | 0.00% | 8.49E-01 | 2.07E+00 | 0.00E+00 | 1.18E-01 | 1.32E+00 | 0.00E+00 | 0.00E+00 | 0.00E+00 | 0.00E+00 | 0.00E+00 |
| 4 | 0.00E+00 | 0.00% | 2.10E-01 | 5.12E-01 | 0.00E+00 | 7.75E-02 | 6.22E-01 | 0.00E+00 | 0.00E+00 | 0.00E+00 | 0.00E+00 | 0.00E+00 |
| 5 | 0.00E+00 | 0.00% | 1.50E-01 | 3.65E-01 | 0.00E+00 | 1.66E-01 | 6.35E-01 | 0.00E+00 | 0.00E+00 | 0.00E+00 | 0.00E+00 | 0.00E+00 |
| 6 | 2.73E-11 | 90.71% | 2.30E-01 | 5.59E-01 | 0.00E+00 | 2.40E-01 | 8.25E-01 | 6.26E-12 | 1.52E-11 | 0.00E+00 | 6.53E-12 | 2.25E-11 |
| 7 | 6.83E-11 | 55.96% | 2.07E-01 | 5.04E-01 | 0.00E+00 | 9.99E-02 | 5.57E-01 | 1.41E-11 | 3.44E-11 | 0.00E+00 | 6.82E-12 | 3.80E-11 |
| 8 | 3.35E-10 | 28.89% | 1.82E-01 | 4.42E-01 | 0.00E+00 | 1.08E-01 | 6.07E-01 | 6.09E-11 | 1.48E-10 | 0.00E+00 | 3.63E-11 | 2.03E-10 |
| 9 | 2.26E-09 | 11.52% | 1.39E-01 | 3.38E-01 | 0.00E+00 | 6.21E-02 | 5.21E-01 | 3.14E-10 | 7.64E-10 | 0.00E+00 | 1.41E-10 | 1.18E-09 |
| 10 | 3.64E-08 | 3.09% | 9.95E-02 | 2.42E-01 | 0.00E+00 | 5.39E-02 | 4.90E-01 | 3.62E-09 | 8.81E-09 | 0.00E+00 | 1.96E-09 | 1.78E-08 |
| 11 | 1.30E-07 | 1.70% | 6.46E-02 | 1.57E-01 | 0.00E+00 | 3.06E-02 | 8.01E-01 | 8.41E-09 | 2.05E-08 | 0.00E+00 | 3.98E-09 | 1.04E-07 |
| 12 | 7.93E-07 | 0.85% | 4.35E-02 | 1.06E-01 | 0.00E+00 | 1.71E-02 | 4.72E-01 | 3.45E-08 | 8.40E-08 | 0.00E+00 | 1.36E-08 | 3.74E-07 |
| 13 | 4.87E-06 | 0.39% | 3.13E-02 | 7.61E-02 | 0.00E+00 | 1.15E-02 | 4.00E-01 | 1.52E-07 | 3.70E-07 | 0.00E+00 | 5.61E-08 | 1.95E-06 |
| 14 | 1.85E-05 | 0.21% | 2.39E-02 | 5.80E-02 | 0.00E+00 | 8.05E-03 | 3.81E-01 | 4.42E-07 | 1.07E-06 | 0.00E+00 | 1.49E-07 | 7.03E-06 |
| 15 | 5.32E-05 | 0.13% | 1.91E-02 | 4.65E-02 | 0.00E+00 | 5.20E-03 | 3.37E-01 | 1.01E-06 | 2.47E-06 | 0.00E+00 | 2.77E-07 | 1.79E-05 |
| 16 | 4.21E-05 | 0.12% | 1.66E-02 | 4.08E-02 | 0.00E+00 | 3.57E-03 | 3.20E-01 | 6.99E-07 | 1.72E-06 | 0.00E+00 | 1.50E-07 | 1.35E-05 |
| 17 | 4.16E-05 | 0.12% | 1.53E-02 | 3.77E-02 | 0.00E+00 | 2.66E-03 | 3.66E-01 | 6.36E-07 | 1.57E-06 | 0.00E+00 | 1.11E-07 | 1.53E-05 |
| 18 | 5.78E-05 | 0.12% | 1.43E-02 | 3.57E-02 | 0.00E+00 | 1.96E-03 | 2.83E-01 | 8.28E-07 | 2.07E-06 | 0.00E+00 | 1.14E-07 | 1.64E-05 |
| 19 | 4.27E-05 | 0.13% | 1.52E-02 | 3.85E-02 | 0.00E+00 | 1.54E-03 | 2.79E-01 | 6.47E-07 | 1.64E-06 | 0.00E+00 | 6.56E-08 | 1.19E-05 |
| 20 | 2.38E-05 | 0.19% | 1.63E-02 | 4.22E-02 | 0.00E+00 | 1.17E-03 | 2.09E-01 | 3.87E-07 | 1.00E-06 | 0.00E+00 | 2.78E-08 | 4.96E-06 |
| 21 | 2.10E-05 | 0.20% | 1.70E-02 | 4.48E-02 | 0.00E+00 | 8.82E-04 | 2.01E-01 | 3.56E-07 | 9.41E-07 | 0.00E+00 | 1.85E-08 | 4.21E-06 |
| 22 | 2.12E-05 | 0.21% | 1.69E-02 | 4.57E-02 | 0.00E+00 | 5.82E-04 | 1.82E-01 | 3.58E-07 | 9.70E-07 | 0.00E+00 | 1.24E-08 | 3.86E-06 |
| 23 | 1.43E-05 | 0.25% | 1.61E-02 | 4.49E-02 | 0.00E+00 | 3.61E-04 | 2.17E-01 | 2.29E-07 | 6.40E-07 | 0.00E+00 | 5.15E-09 | 3.09E-06 |
| 24 | 1.51E-05 | 0.26% | 1.51E-02 | 4.49E-02 | 1.07E-04 | 2.08E-03 | 2.00E-01 | 2.27E-07 | 6.77E-07 | 1.62E-09 | 3.13E-08 | 3.01E-06 |
| 25 | 2.43E-06 | 0.63% | 1.98E-02 | 6.69E-02 | 4.86E-03 | 0.00E+00 | 1.62E-01 | 4.82E-08 | 1.62E-07 | 1.18E-08 | 0.00E+00 | 3.94E-07 |
| 26 | 7.21E-07 | 1.12% | 2.45E-02 | 8.92E-02 | 9.71E-03 | 0.00E+00 | 1.56E-01 | 1.77E-08 | 6.43E-08 | 7.00E-09 | 0.00E+00 | 1.12E-07 |
| 27 | 1.43E-07 | 2.53% | 2.39E-02 | 9.43E-02 | 1.38E-02 | 0.00E+00 | 1.57E-01 | 3.42E-09 | 1.35E-08 | 1.97E-09 | 0.00E+00 | 2.25E-08 |
| 28 | 2.48E-08 | 5.72% | 2.52E-02 | 1.06E-01 | 1.30E-02 | 0.00E+00 | 1.60E-01 | 6.25E-10 | 2.62E-09 | 3.22E-10 | 0.00E+00 | 3.97E-09 |
| 29 | 9.80E-09 | 9.42% | 2.84E-02 | 1.25E-01 | 1.04E-02 | 0.00E+00 | 1.65E-01 | 2.78E-10 | 1.23E-09 | 1.02E-10 | 0.00E+00 | 1.61E-09 |
| 30 | 2.81E-09 | 17.18% | 2.86E-02 | 1.32E-01 | 9.11E-03 | 0.00E+00 | 1.65E-01 | 8.06E-11 | 3.72E-10 | 2.56E-11 | 0.00E+00 | 4.65E-10 |
| Total | 3.60E-04 | 0.04% | 7.50E+00 | 1.85E+01 | 6.10E-02 | 1.95E+00 | 1.78E+01 | 6.09E-06 | 1.55E-05 | 2.28E-08 | 1.04E-06 | 1.04E-04 |

TABLE 14
MCNP reaction rates and reaction rate comparison in SCR tally region 1

| Energy Group | MCNP RRD (cm ⁻³) | | | | | MCNP Standard Deviation | | | | | Partial Percent Error (TXSAMC-MCNP)/MCNP | | | | |
|--------------|------------------------------|----------|----------|----------|----------|-------------------------|--------|--------|---------|--------|--|--------|--------|---------|--------|
| | fission | nusigf | n2n | abs-fis | total | fission | nusigf | n2n | abs-fis | total | fission | nusigf | n2n | abs-fis | total |
| 1 | 0.00E+00 | 0.00E+00 | 0.00E+00 | 0.00E+00 | 0.00E+00 | N/A | N/A | N/A | N/A | N/A | N/A | N/A | N/A | N/A | N/A |
| 2 | 0.00E+00 | 0.00E+00 | 0.00E+00 | 0.00E+00 | 0.00E+00 | N/A | N/A | N/A | N/A | N/A | N/A | N/A | N/A | N/A | N/A |
| 3 | 0.00E+00 | 0.00E+00 | 0.00E+00 | 0.00E+00 | 0.00E+00 | N/A | N/A | N/A | N/A | N/A | N/A | N/A | N/A | N/A | N/A |
| 4 | 0.00E+00 | 0.00E+00 | 0.00E+00 | 0.00E+00 | 0.00E+00 | N/A | N/A | N/A | N/A | N/A | N/A | N/A | N/A | N/A | N/A |
| 5 | 0.00E+00 | 0.00E+00 | 0.00E+00 | 0.00E+00 | 0.00E+00 | N/A | N/A | N/A | N/A | N/A | N/A | N/A | N/A | N/A | N/A |
| 6 | 4.73E-12 | 1.15E-11 | 0.00E+00 | 1.88E-12 | 1.45E-11 | 84.59% | 84.59% | N/A | 75.72% | 61.02% | 0.00% | 0.00% | N/A | 0.00% | 0.00% |
| 7 | 2.01E-11 | 4.90E-11 | 0.00E+00 | 9.22E-12 | 4.97E-11 | 47.71% | 47.71% | N/A | 51.67% | 42.43% | 0.00% | 0.00% | N/A | 0.00% | 0.00% |
| 8 | 7.37E-11 | 1.79E-10 | 0.00E+00 | 5.08E-11 | 2.46E-10 | 27.71% | 27.71% | N/A | 29.55% | 25.65% | 0.00% | 0.00% | N/A | 0.00% | 0.00% |
| 9 | 3.63E-10 | 8.82E-10 | 0.00E+00 | 1.74E-10 | 1.29E-09 | 11.74% | 11.74% | N/A | 13.40% | 10.28% | 0.00% | 0.00% | N/A | 0.00% | 0.00% |
| 10 | 3.82E-09 | 9.29E-09 | 0.00E+00 | 2.08E-09 | 1.88E-08 | 3.21% | 3.21% | N/A | 3.20% | 2.70% | 0.00% | 0.00% | N/A | -0.10% | 0.00% |
| 11 | 9.43E-09 | 2.30E-08 | 0.00E+00 | 5.05E-09 | 1.08E-07 | 1.82% | 1.82% | N/A | 1.79% | 1.22% | -0.02% | -0.02% | N/A | -0.10% | 0.00% |
| 12 | 3.56E-08 | 8.66E-08 | 0.00E+00 | 1.42E-08 | 3.95E-07 | 0.89% | 0.89% | N/A | 0.86% | 0.66% | -0.02% | -0.02% | N/A | -0.05% | -0.02% |
| 13 | 1.59E-07 | 3.86E-07 | 0.00E+00 | 5.86E-08 | 2.04E-06 | 0.40% | 0.40% | N/A | 0.40% | 0.31% | -0.10% | -0.10% | N/A | -0.22% | -0.08% |
| 14 | 4.61E-07 | 1.12E-06 | 0.00E+00 | 1.56E-07 | 7.33E-06 | 0.21% | 0.21% | N/A | 0.21% | 0.17% | -0.30% | -0.28% | N/A | -0.63% | -0.28% |
| 15 | 1.06E-06 | 2.57E-06 | 0.00E+00 | 2.88E-07 | 1.87E-05 | 0.13% | 0.13% | N/A | 0.13% | 0.10% | -0.65% | -0.62% | N/A | -1.06% | -0.67% |
| 16 | 7.25E-07 | 1.78E-06 | 0.00E+00 | 1.56E-07 | 1.40E-05 | 0.12% | 0.12% | N/A | 0.12% | 0.09% | -0.41% | -0.40% | N/A | -0.49% | -0.46% |
| 17 | 6.61E-07 | 1.63E-06 | 0.00E+00 | 1.16E-07 | 1.59E-05 | 0.12% | 0.12% | N/A | 0.12% | 0.11% | -0.40% | -0.39% | N/A | -0.47% | -0.64% |
| 18 | 8.62E-07 | 2.15E-06 | 0.00E+00 | 1.19E-07 | 1.71E-05 | 0.12% | 0.12% | N/A | 0.12% | 0.09% | -0.52% | -0.51% | N/A | -0.46% | -0.69% |
| 19 | 6.72E-07 | 1.71E-06 | 0.00E+00 | 6.80E-08 | 1.23E-05 | 0.14% | 0.14% | N/A | 0.14% | 0.11% | -0.40% | -0.40% | N/A | -0.22% | -0.38% |
| 20 | 4.02E-07 | 1.04E-06 | 0.00E+00 | 2.90E-08 | 5.16E-06 | 0.19% | 0.19% | N/A | 0.19% | 0.15% | -0.24% | -0.24% | N/A | -0.11% | -0.18% |
| 21 | 3.70E-07 | 9.78E-07 | 0.00E+00 | 1.93E-08 | 4.38E-06 | 0.20% | 0.20% | N/A | 0.20% | 0.16% | -0.22% | -0.23% | N/A | -0.07% | -0.16% |
| 22 | 3.73E-07 | 1.01E-06 | 0.00E+00 | 1.29E-08 | 4.02E-06 | 0.21% | 0.21% | N/A | 0.20% | 0.16% | -0.23% | -0.24% | N/A | -0.05% | -0.14% |
| 23 | 2.39E-07 | 6.66E-07 | 0.00E+00 | 5.37E-09 | 3.22E-06 | 0.25% | 0.25% | N/A | 0.24% | 0.21% | -0.15% | -0.16% | N/A | -0.02% | -0.12% |
| 24 | 2.36E-07 | 7.05E-07 | 1.74E-09 | 3.42E-08 | 3.14E-06 | 0.26% | 0.26% | 0.84% | 0.32% | 0.22% | -0.15% | -0.18% | -0.51% | -0.26% | -0.12% |
| 25 | 4.99E-08 | 1.68E-07 | 1.22E-08 | 1.15E-08 | 4.10E-07 | 0.64% | 0.64% | 0.66% | 0.61% | 0.51% | -0.03% | -0.04% | -1.59% | -1.05% | -0.01% |
| 26 | 1.84E-08 | 6.67E-08 | 7.25E-09 | 4.39E-09 | 1.17E-07 | 1.13% | 1.13% | 1.11% | 0.94% | 0.92% | -0.01% | -0.02% | -1.07% | -0.40% | 0.00% |
| 27 | 3.56E-09 | 1.40E-08 | 2.06E-09 | 1.52E-09 | 2.34E-08 | 2.54% | 2.54% | 2.34% | 2.01% | 2.07% | 0.00% | 0.00% | -0.35% | -0.14% | 0.00% |
| 28 | 6.65E-10 | 2.79E-09 | 3.40E-10 | 2.47E-10 | 4.19E-09 | 5.68% | 5.69% | 5.07% | 4.37% | 4.67% | 0.00% | 0.00% | -0.08% | -0.02% | 0.00% |
| 29 | 2.88E-10 | 1.27E-09 | 1.06E-10 | 8.97E-11 | 1.68E-09 | 9.42% | 9.43% | 7.47% | 7.20% | 7.74% | 0.00% | 0.00% | -0.02% | -0.01% | 0.00% |
| 30 | 8.93E-11 | 4.17E-10 | 2.63E-11 | 2.14E-11 | 5.02E-10 | 16.99% | 17.08% | 11.28% | 12.65% | 14.26% | 0.00% | 0.00% | 0.00% | 0.00% | 0.00% |
| Total | 6.34E-06 | 1.61E-05 | 2.37E-08 | 1.10E-06 | 1.08E-04 | 0.05% | 0.05% | 0.55% | 0.08% | 0.04% | -3.85% | -3.85% | -3.61% | -5.83% | -3.97% |

From the first table, we observe the fast nature of the system with no tallied scalar flux in the lowest five energy groups. We also observe an overall error of $\sim 4\%$ for all five reaction rates measured in this survey. This is greater error than was observed in the 30 group SSR test case which is not surprising given that it is a more complex system that does not easily fit into the TRANSX module of TXSAMC. That is, it is not an infinite lattice and there is significant leakage from the system. It is possible that this amount of error would still be acceptable for design purposes but if not, a potential solution would be to divide this one region into smaller regions to better reflect the differences in flux each smaller region sees. Since a pin near the center of a real reactor (as opposed to the infinite lattices of HSR and SSR) sees a different level (and potentially energy shape) of neutron flux than a pin near the edge, there could be significant differences in the amount of shielding in each region. By dividing the core into smaller pieces, the relative fidelity of the shielding process is increased since one can now shield pin-cells in a manner more reflective of reality. We would still expect to see greater errors than in the HSR and SSR test cases since there are still significant deviations from an infinite lattice but some of the error should be alleviated. This hypothesis appears to bear out in tally regions four and five for this reactor. Another possibility for reducing error in strongly heterogeneous systems would be to modify TXSAMC such that NJOY would employ regional, not core-averaged, spectral weight functions.

In Fig. 8 we see the difference in the TXSAMC and MCNP RRD's for the first tally region displayed graphically. While the overall amount of error is significantly larger than that seen in the SSR, the partial percent error in each energy group is still very modest. It is also apparent that in the mid-range energy groups (13-25), TXSAMC is understating the reaction rates relative to the benchmark. It is not clear at this time why this might be occurring. Even with this understatement, the overall error is still within a range that could be described as reasonable for the projects TXSAMC is designed for (scoping studies, limited evaluations of new systems, etc.).

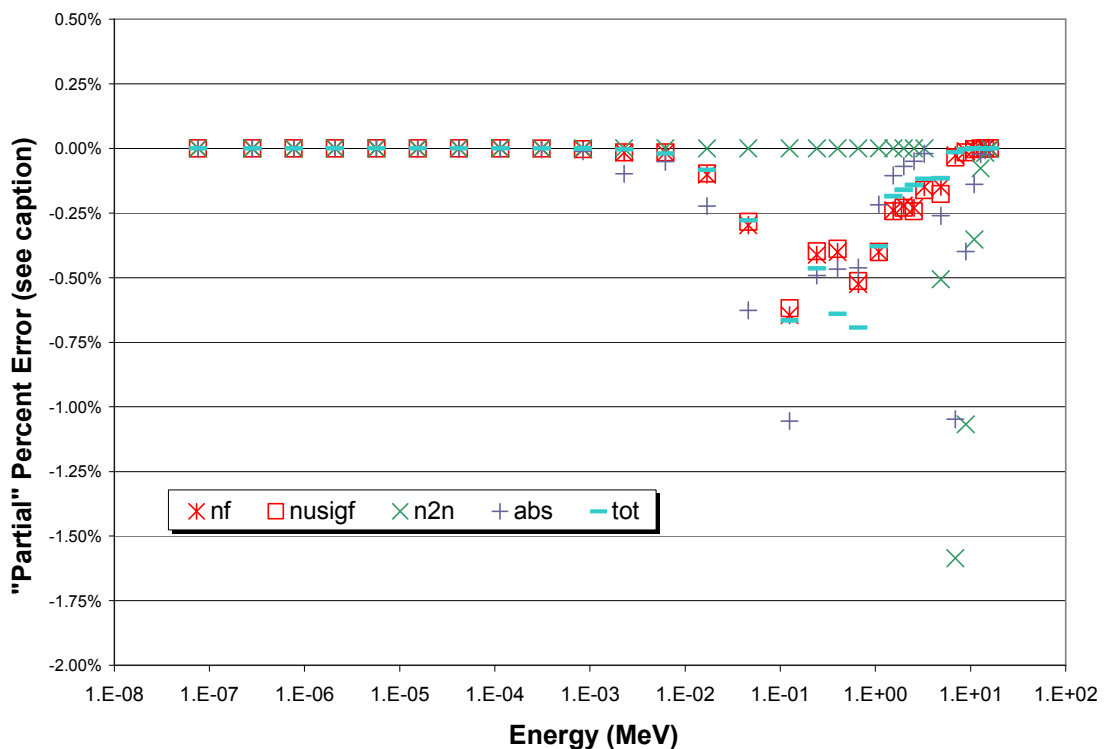


Fig. 8. "Partial" percent errors for reaction-rate densities in SCR tally region 1. Each "partial" error is plotted at the midpoint energy of its group. The percent error in a given reaction rate is the sum of the 30 partial percent errors.

The second tally region is made up of the control rod pin-cells which consist of an AgInCd cylinder in a SS316L sleeve surrounded by coolant. In Table 15 we show the MCNP-tallied scalar flux for the pin-cell, its relative standard deviation, the TXSAMC-generated cross sections and the TXSAMC-generated reaction rate densities for the second tally region. Table 16 shows the MCNP-tallied reaction rate densities, their standard deviations and the partial percent error between the TXSAMC-generated reaction rates and the MCNP-tallied reaction rates for the second tally region.

TABLE 15
MCNP scalar flux, TXSAMC cross sections and reaction rates in SCR tally region 2

| Energy Group | Scalar Flux (n/cm ² /nps) | Rel. Error (1 σ) | TXSAMC SIGMA (cm ⁻¹) | | | | | TXSAMC RRD (cm ⁻³) | | | | |
|--------------|--------------------------------------|--------------------------|----------------------------------|----------|----------|----------|----------|--------------------------------|----------|----------|----------|----------|
| | | | fission | nusigf | n2n | abs-fis | total | fission | nusigf | n2n | abs-fis | total |
| 1 | 0.00E+00 | 0.00% | 0.00E+00 | 0.00E+00 | 0.00E+00 | 1.30E+00 | 1.51E+00 | 0.00E+00 | 0.00E+00 | 0.00E+00 | 0.00E+00 | 0.00E+00 |
| 2 | 0.00E+00 | 0.00% | 0.00E+00 | 0.00E+00 | 0.00E+00 | 5.84E-01 | 7.91E-01 | 0.00E+00 | 0.00E+00 | 0.00E+00 | 0.00E+00 | 0.00E+00 |
| 3 | 0.00E+00 | 0.00% | 0.00E+00 | 0.00E+00 | 0.00E+00 | 2.02E-01 | 4.04E-01 | 0.00E+00 | 0.00E+00 | 0.00E+00 | 0.00E+00 | 0.00E+00 |
| 4 | 0.00E+00 | 0.00% | 0.00E+00 | 0.00E+00 | 0.00E+00 | 2.46E-01 | 4.58E-01 | 0.00E+00 | 0.00E+00 | 0.00E+00 | 0.00E+00 | 0.00E+00 |
| 5 | 0.00E+00 | 0.00% | 0.00E+00 | 0.00E+00 | 0.00E+00 | 2.48E-01 | 4.72E-01 | 0.00E+00 | 0.00E+00 | 0.00E+00 | 0.00E+00 | 0.00E+00 |
| 6 | 0.00E+00 | 0.00% | 0.00E+00 | 0.00E+00 | 0.00E+00 | 1.63E-02 | 2.20E-01 | 0.00E+00 | 0.00E+00 | 0.00E+00 | 0.00E+00 | 0.00E+00 |
| 7 | 0.00E+00 | 0.00% | 0.00E+00 | 0.00E+00 | 0.00E+00 | 4.03E-02 | 2.48E-01 | 0.00E+00 | 0.00E+00 | 0.00E+00 | 0.00E+00 | 0.00E+00 |
| 8 | 4.40E-10 | 100.00% | 0.00E+00 | 0.00E+00 | 0.00E+00 | 5.62E-02 | 4.13E-01 | 0.00E+00 | 0.00E+00 | 0.00E+00 | 2.47E-11 | 1.82E-10 |
| 9 | 6.59E-09 | 71.21% | 0.00E+00 | 0.00E+00 | 0.00E+00 | 1.17E-02 | 2.19E-01 | 0.00E+00 | 0.00E+00 | 0.00E+00 | 7.68E-11 | 1.44E-09 |
| 10 | 3.38E-08 | 28.92% | 0.00E+00 | 0.00E+00 | 0.00E+00 | 6.85E-03 | 2.23E-01 | 0.00E+00 | 0.00E+00 | 0.00E+00 | 2.32E-10 | 7.55E-09 |
| 11 | 1.89E-07 | 13.81% | 0.00E+00 | 0.00E+00 | 0.00E+00 | 5.50E-03 | 1.31E+00 | 0.00E+00 | 0.00E+00 | 0.00E+00 | 1.04E-09 | 2.47E-07 |
| 12 | 9.90E-07 | 5.76% | 0.00E+00 | 0.00E+00 | 0.00E+00 | 7.97E-03 | 4.44E-01 | 0.00E+00 | 0.00E+00 | 0.00E+00 | 7.89E-09 | 4.40E-07 |
| 13 | 6.32E-06 | 2.20% | 0.00E+00 | 0.00E+00 | 0.00E+00 | 5.52E-03 | 2.58E-01 | 0.00E+00 | 0.00E+00 | 0.00E+00 | 3.49E-08 | 1.63E-06 |
| 14 | 2.43E-05 | 1.15% | 0.00E+00 | 0.00E+00 | 0.00E+00 | 3.75E-03 | 2.67E-01 | 0.00E+00 | 0.00E+00 | 0.00E+00 | 9.10E-08 | 6.49E-06 |
| 15 | 6.98E-05 | 0.72% | 0.00E+00 | 0.00E+00 | 0.00E+00 | 2.35E-03 | 2.08E-01 | 0.00E+00 | 0.00E+00 | 0.00E+00 | 1.64E-07 | 1.45E-05 |
| 16 | 5.46E-05 | 0.82% | 0.00E+00 | 0.00E+00 | 0.00E+00 | 1.64E-03 | 2.30E-01 | 0.00E+00 | 0.00E+00 | 0.00E+00 | 8.98E-08 | 1.26E-05 |
| 17 | 5.45E-05 | 0.86% | 0.00E+00 | 0.00E+00 | 0.00E+00 | 1.17E-03 | 2.04E-01 | 0.00E+00 | 0.00E+00 | 0.00E+00 | 6.40E-08 | 1.11E-05 |
| 18 | 7.36E-05 | 0.76% | 0.00E+00 | 0.00E+00 | 0.00E+00 | 8.57E-04 | 2.60E-01 | 0.00E+00 | 0.00E+00 | 0.00E+00 | 6.31E-08 | 1.91E-05 |
| 19 | 5.42E-05 | 0.90% | 0.00E+00 | 0.00E+00 | 0.00E+00 | 6.57E-04 | 2.07E-01 | 0.00E+00 | 0.00E+00 | 0.00E+00 | 3.56E-08 | 1.12E-05 |
| 20 | 2.97E-05 | 1.21% | 0.00E+00 | 0.00E+00 | 0.00E+00 | 5.52E-04 | 1.59E-01 | 0.00E+00 | 0.00E+00 | 0.00E+00 | 1.64E-08 | 4.73E-06 |
| 21 | 2.54E-05 | 1.30% | 0.00E+00 | 0.00E+00 | 0.00E+00 | 4.82E-04 | 1.62E-01 | 0.00E+00 | 0.00E+00 | 0.00E+00 | 1.23E-08 | 4.13E-06 |
| 22 | 2.55E-05 | 1.29% | 0.00E+00 | 0.00E+00 | 0.00E+00 | 4.21E-04 | 1.60E-01 | 0.00E+00 | 0.00E+00 | 0.00E+00 | 1.07E-08 | 4.08E-06 |
| 23 | 1.71E-05 | 1.59% | 0.00E+00 | 0.00E+00 | 0.00E+00 | 3.69E-04 | 1.34E-01 | 0.00E+00 | 0.00E+00 | 0.00E+00 | 6.30E-09 | 2.30E-06 |
| 24 | 1.79E-05 | 1.55% | 0.00E+00 | 0.00E+00 | 0.00E+00 | 4.87E-04 | 1.25E-01 | 0.00E+00 | 0.00E+00 | 0.00E+00 | 8.71E-09 | 2.23E-06 |
| 25 | 2.88E-06 | 3.74% | 0.00E+00 | 0.00E+00 | 5.37E-08 | 2.37E-03 | 1.12E-01 | 0.00E+00 | 0.00E+00 | 1.54E-13 | 6.81E-09 | 3.22E-07 |
| 26 | 8.81E-07 | 6.68% | 0.00E+00 | 0.00E+00 | 5.72E-05 | 5.25E-03 | 1.07E-01 | 0.00E+00 | 0.00E+00 | 5.04E-11 | 4.63E-09 | 9.41E-08 |
| 27 | 1.25E-07 | 17.00% | 0.00E+00 | 0.00E+00 | 2.17E-03 | 7.62E-03 | 1.03E-01 | 0.00E+00 | 0.00E+00 | 2.70E-10 | 9.49E-10 | 1.29E-08 |
| 28 | 4.03E-08 | 35.00% | 0.00E+00 | 0.00E+00 | 5.85E-03 | 4.67E-03 | 1.04E-01 | 0.00E+00 | 0.00E+00 | 2.36E-10 | 1.88E-10 | 4.20E-09 |
| 29 | 1.07E-08 | 54.53% | 0.00E+00 | 0.00E+00 | 2.12E-02 | 0.00E+00 | 1.31E-01 | 0.00E+00 | 0.00E+00 | 2.27E-10 | 0.00E+00 | 1.39E-09 |
| 30 | 0.00E+00 | 0.00% | 0.00E+00 | 0.00E+00 | 1.31E-02 | 0.00E+00 | 1.08E-01 | 0.00E+00 | 0.00E+00 | 0.00E+00 | 0.00E+00 | 0.00E+00 |
| Total | 4.58E-04 | 0.32% | 0.00E+00 | 0.00E+00 | 4.24E-02 | 2.76E+00 | 9.75E+00 | 0.00E+00 | 0.00E+00 | 7.83E-10 | 6.19E-07 | 9.53E-05 |

TABLE 16
MCNP reaction rates and reaction rate comparison in SCR tally region 2

| Energy | MCNP RRD (cm ⁻³) | | | | | MCNP Standard Deviation | | | | | Partial Percent Error (TXSAMC-MCNP)/MCNP | | | | |
|--------|------------------------------|----------|----------|----------|----------|-------------------------|--------|--------|---------|---------|--|--------|--------|---------|--------|
| | fission | nusigf | n2n | abs-fis | total | fission | nusigf | n2n | abs-fis | total | fission | nusigf | n2n | abs-fis | total |
| 1 | 0.00E+00 | 0.00E+00 | 0.00E+00 | 0.00E+00 | 0.00E+00 | N/A | N/A | N/A | N/A | N/A | N/A | N/A | N/A | N/A | N/A |
| 2 | 0.00E+00 | 0.00E+00 | 0.00E+00 | 0.00E+00 | 0.00E+00 | N/A | N/A | N/A | N/A | N/A | N/A | N/A | N/A | N/A | N/A |
| 3 | 0.00E+00 | 0.00E+00 | 0.00E+00 | 0.00E+00 | 0.00E+00 | N/A | N/A | N/A | N/A | N/A | N/A | N/A | N/A | N/A | N/A |
| 4 | 0.00E+00 | 0.00E+00 | 0.00E+00 | 0.00E+00 | 0.00E+00 | N/A | N/A | N/A | N/A | N/A | N/A | N/A | N/A | N/A | N/A |
| 5 | 0.00E+00 | 0.00E+00 | 0.00E+00 | 0.00E+00 | 0.00E+00 | N/A | N/A | N/A | N/A | N/A | N/A | N/A | N/A | N/A | N/A |
| 6 | 0.00E+00 | 0.00E+00 | 0.00E+00 | 0.00E+00 | 0.00E+00 | N/A | N/A | N/A | N/A | N/A | N/A | N/A | N/A | N/A | N/A |
| 7 | 0.00E+00 | 0.00E+00 | 0.00E+00 | 0.00E+00 | 0.00E+00 | N/A | N/A | N/A | N/A | N/A | N/A | N/A | N/A | N/A | N/A |
| 8 | 0.00E+00 | 0.00E+00 | 0.00E+00 | 1.68E-13 | 7.19E-11 | N/A | N/A | N/A | 100.00% | 100.00% | N/A | N/A | N/A | 0.00% | 0.00% |
| 9 | 0.00E+00 | 0.00E+00 | 0.00E+00 | 3.73E-10 | 2.07E-09 | N/A | N/A | N/A | 71.70% | 42.95% | N/A | N/A | N/A | -0.05% | 0.00% |
| 10 | 0.00E+00 | 0.00E+00 | 0.00E+00 | 1.11E-10 | 7.30E-09 | N/A | N/A | N/A | 59.90% | 24.87% | N/A | N/A | N/A | 0.02% | 0.00% |
| 11 | 0.00E+00 | 0.00E+00 | 0.00E+00 | 1.65E-09 | 1.90E-07 | N/A | N/A | N/A | 41.52% | 13.96% | N/A | N/A | N/A | -0.10% | 0.06% |
| 12 | 0.00E+00 | 0.00E+00 | 0.00E+00 | 8.50E-09 | 4.45E-07 | N/A | N/A | N/A | 9.55% | 5.03% | N/A | N/A | N/A | -0.10% | -0.01% |
| 13 | 0.00E+00 | 0.00E+00 | 0.00E+00 | 3.52E-08 | 1.65E-06 | N/A | N/A | N/A | 3.70% | 1.77% | N/A | N/A | N/A | -0.04% | -0.01% |
| 14 | 0.00E+00 | 0.00E+00 | 0.00E+00 | 9.51E-08 | 6.53E-06 | N/A | N/A | N/A | 1.96% | 0.95% | N/A | N/A | N/A | -0.65% | -0.04% |
| 15 | 0.00E+00 | 0.00E+00 | 0.00E+00 | 1.65E-07 | 1.46E-05 | N/A | N/A | N/A | 1.18% | 0.57% | N/A | N/A | N/A | -0.05% | -0.11% |
| 16 | 0.00E+00 | 0.00E+00 | 0.00E+00 | 8.92E-08 | 1.25E-05 | N/A | N/A | N/A | 1.38% | 0.69% | N/A | N/A | N/A | 0.10% | 0.11% |
| 17 | 0.00E+00 | 0.00E+00 | 0.00E+00 | 6.41E-08 | 1.10E-05 | N/A | N/A | N/A | 1.45% | 0.71% | N/A | N/A | N/A | -0.02% | 0.13% |
| 18 | 0.00E+00 | 0.00E+00 | 0.00E+00 | 6.31E-08 | 1.91E-05 | N/A | N/A | N/A | 1.28% | 0.68% | N/A | N/A | N/A | 0.01% | 0.00% |
| 19 | 0.00E+00 | 0.00E+00 | 0.00E+00 | 3.70E-08 | 1.12E-05 | N/A | N/A | N/A | 1.54% | 0.75% | N/A | N/A | N/A | -0.22% | -0.01% |
| 20 | 0.00E+00 | 0.00E+00 | 0.00E+00 | 1.63E-08 | 4.71E-06 | N/A | N/A | N/A | 2.14% | 1.00% | N/A | N/A | N/A | 0.02% | 0.01% |
| 21 | 0.00E+00 | 0.00E+00 | 0.00E+00 | 1.24E-08 | 4.14E-06 | N/A | N/A | N/A | 2.28% | 1.07% | N/A | N/A | N/A | -0.02% | -0.01% |
| 22 | 0.00E+00 | 0.00E+00 | 0.00E+00 | 1.07E-08 | 4.08E-06 | N/A | N/A | N/A | 2.07% | 1.06% | N/A | N/A | N/A | 0.01% | 0.01% |
| 23 | 0.00E+00 | 0.00E+00 | 0.00E+00 | 6.44E-09 | 2.29E-06 | N/A | N/A | N/A | 2.19% | 1.29% | N/A | N/A | N/A | -0.02% | 0.01% |
| 24 | 0.00E+00 | 0.00E+00 | 0.00E+00 | 9.06E-09 | 2.25E-06 | N/A | N/A | N/A | 1.64% | 1.23% | N/A | N/A | N/A | -0.05% | -0.02% |
| 25 | 0.00E+00 | 0.00E+00 | 1.67E-13 | 6.81E-09 | 3.31E-07 | N/A | N/A | 26.57% | 3.29% | 2.93% | N/A | N/A | 0.00% | 0.00% | -0.01% |
| 26 | 0.00E+00 | 0.00E+00 | 6.86E-11 | 4.72E-09 | 9.45E-08 | N/A | N/A | 20.88% | 6.23% | 5.32% | N/A | N/A | -2.88% | -0.01% | 0.00% |
| 27 | 0.00E+00 | 0.00E+00 | 1.57E-10 | 1.28E-09 | 1.21E-08 | N/A | N/A | 46.25% | 16.12% | 14.51% | N/A | N/A | 17.98% | -0.05% | 0.00% |
| 28 | 0.00E+00 | 0.00E+00 | 2.79E-10 | 4.21E-10 | 4.38E-09 | N/A | N/A | 65.68% | 29.54% | 27.51% | N/A | N/A | -6.81% | -0.04% | 0.00% |
| 29 | 0.00E+00 | 0.00E+00 | 1.25E-10 | 9.83E-11 | 1.16E-09 | N/A | N/A | 82.10% | 50.89% | 46.01% | N/A | N/A | 16.10% | -0.02% | 0.00% |
| 30 | 0.00E+00 | 0.00E+00 | 0.00E+00 | 0.00E+00 | 0.00E+00 | N/A | N/A | N/A | N/A | N/A | N/A | N/A | N/A | N/A | N/A |
| Total | 0.00E+00 | 0.00E+00 | 6.30E-10 | 6.27E-07 | 9.52E-05 | N/A | N/A | 35.35% | 0.61% | 0.28% | N/A | N/A | 24.39% | -1.28% | 0.10% |

Since this region is composed of non-fissionable materials, there is obviously no fission or nusigf RRD. The total and non-fission absorption RRD's show good agreement with the MCNP-tallied RRD's but the (n,2n) cross section shows significant disagreement. It is not clear why the (n,2n) cross section shows this disagreement but it is possible that it may be related to the very poor statistics on the tallied (n,2n) reaction rate density. The standard deviation on the RRD's for this reaction are very poor compared both to other reactions in these cells and to other tally regions with relative standard deviations as high as 82%.

In Fig. 9 we see the difference in the TXSAMC and MCNP RRD's for the second tally region displayed graphically. This plot clearly shows the relatively poor

agreement at high energies in the (n,2n) reaction rate. With partial percent errors from 3-18%, the partial percent error for (n,2n) is as much as 1800 times larger than the typical partial percent error in the total or non-fission absorption cross sections. There are clearly some issues in TXSAMC with modeling the (n,2n) reaction when the reaction rate is very low.

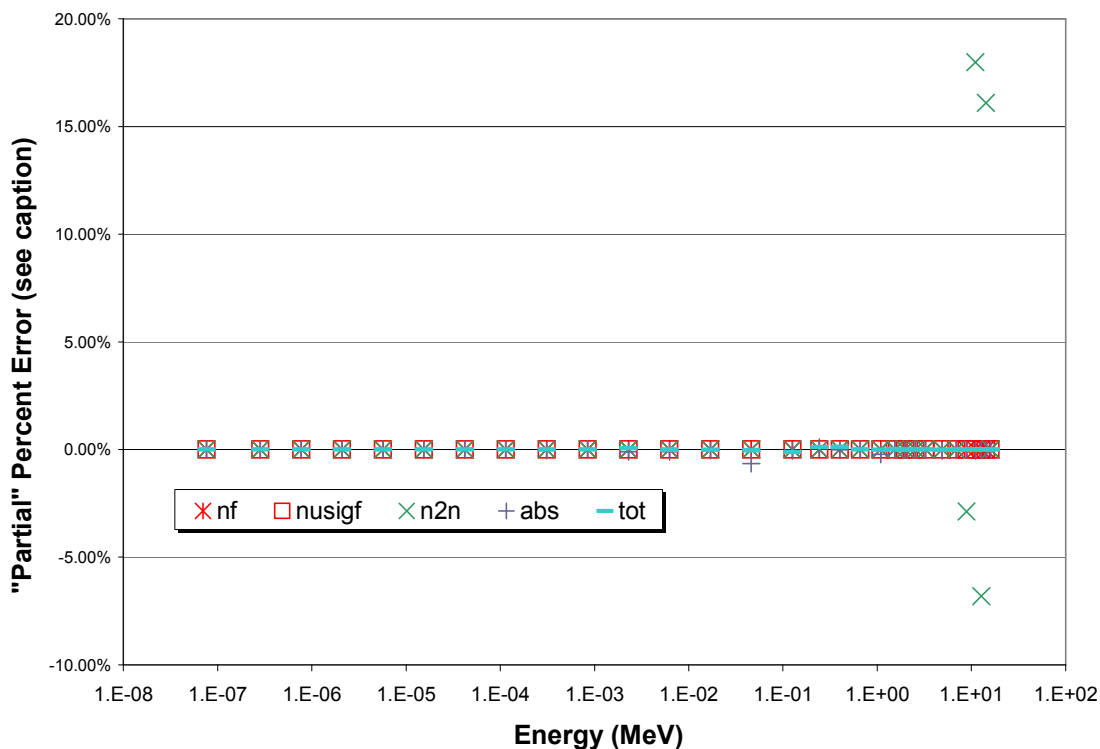


Fig. 9. "Partial" percent errors for reaction-rate densities in SCR tally region 2. Each "partial" error is plotted at the midpoint energy of its group. The percent error in a given reaction rate is the sum of the 30 partial percent errors.

The third tally region is composed of coolant channels filled with liquid sodium. In Table 17 we show the MCNP-tallied scalar flux for the pin-cell, its relative standard deviation, the TXSAMC-generated cross sections and the TXSAMC-generated reaction rate densities for the third tally region. Table 18 shows the MCNP-tallied reaction rate

densities, their standard deviations and the partial percent error between the TXSAMC-generated reaction rates and the MCNP-tallied reaction rates for the third tally region. It should be noted that as a result of the homogenous nature of these cells, there is no heterogeneity option applied in the TRANSX module of TXSAMC and no mixing (since it is all one nuclide). Essentially, this cell is modeled as an infinite dilute (σ_0 equivalent to infinity) mixture of sodium in an infinite cell (no spatial effects).

TABLE 17
MCNP scalar flux, TXSAMC cross sections and reaction rates in SCR tally region 3

| Energy Group | Scalar Flux (n/cm ² /nps) | Rel. Error (1 σ) | TXSAMC SIGMA (cm ⁻¹) | | | | | TXSAMC RRD (cm ⁻³) | | | | | |
|--------------|--------------------------------------|--------------------------|----------------------------------|----------|----------|----------|----------|--------------------------------|----------|----------|----------|----------|----------|
| | | | fission | nusigf | n2n | abs-fis | total | fission | nusigf | n2n | abs-fis | total | |
| 1 | 0.00E+00 | 0.00% | 0.00E+00 | 0.00E+00 | 0.00E+00 | 1.34E-02 | 1.87E-01 | 0.00E+00 | 0.00E+00 | 0.00E+00 | 0.00E+00 | 0.00E+00 | 0.00E+00 |
| 2 | 0.00E+00 | 0.00% | 0.00E+00 | 0.00E+00 | 0.00E+00 | 8.73E-03 | 1.80E-01 | 0.00E+00 | 0.00E+00 | 0.00E+00 | 0.00E+00 | 0.00E+00 | 0.00E+00 |
| 3 | 0.00E+00 | 0.00% | 0.00E+00 | 0.00E+00 | 0.00E+00 | 5.38E-03 | 1.74E-01 | 0.00E+00 | 0.00E+00 | 0.00E+00 | 0.00E+00 | 0.00E+00 | 0.00E+00 |
| 4 | 0.00E+00 | 0.00% | 0.00E+00 | 0.00E+00 | 0.00E+00 | 3.27E-03 | 1.70E-01 | 0.00E+00 | 0.00E+00 | 0.00E+00 | 0.00E+00 | 0.00E+00 | 0.00E+00 |
| 5 | 0.00E+00 | 0.00% | 0.00E+00 | 0.00E+00 | 0.00E+00 | 1.99E-03 | 1.68E-01 | 0.00E+00 | 0.00E+00 | 0.00E+00 | 0.00E+00 | 0.00E+00 | 0.00E+00 |
| 6 | 0.00E+00 | 0.00% | 0.00E+00 | 0.00E+00 | 0.00E+00 | 1.04E-03 | 1.65E-01 | 0.00E+00 | 0.00E+00 | 0.00E+00 | 0.00E+00 | 0.00E+00 | 0.00E+00 |
| 7 | 0.00E+00 | 0.00% | 0.00E+00 | 0.00E+00 | 0.00E+00 | 6.55E-04 | 1.65E-01 | 0.00E+00 | 0.00E+00 | 0.00E+00 | 0.00E+00 | 0.00E+00 | 0.00E+00 |
| 8 | 0.00E+00 | 0.00% | 0.00E+00 | 0.00E+00 | 0.00E+00 | 4.52E-04 | 1.65E-01 | 0.00E+00 | 0.00E+00 | 0.00E+00 | 0.00E+00 | 0.00E+00 | 0.00E+00 |
| 9 | 0.00E+00 | 0.00% | 0.00E+00 | 0.00E+00 | 0.00E+00 | 3.16E-04 | 1.68E-01 | 0.00E+00 | 0.00E+00 | 0.00E+00 | 0.00E+00 | 0.00E+00 | 0.00E+00 |
| 10 | 2.94E-08 | 30.25% | 0.00E+00 | 0.00E+00 | 0.00E+00 | 3.30E-04 | 1.91E-01 | 0.00E+00 | 0.00E+00 | 0.00E+00 | 9.72E-12 | 5.63E-09 | |
| 11 | 2.03E-07 | 11.42% | 0.00E+00 | 0.00E+00 | 0.00E+00 | 5.00E-03 | 5.24E+00 | 0.00E+00 | 0.00E+00 | 0.00E+00 | 1.01E-09 | 1.06E-06 | |
| 12 | 9.59E-07 | 5.41% | 0.00E+00 | 0.00E+00 | 0.00E+00 | 1.33E-04 | 4.82E-01 | 0.00E+00 | 0.00E+00 | 0.00E+00 | 1.28E-10 | 4.62E-07 | |
| 13 | 6.59E-06 | 2.15% | 0.00E+00 | 0.00E+00 | 0.00E+00 | 2.45E-06 | 2.32E-01 | 0.00E+00 | 0.00E+00 | 0.00E+00 | 1.61E-11 | 1.53E-06 | |
| 14 | 2.47E-05 | 1.13% | 0.00E+00 | 0.00E+00 | 0.00E+00 | 9.75E-05 | 2.71E-01 | 0.00E+00 | 0.00E+00 | 0.00E+00 | 2.41E-09 | 6.70E-06 | |
| 15 | 7.03E-05 | 0.72% | 0.00E+00 | 0.00E+00 | 0.00E+00 | 3.43E-05 | 1.81E-01 | 0.00E+00 | 0.00E+00 | 0.00E+00 | 2.41E-09 | 1.27E-05 | |
| 16 | 5.52E-05 | 0.83% | 0.00E+00 | 0.00E+00 | 0.00E+00 | 5.29E-05 | 2.21E-01 | 0.00E+00 | 0.00E+00 | 0.00E+00 | 2.92E-09 | 1.22E-05 | |
| 17 | 5.50E-05 | 0.87% | 0.00E+00 | 0.00E+00 | 0.00E+00 | 2.29E-05 | 1.84E-01 | 0.00E+00 | 0.00E+00 | 0.00E+00 | 1.26E-09 | 1.01E-05 | |
| 18 | 7.43E-05 | 0.76% | 0.00E+00 | 0.00E+00 | 0.00E+00 | 1.68E-05 | 2.66E-01 | 0.00E+00 | 0.00E+00 | 0.00E+00 | 1.25E-09 | 1.98E-05 | |
| 19 | 5.35E-05 | 0.91% | 0.00E+00 | 0.00E+00 | 0.00E+00 | 1.20E-05 | 1.98E-01 | 0.00E+00 | 0.00E+00 | 0.00E+00 | 6.42E-10 | 1.06E-05 | |
| 20 | 2.99E-05 | 1.20% | 0.00E+00 | 0.00E+00 | 0.00E+00 | 1.08E-05 | 1.42E-01 | 0.00E+00 | 0.00E+00 | 0.00E+00 | 3.22E-10 | 4.24E-06 | |
| 21 | 2.63E-05 | 1.29% | 0.00E+00 | 0.00E+00 | 0.00E+00 | 1.01E-05 | 1.49E-01 | 0.00E+00 | 0.00E+00 | 0.00E+00 | 2.65E-10 | 3.92E-06 | |
| 22 | 2.56E-05 | 1.28% | 0.00E+00 | 0.00E+00 | 0.00E+00 | 9.46E-06 | 1.48E-01 | 0.00E+00 | 0.00E+00 | 0.00E+00 | 2.42E-10 | 3.79E-06 | |
| 23 | 1.74E-05 | 1.59% | 0.00E+00 | 0.00E+00 | 0.00E+00 | 8.87E-06 | 1.20E-01 | 0.00E+00 | 0.00E+00 | 0.00E+00 | 1.55E-10 | 2.09E-06 | |
| 24 | 1.81E-05 | 1.54% | 0.00E+00 | 0.00E+00 | 0.00E+00 | 1.91E-04 | 1.09E-01 | 0.00E+00 | 0.00E+00 | 0.00E+00 | 3.46E-09 | 1.98E-06 | |
| 25 | 2.82E-06 | 3.80% | 0.00E+00 | 0.00E+00 | 0.00E+00 | 2.31E-03 | 9.46E-02 | 0.00E+00 | 0.00E+00 | 0.00E+00 | 6.52E-09 | 2.67E-07 | |
| 26 | 8.89E-07 | 6.71% | 0.00E+00 | 0.00E+00 | 0.00E+00 | 5.70E-03 | 8.67E-02 | 0.00E+00 | 0.00E+00 | 0.00E+00 | 5.07E-09 | 7.70E-08 | |
| 27 | 1.55E-07 | 15.72% | 0.00E+00 | 0.00E+00 | 0.00E+00 | 1.08E-02 | 8.62E-02 | 0.00E+00 | 0.00E+00 | 0.00E+00 | 1.67E-09 | 1.34E-08 | |
| 28 | 2.71E-08 | 36.99% | 0.00E+00 | 0.00E+00 | 5.13E-05 | 1.15E-02 | 8.85E-02 | 0.00E+00 | 0.00E+00 | 1.39E-12 | 3.12E-10 | 2.40E-09 | |
| 29 | 1.40E-08 | 52.58% | 0.00E+00 | 0.00E+00 | 1.49E-03 | 8.92E-03 | 9.01E-02 | 0.00E+00 | 0.00E+00 | 2.09E-11 | 1.25E-10 | 1.26E-09 | |
| 30 | 1.96E-10 | 100.00% | 0.00E+00 | 0.00E+00 | 4.50E-03 | 5.16E-03 | 9.20E-02 | 0.00E+00 | 0.00E+00 | 8.81E-13 | 1.01E-12 | 1.80E-11 | |
| Total | 4.62E-04 | 0.32% | 0.00E+00 | 0.00E+00 | 6.05E-03 | 8.55E-02 | 1.02E+01 | 0.00E+00 | 0.00E+00 | 0.00E+00 | 2.32E-11 | 3.02E-08 | 9.15E-05 |

TABLE 18
MCNP reaction rates and reaction rate comparison in SCR tally region 3

| Energy Group | MCNP RRD (cm ⁻³) | | | | | MCNP Standard Deviation | | | | | Partial Percent Error (TXSAMC-MCNP)/MCNP | | | | |
|-----------------|------------------------------|----------|----------|----------|----------|-------------------------|--------|---------|---------|---------|--|--------|---------|---------|-------|
| | fission | nusigf | n2n | abs-fis | total | fission | nusigf | n2n | abs-fis | total | fission | nusigf | n2n | abs-fis | total |
| 1 | 0.00E+00 | 0.00E+00 | 0.00E+00 | 0.00E+00 | 0.00E+00 | N/A | N/A | N/A | N/A | N/A | N/A | N/A | N/A | N/A | N/A |
| 2 | 0.00E+00 | 0.00E+00 | 0.00E+00 | 0.00E+00 | 0.00E+00 | N/A | N/A | N/A | N/A | N/A | N/A | N/A | N/A | N/A | N/A |
| 3 | 0.00E+00 | 0.00E+00 | 0.00E+00 | 0.00E+00 | 0.00E+00 | N/A | N/A | N/A | N/A | N/A | N/A | N/A | N/A | N/A | N/A |
| 4 | 0.00E+00 | 0.00E+00 | 0.00E+00 | 0.00E+00 | 0.00E+00 | N/A | N/A | N/A | N/A | N/A | N/A | N/A | N/A | N/A | N/A |
| 5 | 0.00E+00 | 0.00E+00 | 0.00E+00 | 0.00E+00 | 0.00E+00 | N/A | N/A | N/A | N/A | N/A | N/A | N/A | N/A | N/A | N/A |
| 6 | 0.00E+00 | 0.00E+00 | 0.00E+00 | 0.00E+00 | 0.00E+00 | N/A | N/A | N/A | N/A | N/A | N/A | N/A | N/A | N/A | N/A |
| 7 | 0.00E+00 | 0.00E+00 | 0.00E+00 | 0.00E+00 | 0.00E+00 | N/A | N/A | N/A | N/A | N/A | N/A | N/A | N/A | N/A | N/A |
| 8 | 0.00E+00 | 0.00E+00 | 0.00E+00 | 0.00E+00 | 0.00E+00 | N/A | N/A | N/A | N/A | N/A | N/A | N/A | N/A | N/A | N/A |
| 9 | 0.00E+00 | 0.00E+00 | 0.00E+00 | 0.00E+00 | 0.00E+00 | N/A | N/A | N/A | N/A | N/A | N/A | N/A | N/A | N/A | N/A |
| 10 | 0.00E+00 | 0.00E+00 | 0.00E+00 | 9.95E-12 | 5.74E-09 | N/A | N/A | N/A | 29.72% | 29.84% | N/A | N/A | N/A | 0.00% | 0.00% |
| 11 | 0.00E+00 | 0.00E+00 | 0.00E+00 | 3.26E-10 | 2.68E-07 | N/A | N/A | N/A | 12.67% | 13.38% | N/A | N/A | N/A | 2.45% | 0.91% |
| 12 | 0.00E+00 | 0.00E+00 | 0.00E+00 | 8.24E-11 | 4.14E-07 | N/A | N/A | N/A | 9.73% | 5.88% | N/A | N/A | N/A | 0.16% | 0.06% |
| 13 | 0.00E+00 | 0.00E+00 | 0.00E+00 | 1.63E-11 | 1.53E-06 | N/A | N/A | N/A | 2.58% | 2.16% | N/A | N/A | N/A | 0.00% | 0.00% |
| 14 | 0.00E+00 | 0.00E+00 | 0.00E+00 | 1.79E-09 | 5.82E-06 | N/A | N/A | N/A | 21.35% | 1.18% | N/A | N/A | N/A | 2.22% | 1.00% |
| 15 | 0.00E+00 | 0.00E+00 | 0.00E+00 | 1.82E-09 | 1.27E-05 | N/A | N/A | N/A | 11.13% | 0.72% | N/A | N/A | N/A | 2.11% | 0.01% |
| 16 | 0.00E+00 | 0.00E+00 | 0.00E+00 | 2.59E-09 | 1.14E-05 | N/A | N/A | N/A | 4.67% | 0.86% | N/A | N/A | N/A | 1.18% | 0.86% |
| 17 | 0.00E+00 | 0.00E+00 | 0.00E+00 | 1.20E-09 | 9.78E-06 | N/A | N/A | N/A | 4.71% | 0.89% | N/A | N/A | N/A | 0.21% | 0.39% |
| 18 | 0.00E+00 | 0.00E+00 | 0.00E+00 | 1.25E-09 | 1.89E-05 | N/A | N/A | N/A | 0.77% | 0.81% | N/A | N/A | N/A | 0.02% | 0.99% |
| 19 | 0.00E+00 | 0.00E+00 | 0.00E+00 | 6.41E-10 | 1.05E-05 | N/A | N/A | N/A | 0.91% | 0.93% | N/A | N/A | N/A | 0.00% | 0.11% |
| 20 | 0.00E+00 | 0.00E+00 | 0.00E+00 | 3.22E-10 | 4.21E-06 | N/A | N/A | N/A | 1.20% | 1.21% | N/A | N/A | N/A | 0.00% | 0.04% |
| 21 | 0.00E+00 | 0.00E+00 | 0.00E+00 | 2.65E-10 | 3.89E-06 | N/A | N/A | N/A | 1.29% | 1.31% | N/A | N/A | N/A | 0.00% | 0.03% |
| 22 | 0.00E+00 | 0.00E+00 | 0.00E+00 | 2.42E-10 | 3.78E-06 | N/A | N/A | N/A | 1.28% | 1.28% | N/A | N/A | N/A | 0.00% | 0.01% |
| 23 | 0.00E+00 | 0.00E+00 | 0.00E+00 | 1.55E-10 | 2.08E-06 | N/A | N/A | N/A | 1.59% | 1.60% | N/A | N/A | N/A | 0.00% | 0.01% |
| 24 | 0.00E+00 | 0.00E+00 | 0.00E+00 | 3.43E-09 | 1.97E-06 | N/A | N/A | N/A | 3.36% | 1.54% | N/A | N/A | N/A | 0.08% | 0.01% |
| 25 | 0.00E+00 | 0.00E+00 | 0.00E+00 | 6.64E-09 | 2.67E-07 | N/A | N/A | N/A | 4.00% | 3.82% | N/A | N/A | N/A | -0.42% | 0.00% |
| 26 | 0.00E+00 | 0.00E+00 | 0.00E+00 | 5.05E-09 | 7.68E-08 | N/A | N/A | N/A | 6.83% | 6.71% | N/A | N/A | N/A | 0.08% | 0.00% |
| 27 | 0.00E+00 | 0.00E+00 | 0.00E+00 | 1.69E-09 | 1.34E-08 | N/A | N/A | N/A | 15.77% | 15.73% | N/A | N/A | N/A | -0.05% | 0.00% |
| 28 | 0.00E+00 | 0.00E+00 | 1.63E-12 | 3.15E-10 | 2.40E-09 | N/A | N/A | 72.48% | 36.94% | 37.00% | N/A | N/A | -0.77% | -0.01% | 0.00% |
| 29 | 0.00E+00 | 0.00E+00 | 2.88E-11 | 1.43E-10 | 1.27E-09 | N/A | N/A | 54.37% | 52.72% | 52.55% | N/A | N/A | -25.10% | -0.06% | 0.00% |
| 30 | 0.00E+00 | 0.00E+00 | 9.05E-13 | 1.89E-12 | 1.80E-11 | N/A | N/A | 100.00% | 100.00% | 100.00% | N/A | N/A | -0.07% | 0.00% | 0.00% |
| Total | 0.00E+00 | 0.00E+00 | 3.13E-11 | 2.80E-08 | 8.77E-05 | N/A | N/A | 51.37% | 2.56% | 0.34% | N/A | N/A | -25.95% | 7.96% | 4.42% |

As expected, this region of non-fissionable material had no fission or fission neutron emission reactions and a fairly small number of (n,2n) reactions. It is readily apparent that this region has a greater error in the overall reaction rates than other regions examined so far. Part of this error comes from the area around the sodium resonance in group 11. Most of the rest of the error shows up in a modest overstatement of the RRD by TXSAMC in higher energy groups. Fortunately, the flux is already relatively small in that group so the total error is a more manageable 5-10%. The above-mentioned 2.8 keV sodium resonance can be clearly seen in Fig. 10³.

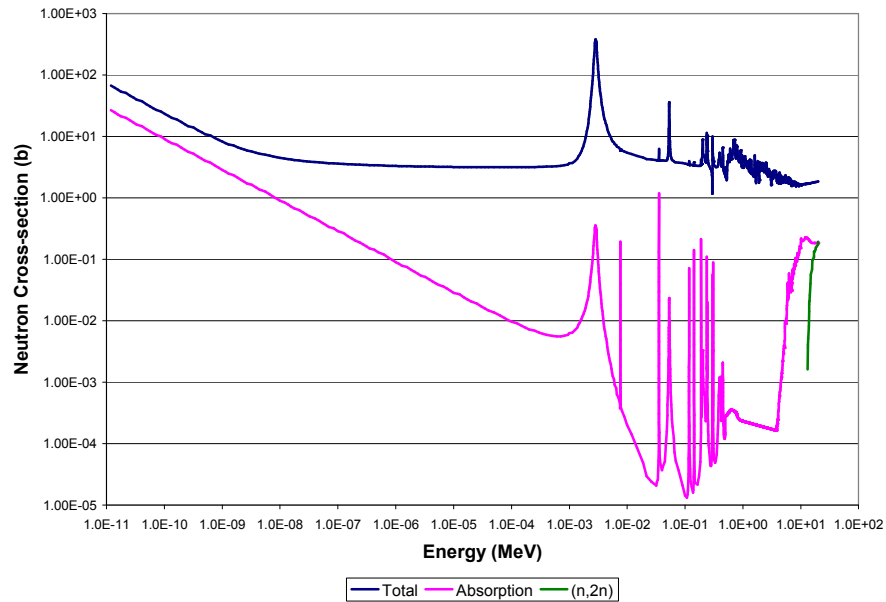


Fig. 10. Plot of total, absorption and (n,2n) cross sections for ^{23}Na .

In Fig. 11 we see the difference in the TXSAMC and MCNP RRD's for the third tally region displayed graphically. We see very little difference between the two reaction rates at low energies. There is a significant but still modest difference located in the region of the large sodium resonance. At very high energies we see significant error in the (n,2n) reaction rate. The (n,2n) reaction in group 29 shows the largest error seen in any group in any region or test problem. It is important to note that away from the resonance and the upper thresholds, the error is actually quite low.

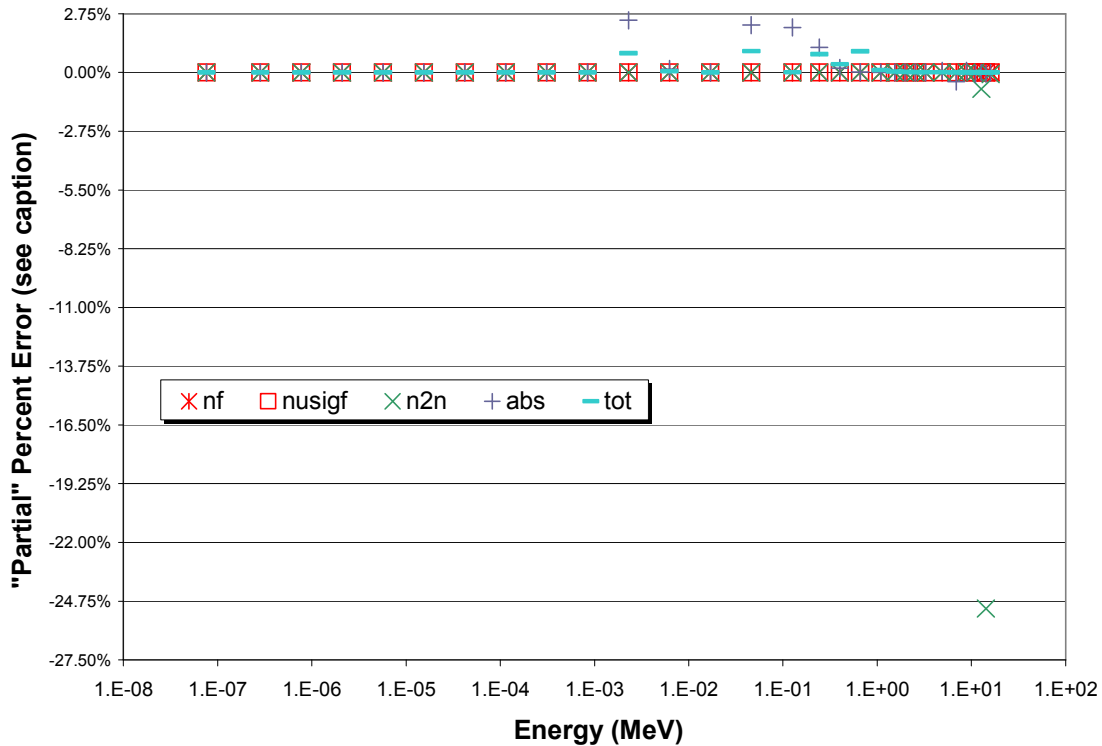


Fig. 11. "Partial" percent errors for reaction-rate densities in SCR tally region 3. Each "partial" error is plotted at the midpoint energy of its group. The percent error in a given reaction rate is the sum of the 30 partial percent errors.

The fourth tally region is composed of the eight nearest fuel pin-cells to each control rod location for a total of sixteen cells. In Table 19 we show the MCNP-tallied scalar flux for the pin-cell, its relative standard deviation, the TXSAMC-generated cross sections and the TXSAMC-generated reaction rate densities for the fourth tally region. Table 20 shows the MCNP-tallied reaction rate densities, their standard deviations and the partial percent error between the TXSAMC-generated reaction rates and the MCNP-tallied reaction rates for the fourth tally region. The hope with modeling this region was to obtain a more accurate picture of the cross sections in this region of depressed flux

due to the presence of the control rod. It should be noted that the presence of a control rod in a fast system has less of an effect than it might in a thermal system since much of the absorbing power of the rod is in thermal regions.

TABLE 19
MCNP scalar flux, TXSAMC cross sections and reaction rates in SCR tally region 4

| Energy | Scalar Flux | Rel. Error | TXSAMC SIGMA (cm ⁻¹) | | | | | TXSAMC RRD (cm ⁻³) | | | | |
|--------|--------------------------|---------------|----------------------------------|----------|----------|----------|----------|--------------------------------|----------|----------|----------|----------|
| Group | (n/cm ² /nps) | (1 σ) | fission | nusigf | n2n | abs-fis | total | fission | nusigf | n2n | abs-fis | total |
| 1 | 0.00E+00 | 0.00% | 2.89E+00 | 7.04E+00 | 0.00E+00 | 5.00E-01 | 3.76E+00 | 0.00E+00 | 0.00E+00 | 0.00E+00 | 0.00E+00 | 0.00E+00 |
| 2 | 0.00E+00 | 0.00% | 2.06E+00 | 5.03E+00 | 0.00E+00 | 4.35E-01 | 2.86E+00 | 0.00E+00 | 0.00E+00 | 0.00E+00 | 0.00E+00 | 0.00E+00 |
| 3 | 0.00E+00 | 0.00% | 8.49E-01 | 2.07E+00 | 0.00E+00 | 1.18E-01 | 1.32E+00 | 0.00E+00 | 0.00E+00 | 0.00E+00 | 0.00E+00 | 0.00E+00 |
| 4 | 0.00E+00 | 0.00% | 2.10E-01 | 5.12E-01 | 0.00E+00 | 7.75E-02 | 6.22E-01 | 0.00E+00 | 0.00E+00 | 0.00E+00 | 0.00E+00 | 0.00E+00 |
| 5 | 0.00E+00 | 0.00% | 1.50E-01 | 3.65E-01 | 0.00E+00 | 1.66E-01 | 6.35E-01 | 0.00E+00 | 0.00E+00 | 0.00E+00 | 0.00E+00 | 0.00E+00 |
| 6 | 0.00E+00 | 0.00% | 2.30E-01 | 5.59E-01 | 0.00E+00 | 2.40E-01 | 8.25E-01 | 0.00E+00 | 0.00E+00 | 0.00E+00 | 0.00E+00 | 0.00E+00 |
| 7 | 2.14E-11 | 100.00% | 2.66E-01 | 6.47E-01 | 0.00E+00 | 1.28E-01 | 6.66E-01 | 5.69E-12 | 1.39E-11 | 0.00E+00 | 2.74E-12 | 1.43E-11 |
| 8 | 1.98E-10 | 78.96% | 7.42E-02 | 1.81E-01 | 0.00E+00 | 4.44E-02 | 3.43E-01 | 1.47E-11 | 3.57E-11 | 0.00E+00 | 8.78E-12 | 6.78E-11 |
| 9 | 1.33E-09 | 56.69% | 1.56E-01 | 3.79E-01 | 0.00E+00 | 6.96E-02 | 5.63E-01 | 2.07E-10 | 5.03E-10 | 0.00E+00 | 9.25E-11 | 7.48E-10 |
| 10 | 2.16E-08 | 17.12% | 1.02E-01 | 2.48E-01 | 0.00E+00 | 5.51E-02 | 4.99E-01 | 2.20E-09 | 5.35E-09 | 0.00E+00 | 1.19E-09 | 1.08E-08 |
| 11 | 1.40E-07 | 7.39% | 6.60E-02 | 1.61E-01 | 0.00E+00 | 3.12E-02 | 7.80E-01 | 9.27E-09 | 2.26E-08 | 0.00E+00 | 4.38E-09 | 1.09E-07 |
| 12 | 9.20E-07 | 2.89% | 4.35E-02 | 1.06E-01 | 0.00E+00 | 1.71E-02 | 4.71E-01 | 4.00E-08 | 9.74E-08 | 0.00E+00 | 1.58E-08 | 4.33E-07 |
| 13 | 6.08E-06 | 1.20% | 3.16E-02 | 7.68E-02 | 0.00E+00 | 1.16E-02 | 4.01E-01 | 1.92E-07 | 4.66E-07 | 0.00E+00 | 7.07E-08 | 2.44E-06 |
| 14 | 2.38E-05 | 0.64% | 2.39E-02 | 5.80E-02 | 0.00E+00 | 8.05E-03 | 3.81E-01 | 5.70E-07 | 1.38E-06 | 0.00E+00 | 1.92E-07 | 9.06E-06 |
| 15 | 6.90E-05 | 0.40% | 1.91E-02 | 4.65E-02 | 0.00E+00 | 5.20E-03 | 3.37E-01 | 1.32E-06 | 3.21E-06 | 0.00E+00 | 3.59E-07 | 2.33E-05 |
| 16 | 5.48E-05 | 0.43% | 1.66E-02 | 4.08E-02 | 0.00E+00 | 3.58E-03 | 3.20E-01 | 9.12E-07 | 2.24E-06 | 0.00E+00 | 1.96E-07 | 1.75E-05 |
| 17 | 5.41E-05 | 0.44% | 1.53E-02 | 3.77E-02 | 0.00E+00 | 2.66E-03 | 3.67E-01 | 8.26E-07 | 2.04E-06 | 0.00E+00 | 1.44E-07 | 1.98E-05 |
| 18 | 7.50E-05 | 0.40% | 1.43E-02 | 3.57E-02 | 0.00E+00 | 1.96E-03 | 2.83E-01 | 1.07E-06 | 2.67E-06 | 0.00E+00 | 1.47E-07 | 2.12E-05 |
| 19 | 5.53E-05 | 0.46% | 1.52E-02 | 3.86E-02 | 0.00E+00 | 1.54E-03 | 2.79E-01 | 8.42E-07 | 2.14E-06 | 0.00E+00 | 8.54E-08 | 1.54E-05 |
| 20 | 3.09E-05 | 0.59% | 1.63E-02 | 4.22E-02 | 0.00E+00 | 1.17E-03 | 2.09E-01 | 5.03E-07 | 1.31E-06 | 0.00E+00 | 3.62E-08 | 6.45E-06 |
| 21 | 2.70E-05 | 0.64% | 1.70E-02 | 4.49E-02 | 0.00E+00 | 8.83E-04 | 2.01E-01 | 4.58E-07 | 1.21E-06 | 0.00E+00 | 2.38E-08 | 5.42E-06 |
| 22 | 2.74E-05 | 0.64% | 1.69E-02 | 4.58E-02 | 0.00E+00 | 5.83E-04 | 1.82E-01 | 4.62E-07 | 1.25E-06 | 0.00E+00 | 1.60E-08 | 4.98E-06 |
| 23 | 1.85E-05 | 0.77% | 1.61E-02 | 4.49E-02 | 0.00E+00 | 3.61E-04 | 2.17E-01 | 2.98E-07 | 8.31E-07 | 0.00E+00 | 6.69E-09 | 4.01E-06 |
| 24 | 1.94E-05 | 0.77% | 1.51E-02 | 4.49E-02 | 1.07E-04 | 2.08E-03 | 2.00E-01 | 2.92E-07 | 8.69E-07 | 2.08E-09 | 4.02E-08 | 3.87E-06 |
| 25 | 3.16E-06 | 1.85% | 2.00E-02 | 6.75E-02 | 4.91E-03 | 0.00E+00 | 1.63E-01 | 6.33E-08 | 2.13E-07 | 1.55E-08 | 0.00E+00 | 5.15E-07 |
| 26 | 9.53E-07 | 3.32% | 2.43E-02 | 8.86E-02 | 9.65E-03 | 0.00E+00 | 1.55E-01 | 2.32E-08 | 8.44E-08 | 9.20E-09 | 0.00E+00 | 1.48E-07 |
| 27 | 1.66E-07 | 7.82% | 2.45E-02 | 9.64E-02 | 1.41E-02 | 0.00E+00 | 1.59E-01 | 4.06E-09 | 1.60E-08 | 2.34E-09 | 0.00E+00 | 2.64E-08 |
| 28 | 3.51E-08 | 18.19% | 2.60E-02 | 1.09E-01 | 1.33E-02 | 0.00E+00 | 1.62E-01 | 9.10E-10 | 3.82E-09 | 4.67E-10 | 0.00E+00 | 5.69E-09 |
| 29 | 1.52E-08 | 26.34% | 2.83E-02 | 1.25E-01 | 1.12E-02 | 0.00E+00 | 1.63E-01 | 4.31E-10 | 1.90E-09 | 1.71E-10 | 0.00E+00 | 2.49E-09 |
| 30 | 3.63E-09 | 53.02% | 2.72E-02 | 1.25E-01 | 9.14E-03 | 0.00E+00 | 1.61E-01 | 9.86E-11 | 4.55E-10 | 3.32E-11 | 0.00E+00 | 5.84E-10 |
| Total | 4.67E-04 | 0.18% | 7.47E+00 | 1.85E+01 | 6.25E-02 | 1.92E+00 | 1.77E+01 | 7.89E-06 | 2.01E-05 | 2.98E-08 | 1.34E-06 | 1.35E-04 |

TABLE 20
MCNP reaction rates and reaction rate comparison in SCR tally region 4

| Energy Group | MCNP RRD (cm ⁻³) | | | | | MCNP Standard Deviation | | | | | Partial Percent Error (TXSAMC-MCNP)/MCNP | | | | |
|-----------------|------------------------------|----------|----------|----------|----------|-------------------------|---------|--------|---------|---------|--|--------|--------|---------|--------|
| | fission | nusigf | n2n | abs-fis | total | fission | nusigf | n2n | abs-fis | total | fission | nusigf | n2n | abs-fis | total |
| 1 | 0.00E+00 | 0.00E+00 | 0.00E+00 | 0.00E+00 | 0.00E+00 | N/A | N/A | N/A | N/A | N/A | N/A | N/A | N/A | N/A | N/A |
| 2 | 0.00E+00 | 0.00E+00 | 0.00E+00 | 0.00E+00 | 0.00E+00 | N/A | N/A | N/A | N/A | N/A | N/A | N/A | N/A | N/A | N/A |
| 3 | 0.00E+00 | 0.00E+00 | 0.00E+00 | 0.00E+00 | 0.00E+00 | N/A | N/A | N/A | N/A | N/A | N/A | N/A | N/A | N/A | N/A |
| 4 | 0.00E+00 | 0.00E+00 | 0.00E+00 | 0.00E+00 | 0.00E+00 | N/A | N/A | N/A | N/A | N/A | N/A | N/A | N/A | N/A | N/A |
| 5 | 0.00E+00 | 0.00E+00 | 0.00E+00 | 0.00E+00 | 0.00E+00 | N/A | N/A | N/A | N/A | N/A | N/A | N/A | N/A | N/A | N/A |
| 6 | 0.00E+00 | 0.00E+00 | 0.00E+00 | 0.00E+00 | 0.00E+00 | N/A | N/A | N/A | N/A | N/A | N/A | N/A | N/A | N/A | N/A |
| 7 | 7.40E-11 | 1.80E-10 | 0.00E+00 | 2.71E-11 | 1.10E-10 | 100.00% | 100.00% | N/A | 100.00% | 100.00% | 0.00% | 0.00% | N/A | 0.00% | 0.00% |
| 8 | 1.85E-11 | 4.49E-11 | 0.00E+00 | 2.33E-11 | 1.21E-10 | 93.25% | 93.25% | N/A | 94.73% | 92.10% | 0.00% | 0.00% | N/A | 0.00% | 0.00% |
| 9 | 2.14E-10 | 5.21E-10 | 0.00E+00 | 1.00E-10 | 7.79E-10 | 56.78% | 56.78% | N/A | 61.83% | 53.76% | 0.00% | 0.00% | N/A | 0.00% | 0.00% |
| 10 | 2.03E-09 | 4.94E-09 | 0.00E+00 | 1.12E-09 | 1.04E-08 | 17.86% | 17.86% | N/A | 17.79% | 15.00% | 0.00% | 0.00% | N/A | 0.01% | 0.00% |
| 11 | 9.37E-09 | 2.28E-08 | 0.00E+00 | 5.13E-09 | 1.20E-07 | 8.11% | 8.11% | N/A | 7.94% | 5.68% | 0.00% | 0.00% | N/A | -0.05% | -0.01% |
| 12 | 4.02E-08 | 9.80E-08 | 0.00E+00 | 1.61E-08 | 4.45E-07 | 3.13% | 3.13% | N/A | 3.04% | 2.33% | 0.00% | 0.00% | N/A | -0.02% | -0.01% |
| 13 | 1.91E-07 | 4.65E-07 | 0.00E+00 | 7.06E-08 | 2.45E-06 | 1.28% | 1.28% | N/A | 1.28% | 1.02% | 0.01% | 0.01% | N/A | 0.01% | -0.01% |
| 14 | 5.74E-07 | 1.39E-06 | 0.00E+00 | 1.94E-07 | 9.14E-06 | 0.67% | 0.67% | N/A | 0.67% | 0.53% | -0.06% | -0.06% | N/A | -0.16% | -0.06% |
| 15 | 1.32E-06 | 3.23E-06 | 0.00E+00 | 3.62E-07 | 2.34E-05 | 0.42% | 0.42% | N/A | 0.42% | 0.34% | -0.11% | -0.10% | N/A | -0.21% | -0.11% |
| 16 | 9.15E-07 | 2.25E-06 | 0.00E+00 | 1.96E-07 | 1.76E-05 | 0.45% | 0.45% | N/A | 0.44% | 0.35% | -0.04% | -0.04% | N/A | -0.03% | -0.04% |
| 17 | 8.33E-07 | 2.06E-06 | 0.00E+00 | 1.46E-07 | 2.00E-05 | 0.47% | 0.47% | N/A | 0.46% | 0.40% | -0.09% | -0.08% | N/A | -0.15% | -0.17% |
| 18 | 1.08E-06 | 2.70E-06 | 0.00E+00 | 1.49E-07 | 2.14E-05 | 0.42% | 0.42% | N/A | 0.41% | 0.31% | -0.13% | -0.12% | N/A | -0.15% | -0.19% |
| 19 | 8.45E-07 | 2.15E-06 | 0.00E+00 | 8.55E-08 | 1.55E-05 | 0.49% | 0.49% | N/A | 0.48% | 0.38% | -0.04% | -0.04% | N/A | -0.01% | -0.01% |
| 20 | 5.07E-07 | 1.31E-06 | 0.00E+00 | 3.65E-08 | 6.50E-06 | 0.64% | 0.64% | N/A | 0.62% | 0.50% | -0.04% | -0.04% | N/A | -0.02% | -0.04% |
| 21 | 4.61E-07 | 1.22E-06 | 0.00E+00 | 2.40E-08 | 5.46E-06 | 0.68% | 0.68% | N/A | 0.67% | 0.54% | -0.03% | -0.03% | N/A | -0.01% | -0.03% |
| 22 | 4.64E-07 | 1.26E-06 | 0.00E+00 | 1.61E-08 | 5.00E-06 | 0.68% | 0.68% | N/A | 0.67% | 0.52% | -0.02% | -0.02% | N/A | -0.01% | -0.02% |
| 23 | 3.01E-07 | 8.39E-07 | 0.00E+00 | 6.78E-09 | 4.05E-06 | 0.82% | 0.82% | N/A | 0.81% | 0.69% | -0.04% | -0.04% | N/A | -0.01% | -0.03% |
| 24 | 2.94E-07 | 8.77E-07 | 2.22E-09 | 4.22E-08 | 3.90E-06 | 0.82% | 0.82% | 2.73% | 1.02% | 0.68% | -0.03% | -0.04% | -0.49% | -0.14% | -0.03% |
| 25 | 6.30E-08 | 2.12E-07 | 1.54E-08 | 1.47E-08 | 5.17E-07 | 1.99% | 1.99% | 2.06% | 1.92% | 1.60% | 0.00% | 0.01% | 0.44% | -1.07% | 0.00% |
| 26 | 2.38E-08 | 8.66E-08 | 9.44E-09 | 5.68E-09 | 1.50E-07 | 3.56% | 3.56% | 3.50% | 2.93% | 2.89% | -0.01% | -0.01% | -0.81% | -0.41% | 0.00% |
| 27 | 3.87E-09 | 1.53E-08 | 2.25E-09 | 1.68E-09 | 2.58E-08 | 8.45% | 8.46% | 7.82% | 6.45% | 6.78% | 0.00% | 0.00% | 0.30% | -0.12% | 0.00% |
| 28 | 9.42E-10 | 3.95E-09 | 4.74E-10 | 3.39E-10 | 5.82E-09 | 18.61% | 18.64% | 16.58% | 14.17% | 15.45% | 0.00% | 0.00% | -0.02% | -0.02% | 0.00% |
| 29 | 4.45E-10 | 1.96E-09 | 1.57E-10 | 1.39E-10 | 2.57E-09 | 27.42% | 27.40% | 22.73% | 20.64% | 22.72% | 0.00% | 0.00% | 0.05% | -0.01% | 0.00% |
| 30 | 1.29E-10 | 5.98E-10 | 3.51E-11 | 2.90E-11 | 6.80E-10 | 56.63% | 56.62% | 40.17% | 47.43% | 49.82% | 0.00% | 0.00% | -0.01% | 0.00% | 0.00% |
| Total | 7.93E-06 | 2.02E-05 | 3.00E-08 | 1.37E-06 | 1.36E-04 | 0.19% | 0.19% | 1.70% | 0.24% | 0.16% | -0.62% | -0.61% | -0.53% | -2.61% | -0.73% |

From the second table, it appears that this goal was achieved as the relative difference in the reaction rates is significantly smaller than that of the first tally region. It appears that overall the cross sections reproduce the reaction rates very well. It is likely that this increase in accuracy is due to a greater uniformity in the flux seen in each cell; the flux seen by pins near a control rod can be significantly different than that seen by pins elsewhere in the reactor. This suggests that smaller regions do work better in the TXSAMC process and are useful for shielding areas with a depressed flux.

In Fig. 12 we see the difference in the TXSAMC and MCNP RRD's for the fourth tally region displayed graphically. The very small errors in the low energy range are quite obvious in this plot as well as the small error near the sodium resonance. At

very high energies we see modest error in the (n,2n) and fission/nusigf reaction rates. It is important to note that away from the resonance and the upper thresholds, the error is quite low. In fact, for much of the energy spectrum, the error is near zero. Even in the “worst” groups for error, the error is never more than one and half percent. It is also apparent that the error in this tally region is significantly less than that for the first three tally regions.

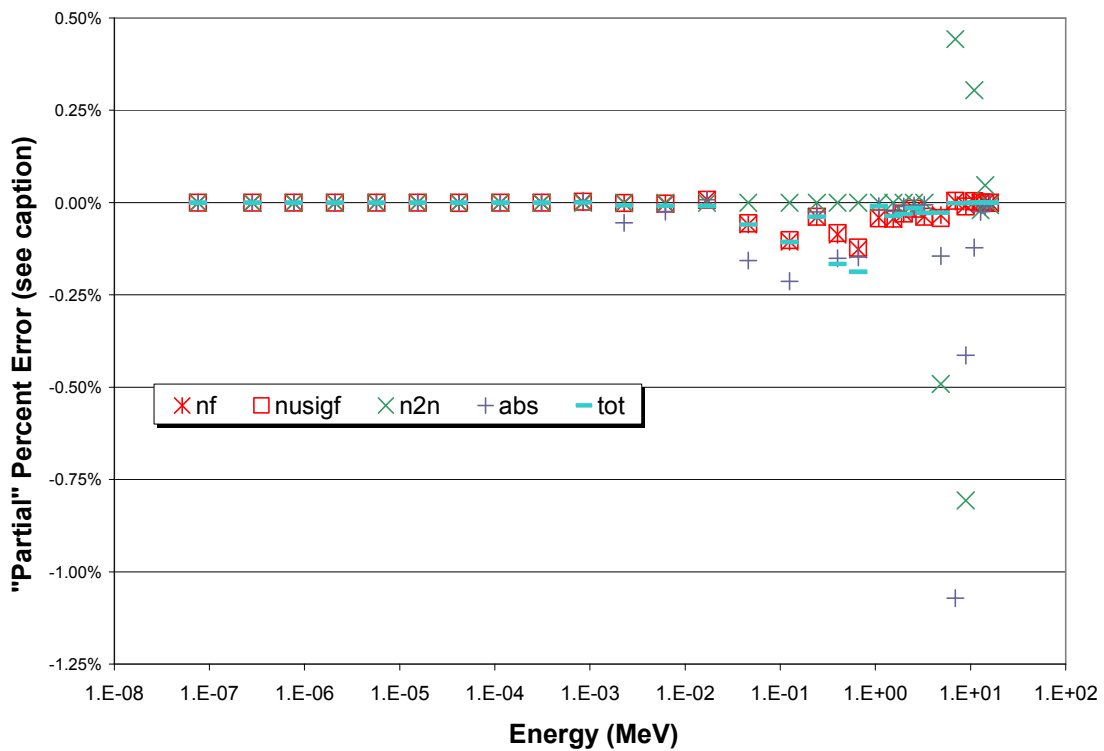


Fig. 12. “Partial” percent errors for reaction-rate densities in SCR tally region 4. Each “partial” error is plotted at the midpoint energy of its group. The percent error in a given reaction rate is the sum of the 30 partial percent errors.

The fifth tally region is composed of the eight nearest fuel pin-cells to each coolant channel location for a total of sixteen cells. In Table 21 we show the MCNP-tallied scalar flux for the pin-cell, its relative standard deviation, the TXSAMC-generated cross sections and the TXSAMC-generated reaction rate densities for the fifth tally region. Table 22 shows the MCNP-tallied reaction rate densities, their standard deviations and the partial percent error between the TXSAMC-generated reaction rates and the MCNP-tallied reaction rates for the fifth tally region.

TABLE 21
MCNP scalar flux, TXSAMC cross sections and reaction rates in SCR tally region 5

| Energy Group | Scalar Flux (n/cm ² /nps) | Rel. Error (1 σ) | TXSAMC SIGMA (cm ⁻¹) | | | | | TXSAMC RRD (cm ⁻³) | | | | | |
|--------------|--------------------------------------|--------------------------|----------------------------------|----------|----------|----------|----------|--------------------------------|----------|----------|----------|----------|----------|
| | | | fission | nusigf | n2n | abs-fis | total | fission | nusigf | n2n | abs-fis | total | |
| 1 | 0.00E+00 | 0.00% | 0.00E+00 | 0.00E+00 | 0.00E+00 | 0.00E+00 | 0.00E+00 | 0.00E+00 | 0.00E+00 | 0.00E+00 | 0.00E+00 | 0.00E+00 | 0.00E+00 |
| 2 | 0.00E+00 | 0.00% | 0.00E+00 | 0.00E+00 | 0.00E+00 | 0.00E+00 | 0.00E+00 | 0.00E+00 | 0.00E+00 | 0.00E+00 | 0.00E+00 | 0.00E+00 | 0.00E+00 |
| 3 | 0.00E+00 | 0.00% | 0.00E+00 | 0.00E+00 | 0.00E+00 | 0.00E+00 | 0.00E+00 | 0.00E+00 | 0.00E+00 | 0.00E+00 | 0.00E+00 | 0.00E+00 | 0.00E+00 |
| 4 | 0.00E+00 | 0.00% | 0.00E+00 | 0.00E+00 | 0.00E+00 | 0.00E+00 | 0.00E+00 | 0.00E+00 | 0.00E+00 | 0.00E+00 | 0.00E+00 | 0.00E+00 | 0.00E+00 |
| 5 | 0.00E+00 | 0.00% | 0.00E+00 | 0.00E+00 | 0.00E+00 | 0.00E+00 | 0.00E+00 | 0.00E+00 | 0.00E+00 | 0.00E+00 | 0.00E+00 | 0.00E+00 | 0.00E+00 |
| 6 | 0.00E+00 | 0.00% | 0.00E+00 | 0.00E+00 | 0.00E+00 | 0.00E+00 | 0.00E+00 | 0.00E+00 | 0.00E+00 | 0.00E+00 | 0.00E+00 | 0.00E+00 | 0.00E+00 |
| 7 | 0.00E+00 | 0.00% | 0.00E+00 | 0.00E+00 | 0.00E+00 | 0.00E+00 | 0.00E+00 | 0.00E+00 | 0.00E+00 | 0.00E+00 | 0.00E+00 | 0.00E+00 | 0.00E+00 |
| 8 | 0.00E+00 | 0.00% | 0.00E+00 | 0.00E+00 | 0.00E+00 | 0.00E+00 | 0.00E+00 | 0.00E+00 | 0.00E+00 | 0.00E+00 | 0.00E+00 | 0.00E+00 | 0.00E+00 |
| 9 | 1.15E-09 | 50.52% | 1.59E-10 | 3.88E-10 | 0.00E+00 | 7.14E-11 | 5.97E-10 | 1.78E-10 | 4.33E-10 | 0.00E+00 | 8.30E-11 | 6.47E-10 | 6.47E-10 |
| 10 | 2.28E-08 | 15.94% | 2.36E-09 | 5.74E-09 | 0.00E+00 | 1.28E-09 | 1.15E-08 | 2.42E-09 | 5.89E-09 | 0.00E+00 | 1.32E-09 | 1.21E-08 | 1.21E-08 |
| 11 | 1.59E-07 | 6.68% | 1.03E-08 | 2.51E-08 | 0.00E+00 | 4.88E-09 | 1.28E-07 | 1.13E-08 | 2.75E-08 | 0.00E+00 | 6.11E-09 | 1.30E-07 | 1.30E-07 |
| 12 | 9.70E-07 | 2.90% | 4.29E-08 | 1.04E-07 | 0.00E+00 | 1.69E-08 | 4.59E-07 | 4.20E-08 | 1.02E-07 | 0.00E+00 | 1.67E-08 | 4.69E-07 | 4.69E-07 |
| 13 | 6.21E-06 | 1.20% | 1.96E-07 | 4.75E-07 | 0.00E+00 | 7.20E-08 | 2.49E-06 | 1.96E-07 | 4.76E-07 | 0.00E+00 | 7.21E-08 | 2.51E-06 | 2.51E-06 |
| 14 | 2.39E-05 | 0.64% | 5.73E-07 | 1.39E-06 | 0.00E+00 | 1.93E-07 | 9.10E-06 | 5.77E-07 | 1.40E-06 | 0.00E+00 | 1.95E-07 | 9.17E-06 | 9.17E-06 |
| 15 | 6.90E-05 | 0.40% | 1.32E-06 | 3.21E-06 | 0.00E+00 | 3.59E-07 | 2.33E-05 | 1.32E-06 | 3.22E-06 | 0.00E+00 | 3.61E-07 | 2.34E-05 | 2.34E-05 |
| 16 | 5.50E-05 | 0.43% | 9.14E-07 | 2.24E-06 | 0.00E+00 | 1.97E-07 | 1.76E-05 | 9.17E-07 | 2.25E-06 | 0.00E+00 | 1.97E-07 | 1.76E-05 | 1.76E-05 |
| 17 | 5.42E-05 | 0.44% | 8.27E-07 | 2.04E-06 | 0.00E+00 | 1.44E-07 | 1.98E-05 | 8.31E-07 | 2.05E-06 | 0.00E+00 | 1.46E-07 | 2.01E-05 | 2.01E-05 |
| 18 | 7.56E-05 | 0.39% | 1.08E-06 | 2.70E-06 | 0.00E+00 | 1.48E-07 | 2.14E-05 | 1.09E-06 | 2.71E-06 | 0.00E+00 | 1.50E-07 | 2.16E-05 | 2.16E-05 |
| 19 | 5.52E-05 | 0.46% | 8.35E-07 | 2.12E-06 | 0.00E+00 | 8.47E-08 | 1.54E-05 | 8.41E-07 | 2.14E-06 | 0.00E+00 | 8.50E-08 | 1.54E-05 | 1.54E-05 |
| 20 | 3.10E-05 | 0.59% | 5.05E-07 | 1.31E-06 | 0.00E+00 | 3.63E-08 | 6.47E-06 | 5.07E-07 | 1.32E-06 | 0.00E+00 | 3.66E-08 | 6.51E-06 | 6.51E-06 |
| 21 | 2.69E-05 | 0.64% | 4.58E-07 | 1.21E-06 | 0.00E+00 | 2.38E-08 | 5.40E-06 | 4.59E-07 | 1.21E-06 | 0.00E+00 | 2.39E-08 | 5.43E-06 | 5.43E-06 |
| 22 | 2.74E-05 | 0.64% | 4.61E-07 | 1.25E-06 | 0.00E+00 | 1.59E-08 | 4.98E-06 | 4.67E-07 | 1.26E-06 | 0.00E+00 | 1.62E-08 | 5.02E-06 | 5.02E-06 |
| 23 | 1.85E-05 | 0.77% | 2.97E-07 | 8.31E-07 | 0.00E+00 | 6.69E-09 | 4.01E-06 | 3.01E-07 | 8.39E-07 | 0.00E+00 | 6.78E-09 | 4.04E-06 | 4.04E-06 |
| 24 | 1.95E-05 | 0.76% | 2.93E-07 | 8.73E-07 | 2.09E-09 | 4.04E-08 | 3.89E-06 | 2.96E-07 | 8.82E-07 | 2.15E-09 | 4.29E-08 | 3.93E-06 | 3.93E-06 |
| 25 | 3.12E-06 | 1.85% | 6.21E-08 | 2.09E-07 | 1.52E-08 | 0.00E+00 | 5.06E-07 | 6.15E-08 | 2.07E-07 | 1.50E-08 | 1.43E-08 | 5.07E-07 | 5.07E-07 |
| 26 | 9.56E-07 | 3.33% | 2.38E-08 | 8.65E-08 | 9.41E-09 | 0.00E+00 | 1.50E-07 | 2.40E-08 | 8.72E-08 | 9.45E-09 | 5.65E-09 | 1.51E-07 | 1.51E-07 |
| 27 | 1.76E-07 | 7.68% | 4.27E-09 | 1.68E-08 | 2.44E-09 | 0.00E+00 | 2.79E-08 | 4.37E-09 | 1.73E-08 | 2.53E-09 | 1.85E-09 | 2.84E-08 | 2.84E-08 |
| 28 | 2.69E-08 | 18.41% | 6.57E-10 | 2.76E-09 | 3.42E-10 | 0.00E+00 | 4.24E-09 | 6.87E-10 | 2.89E-09 | 3.46E-10 | 2.55E-10 | 4.34E-09 | 4.34E-09 |
| 29 | 9.02E-09 | 32.86% | 2.70E-10 | 1.19E-09 | 9.50E-11 | 0.00E+00 | 1.53E-09 | 2.29E-10 | 1.01E-09 | 8.92E-11 | 7.99E-11 | 1.41E-09 | 1.41E-09 |
| 30 | 4.04E-09 | 47.73% | 1.11E-10 | 5.13E-10 | 3.55E-11 | 0.00E+00 | 6.56E-10 | 1.17E-10 | 5.39E-10 | 3.42E-11 | 3.31E-11 | 6.75E-10 | 6.75E-10 |
| Total | 4.68E-04 | 0.18% | 7.91E-06 | 2.01E-05 | 2.96E-08 | 1.34E-06 | 1.35E-04 | 7.95E-06 | 2.02E-05 | 2.96E-08 | 1.38E-06 | 1.36E-04 | 1.36E-04 |

TABLE 22
MCNP reaction rates and reaction rate comparison in SCR tally region 5

| Energy Group | MCNP RRD (cm ⁻³) | | | | | MCNP Standard Deviation | | | | | Relative Difference (TXSAMC-MCNP)/MCNP | | | | |
|-----------------|------------------------------|----------|----------|----------|----------|-------------------------|--------|--------|---------|--------|--|--------|--------|---------|--------|
| | fission | nusigf | n2n | abs-fis | total | fission | nusigf | n2n | abs-fis | total | fission | nusigf | n2n | abs-fis | total |
| 1 | 0.00E+00 | 0.00E+00 | 0.00E+00 | 0.00E+00 | 0.00E+00 | N/A | N/A | N/A | N/A | N/A | N/A | N/A | N/A | N/A | N/A |
| 2 | 0.00E+00 | 0.00E+00 | 0.00E+00 | 0.00E+00 | 0.00E+00 | N/A | N/A | N/A | N/A | N/A | N/A | N/A | N/A | N/A | N/A |
| 3 | 0.00E+00 | 0.00E+00 | 0.00E+00 | 0.00E+00 | 0.00E+00 | N/A | N/A | N/A | N/A | N/A | N/A | N/A | N/A | N/A | N/A |
| 4 | 0.00E+00 | 0.00E+00 | 0.00E+00 | 0.00E+00 | 0.00E+00 | N/A | N/A | N/A | N/A | N/A | N/A | N/A | N/A | N/A | N/A |
| 5 | 0.00E+00 | 0.00E+00 | 0.00E+00 | 0.00E+00 | 0.00E+00 | N/A | N/A | N/A | N/A | N/A | N/A | N/A | N/A | N/A | N/A |
| 6 | 0.00E+00 | 0.00E+00 | 0.00E+00 | 0.00E+00 | 0.00E+00 | N/A | N/A | N/A | N/A | N/A | N/A | N/A | N/A | N/A | N/A |
| 7 | 0.00E+00 | 0.00E+00 | 0.00E+00 | 0.00E+00 | 0.00E+00 | N/A | N/A | N/A | N/A | N/A | N/A | N/A | N/A | N/A | N/A |
| 8 | 0.00E+00 | 0.00E+00 | 0.00E+00 | 0.00E+00 | 0.00E+00 | N/A | N/A | N/A | N/A | N/A | N/A | N/A | N/A | N/A | N/A |
| 9 | 1.78E-10 | 4.33E-10 | 0.00E+00 | 8.30E-11 | 6.47E-10 | 60.72% | 60.72% | N/A | 52.02% | 50.39% | 0.00% | 0.00% | N/A | 0.00% | 0.00% |
| 10 | 2.42E-09 | 5.89E-09 | 0.00E+00 | 1.32E-09 | 1.21E-08 | 17.17% | 17.17% | N/A | 16.53% | 14.97% | 0.00% | 0.00% | N/A | 0.00% | 0.00% |
| 11 | 1.13E-08 | 2.75E-08 | 0.00E+00 | 6.11E-09 | 1.30E-07 | 7.52% | 7.52% | N/A | 7.32% | 5.16% | -0.01% | -0.01% | N/A | -0.09% | 0.00% |
| 12 | 4.20E-08 | 1.02E-07 | 0.00E+00 | 1.67E-08 | 4.69E-07 | 3.14% | 3.14% | N/A | 3.05% | 2.32% | 0.01% | 0.01% | N/A | 0.01% | -0.01% |
| 13 | 1.96E-07 | 4.76E-07 | 0.00E+00 | 7.21E-08 | 2.51E-06 | 1.28% | 1.28% | N/A | 1.27% | 1.01% | 0.00% | 0.00% | N/A | -0.01% | -0.02% |
| 14 | 5.77E-07 | 1.40E-06 | 0.00E+00 | 1.95E-07 | 9.17E-06 | 0.67% | 0.67% | N/A | 0.67% | 0.53% | -0.05% | -0.05% | N/A | -0.15% | -0.05% |
| 15 | 1.32E-06 | 3.22E-06 | 0.00E+00 | 3.61E-07 | 2.34E-05 | 0.42% | 0.42% | N/A | 0.42% | 0.34% | -0.04% | -0.04% | N/A | -0.11% | -0.07% |
| 16 | 9.17E-07 | 2.25E-06 | 0.00E+00 | 1.97E-07 | 1.76E-05 | 0.45% | 0.45% | N/A | 0.44% | 0.35% | -0.04% | -0.04% | N/A | -0.03% | -0.04% |
| 17 | 8.31E-07 | 2.05E-06 | 0.00E+00 | 1.46E-07 | 2.01E-05 | 0.47% | 0.47% | N/A | 0.46% | 0.40% | -0.06% | -0.06% | N/A | -0.12% | -0.16% |
| 18 | 1.09E-06 | 2.71E-06 | 0.00E+00 | 1.50E-07 | 2.16E-05 | 0.42% | 0.42% | N/A | 0.41% | 0.31% | -0.07% | -0.07% | N/A | -0.11% | -0.18% |
| 19 | 8.41E-07 | 2.14E-06 | 0.00E+00 | 8.50E-08 | 1.54E-05 | 0.49% | 0.49% | N/A | 0.48% | 0.38% | -0.08% | -0.08% | N/A | -0.02% | -0.03% |
| 20 | 5.07E-07 | 1.32E-06 | 0.00E+00 | 3.66E-08 | 6.51E-06 | 0.64% | 0.64% | N/A | 0.62% | 0.50% | -0.03% | -0.03% | N/A | -0.02% | -0.03% |
| 21 | 4.59E-07 | 1.21E-06 | 0.00E+00 | 2.39E-08 | 5.43E-06 | 0.68% | 0.68% | N/A | 0.67% | 0.53% | -0.01% | -0.01% | N/A | -0.01% | -0.02% |
| 22 | 4.67E-07 | 1.26E-06 | 0.00E+00 | 1.62E-08 | 5.02E-06 | 0.68% | 0.68% | N/A | 0.67% | 0.52% | -0.07% | -0.08% | N/A | -0.02% | -0.03% |
| 23 | 3.01E-07 | 8.39E-07 | 0.00E+00 | 6.78E-09 | 4.04E-06 | 0.82% | 0.82% | N/A | 0.81% | 0.68% | -0.04% | -0.04% | N/A | -0.01% | -0.03% |
| 24 | 2.96E-07 | 8.82E-07 | 2.15E-09 | 4.29E-08 | 3.93E-06 | 0.81% | 0.81% | 2.70% | 1.01% | 0.67% | -0.04% | -0.05% | -0.23% | -0.18% | -0.03% |
| 25 | 6.15E-08 | 2.07E-07 | 1.50E-08 | 1.43E-08 | 5.07E-07 | 1.99% | 2.00% | 2.07% | 1.91% | 1.60% | 0.01% | 0.01% | 0.88% | -1.04% | 0.00% |
| 26 | 2.40E-08 | 8.72E-08 | 9.45E-09 | 5.65E-09 | 1.51E-07 | 3.51% | 3.51% | 3.46% | 2.89% | 2.86% | 0.00% | 0.00% | -0.12% | -0.41% | 0.00% |
| 27 | 4.37E-09 | 1.73E-08 | 2.53E-09 | 1.85E-09 | 2.84E-08 | 8.16% | 8.17% | 7.57% | 6.49% | 6.72% | 0.00% | 0.00% | -0.28% | -0.13% | 0.00% |
| 28 | 6.87E-10 | 2.89E-09 | 3.46E-10 | 2.55E-10 | 4.34E-09 | 19.96% | 20.00% | 17.41% | 14.90% | 16.16% | 0.00% | 0.00% | -0.01% | -0.02% | 0.00% |
| 29 | 2.29E-10 | 1.01E-09 | 8.92E-11 | 7.99E-11 | 1.41E-09 | 33.32% | 33.27% | 26.56% | 24.59% | 26.32% | 0.00% | 0.00% | 0.02% | -0.01% | 0.00% |
| 30 | 1.17E-10 | 5.39E-10 | 3.42E-11 | 3.31E-11 | 6.75E-10 | 47.87% | 47.89% | 32.77% | 35.53% | 39.13% | 0.00% | 0.00% | 0.00% | 0.00% | 0.00% |
| Total | 7.95E-06 | 2.02E-05 | 2.96E-08 | 1.38E-06 | 1.36E-04 | 0.19% | 0.19% | 1.71% | 0.24% | 0.16% | -0.53% | -0.54% | 0.25% | -2.46% | -0.70% |

Similar to the fourth tally region, this region shows less difference between the TXSAMC and MCNP RRD's than the first tally region. It is likely that this is due to the greater uniformity of flux in this smaller region. The overall error is very manageable at less than one percent for all but the absorption RRD. It should be noted that some of the groups that show up as having a very low partial percent error actually have significant differences between the MCNP-tallied RRD and the TXSAMC-produced RRD. One of the benefits to this statistical weighting approach (through the MCNP-derived scalar flux) is that many of the regions/energy groups with the worst error contribute least to the overall reaction rate so, to a certain extent, the high errors in certain energy groups are not important.

In Fig. 13 we see the difference in the TXSAMC and MCNP RRD's for the fifth tally region displayed graphically. The very low errors in the low energy range are quite obvious in this plot as well as the small error near the sodium resonance. The greater contributor to the overall difference is in the (n,2n) and fission/nusigf reaction rates at higher energies. It is important to note that away from the resonance and the upper thresholds, the error is quite low. In fact, for much of the energy spectrum, the error is near zero. It is also apparent that the error in this tally region is significantly less than that for the first three tally regions.

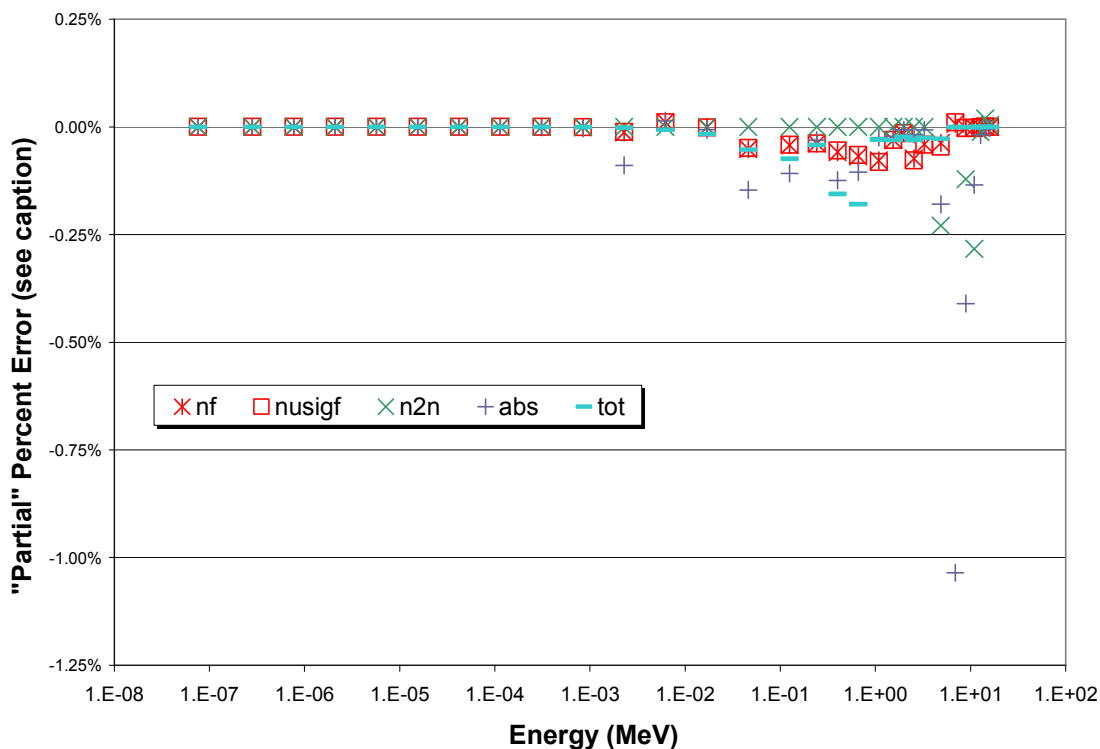


Fig. 13. "Partial" percent errors for reaction-rate densities in SCR tally region 5. Each "partial" error is plotted at the midpoint energy of its group. The percent error in a given reaction rate is the sum of the 30 partial percent errors.

Overall, it appears that the various tally regions in the SCR are reasonably well represented by the homogenized cross sections generated for each region. As expected, the smaller fuel tally regions (four and five) have a lower percent error than the core wide tally region (region one). This is probably due to the greater uniformity of flux in each pin-cell of the smaller regions relative to the larger region. It should be noted that while the error in the largest region is in the mid- to low-single digits, this is still decent performance and may be acceptable for certain applications. Obviously, the much lower error in the smaller regions is probably more broadly applicable. We also note that the problem of threshold reactions and major resonances is most apparent in the coolant channels so it might be suggested that in actual applications, the coolant channel cell cross sections should be smeared into the surrounding homogenized fuel cross sections. Again, TXSAMC appears to work fairly well for the square lattice reactor problem with heterogeneities.

SQUARE-COMPLEX REACTOR ALTERNATE

In order to test one of the features of TXSAMC, an alternate SCR problem (SCRA) was run that used a 187 group weighting function in the GROUPT module instead of the 30 group weighting function. All of the geometry and material layouts remained the same. We still produced 30 group cross sections in NJOY and shielded them in the same manner in TRANSX. The only differences from the SCR were the weighting function and the number of histories used in the MCNP portion of TXSAMC. In order to counter the increase in variance with the increase in the number of energy

bins used to produce the 187 group core-averaged scalar flux, the number of histories was increased from 2,000,000 to 10,000,000. One of the main goals with this test was to determine if we could reduce the difference between the TXSAMC-generated RRD's and the MCNP-tallied RRD's by calculating the within-group shape of the flux to create more accurate MGXS from NJOY. The results within each tally region are presented below.

The weighting function that is used in the NJOY module of TXSAMC is based on a core-averaged scalar flux for this reactor as tallied by MCNP using 187 energy bins. The group structure that defines these energy bins is shown in Table 4 in Chapter II. The multiplying scalar flux used to produce the TXSAMC RRD's is the cell-averaged scalar flux for the pin-cells within the specified tally region. The normalization of this scalar flux is over the combined cell volumes of the entire region. Since the TXSAMC-produced cross sections assume a one dimensional representation of the pin-cell, the MCNP-produced RRD's are adjusted to reflect this. For example, in the fuel pin-cells the MCNP RRD for each component (meat, clad, coolant) is multiplied by the cross-sectional area in the x-y plane of that component and divided by the total pin-cell cross-sectional area. The net effect of this adjustment is small as long as the pin length and vessel length are similar (i.e. not a lot of extra coolant) since the TXSAMC cross sections are produced by appropriately volume-normalized RZFLUX files and the MCNP RRD is also volume-normalized.

The first tally region is made up of all fuel pin-cells not adjacent to the coolant channels or control rods. In Tables 23 we show the MCNP-tallied scalar flux for the pin-

cell, its relative standard deviation, the TXSAMC-generated cross sections and the TXSAMC-generated reaction rate densities for the first tally region. Table 24 shows the MCNP-tallied reaction rate densities, their standard deviations and the partial percent error between the TXSAMC-generated reaction rates and the MCNP-tallied reaction rates for the first tally region.

TABLE 23
MCNP scalar flux, TXSAMC cross sections and reaction rates in SCRA tally region 1

| Energy Group | Scalar Flux (n/cm ² /hps) | Rel. Error (1 σ) | TXSAMC SIGMA (cm ⁻¹) | | | | | TXSAMC RRD (cm ⁻³) | | | | |
|--------------|--------------------------------------|--------------------------|----------------------------------|----------|----------|----------|----------|--------------------------------|----------|----------|----------|----------|
| | | | fission | nusigf | n2n | abs-fis | total | fission | nusigf | n2n | abs-fis | total |
| 1 | 0.00E+00 | 0.00% | 5.57E+00 | 1.36E+01 | 0.00E+00 | 9.86E-01 | 6.97E+00 | 0.00E+00 | 0.00E+00 | 0.00E+00 | 0.00E+00 | 0.00E+00 |
| 2 | 0.00E+00 | 0.00% | 2.14E+00 | 5.22E+00 | 0.00E+00 | 4.63E-01 | 2.96E+00 | 0.00E+00 | 0.00E+00 | 0.00E+00 | 0.00E+00 | 0.00E+00 |
| 3 | 0.00E+00 | 0.00% | 8.70E-01 | 2.12E+00 | 0.00E+00 | 1.41E-01 | 1.36E+00 | 0.00E+00 | 0.00E+00 | 0.00E+00 | 0.00E+00 | 0.00E+00 |
| 4 | 0.00E+00 | 0.00% | 2.36E-01 | 5.75E-01 | 0.00E+00 | 8.20E-02 | 6.53E-01 | 0.00E+00 | 0.00E+00 | 0.00E+00 | 0.00E+00 | 0.00E+00 |
| 5 | 0.00E+00 | 0.00% | 2.80E-01 | 6.80E-01 | 0.00E+00 | 7.22E-02 | 7.84E-01 | 0.00E+00 | 0.00E+00 | 0.00E+00 | 0.00E+00 | 0.00E+00 |
| 6 | 2.52E-11 | 48.42% | 3.29E-01 | 8.01E-01 | 0.00E+00 | 1.63E-01 | 7.95E-01 | 8.28E-12 | 2.02E-11 | 0.00E+00 | 4.09E-12 | 2.00E-11 |
| 7 | 4.72E-11 | 33.47% | 3.66E-01 | 8.92E-01 | 0.00E+00 | 1.79E-01 | 8.71E-01 | 1.73E-11 | 4.21E-11 | 0.00E+00 | 8.44E-12 | 4.11E-11 |
| 8 | 3.12E-10 | 14.85% | 1.91E-01 | 4.65E-01 | 0.00E+00 | 1.16E-01 | 6.33E-01 | 5.96E-11 | 1.45E-10 | 0.00E+00 | 3.61E-11 | 1.97E-10 |
| 9 | 2.48E-09 | 5.06% | 1.36E-01 | 3.31E-01 | 0.00E+00 | 6.07E-02 | 5.18E-01 | 3.38E-10 | 8.21E-10 | 0.00E+00 | 1.50E-10 | 1.28E-09 |
| 10 | 3.51E-08 | 1.41% | 9.75E-02 | 2.37E-01 | 0.00E+00 | 5.31E-02 | 4.88E-01 | 3.43E-09 | 8.34E-09 | 0.00E+00 | 1.86E-09 | 1.71E-08 |
| 11 | 1.29E-07 | 0.77% | 6.93E-02 | 1.69E-01 | 0.00E+00 | 3.69E-02 | 5.81E-01 | 8.96E-09 | 2.18E-08 | 0.00E+00 | 4.76E-09 | 7.51E-08 |
| 12 | 7.91E-07 | 0.38% | 4.28E-02 | 1.04E-01 | 0.00E+00 | 1.70E-02 | 4.64E-01 | 3.38E-08 | 8.23E-08 | 0.00E+00 | 1.34E-08 | 3.67E-07 |
| 13 | 4.88E-06 | 0.17% | 3.13E-02 | 7.61E-02 | 0.00E+00 | 1.15E-02 | 4.00E-01 | 1.53E-07 | 3.72E-07 | 0.00E+00 | 5.63E-08 | 1.95E-06 |
| 14 | 1.84E-05 | 0.09% | 2.40E-02 | 5.82E-02 | 0.00E+00 | 8.10E-03 | 3.80E-01 | 4.43E-07 | 1.07E-06 | 0.00E+00 | 1.49E-07 | 7.01E-06 |
| 15 | 5.33E-05 | 0.06% | 1.91E-02 | 4.65E-02 | 0.00E+00 | 5.20E-03 | 3.37E-01 | 1.02E-06 | 2.48E-06 | 0.00E+00 | 2.77E-07 | 1.80E-05 |
| 16 | 4.21E-05 | 0.05% | 1.66E-02 | 4.07E-02 | 0.00E+00 | 3.56E-03 | 3.19E-01 | 6.98E-07 | 1.71E-06 | 0.00E+00 | 1.50E-07 | 1.34E-05 |
| 17 | 4.16E-05 | 0.05% | 1.53E-02 | 3.77E-02 | 0.00E+00 | 2.68E-03 | 3.58E-01 | 6.36E-07 | 1.57E-06 | 0.00E+00 | 1.11E-07 | 1.49E-05 |
| 18 | 5.78E-05 | 0.05% | 1.43E-02 | 3.57E-02 | 0.00E+00 | 1.97E-03 | 2.82E-01 | 8.28E-07 | 2.06E-06 | 0.00E+00 | 1.14E-07 | 1.63E-05 |
| 19 | 4.27E-05 | 0.06% | 1.52E-02 | 3.85E-02 | 0.00E+00 | 1.53E-03 | 2.76E-01 | 6.48E-07 | 1.64E-06 | 0.00E+00 | 6.54E-08 | 1.18E-05 |
| 20 | 2.37E-05 | 0.08% | 1.63E-02 | 4.22E-02 | 0.00E+00 | 1.17E-03 | 2.09E-01 | 3.87E-07 | 1.00E-06 | 0.00E+00 | 2.78E-08 | 4.95E-06 |
| 21 | 2.09E-05 | 0.09% | 1.70E-02 | 4.48E-02 | 0.00E+00 | 8.81E-04 | 2.01E-01 | 3.55E-07 | 9.39E-07 | 0.00E+00 | 1.85E-08 | 4.20E-06 |
| 22 | 2.12E-05 | 0.09% | 1.69E-02 | 4.56E-02 | 0.00E+00 | 5.82E-04 | 1.82E-01 | 3.57E-07 | 9.68E-07 | 0.00E+00 | 1.23E-08 | 3.85E-06 |
| 23 | 1.42E-05 | 0.11% | 1.61E-02 | 4.49E-02 | 0.00E+00 | 3.63E-04 | 2.15E-01 | 2.29E-07 | 6.39E-07 | 0.00E+00 | 5.16E-09 | 3.07E-06 |
| 24 | 1.51E-05 | 0.11% | 1.51E-02 | 4.49E-02 | 1.12E-04 | 2.07E-03 | 2.00E-01 | 2.27E-07 | 6.78E-07 | 1.69E-09 | 3.12E-08 | 3.01E-06 |
| 25 | 2.43E-06 | 0.28% | 1.98E-02 | 6.66E-02 | 4.83E-03 | 0.00E+00 | 1.62E-01 | 4.81E-08 | 1.62E-07 | 1.17E-08 | 0.00E+00 | 3.94E-07 |
| 26 | 7.30E-07 | 0.50% | 2.44E-02 | 8.88E-02 | 9.68E-03 | 0.00E+00 | 1.56E-01 | 1.78E-08 | 6.49E-08 | 7.07E-09 | 0.00E+00 | 1.14E-07 |
| 27 | 1.40E-07 | 1.13% | 2.41E-02 | 9.48E-02 | 1.39E-02 | 0.00E+00 | 1.58E-01 | 3.36E-09 | 1.33E-08 | 1.94E-09 | 0.00E+00 | 2.20E-08 |
| 28 | 2.61E-08 | 2.55% | 2.55E-02 | 1.07E-01 | 1.31E-02 | 0.00E+00 | 1.61E-01 | 6.65E-10 | 2.79E-09 | 3.42E-10 | 0.00E+00 | 4.20E-09 |
| 29 | 9.20E-09 | 4.36% | 2.86E-02 | 1.26E-01 | 1.04E-02 | 0.00E+00 | 1.66E-01 | 2.64E-10 | 1.16E-09 | 9.56E-11 | 0.00E+00 | 1.52E-09 |
| 30 | 3.04E-09 | 7.49% | 2.82E-02 | 1.31E-01 | 8.95E-03 | 0.00E+00 | 1.64E-01 | 8.59E-11 | 4.00E-10 | 2.73E-11 | 0.00E+00 | 4.98E-10 |
| Total | 3.60E-04 | 0.02% | 1.07E+01 | 2.63E+01 | 6.09E-02 | 2.41E+00 | 2.14E+01 | 6.09E-06 | 1.55E-05 | 2.29E-08 | 1.04E-06 | 1.03E-04 |

The first table shows similar results to the SCR. There are minor differences in the various TXSAMC-generated cross sections but they are very similar overall. At first glance, this suggests that the cross sections are somewhat insensitive to the within group shape of the flux. We also observe overall errors for all five reactions in the second table

that are very similar to those reported in the SCR. Again, this tends to support the idea that using a 187 group spectrum does not materially reduce the amount of error in the cross sections. It should be noted that there is some difficulty in quantifying very small reductions in the amount of difference between TXSAMC and MCNP since the increase in histories resulted in lower variances and slightly different means for the MCNP-tallied RRD's. In effect, changing the weight function also changes the benchmark.

TABLE 24
MCNP reaction rates and reaction rate comparison in SCRA tally region 1

| Energy Group | MCNP RRD (cm ⁻³) | | | | | MCNP Standard Deviation | | | | | Partial Percent Error (TXSAMC-MCNP)/MCNP | | | | |
|--------------|------------------------------|----------|----------|----------|----------|-------------------------|--------|-------|---------|--------|--|--------|--------|---------|--------|
| | fission | nusigf | n2n | abs-fis | total | fission | nusigf | n2n | abs-fis | total | fission | nusigf | n2n | abs-fis | total |
| 1 | 0.00E+00 | 0.00E+00 | 0.00E+00 | 0.00E+00 | 0.00E+00 | N/A | N/A | N/A | N/A | N/A | N/A | N/A | N/A | N/A | N/A |
| 2 | 0.00E+00 | 0.00E+00 | 0.00E+00 | 0.00E+00 | 0.00E+00 | N/A | N/A | N/A | N/A | N/A | N/A | N/A | N/A | N/A | N/A |
| 3 | 0.00E+00 | 0.00E+00 | 0.00E+00 | 0.00E+00 | 0.00E+00 | N/A | N/A | N/A | N/A | N/A | N/A | N/A | N/A | N/A | N/A |
| 4 | 0.00E+00 | 0.00E+00 | 0.00E+00 | 0.00E+00 | 0.00E+00 | N/A | N/A | N/A | N/A | N/A | N/A | N/A | N/A | N/A | N/A |
| 5 | 0.00E+00 | 0.00E+00 | 0.00E+00 | 0.00E+00 | 0.00E+00 | N/A | N/A | N/A | N/A | N/A | N/A | N/A | N/A | N/A | N/A |
| 6 | 6.12E-12 | 1.49E-11 | 0.00E+00 | 2.70E-12 | 1.76E-11 | 37.23% | 37.23% | N/A | 39.53% | 38.44% | 0.00% | 0.00% | N/A | 0.00% | 0.00% |
| 7 | 1.98E-11 | 4.82E-11 | 0.00E+00 | 7.94E-12 | 4.40E-11 | 29.28% | 29.28% | N/A | 28.74% | 26.75% | 0.00% | 0.00% | N/A | 0.00% | 0.00% |
| 8 | 6.41E-11 | 1.56E-10 | 0.00E+00 | 4.03E-11 | 2.13E-10 | 13.85% | 13.85% | N/A | 14.43% | 12.63% | 0.00% | 0.00% | N/A | 0.00% | 0.00% |
| 9 | 3.66E-10 | 8.91E-10 | 0.00E+00 | 1.68E-10 | 1.36E-09 | 5.12% | 5.12% | N/A | 5.55% | 4.42% | 0.00% | 0.00% | N/A | 0.00% | 0.00% |
| 10 | 3.62E-09 | 8.82E-09 | 0.00E+00 | 1.97E-09 | 1.79E-08 | 1.45% | 1.45% | N/A | 1.46% | 1.22% | 0.00% | 0.00% | N/A | -0.01% | 0.00% |
| 11 | 9.36E-09 | 2.28E-08 | 0.00E+00 | 5.02E-09 | 1.07E-07 | 0.82% | 0.82% | N/A | 0.80% | 0.55% | -0.01% | -0.01% | N/A | -0.02% | -0.03% |
| 12 | 3.54E-08 | 8.61E-08 | 0.00E+00 | 1.41E-08 | 3.93E-07 | 0.40% | 0.40% | N/A | 0.38% | 0.29% | -0.02% | -0.02% | N/A | -0.06% | -0.02% |
| 13 | 1.59E-07 | 3.87E-07 | 0.00E+00 | 5.87E-08 | 2.04E-06 | 0.18% | 0.18% | N/A | 0.18% | 0.14% | -0.10% | -0.10% | N/A | -0.22% | -0.08% |
| 14 | 4.61E-07 | 1.12E-06 | 0.00E+00 | 1.55E-07 | 7.33E-06 | 0.10% | 0.10% | N/A | 0.10% | 0.07% | -0.28% | -0.26% | N/A | -0.55% | -0.29% |
| 15 | 1.06E-06 | 2.58E-06 | 0.00E+00 | 2.89E-07 | 1.87E-05 | 0.06% | 0.06% | N/A | 0.06% | 0.05% | -0.65% | -0.62% | N/A | -1.06% | -0.67% |
| 16 | 7.25E-07 | 1.78E-06 | 0.00E+00 | 1.56E-07 | 1.39E-05 | 0.06% | 0.06% | N/A | 0.06% | 0.05% | -0.43% | -0.41% | N/A | -0.54% | -0.50% |
| 17 | 6.61E-07 | 1.63E-06 | 0.00E+00 | 1.16E-07 | 1.60E-05 | 0.06% | 0.06% | N/A | 0.06% | 0.05% | -0.39% | -0.38% | N/A | -0.42% | -0.97% |
| 18 | 8.60E-07 | 2.15E-06 | 0.00E+00 | 1.19E-07 | 1.71E-05 | 0.05% | 0.05% | N/A | 0.05% | 0.04% | -0.52% | -0.51% | N/A | -0.43% | -0.71% |
| 19 | 6.73E-07 | 1.71E-06 | 0.00E+00 | 6.81E-08 | 1.23E-05 | 0.06% | 0.06% | N/A | 0.06% | 0.05% | -0.40% | -0.40% | N/A | -0.24% | -0.50% |
| 20 | 4.02E-07 | 1.04E-06 | 0.00E+00 | 2.90E-08 | 5.15E-06 | 0.08% | 0.08% | N/A | 0.08% | 0.06% | -0.24% | -0.25% | N/A | -0.10% | -0.18% |
| 21 | 3.70E-07 | 9.77E-07 | 0.00E+00 | 1.92E-08 | 4.38E-06 | 0.09% | 0.09% | N/A | 0.09% | 0.07% | -0.23% | -0.23% | N/A | -0.07% | -0.16% |
| 22 | 3.72E-07 | 1.01E-06 | 0.00E+00 | 1.29E-08 | 4.01E-06 | 0.09% | 0.09% | N/A | 0.10% | 0.07% | -0.23% | -0.25% | N/A | -0.05% | -0.14% |
| 23 | 2.39E-07 | 6.66E-07 | 0.00E+00 | 5.37E-09 | 3.22E-06 | 0.11% | 0.11% | N/A | 0.11% | 0.09% | -0.15% | -0.17% | N/A | -0.02% | -0.14% |
| 24 | 2.37E-07 | 7.06E-07 | 1.75E-09 | 3.43E-08 | 3.14E-06 | 0.11% | 0.12% | 0.37% | 0.15% | 0.09% | -0.15% | -0.18% | -0.24% | -0.28% | -0.12% |
| 25 | 4.99E-08 | 1.68E-07 | 1.22E-08 | 1.16E-08 | 4.10E-07 | 0.28% | 0.29% | 0.30% | 0.27% | 0.23% | -0.03% | -0.04% | -1.92% | -1.05% | -0.02% |
| 26 | 1.86E-08 | 6.77E-08 | 7.36E-09 | 4.47E-09 | 1.18E-07 | 0.50% | 0.50% | 0.50% | 0.41% | 0.41% | -0.01% | -0.02% | -1.21% | -0.41% | 0.00% |
| 27 | 3.50E-09 | 1.38E-08 | 2.02E-09 | 1.49E-09 | 2.29E-08 | 1.13% | 1.13% | 1.04% | 0.90% | 0.92% | 0.00% | 0.00% | -0.34% | -0.14% | 0.00% |
| 28 | 6.89E-10 | 2.89E-09 | 3.54E-10 | 2.59E-10 | 4.37E-09 | 2.57% | 2.57% | 2.28% | 1.95% | 2.10% | 0.00% | 0.00% | -0.05% | -0.02% | 0.00% |
| 29 | 2.74E-10 | 1.21E-09 | 1.00E-10 | 8.45E-11 | 1.59E-09 | 4.41% | 4.41% | 3.48% | 3.36% | 3.63% | 0.00% | 0.00% | -0.02% | -0.01% | 0.00% |
| 30 | 9.27E-11 | 4.32E-10 | 2.85E-11 | 2.31E-11 | 5.29E-10 | 7.48% | 7.49% | 5.07% | 5.59% | 6.18% | 0.00% | 0.00% | -0.01% | 0.00% | 0.00% |
| Total | 6.34E-06 | 1.61E-05 | 2.38E-08 | 1.10E-06 | 1.08E-04 | 0.02% | 0.02% | 0.25% | 0.03% | 0.02% | -3.84% | -3.84% | -3.79% | -5.70% | -4.53% |

In Fig. 14 we see the difference in the TXSAMC and MCNP RRD's for the first tally region displayed graphically. This plot looks very similar to that for the corresponding region in SCR with only a few small differences. The amount of error did not significantly decrease with the new weighting function but it also did not increase.

At this stage, it appears that while we are not doing much good with the new weight function, we are also not doing much harm (other than a large increase in computer time to obtain similar results).

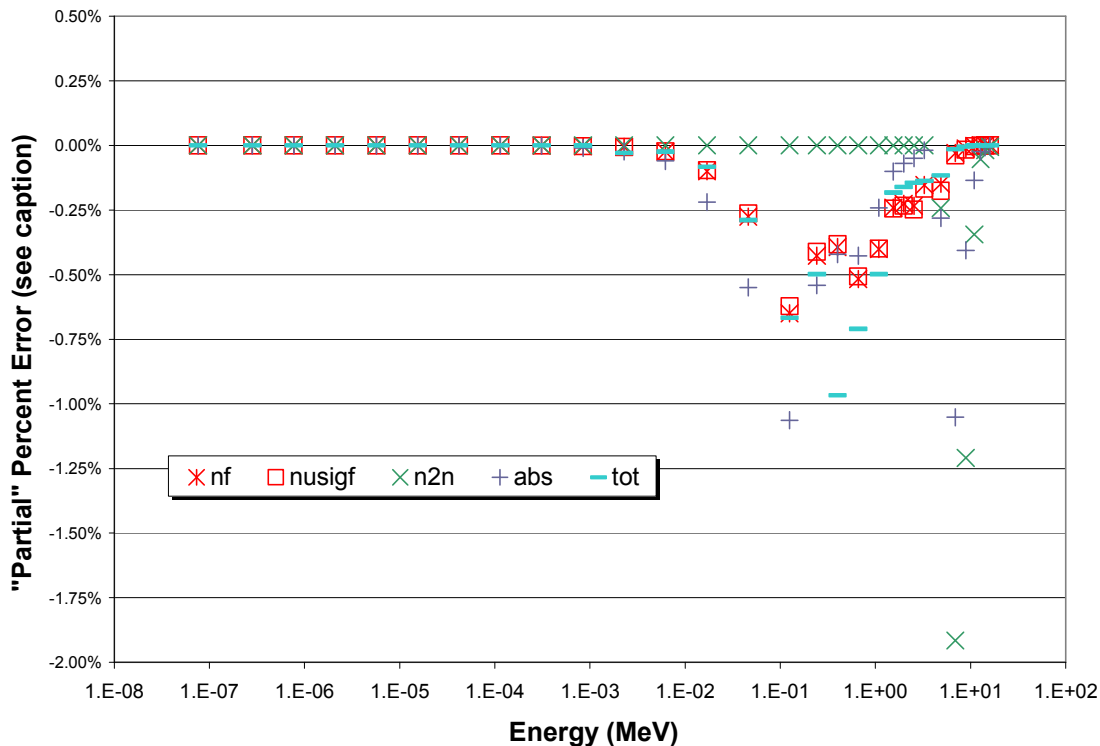


Fig. 14. "Partial" percent errors for reaction-rate densities in SCRA tally region 1. Each "partial" error is plotted at the midpoint energy of its group. The percent error in a given reaction rate is the sum of the 30 partial percent errors.

The second tally region is made up of the control rod pin-cells which consist of an AgInCd cylinder in a SS316L sleeve surrounded by coolant. In Table 25 we show the MCNP-tallied scalar flux for the pin-cell, its relative standard deviation, the TXSAMC-generated cross sections and the TXSAMC-generated reaction rate densities for the

second tally region. Table 26 shows the MCNP-tallied reaction rate densities, their standard deviations and the partial percent error between the TXSAMC-generated reaction rates and the MCNP-tallied reaction rates for the second tally region. Since this region is composed of non-fissionable materials, there is obviously no fission or nusigf RRD. Unlike the first tally region, we do see some significant improvement in the (n,2n) reaction rate when compared to the SCR. We also see a modest improvement in the non-fission absorption cross section and a slight increase in error in the total cross section. Given the very small difference in the latter compared to the reduction in the variance of the MCNP-tallied total RRD, it is possible that this is due more to improved calculation of the benchmark RRD and not an actual change in the TXSAMC RRD. The numbers in the first table seem to bear this out but it is not conclusive. Further studies will attempt to quantify the amount of change due to shifts in the benchmark versus shifts of the actual TXSAMC RRD.

TABLE 25
MCNP scalar flux, TXSAMC cross sections and reaction rates in SCRA tally region 2

| Energy Group | Scalar Flux (n/cm ² /hps) | Rel. Error (1 σ) | TXSAMC SIGMA (cm ⁻¹) | | | | TXSAMC RRD (cm ⁻³) | | | | | |
|--------------|---|-----------------------------|----------------------------------|----------|----------|----------|--------------------------------|----------|----------|----------|----------|----------|
| | | | fission | nusigf | n2n | abs-fis | total | fission | nusigf | n2n | abs-fis | total |
| 1 | 0.00E+00 | 0.00% | 0.00E+00 | 0.00E+00 | 0.00E+00 | 1.62E+00 | 1.85E+00 | 0.00E+00 | 0.00E+00 | 0.00E+00 | 0.00E+00 | 0.00E+00 |
| 2 | 0.00E+00 | 0.00% | 0.00E+00 | 0.00E+00 | 0.00E+00 | 5.79E-01 | 7.86E-01 | 0.00E+00 | 0.00E+00 | 0.00E+00 | 0.00E+00 | 0.00E+00 |
| 3 | 0.00E+00 | 0.00% | 0.00E+00 | 0.00E+00 | 0.00E+00 | 2.55E-01 | 4.57E-01 | 0.00E+00 | 0.00E+00 | 0.00E+00 | 0.00E+00 | 0.00E+00 |
| 4 | 0.00E+00 | 0.00% | 0.00E+00 | 0.00E+00 | 0.00E+00 | 2.86E-01 | 4.99E-01 | 0.00E+00 | 0.00E+00 | 0.00E+00 | 0.00E+00 | 0.00E+00 |
| 5 | 0.00E+00 | 0.00% | 0.00E+00 | 0.00E+00 | 0.00E+00 | 8.07E+00 | 9.14E+00 | 0.00E+00 | 0.00E+00 | 0.00E+00 | 0.00E+00 | 0.00E+00 |
| 6 | 0.00E+00 | 0.00% | 0.00E+00 | 0.00E+00 | 0.00E+00 | 2.32E-02 | 2.30E-01 | 0.00E+00 | 0.00E+00 | 0.00E+00 | 0.00E+00 | 0.00E+00 |
| 7 | 0.00E+00 | 0.00% | 0.00E+00 | 0.00E+00 | 0.00E+00 | 3.51E-02 | 2.42E-01 | 0.00E+00 | 0.00E+00 | 0.00E+00 | 0.00E+00 | 0.00E+00 |
| 8 | 8.80E-11 | 100.00% | 0.00E+00 | 0.00E+00 | 0.00E+00 | 2.84E-02 | 2.61E-01 | 0.00E+00 | 0.00E+00 | 0.00E+00 | 2.49E-12 | 2.30E-11 |
| 9 | 1.52E-09 | 63.15% | 0.00E+00 | 0.00E+00 | 0.00E+00 | 1.16E-02 | 2.19E-01 | 0.00E+00 | 0.00E+00 | 0.00E+00 | 1.76E-11 | 3.33E-10 |
| 10 | 2.55E-08 | 15.13% | 0.00E+00 | 0.00E+00 | 0.00E+00 | 6.04E-03 | 2.23E-01 | 0.00E+00 | 0.00E+00 | 0.00E+00 | 1.54E-10 | 5.69E-09 |
| 11 | 1.63E-07 | 6.13% | 0.00E+00 | 0.00E+00 | 0.00E+00 | 6.57E-03 | 6.10E-01 | 0.00E+00 | 0.00E+00 | 0.00E+00 | 1.07E-09 | 9.93E-08 |
| 12 | 9.44E-07 | 2.49% | 0.00E+00 | 0.00E+00 | 0.00E+00 | 8.19E-03 | 4.23E-01 | 0.00E+00 | 0.00E+00 | 0.00E+00 | 7.73E-09 | 4.00E-07 |
| 13 | 6.32E-06 | 0.98% | 0.00E+00 | 0.00E+00 | 0.00E+00 | 5.45E-03 | 2.58E-01 | 0.00E+00 | 0.00E+00 | 0.00E+00 | 3.45E-08 | 1.63E-06 |
| 14 | 2.42E-05 | 0.51% | 0.00E+00 | 0.00E+00 | 0.00E+00 | 3.75E-03 | 2.64E-01 | 0.00E+00 | 0.00E+00 | 0.00E+00 | 9.07E-08 | 6.40E-06 |
| 15 | 7.05E-05 | 0.32% | 0.00E+00 | 0.00E+00 | 0.00E+00 | 2.34E-03 | 2.08E-01 | 0.00E+00 | 0.00E+00 | 0.00E+00 | 1.65E-07 | 1.47E-05 |
| 16 | 5.45E-05 | 0.37% | 0.00E+00 | 0.00E+00 | 0.00E+00 | 1.65E-03 | 2.28E-01 | 0.00E+00 | 0.00E+00 | 0.00E+00 | 8.98E-08 | 1.24E-05 |
| 17 | 5.45E-05 | 0.39% | 0.00E+00 | 0.00E+00 | 0.00E+00 | 1.18E-03 | 2.02E-01 | 0.00E+00 | 0.00E+00 | 0.00E+00 | 6.42E-08 | 1.10E-05 |
| 18 | 7.37E-05 | 0.34% | 0.00E+00 | 0.00E+00 | 0.00E+00 | 8.62E-04 | 2.57E-01 | 0.00E+00 | 0.00E+00 | 0.00E+00 | 6.36E-08 | 1.89E-05 |
| 19 | 5.42E-05 | 0.40% | 0.00E+00 | 0.00E+00 | 0.00E+00 | 6.66E-04 | 2.07E-01 | 0.00E+00 | 0.00E+00 | 0.00E+00 | 3.61E-08 | 1.12E-05 |
| 20 | 2.98E-05 | 0.53% | 0.00E+00 | 0.00E+00 | 0.00E+00 | 5.60E-04 | 1.59E-01 | 0.00E+00 | 0.00E+00 | 0.00E+00 | 1.67E-08 | 4.75E-06 |
| 21 | 2.59E-05 | 0.57% | 0.00E+00 | 0.00E+00 | 0.00E+00 | 4.87E-04 | 1.62E-01 | 0.00E+00 | 0.00E+00 | 0.00E+00 | 1.26E-08 | 4.21E-06 |
| 22 | 2.56E-05 | 0.57% | 0.00E+00 | 0.00E+00 | 0.00E+00 | 4.24E-04 | 1.60E-01 | 0.00E+00 | 0.00E+00 | 0.00E+00 | 1.09E-08 | 4.10E-06 |
| 23 | 1.70E-05 | 0.71% | 0.00E+00 | 0.00E+00 | 0.00E+00 | 3.78E-04 | 1.35E-01 | 0.00E+00 | 0.00E+00 | 0.00E+00 | 6.42E-09 | 2.28E-06 |
| 24 | 1.78E-05 | 0.70% | 0.00E+00 | 0.00E+00 | 0.00E+00 | 5.01E-04 | 1.25E-01 | 0.00E+00 | 0.00E+00 | 0.00E+00 | 8.93E-09 | 2.23E-06 |
| 25 | 2.76E-06 | 1.72% | 0.00E+00 | 0.00E+00 | 6.28E-08 | 2.36E-03 | 1.15E-01 | 0.00E+00 | 0.00E+00 | 1.73E-13 | 6.51E-09 | 3.17E-07 |
| 26 | 8.64E-07 | 3.10% | 0.00E+00 | 0.00E+00 | 6.09E-05 | 5.21E-03 | 1.08E-01 | 0.00E+00 | 0.00E+00 | 5.26E-11 | 4.50E-09 | 9.31E-08 |
| 27 | 1.43E-07 | 7.19% | 0.00E+00 | 0.00E+00 | 2.25E-03 | 7.49E-03 | 1.05E-01 | 0.00E+00 | 0.00E+00 | 3.21E-10 | 1.07E-09 | 1.50E-08 |
| 28 | 3.54E-08 | 15.25% | 0.00E+00 | 0.00E+00 | 7.53E-03 | 2.73E-03 | 1.10E-01 | 0.00E+00 | 0.00E+00 | 2.67E-10 | 9.67E-11 | 3.90E-09 |
| 29 | 7.90E-09 | 30.47% | 0.00E+00 | 0.00E+00 | 9.34E-03 | 9.63E-05 | 1.05E-01 | 0.00E+00 | 0.00E+00 | 7.37E-11 | 7.61E-13 | 8.33E-10 |
| 30 | 2.72E-09 | 50.41% | 0.00E+00 | 0.00E+00 | 9.98E-03 | 0.00E+00 | 1.01E-01 | 0.00E+00 | 0.00E+00 | 2.72E-11 | 0.00E+00 | 2.76E-10 |
| Total | 4.59E-04 | 0.14% | 0.00E+00 | 0.00E+00 | 2.92E-02 | 1.10E+01 | 1.80E+01 | 0.00E+00 | 0.00E+00 | 7.41E-10 | 6.21E-07 | 9.48E-05 |

TABLE 26
MCNP reaction rates and reaction rate comparison in SCRA tally region 2

| Energy | MCNP RRD (cm ⁻³) | | | | | MCNP Standard Deviation | | | | | Partial Percent Error (TXSAMC-MCNP)/MCNP | | | | |
|--------|------------------------------|----------|----------|----------|----------|-------------------------|--------|--------|---------|---------|--|--------|--------|---------|--------|
| | fission | nusigf | n2n | abs-fis | total | fission | nusigf | n2n | abs-fis | total | fission | nusigf | n2n | abs-fis | total |
| 1 | 0.00E+00 | 0.00E+00 | 0.00E+00 | 0.00E+00 | 0.00E+00 | N/A | N/A | N/A | N/A | N/A | N/A | N/A | N/A | N/A | N/A |
| 2 | 0.00E+00 | 0.00E+00 | 0.00E+00 | 0.00E+00 | 0.00E+00 | N/A | N/A | N/A | N/A | N/A | N/A | N/A | N/A | N/A | N/A |
| 3 | 0.00E+00 | 0.00E+00 | 0.00E+00 | 0.00E+00 | 0.00E+00 | N/A | N/A | N/A | N/A | N/A | N/A | N/A | N/A | N/A | N/A |
| 4 | 0.00E+00 | 0.00E+00 | 0.00E+00 | 0.00E+00 | 0.00E+00 | N/A | N/A | N/A | N/A | N/A | N/A | N/A | N/A | N/A | N/A |
| 5 | 0.00E+00 | 0.00E+00 | 0.00E+00 | 0.00E+00 | 0.00E+00 | N/A | N/A | N/A | N/A | N/A | N/A | N/A | N/A | N/A | N/A |
| 6 | 0.00E+00 | 0.00E+00 | 0.00E+00 | 0.00E+00 | 0.00E+00 | N/A | N/A | N/A | N/A | N/A | N/A | N/A | N/A | N/A | N/A |
| 7 | 0.00E+00 | 0.00E+00 | 0.00E+00 | 0.00E+00 | 0.00E+00 | N/A | N/A | N/A | N/A | N/A | N/A | N/A | N/A | N/A | N/A |
| 8 | 0.00E+00 | 0.00E+00 | 0.00E+00 | 3.35E-14 | 1.44E-11 | N/A | N/A | N/A | 100.00% | 100.00% | N/A | N/A | N/A | 0.00% | 0.00% |
| 9 | 0.00E+00 | 0.00E+00 | 0.00E+00 | 7.46E-11 | 4.48E-10 | N/A | N/A | N/A | 71.63% | 40.46% | N/A | N/A | N/A | -0.01% | 0.00% |
| 10 | 0.00E+00 | 0.00E+00 | 0.00E+00 | 1.70E-10 | 5.85E-09 | N/A | N/A | N/A | 43.70% | 12.15% | N/A | N/A | N/A | 0.00% | 0.00% |
| 11 | 0.00E+00 | 0.00E+00 | 0.00E+00 | 1.39E-09 | 1.83E-07 | N/A | N/A | N/A | 14.33% | 6.12% | N/A | N/A | N/A | -0.05% | -0.09% |
| 12 | 0.00E+00 | 0.00E+00 | 0.00E+00 | 7.75E-09 | 4.33E-07 | N/A | N/A | N/A | 4.43% | 2.20% | N/A | N/A | N/A | 0.00% | -0.04% |
| 13 | 0.00E+00 | 0.00E+00 | 0.00E+00 | 3.53E-08 | 1.65E-06 | N/A | N/A | N/A | 1.66% | 0.79% | N/A | N/A | N/A | -0.13% | -0.02% |
| 14 | 0.00E+00 | 0.00E+00 | 0.00E+00 | 9.29E-08 | 6.48E-06 | N/A | N/A | N/A | 0.86% | 0.43% | N/A | N/A | N/A | -0.35% | -0.09% |
| 15 | 0.00E+00 | 0.00E+00 | 0.00E+00 | 1.65E-07 | 1.48E-05 | N/A | N/A | N/A | 0.53% | 0.26% | N/A | N/A | N/A | 0.00% | -0.12% |
| 16 | 0.00E+00 | 0.00E+00 | 0.00E+00 | 8.93E-08 | 1.25E-05 | N/A | N/A | N/A | 0.62% | 0.31% | N/A | N/A | N/A | 0.08% | -0.02% |
| 17 | 0.00E+00 | 0.00E+00 | 0.00E+00 | 6.44E-08 | 1.10E-05 | N/A | N/A | N/A | 0.65% | 0.32% | N/A | N/A | N/A | -0.02% | -0.01% |
| 18 | 0.00E+00 | 0.00E+00 | 0.00E+00 | 6.39E-08 | 1.92E-05 | N/A | N/A | N/A | 0.57% | 0.30% | N/A | N/A | N/A | -0.04% | -0.25% |
| 19 | 0.00E+00 | 0.00E+00 | 0.00E+00 | 3.62E-08 | 1.12E-05 | N/A | N/A | N/A | 0.69% | 0.34% | N/A | N/A | N/A | -0.03% | -0.04% |
| 20 | 0.00E+00 | 0.00E+00 | 0.00E+00 | 1.63E-08 | 4.73E-06 | N/A | N/A | N/A | 0.94% | 0.44% | N/A | N/A | N/A | 0.06% | 0.02% |
| 21 | 0.00E+00 | 0.00E+00 | 0.00E+00 | 1.25E-08 | 4.22E-06 | N/A | N/A | N/A | 0.98% | 0.47% | N/A | N/A | N/A | 0.01% | 0.00% |
| 22 | 0.00E+00 | 0.00E+00 | 0.00E+00 | 1.10E-08 | 4.11E-06 | N/A | N/A | N/A | 0.92% | 0.47% | N/A | N/A | N/A | -0.02% | -0.01% |
| 23 | 0.00E+00 | 0.00E+00 | 0.00E+00 | 6.36E-09 | 2.28E-06 | N/A | N/A | N/A | 0.98% | 0.58% | N/A | N/A | N/A | 0.01% | 0.01% |
| 24 | 0.00E+00 | 0.00E+00 | 0.00E+00 | 8.98E-09 | 2.23E-06 | N/A | N/A | N/A | 0.75% | 0.55% | N/A | N/A | N/A | -0.01% | 0.00% |
| 25 | 0.00E+00 | 0.00E+00 | 1.74E-13 | 6.47E-09 | 3.17E-07 | N/A | N/A | 11.92% | 1.51% | 1.35% | N/A | N/A | 0.00% | 0.01% | 0.00% |
| 26 | 0.00E+00 | 0.00E+00 | 5.51E-11 | 4.60E-09 | 9.29E-08 | N/A | N/A | 8.82% | 2.86% | 2.45% | N/A | N/A | -0.31% | -0.02% | 0.00% |
| 27 | 0.00E+00 | 0.00E+00 | 3.40E-10 | 1.38E-09 | 1.51E-08 | N/A | N/A | 14.33% | 6.78% | 5.80% | N/A | N/A | -2.46% | -0.05% | 0.00% |
| 28 | 0.00E+00 | 0.00E+00 | 2.78E-10 | 3.60E-10 | 3.91E-09 | N/A | N/A | 24.97% | 13.37% | 12.01% | N/A | N/A | -1.48% | -0.04% | 0.00% |
| 29 | 0.00E+00 | 0.00E+00 | 6.47E-11 | 7.54E-11 | 8.14E-10 | N/A | N/A | 43.65% | 28.92% | 26.06% | N/A | N/A | 1.15% | -0.01% | 0.00% |
| 30 | 0.00E+00 | 0.00E+00 | 4.54E-11 | 2.33E-11 | 3.06E-10 | N/A | N/A | 47.36% | 44.54% | 38.06% | N/A | N/A | -2.33% | 0.00% | 0.00% |
| Total | 0.00E+00 | 0.00E+00 | 7.84E-10 | 6.25E-07 | 9.54E-05 | N/A | N/A | 11.76% | 0.27% | 0.12% | N/A | N/A | -5.42% | -0.63% | -0.66% |

In Fig. 15 we see the difference in the TXSAMC and MCNP RRD's for the second tally region displayed graphically. This plot clearly shows the decrease in error when compared to the SCR. The largest error in any single group for any reaction is less than 3% whereas in the SCR it was 82%. Again, it is not clear at this time if this reduction is due to a reduction in variance of the benchmark, better cross sections produced by TXSAMC or some unknown cause.

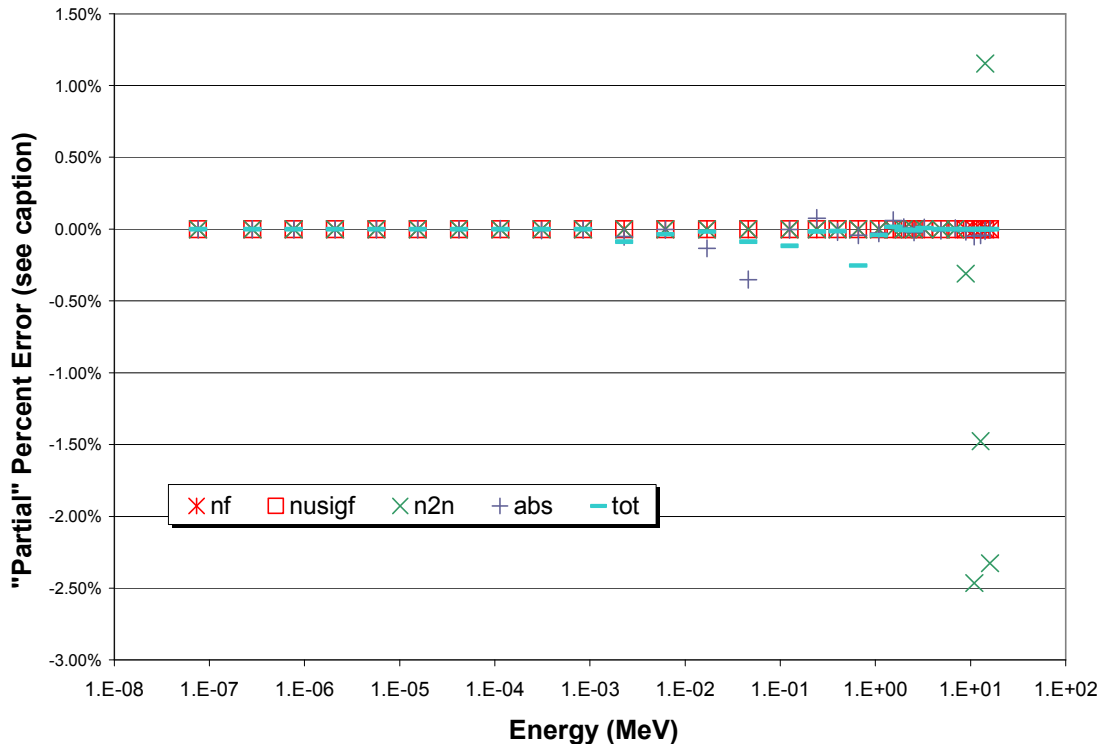


Fig. 15. "Partial" percent errors for reaction-rate densities in SCRA tally region 2. Each "partial" error is plotted at the midpoint energy of its group. The percent error in a given reaction rate is the sum of the 30 partial percent errors.

The third tally region is composed of coolant channels filled with liquid sodium. In Table 27 we show the MCNP-tallied scalar flux for the pin-cell, its relative standard deviation, the TXSAMC-generated cross sections and the TXSAMC-generated reaction rate densities for the third tally region. Table 28 shows the MCNP-tallied reaction rate densities, their standard deviations and the partial percent error between the TXSAMC-generated reaction rates and the MCNP-tallied reaction rates for the third tally region. It should be noted that as a result of the homogenous nature of these cells, there is no heterogeneity option applied in the TRANSX module of TXSAMC and no mixing (since it is all one nuclide).

TABLE 27
MCNP scalar flux, TXSAMC cross sections and reaction rates in SCRA tally region 3

| Energy Group | Scalar Flux (n/cm ² /hps) | Rel. Error (1 σ) | TXSAMC SIGMA (cm ⁻¹) | | | | | TXSAMC RRD (cm ⁻³) | | | | | |
|--------------|--------------------------------------|--------------------------|----------------------------------|----------|----------|----------|----------|--------------------------------|----------|----------|----------|----------|----------|
| | | | fission | nusigf | n2n | abs-fis | total | fission | nusigf | n2n | abs-fis | total | |
| 1 | 0.00E+00 | 0.00% | 0.00E+00 | 0.00E+00 | 0.00E+00 | 4.90E-02 | 2.59E-01 | 0.00E+00 | 0.00E+00 | 0.00E+00 | 0.00E+00 | 0.00E+00 | 0.00E+00 |
| 2 | 0.00E+00 | 0.00% | 0.00E+00 | 0.00E+00 | 0.00E+00 | 8.70E-03 | 1.80E-01 | 0.00E+00 | 0.00E+00 | 0.00E+00 | 0.00E+00 | 0.00E+00 | 0.00E+00 |
| 3 | 0.00E+00 | 0.00% | 0.00E+00 | 0.00E+00 | 0.00E+00 | 4.72E-03 | 1.72E-01 | 0.00E+00 | 0.00E+00 | 0.00E+00 | 0.00E+00 | 0.00E+00 | 0.00E+00 |
| 4 | 0.00E+00 | 0.00% | 0.00E+00 | 0.00E+00 | 0.00E+00 | 3.37E-03 | 1.70E-01 | 0.00E+00 | 0.00E+00 | 0.00E+00 | 0.00E+00 | 0.00E+00 | 0.00E+00 |
| 5 | 0.00E+00 | 0.00% | 0.00E+00 | 0.00E+00 | 0.00E+00 | 1.91E-03 | 1.68E-01 | 0.00E+00 | 0.00E+00 | 0.00E+00 | 0.00E+00 | 0.00E+00 | 0.00E+00 |
| 6 | 0.00E+00 | 0.00% | 0.00E+00 | 0.00E+00 | 0.00E+00 | 1.05E-03 | 1.65E-01 | 0.00E+00 | 0.00E+00 | 0.00E+00 | 0.00E+00 | 0.00E+00 | 0.00E+00 |
| 7 | 0.00E+00 | 0.00% | 0.00E+00 | 0.00E+00 | 0.00E+00 | 6.61E-04 | 1.65E-01 | 0.00E+00 | 0.00E+00 | 0.00E+00 | 0.00E+00 | 0.00E+00 | 0.00E+00 |
| 8 | 0.00E+00 | 0.00% | 0.00E+00 | 0.00E+00 | 0.00E+00 | 4.48E-04 | 1.65E-01 | 0.00E+00 | 0.00E+00 | 0.00E+00 | 0.00E+00 | 0.00E+00 | 0.00E+00 |
| 9 | 8.62E-10 | 65.10% | 0.00E+00 | 0.00E+00 | 0.00E+00 | 3.13E-04 | 1.68E-01 | 0.00E+00 | 0.00E+00 | 0.00E+00 | 2.70E-13 | 1.45E-10 | 1.45E-10 |
| 10 | 2.60E-08 | 14.26% | 0.00E+00 | 0.00E+00 | 0.00E+00 | 3.36E-04 | 1.94E-01 | 0.00E+00 | 0.00E+00 | 0.00E+00 | 8.74E-12 | 5.05E-09 | 5.05E-09 |
| 11 | 1.83E-07 | 5.53% | 0.00E+00 | 0.00E+00 | 0.00E+00 | 2.02E-03 | 1.83E+00 | 0.00E+00 | 0.00E+00 | 0.00E+00 | 3.70E-10 | 3.34E-07 | 3.34E-07 |
| 12 | 9.64E-07 | 2.48% | 0.00E+00 | 0.00E+00 | 0.00E+00 | 1.04E-04 | 4.30E-01 | 0.00E+00 | 0.00E+00 | 0.00E+00 | 1.00E-10 | 4.14E-07 | 4.14E-07 |
| 13 | 6.39E-06 | 0.97% | 0.00E+00 | 0.00E+00 | 0.00E+00 | 2.47E-06 | 2.32E-01 | 0.00E+00 | 0.00E+00 | 0.00E+00 | 1.58E-11 | 1.48E-06 | 1.48E-06 |
| 14 | 2.43E-05 | 0.51% | 0.00E+00 | 0.00E+00 | 0.00E+00 | 9.64E-05 | 2.65E-01 | 0.00E+00 | 0.00E+00 | 0.00E+00 | 2.34E-09 | 6.42E-06 | 6.42E-06 |
| 15 | 7.07E-05 | 0.32% | 0.00E+00 | 0.00E+00 | 0.00E+00 | 3.37E-05 | 1.81E-01 | 0.00E+00 | 0.00E+00 | 0.00E+00 | 2.38E-09 | 1.28E-05 | 1.28E-05 |
| 16 | 5.47E-05 | 0.37% | 0.00E+00 | 0.00E+00 | 0.00E+00 | 5.22E-05 | 2.18E-01 | 0.00E+00 | 0.00E+00 | 0.00E+00 | 2.85E-09 | 1.19E-05 | 1.19E-05 |
| 17 | 5.41E-05 | 0.39% | 0.00E+00 | 0.00E+00 | 0.00E+00 | 2.24E-05 | 1.81E-01 | 0.00E+00 | 0.00E+00 | 0.00E+00 | 1.21E-09 | 9.81E-06 | 9.81E-06 |
| 18 | 7.34E-05 | 0.34% | 0.00E+00 | 0.00E+00 | 0.00E+00 | 1.68E-05 | 2.62E-01 | 0.00E+00 | 0.00E+00 | 0.00E+00 | 1.23E-09 | 1.92E-05 | 1.92E-05 |
| 19 | 5.39E-05 | 0.41% | 0.00E+00 | 0.00E+00 | 0.00E+00 | 1.20E-05 | 1.98E-01 | 0.00E+00 | 0.00E+00 | 0.00E+00 | 6.46E-10 | 1.07E-05 | 1.07E-05 |
| 20 | 3.00E-05 | 0.53% | 0.00E+00 | 0.00E+00 | 0.00E+00 | 1.08E-05 | 1.42E-01 | 0.00E+00 | 0.00E+00 | 0.00E+00 | 3.23E-10 | 4.26E-06 | 4.26E-06 |
| 21 | 2.66E-05 | 0.57% | 0.00E+00 | 0.00E+00 | 0.00E+00 | 1.01E-05 | 1.49E-01 | 0.00E+00 | 0.00E+00 | 0.00E+00 | 2.68E-10 | 3.96E-06 | 3.96E-06 |
| 22 | 2.54E-05 | 0.58% | 0.00E+00 | 0.00E+00 | 0.00E+00 | 9.46E-06 | 1.48E-01 | 0.00E+00 | 0.00E+00 | 0.00E+00 | 2.41E-10 | 3.78E-06 | 3.78E-06 |
| 23 | 1.72E-05 | 0.71% | 0.00E+00 | 0.00E+00 | 0.00E+00 | 8.88E-06 | 1.20E-01 | 0.00E+00 | 0.00E+00 | 0.00E+00 | 1.53E-10 | 2.06E-06 | 2.06E-06 |
| 24 | 1.80E-05 | 0.70% | 0.00E+00 | 0.00E+00 | 0.00E+00 | 1.96E-04 | 1.09E-01 | 0.00E+00 | 0.00E+00 | 0.00E+00 | 3.52E-09 | 1.96E-06 | 1.96E-06 |
| 25 | 2.93E-06 | 1.70% | 0.00E+00 | 0.00E+00 | 0.00E+00 | 2.31E-03 | 9.47E-02 | 0.00E+00 | 0.00E+00 | 0.00E+00 | 6.76E-09 | 2.77E-07 | 2.77E-07 |
| 26 | 8.59E-07 | 3.03% | 0.00E+00 | 0.00E+00 | 0.00E+00 | 5.71E-03 | 8.67E-02 | 0.00E+00 | 0.00E+00 | 0.00E+00 | 4.91E-09 | 7.45E-08 | 7.45E-08 |
| 27 | 1.66E-07 | 7.16% | 0.00E+00 | 0.00E+00 | 0.00E+00 | 1.08E-02 | 8.62E-02 | 0.00E+00 | 0.00E+00 | 0.00E+00 | 1.79E-09 | 1.43E-08 | 1.43E-08 |
| 28 | 3.56E-08 | 15.11% | 0.00E+00 | 0.00E+00 | 5.03E-05 | 1.15E-02 | 8.85E-02 | 0.00E+00 | 0.00E+00 | 1.79E-12 | 4.11E-10 | 3.15E-09 | 3.15E-09 |
| 29 | 1.33E-08 | 27.77% | 0.00E+00 | 0.00E+00 | 1.52E-03 | 8.89E-03 | 9.01E-02 | 0.00E+00 | 0.00E+00 | 2.02E-11 | 1.18E-10 | 1.20E-09 | 1.20E-09 |
| 30 | 2.36E-09 | 57.50% | 0.00E+00 | 0.00E+00 | 5.03E-03 | 4.64E-03 | 9.23E-02 | 0.00E+00 | 0.00E+00 | 1.18E-11 | 1.09E-11 | 2.18E-10 | 2.18E-10 |
| Total | 4.60E-04 | 0.14% | 0.00E+00 | 0.00E+00 | 6.59E-03 | 1.17E-01 | 6.81E+00 | 0.00E+00 | 0.00E+00 | 3.38E-11 | 2.97E-08 | 8.95E-05 | 8.95E-05 |

TABLE 28
MCNP reaction rated and reaction rate comparison in SCRA tally region 3

| Energy Group | MCNP RRD (cm ⁻³) | | | | | MCNP Standard Deviation | | | | | Partial Percent Error (TXSAMC-MCNP)/MCNP | | | | |
|--------------|------------------------------|----------|----------|----------|----------|-------------------------|--------|--------|---------|--------|--|--------|---------|---------|-------|
| | fission | nusigf | n2n | abs-fis | total | fission | nusigf | n2n | abs-fis | total | fission | nusigf | n2n | abs-fis | total |
| 1 | 0.00E+00 | 0.00E+00 | 0.00E+00 | 0.00E+00 | 0.00E+00 | N/A | N/A | 0.00% | 0.00% | 0.00% | N/A | N/A | N/A | N/A | N/A |
| 2 | 0.00E+00 | 0.00E+00 | 0.00E+00 | 0.00E+00 | 0.00E+00 | N/A | N/A | 0.00% | 0.00% | 0.00% | N/A | N/A | N/A | N/A | N/A |
| 3 | 0.00E+00 | 0.00E+00 | 0.00E+00 | 0.00E+00 | 0.00E+00 | N/A | N/A | 0.00% | 0.00% | 0.00% | N/A | N/A | N/A | N/A | N/A |
| 4 | 0.00E+00 | 0.00E+00 | 0.00E+00 | 0.00E+00 | 0.00E+00 | N/A | N/A | 0.00% | 0.00% | 0.00% | N/A | N/A | N/A | N/A | N/A |
| 5 | 0.00E+00 | 0.00E+00 | 0.00E+00 | 0.00E+00 | 0.00E+00 | N/A | N/A | 0.00% | 0.00% | 0.00% | N/A | N/A | N/A | N/A | N/A |
| 6 | 0.00E+00 | 0.00E+00 | 0.00E+00 | 0.00E+00 | 0.00E+00 | N/A | N/A | 0.00% | 0.00% | 0.00% | N/A | N/A | N/A | N/A | N/A |
| 7 | 0.00E+00 | 0.00E+00 | 0.00E+00 | 0.00E+00 | 0.00E+00 | N/A | N/A | 0.00% | 0.00% | 0.00% | N/A | N/A | N/A | N/A | N/A |
| 8 | 0.00E+00 | 0.00E+00 | 0.00E+00 | 0.00E+00 | 0.00E+00 | N/A | N/A | 0.00% | 0.00% | 0.00% | N/A | N/A | N/A | N/A | N/A |
| 9 | 0.00E+00 | 0.00E+00 | 0.00E+00 | 2.64E-13 | 1.45E-10 | N/A | N/A | 0.00% | 64.96% | 65.12% | N/A | N/A | N/A | 0.00% | 0.00% |
| 10 | 0.00E+00 | 0.00E+00 | 0.00E+00 | 8.85E-12 | 5.10E-09 | N/A | N/A | 0.00% | 14.32% | 14.30% | N/A | N/A | N/A | 0.00% | 0.00% |
| 11 | 0.00E+00 | 0.00E+00 | 0.00E+00 | 2.82E-10 | 2.30E-07 | N/A | N/A | 0.00% | 5.93% | 6.29% | N/A | N/A | N/A | 0.32% | 0.12% |
| 12 | 0.00E+00 | 0.00E+00 | 0.00E+00 | 9.43E-11 | 4.09E-07 | N/A | N/A | 0.00% | 8.00% | 2.72% | N/A | N/A | N/A | 0.02% | 0.01% |
| 13 | 0.00E+00 | 0.00E+00 | 0.00E+00 | 1.56E-11 | 1.48E-06 | N/A | N/A | 0.00% | 1.16% | 0.98% | N/A | N/A | N/A | 0.00% | 0.00% |
| 14 | 0.00E+00 | 0.00E+00 | 0.00E+00 | 1.72E-09 | 5.72E-06 | N/A | N/A | 0.00% | 7.93% | 0.54% | N/A | N/A | N/A | 2.23% | 0.81% |
| 15 | 0.00E+00 | 0.00E+00 | 0.00E+00 | 1.87E-09 | 1.28E-05 | N/A | N/A | 0.00% | 5.06% | 0.32% | N/A | N/A | N/A | 1.81% | 0.01% |
| 16 | 0.00E+00 | 0.00E+00 | 0.00E+00 | 2.40E-09 | 1.13E-05 | N/A | N/A | 0.00% | 2.08% | 0.39% | N/A | N/A | N/A | 1.62% | 0.68% |
| 17 | 0.00E+00 | 0.00E+00 | 0.00E+00 | 1.12E-09 | 9.61E-06 | N/A | N/A | 0.00% | 1.94% | 0.40% | N/A | N/A | N/A | 0.34% | 0.23% |
| 18 | 0.00E+00 | 0.00E+00 | 0.00E+00 | 1.23E-09 | 1.87E-05 | N/A | N/A | 0.00% | 0.34% | 0.36% | N/A | N/A | N/A | 0.01% | 0.64% |
| 19 | 0.00E+00 | 0.00E+00 | 0.00E+00 | 6.46E-10 | 1.06E-05 | N/A | N/A | 0.00% | 0.41% | 0.41% | N/A | N/A | N/A | 0.00% | 0.08% |
| 20 | 0.00E+00 | 0.00E+00 | 0.00E+00 | 3.23E-10 | 4.22E-06 | N/A | N/A | 0.00% | 0.53% | 0.54% | N/A | N/A | N/A | 0.00% | 0.04% |
| 21 | 0.00E+00 | 0.00E+00 | 0.00E+00 | 2.68E-10 | 3.94E-06 | N/A | N/A | 0.00% | 0.57% | 0.58% | N/A | N/A | N/A | 0.00% | 0.02% |
| 22 | 0.00E+00 | 0.00E+00 | 0.00E+00 | 2.41E-10 | 3.76E-06 | N/A | N/A | 0.00% | 0.58% | 0.58% | N/A | N/A | N/A | 0.00% | 0.01% |
| 23 | 0.00E+00 | 0.00E+00 | 0.00E+00 | 1.53E-10 | 2.05E-06 | N/A | N/A | 0.00% | 0.71% | 0.71% | N/A | N/A | N/A | 0.00% | 0.01% |
| 24 | 0.00E+00 | 0.00E+00 | 0.00E+00 | 3.41E-09 | 1.95E-06 | N/A | N/A | 0.00% | 1.48% | 0.70% | N/A | N/A | N/A | 0.39% | 0.01% |
| 25 | 0.00E+00 | 0.00E+00 | 0.00E+00 | 6.76E-09 | 2.78E-07 | N/A | N/A | 0.00% | 1.78% | 1.70% | N/A | N/A | N/A | 0.01% | 0.00% |
| 26 | 0.00E+00 | 0.00E+00 | 0.00E+00 | 4.94E-09 | 7.45E-08 | N/A | N/A | 0.00% | 3.11% | 3.03% | N/A | N/A | N/A | -0.12% | 0.00% |
| 27 | 0.00E+00 | 0.00E+00 | 0.00E+00 | 1.79E-09 | 1.43E-08 | N/A | N/A | 0.00% | 7.15% | 7.16% | N/A | N/A | N/A | 0.00% | 0.00% |
| 28 | 0.00E+00 | 0.00E+00 | 7.85E-13 | 4.14E-10 | 3.15E-09 | N/A | N/A | 40.16% | 15.12% | 15.10% | N/A | N/A | 2.74% | -0.01% | 0.00% |
| 29 | 0.00E+00 | 0.00E+00 | 2.53E-11 | 1.36E-10 | 1.20E-09 | N/A | N/A | 27.90% | 27.85% | 27.76% | N/A | N/A | -14.00% | -0.06% | 0.00% |
| 30 | 0.00E+00 | 0.00E+00 | 1.07E-11 | 2.28E-11 | 2.17E-10 | N/A | N/A | 56.79% | 57.50% | 57.48% | N/A | N/A | 3.22% | -0.04% | 0.00% |
| Total | 0.00E+00 | 0.00E+00 | 3.68E-11 | 2.78E-08 | 8.72E-05 | N/A | N/A | 25.39% | 1.11% | 0.15% | N/A | N/A | -8.05% | 6.50% | 2.65% |

As expected, this region of non-fissionable material had no fission or fission neutron emission reactions and a fairly small number of $(n,2n)$ reactions. One important feature to note here is that the error in the total and non-fission absorption cross sections in group 11 (located on the largest sodium resonance) has decreased greatly. Since the cross sections produced for this group in this region are probably more dependent on within group shape than any other due to the size and breadth of this resonance, it seems reasonable to surmise that using the 187 group function may have helped map this out better and produced better cross sections in this region. This hypothesis is supported by looking at the differences between the MCNP-tallied RRD's in group 11 for the two functions and the differences between the TXSAMC-generated cross sections in group 11 for each function. There is a small difference in the MCNP-tallied RRD's with both functions which is entirely attributable to the increase in the number of histories. If stochastic effects were the driver in the reduction in error and the 30 group and 187 group weight functions provided roughly the same information about the within group shape, we would expect to see a small change in the TXSAMC-generated cross sections for group 11 on the same order as the MCNP-tallied RRD's. We instead see a 50% decrease from the SCR to the SCRA in the group 11 non-absorption fission and total cross sections. In most other groups, the change in generated cross sections is on the order of a few percent. This strongly suggests that the 187 group spectrum is helpful in the area of this very broad resonance.

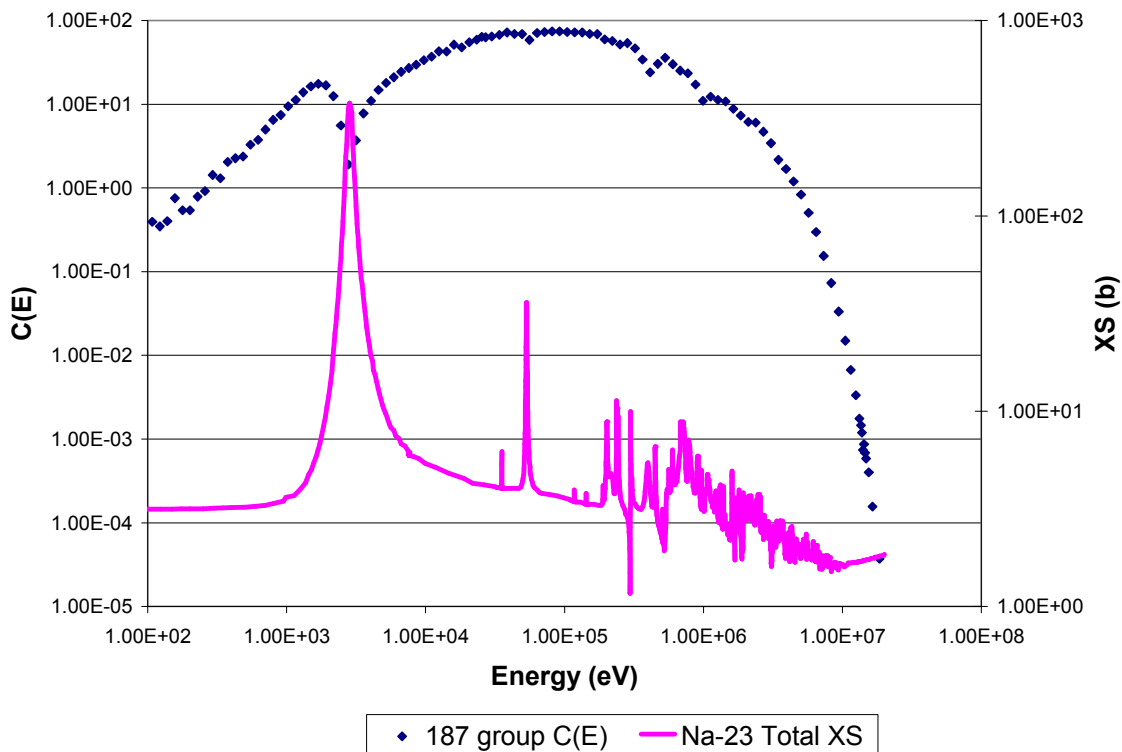


Fig. 16. Plot of 187 group weighting function with sodium cross section.

We also plot in Fig. 16 the 187 group weighting function in the mid range energies along with the sodium cross section. The dip in the weighting function corresponds very nicely with the 2.8 keV resonance. Again, while this is not conclusive, this evidence does suggest that in some cases and for some resonances, a finer group structure might be of some benefit.

In Fig. 17 we see the difference in the TXSAMC and MCNP RRD's for the third tally region displayed graphically. The use of the new weighting function does not seem to have decreased the error by nearly as large of a factor in the higher energies. If one accepts the hypothesis that a better mapping of the 2.8 keV sodium resonance reduced

the error in group 11, it seems possible that the lack of reduction in error at higher energies might be due to a failure to resolve those resonances with the 187 group function. At higher energies, the resonances are simply too many and too narrow to be resolved by anything less than thousands of groups; thus, the 187 group function is not adding any real information about the within group flux shape at these energies.

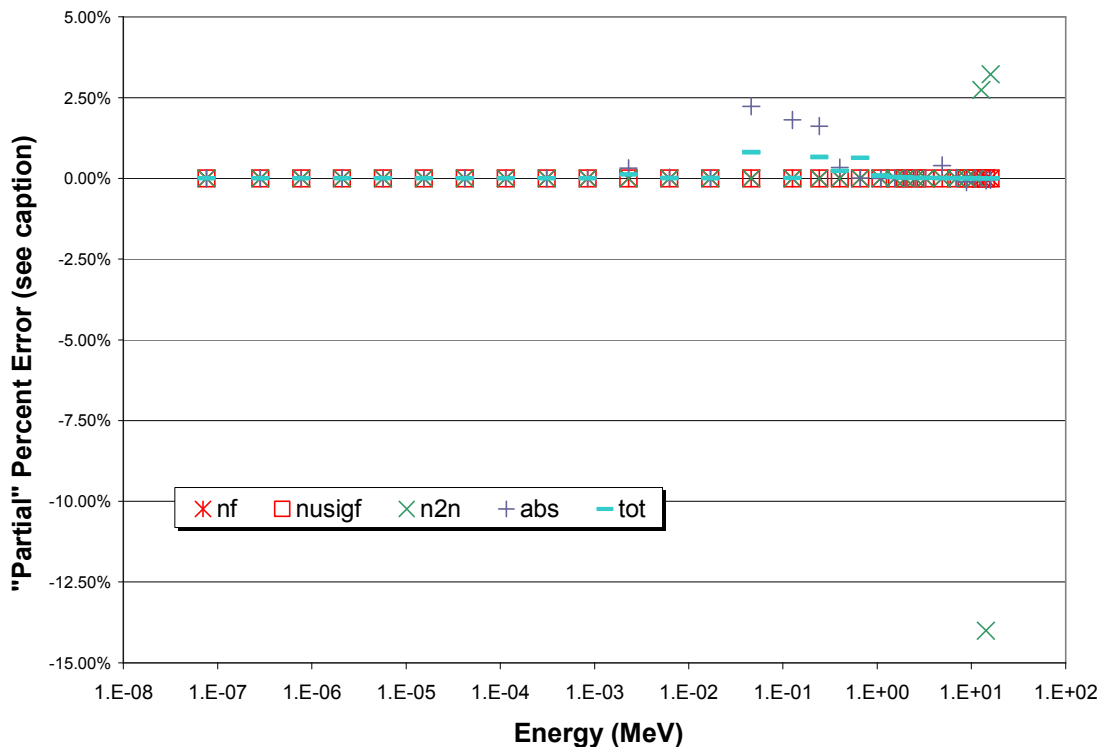


Fig. 17. "Partial" percent errors for reaction-rate densities in SCRA tally region 3. Each "partial" error is plotted at the midpoint energy of its group. The percent error in a given reaction rate is the sum of the 30 partial percent errors.

The fourth tally region is composed of the eight nearest fuel pin-cells to each control rod location for a total of sixteen cells. In Table 29 we show the MCNP-tallied scalar flux for the pin-cell, its relative standard deviation, the TXSAMC-generated cross

sections and the TXSAMC-generated reaction rate densities for the fourth tally region.

Table 30 shows the MCNP-tallied reaction rate densities, their standard deviations and the partial percent error between the TXSAMC-generated reaction rates and the MCNP-tallied reaction rates for the fourth tally region.

TABLE 29
MCNP scalar flux, TXSAMC cross sections and reaction rates in SCRA tally region 4

| Energy Group | Scalar Flux (n/cm ² /hps) | Rel. Error (1 σ) | TXSAMC SIGMA (cm ⁻¹) | | | | | TXSAMC RRD (cm ⁻³) | | | | |
|--------------|--------------------------------------|--------------------------|----------------------------------|----------|----------|----------|----------|--------------------------------|----------|----------|----------|----------|
| | | | fission | nusigf | n2n | abs-fis | total | fission | nusigf | n2n | abs-fis | total |
| 1 | 0.00E+00 | 0.00% | 5.57E+00 | 1.36E+01 | 0.00E+00 | 9.86E-01 | 6.97E+00 | 0.00E+00 | 0.00E+00 | 0.00E+00 | 0.00E+00 | 0.00E+00 |
| 2 | 0.00E+00 | 0.00% | 2.14E+00 | 5.22E+00 | 0.00E+00 | 4.63E-01 | 2.96E+00 | 0.00E+00 | 0.00E+00 | 0.00E+00 | 0.00E+00 | 0.00E+00 |
| 3 | 0.00E+00 | 0.00% | 8.70E-01 | 2.12E+00 | 0.00E+00 | 1.41E-01 | 1.36E+00 | 0.00E+00 | 0.00E+00 | 0.00E+00 | 0.00E+00 | 0.00E+00 |
| 4 | 0.00E+00 | 0.00% | 2.36E-01 | 5.75E-01 | 0.00E+00 | 8.20E-02 | 6.53E-01 | 0.00E+00 | 0.00E+00 | 0.00E+00 | 0.00E+00 | 0.00E+00 |
| 5 | 7.13E-12 | 100.00% | 1.61E-01 | 3.93E-01 | 0.00E+00 | 4.22E-02 | 5.16E-01 | 1.15E-12 | 2.80E-12 | 0.00E+00 | 3.01E-13 | 3.68E-12 |
| 6 | 0.00E+00 | 0.00% | 5.61E-01 | 1.36E+00 | 0.00E+00 | 2.76E-01 | 1.25E+00 | 0.00E+00 | 0.00E+00 | 0.00E+00 | 0.00E+00 | 0.00E+00 |
| 7 | 1.02E-11 | 71.60% | 3.90E-01 | 9.48E-01 | 0.00E+00 | 1.90E-01 | 9.16E-01 | 3.97E-12 | 9.66E-12 | 0.00E+00 | 1.94E-12 | 9.34E-12 |
| 8 | 2.16E-10 | 69.32% | 2.39E-01 | 5.81E-01 | 0.00E+00 | 1.44E-01 | 7.52E-01 | 5.14E-11 | 1.25E-10 | 0.00E+00 | 3.11E-11 | 1.62E-10 |
| 9 | 9.21E-10 | 32.18% | 1.21E-01 | 2.94E-01 | 0.00E+00 | 5.40E-02 | 4.77E-01 | 1.11E-10 | 2.71E-10 | 0.00E+00 | 4.97E-11 | 4.39E-10 |
| 10 | 2.23E-08 | 7.88% | 9.88E-02 | 2.40E-01 | 0.00E+00 | 5.37E-02 | 4.92E-01 | 2.20E-09 | 5.36E-09 | 0.00E+00 | 1.20E-09 | 1.10E-08 |
| 11 | 1.40E-07 | 3.11% | 6.97E-02 | 1.70E-01 | 0.00E+00 | 3.71E-02 | 5.80E-01 | 9.80E-09 | 2.38E-08 | 0.00E+00 | 5.21E-09 | 8.15E-08 |
| 12 | 9.37E-07 | 1.30% | 4.28E-02 | 1.04E-01 | 0.00E+00 | 1.70E-02 | 4.64E-01 | 4.01E-08 | 9.76E-08 | 0.00E+00 | 1.59E-08 | 4.35E-07 |
| 13 | 6.11E-06 | 0.54% | 3.13E-02 | 7.61E-02 | 0.00E+00 | 1.15E-02 | 4.00E-01 | 1.91E-07 | 4.65E-07 | 0.00E+00 | 7.05E-08 | 2.44E-06 |
| 14 | 2.38E-05 | 0.29% | 2.40E-02 | 5.82E-02 | 0.00E+00 | 8.10E-03 | 3.80E-01 | 5.72E-07 | 1.39E-06 | 0.00E+00 | 1.93E-07 | 9.05E-06 |
| 15 | 6.93E-05 | 0.18% | 1.91E-02 | 4.65E-02 | 0.00E+00 | 5.20E-03 | 3.37E-01 | 1.32E-06 | 3.22E-06 | 0.00E+00 | 3.60E-07 | 2.34E-05 |
| 16 | 5.48E-05 | 0.19% | 1.66E-02 | 4.08E-02 | 0.00E+00 | 3.56E-03 | 3.19E-01 | 9.10E-07 | 2.24E-06 | 0.00E+00 | 1.95E-07 | 1.75E-05 |
| 17 | 5.39E-05 | 0.20% | 1.53E-02 | 3.78E-02 | 0.00E+00 | 2.68E-03 | 3.58E-01 | 8.24E-07 | 2.04E-06 | 0.00E+00 | 1.44E-07 | 1.93E-05 |
| 18 | 7.51E-05 | 0.18% | 1.43E-02 | 3.57E-02 | 0.00E+00 | 1.97E-03 | 2.82E-01 | 1.08E-06 | 2.68E-06 | 0.00E+00 | 1.48E-07 | 2.12E-05 |
| 19 | 5.53E-05 | 0.20% | 1.52E-02 | 3.85E-02 | 0.00E+00 | 1.53E-03 | 2.76E-01 | 8.39E-07 | 2.13E-06 | 0.00E+00 | 8.47E-08 | 1.52E-05 |
| 20 | 3.07E-05 | 0.27% | 1.63E-02 | 4.23E-02 | 0.00E+00 | 1.17E-03 | 2.09E-01 | 5.00E-07 | 1.30E-06 | 0.00E+00 | 3.60E-08 | 6.40E-06 |
| 21 | 2.70E-05 | 0.29% | 1.70E-02 | 4.49E-02 | 0.00E+00 | 8.82E-04 | 2.01E-01 | 4.59E-07 | 1.21E-06 | 0.00E+00 | 2.38E-08 | 5.42E-06 |
| 22 | 2.74E-05 | 0.29% | 1.69E-02 | 4.57E-02 | 0.00E+00 | 5.83E-04 | 1.82E-01 | 4.63E-07 | 1.25E-06 | 0.00E+00 | 1.60E-08 | 4.99E-06 |
| 23 | 1.84E-05 | 0.34% | 1.61E-02 | 4.49E-02 | 0.00E+00 | 3.63E-04 | 2.15E-01 | 2.97E-07 | 8.28E-07 | 0.00E+00 | 6.69E-09 | 3.97E-06 |
| 24 | 1.95E-05 | 0.34% | 1.51E-02 | 4.49E-02 | 1.12E-04 | 2.07E-03 | 2.00E-01 | 2.93E-07 | 8.74E-07 | 2.18E-09 | 4.02E-08 | 3.89E-06 |
| 25 | 3.11E-06 | 0.84% | 1.98E-02 | 6.66E-02 | 4.82E-03 | 0.00E+00 | 1.62E-01 | 6.14E-08 | 2.07E-07 | 1.50E-08 | 0.00E+00 | 5.03E-07 |
| 26 | 9.63E-07 | 1.49% | 2.45E-02 | 8.92E-02 | 9.71E-03 | 0.00E+00 | 1.56E-01 | 2.36E-08 | 8.58E-08 | 9.35E-09 | 0.00E+00 | 1.50E-07 |
| 27 | 1.79E-07 | 3.42% | 2.37E-02 | 9.36E-02 | 1.37E-02 | 0.00E+00 | 1.57E-01 | 4.26E-09 | 1.68E-08 | 2.46E-09 | 0.00E+00 | 2.81E-08 |
| 28 | 3.41E-08 | 7.70% | 2.51E-02 | 1.05E-01 | 1.29E-02 | 0.00E+00 | 1.60E-01 | 8.54E-10 | 3.58E-09 | 4.40E-10 | 0.00E+00 | 5.45E-09 |
| 29 | 1.15E-08 | 13.77% | 2.78E-02 | 1.23E-01 | 1.03E-02 | 0.00E+00 | 1.63E-01 | 3.19E-10 | 1.41E-09 | 1.18E-10 | 0.00E+00 | 1.88E-09 |
| 30 | 3.90E-09 | 24.09% | 3.13E-02 | 1.46E-01 | 8.93E-03 | 0.00E+00 | 1.72E-01 | 1.22E-10 | 5.68E-10 | 3.48E-11 | 0.00E+00 | 6.71E-10 |
| Total | 4.67E-04 | 0.08% | 1.09E+01 | 2.68E+01 | 6.05E-02 | 2.53E+00 | 2.17E+01 | 7.89E-06 | 2.01E-05 | 2.96E-08 | 1.34E-06 | 1.34E-04 |

TABLE 30
MCNP reaction rates and reaction rate comparison in SCRA tally region 4

| Energy | MCNP RRD (cm ⁻³) | | | | | MCNP Standard Deviation | | | | | Partial Percent Error (TXSAMC-MCNP)/MCNP | | | | |
|--------|------------------------------|----------|----------|----------|----------|-------------------------|---------|--------|---------|---------|--|--------|--------|---------|--------|
| | fission | nusigf | n2n | abs-fis | total | fission | nusigf | n2n | abs-fis | total | fission | nusigf | n2n | abs-fis | total |
| 1 | 0.00E+00 | 0.00E+00 | 0.00E+00 | 0.00E+00 | 0.00E+00 | N/A | N/A | N/A | N/A | N/A | N/A | N/A | N/A | N/A | N/A |
| 2 | 0.00E+00 | 0.00E+00 | 0.00E+00 | 0.00E+00 | 0.00E+00 | N/A | N/A | N/A | N/A | N/A | N/A | N/A | N/A | N/A | N/A |
| 3 | 0.00E+00 | 0.00E+00 | 0.00E+00 | 0.00E+00 | 0.00E+00 | N/A | N/A | N/A | N/A | N/A | N/A | N/A | N/A | N/A | N/A |
| 4 | 0.00E+00 | 0.00E+00 | 0.00E+00 | 0.00E+00 | 0.00E+00 | N/A | N/A | N/A | N/A | N/A | N/A | N/A | N/A | N/A | N/A |
| 5 | 2.77E-12 | 6.75E-12 | 0.00E+00 | 5.97E-13 | 6.65E-12 | 100.00% | 100.00% | N/A | 100.00% | 100.00% | 0.00% | 0.00% | N/A | 0.00% | 0.00% |
| 6 | 0.00E+00 | 0.00E+00 | 0.00E+00 | 0.00E+00 | 0.00E+00 | N/A | N/A | N/A | N/A | N/A | N/A | N/A | N/A | N/A | N/A |
| 7 | 2.05E-11 | 5.00E-11 | 0.00E+00 | 7.23E-12 | 3.25E-11 | 77.31% | 77.31% | N/A | 78.98% | 75.11% | 0.00% | 0.00% | N/A | 0.00% | 0.00% |
| 8 | 2.85E-11 | 6.92E-11 | 0.00E+00 | 2.28E-11 | 1.09E-10 | 61.87% | 61.87% | N/A | 60.38% | 48.34% | 0.00% | 0.00% | N/A | 0.00% | 0.00% |
| 9 | 1.33E-10 | 3.25E-10 | 0.00E+00 | 6.71E-11 | 5.38E-10 | 33.38% | 33.38% | N/A | 32.05% | 30.00% | 0.00% | 0.00% | N/A | 0.00% | 0.00% |
| 10 | 2.20E-09 | 5.34E-09 | 0.00E+00 | 1.30E-09 | 1.12E-08 | 8.61% | 8.61% | N/A | 9.33% | 7.22% | 0.00% | 0.00% | N/A | -0.01% | 0.00% |
| 11 | 9.53E-09 | 2.32E-08 | 0.00E+00 | 5.23E-09 | 1.19E-07 | 3.44% | 3.44% | N/A | 3.42% | 2.40% | 0.00% | 0.00% | N/A | 0.00% | -0.03% |
| 12 | 4.11E-08 | 1.00E-07 | 0.00E+00 | 1.64E-08 | 4.54E-07 | 1.42% | 1.42% | N/A | 1.38% | 1.05% | -0.01% | -0.01% | N/A | -0.03% | -0.01% |
| 13 | 1.93E-07 | 4.69E-07 | 0.00E+00 | 7.11E-08 | 2.47E-06 | 0.58% | 0.58% | N/A | 0.58% | 0.46% | -0.02% | -0.02% | N/A | -0.05% | -0.02% |
| 14 | 5.75E-07 | 1.39E-06 | 0.00E+00 | 1.94E-07 | 9.15E-06 | 0.30% | 0.30% | N/A | 0.30% | 0.24% | -0.03% | -0.03% | N/A | -0.07% | -0.07% |
| 15 | 1.33E-06 | 3.24E-06 | 0.00E+00 | 3.63E-07 | 2.35E-05 | 0.19% | 0.19% | N/A | 0.19% | 0.15% | -0.10% | -0.10% | N/A | -0.20% | -0.10% |
| 16 | 9.14E-07 | 2.24E-06 | 0.00E+00 | 1.96E-07 | 1.76E-05 | 0.20% | 0.20% | N/A | 0.20% | 0.16% | -0.05% | -0.05% | N/A | -0.07% | -0.07% |
| 17 | 8.28E-07 | 2.05E-06 | 0.00E+00 | 1.45E-07 | 2.00E-05 | 0.21% | 0.21% | N/A | 0.21% | 0.17% | -0.05% | -0.05% | N/A | -0.08% | -0.50% |
| 18 | 1.08E-06 | 2.70E-06 | 0.00E+00 | 1.49E-07 | 2.15E-05 | 0.19% | 0.19% | N/A | 0.19% | 0.14% | -0.08% | -0.08% | N/A | -0.08% | -0.20% |
| 19 | 8.43E-07 | 2.14E-06 | 0.00E+00 | 8.53E-08 | 1.54E-05 | 0.22% | 0.22% | N/A | 0.22% | 0.17% | -0.05% | -0.05% | N/A | -0.04% | -0.13% |
| 20 | 5.02E-07 | 1.30E-06 | 0.00E+00 | 3.62E-08 | 6.44E-06 | 0.28% | 0.28% | N/A | 0.28% | 0.23% | -0.02% | -0.02% | N/A | -0.01% | -0.02% |
| 21 | 4.61E-07 | 1.22E-06 | 0.00E+00 | 2.40E-08 | 5.46E-06 | 0.31% | 0.31% | N/A | 0.30% | 0.24% | -0.03% | -0.03% | N/A | -0.01% | -0.03% |
| 22 | 4.66E-07 | 1.26E-06 | 0.00E+00 | 1.61E-08 | 5.02E-06 | 0.31% | 0.31% | N/A | 0.30% | 0.24% | -0.04% | -0.04% | N/A | -0.01% | -0.02% |
| 23 | 2.99E-07 | 8.35E-07 | 0.00E+00 | 6.74E-09 | 4.03E-06 | 0.37% | 0.37% | N/A | 0.36% | 0.31% | -0.03% | -0.04% | N/A | 0.00% | -0.04% |
| 24 | 2.96E-07 | 8.83E-07 | 2.23E-09 | 4.26E-08 | 3.92E-06 | 0.37% | 0.37% | 1.20% | 0.46% | 0.31% | -0.04% | -0.05% | -0.17% | -0.17% | -0.03% |
| 25 | 6.21E-08 | 2.09E-07 | 1.52E-08 | 1.44E-08 | 5.09E-07 | 0.90% | 0.90% | 0.94% | 0.88% | 0.73% | -0.01% | -0.01% | -0.60% | -1.05% | 0.00% |
| 26 | 2.38E-08 | 8.66E-08 | 9.44E-09 | 5.72E-09 | 1.51E-07 | 1.59% | 1.59% | 1.56% | 1.31% | 1.29% | 0.00% | 0.00% | -0.30% | -0.42% | 0.00% |
| 27 | 4.36E-09 | 1.72E-08 | 2.51E-09 | 1.84E-09 | 2.85E-08 | 3.65% | 3.65% | 3.38% | 2.88% | 2.97% | 0.00% | 0.00% | -0.15% | -0.13% | 0.00% |
| 28 | 8.74E-10 | 3.67E-09 | 4.45E-10 | 3.26E-10 | 5.53E-09 | 8.31% | 8.33% | 7.26% | 6.20% | 6.75% | 0.00% | 0.00% | -0.02% | -0.02% | 0.00% |
| 29 | 3.12E-10 | 1.37E-09 | 1.15E-10 | 1.02E-10 | 1.85E-09 | 14.72% | 14.72% | 11.45% | 10.86% | 11.81% | 0.00% | 0.00% | 0.01% | -0.01% | 0.00% |
| 30 | 1.27E-10 | 5.92E-10 | 3.55E-11 | 2.87E-11 | 6.92E-10 | 24.53% | 24.54% | 17.26% | 19.40% | 21.00% | 0.00% | 0.00% | 0.00% | 0.00% | 0.00% |
| Total | 7.93E-06 | 2.02E-05 | 2.99E-08 | 1.38E-06 | 1.36E-04 | 0.09% | 0.09% | 0.77% | 0.11% | 0.07% | -0.57% | -0.58% | -1.23% | -2.48% | -1.29% |

From the second table, we see results similar to the first tally region in that the amount of error did not significantly decrease when compared to the SCR. Again, if we accept the possibility that a reduction in error would be due to better mapping of the within group flux, it is possible that the many overlapping resonances of the fuel are not mapped any better by 187 groups than 30 groups which results in the same cross sections and the same error as the SCR. Even if we presume that the 187 group spectrum mapped the 2.8 keV resonance well, the relative dearth of sodium in the first and fourth tally regions compared to fuel would reduce the benefits of this effect. In Fig. 18 we see the difference in the TXSAMC and MCNP RRD's for the fourth tally region displayed graphically.

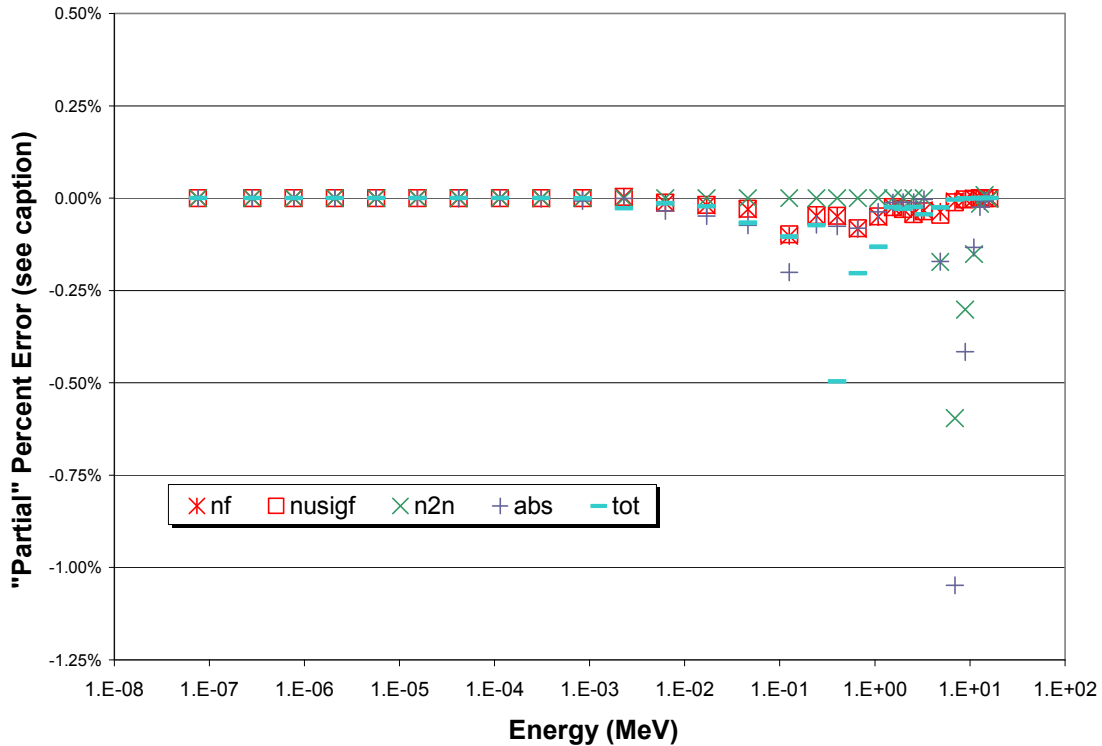


Fig. 18. "Partial" percent errors for reaction-rate densities in SCRA tally region 4. Each "partial" error is plotted at the midpoint energy of its group. The percent error in a given reaction rate is the sum of the 30 partial percent errors.

The fifth tally region is composed of the eight nearest fuel pin-cells to each coolant channel location for a total of sixteen cells. In Table 31 we show the MCNP-tallied scalar flux for the pin-cell, its relative standard deviation, the TXSAMC-generated cross sections and the TXSAMC-generated reaction rate densities for the fifth tally region. Table 32 shows the MCNP-tallied reaction rate densities, their standard deviations and the partial percent error between the TXSAMC-generated reaction rates and the MCNP-tallied reaction rates for the fifth tally region.

TABLE 31
MCNP scalar flux, TXSAMC cross sections and reaction rates in SCRA tally region 5

| Energy Group | Scalar Flux (n/cm ² /hps) | Rel. Error (1 σ) | TXSAMC SIGMA (cm ⁻¹) | | | | TXSAMC RRD (cm ⁻³) | | | | | |
|--------------|--------------------------------------|--------------------------|----------------------------------|----------|----------|----------|--------------------------------|----------|----------|----------|----------|----------|
| | | | fission | nusigf | n2n | abs-fis | total | fission | nusigf | n2n | abs-fis | total |
| 1 | 0.00E+00 | 0.00% | 5.57E+00 | 1.36E+01 | 0.00E+00 | 9.86E-01 | 6.97E+00 | 0.00E+00 | 0.00E+00 | 0.00E+00 | 0.00E+00 | 0.00E+00 |
| 2 | 0.00E+00 | 0.00% | 2.14E+00 | 5.22E+00 | 0.00E+00 | 4.63E-01 | 2.96E+00 | 0.00E+00 | 0.00E+00 | 0.00E+00 | 0.00E+00 | 0.00E+00 |
| 3 | 0.00E+00 | 0.00% | 8.70E-01 | 2.12E+00 | 0.00E+00 | 1.41E-01 | 1.36E+00 | 0.00E+00 | 0.00E+00 | 0.00E+00 | 0.00E+00 | 0.00E+00 |
| 4 | 0.00E+00 | 0.00% | 2.36E-01 | 5.75E-01 | 0.00E+00 | 8.20E-02 | 6.53E-01 | 0.00E+00 | 0.00E+00 | 0.00E+00 | 0.00E+00 | 0.00E+00 |
| 5 | 0.00E+00 | 0.00% | 1.61E-01 | 3.93E-01 | 0.00E+00 | 4.22E-02 | 5.16E-01 | 0.00E+00 | 0.00E+00 | 0.00E+00 | 0.00E+00 | 0.00E+00 |
| 6 | 0.00E+00 | 0.00% | 3.24E-01 | 7.88E-01 | 0.00E+00 | 1.60E-01 | 7.82E-01 | 0.00E+00 | 0.00E+00 | 0.00E+00 | 0.00E+00 | 0.00E+00 |
| 7 | 0.00E+00 | 0.00% | 6.75E-01 | 1.64E+00 | 0.00E+00 | 3.29E-01 | 1.48E+00 | 0.00E+00 | 0.00E+00 | 0.00E+00 | 0.00E+00 | 0.00E+00 |
| 8 | 1.28E-11 | 100.00% | 1.18E-01 | 2.88E-01 | 0.00E+00 | 7.18E-02 | 4.41E-01 | 1.52E-12 | 3.70E-12 | 0.00E+00 | 9.21E-13 | 5.66E-12 |
| 9 | 7.83E-10 | 34.37% | 1.44E-01 | 3.49E-01 | 0.00E+00 | 6.40E-02 | 5.36E-01 | 1.12E-10 | 2.73E-10 | 0.00E+00 | 5.01E-11 | 4.20E-10 |
| 10 | 2.07E-08 | 7.70% | 9.92E-02 | 2.41E-01 | 0.00E+00 | 5.40E-02 | 4.93E-01 | 2.06E-09 | 5.00E-09 | 0.00E+00 | 1.12E-09 | 1.02E-08 |
| 11 | 1.44E-07 | 3.11% | 6.97E-02 | 1.70E-01 | 0.00E+00 | 3.71E-02 | 5.82E-01 | 1.00E-08 | 2.44E-08 | 0.00E+00 | 5.34E-09 | 8.38E-08 |
| 12 | 9.31E-07 | 1.30% | 4.28E-02 | 1.04E-01 | 0.00E+00 | 1.70E-02 | 4.64E-01 | 3.99E-08 | 9.71E-08 | 0.00E+00 | 1.58E-08 | 4.32E-07 |
| 13 | 6.12E-06 | 0.54% | 3.13E-02 | 7.60E-02 | 0.00E+00 | 1.15E-02 | 3.99E-01 | 1.91E-07 | 4.65E-07 | 0.00E+00 | 7.05E-08 | 2.45E-06 |
| 14 | 2.38E-05 | 0.29% | 2.40E-02 | 5.82E-02 | 0.00E+00 | 8.10E-03 | 3.80E-01 | 5.72E-07 | 1.39E-06 | 0.00E+00 | 1.93E-07 | 9.04E-06 |
| 15 | 6.93E-05 | 0.18% | 1.91E-02 | 4.65E-02 | 0.00E+00 | 5.20E-03 | 3.37E-01 | 1.32E-06 | 3.22E-06 | 0.00E+00 | 3.61E-07 | 2.34E-05 |
| 16 | 5.49E-05 | 0.19% | 1.66E-02 | 4.07E-02 | 0.00E+00 | 3.56E-03 | 3.19E-01 | 9.11E-07 | 2.24E-06 | 0.00E+00 | 1.96E-07 | 1.75E-05 |
| 17 | 5.40E-05 | 0.20% | 1.53E-02 | 3.78E-02 | 0.00E+00 | 2.68E-03 | 3.58E-01 | 8.26E-07 | 2.04E-06 | 0.00E+00 | 1.45E-07 | 1.93E-05 |
| 18 | 7.52E-05 | 0.18% | 1.43E-02 | 3.58E-02 | 0.00E+00 | 1.97E-03 | 2.82E-01 | 1.08E-06 | 2.69E-06 | 0.00E+00 | 1.48E-07 | 2.12E-05 |
| 19 | 5.57E-05 | 0.20% | 1.52E-02 | 3.85E-02 | 0.00E+00 | 1.53E-03 | 2.76E-01 | 8.45E-07 | 2.15E-06 | 0.00E+00 | 8.54E-08 | 1.54E-05 |
| 20 | 3.08E-05 | 0.27% | 1.63E-02 | 4.22E-02 | 0.00E+00 | 1.17E-03 | 2.09E-01 | 5.02E-07 | 1.30E-06 | 0.00E+00 | 3.61E-08 | 6.43E-06 |
| 21 | 2.72E-05 | 0.28% | 1.70E-02 | 4.48E-02 | 0.00E+00 | 8.81E-04 | 2.01E-01 | 4.61E-07 | 1.22E-06 | 0.00E+00 | 2.40E-08 | 5.46E-06 |
| 22 | 2.74E-05 | 0.29% | 1.68E-02 | 4.56E-02 | 0.00E+00 | 5.81E-04 | 1.82E-01 | 4.61E-07 | 1.25E-06 | 0.00E+00 | 1.59E-08 | 4.97E-06 |
| 23 | 1.85E-05 | 0.34% | 1.61E-02 | 4.49E-02 | 0.00E+00 | 3.63E-04 | 2.16E-01 | 2.98E-07 | 8.30E-07 | 0.00E+00 | 6.71E-09 | 3.98E-06 |
| 24 | 1.96E-05 | 0.34% | 1.51E-02 | 4.49E-02 | 1.12E-04 | 2.07E-03 | 2.00E-01 | 2.96E-07 | 8.81E-07 | 2.20E-09 | 4.05E-08 | 3.92E-06 |
| 25 | 3.18E-06 | 0.83% | 1.98E-02 | 6.68E-02 | 4.84E-03 | 0.00E+00 | 1.62E-01 | 6.30E-08 | 2.12E-07 | 1.54E-08 | 0.00E+00 | 5.16E-07 |
| 26 | 9.67E-07 | 1.49% | 2.45E-02 | 8.90E-02 | 9.70E-03 | 0.00E+00 | 1.56E-01 | 2.36E-08 | 8.60E-08 | 9.37E-09 | 0.00E+00 | 1.50E-07 |
| 27 | 1.83E-07 | 3.41% | 2.40E-02 | 9.47E-02 | 1.38E-02 | 0.00E+00 | 1.57E-01 | 4.39E-09 | 1.73E-08 | 2.53E-09 | 0.00E+00 | 2.88E-08 |
| 28 | 3.18E-08 | 8.00% | 2.64E-02 | 1.11E-01 | 1.35E-02 | 0.00E+00 | 1.64E-01 | 8.40E-10 | 3.52E-09 | 4.28E-10 | 0.00E+00 | 5.22E-09 |
| 29 | 1.03E-08 | 13.47% | 2.79E-02 | 1.23E-01 | 1.04E-02 | 0.00E+00 | 1.63E-01 | 2.88E-10 | 1.27E-09 | 1.07E-10 | 0.00E+00 | 1.69E-09 |
| 30 | 3.10E-09 | 22.35% | 2.84E-02 | 1.33E-01 | 8.64E-03 | 0.00E+00 | 1.65E-01 | 8.81E-11 | 4.10E-10 | 2.68E-11 | 0.00E+00 | 5.11E-10 |
| Total | 4.68E-04 | 0.08% | 1.08E+01 | 2.66E+01 | 6.10E-02 | 2.49E+00 | 2.16E+01 | 7.91E-06 | 2.01E-05 | 3.00E-08 | 1.34E-06 | 1.34E-04 |

Similar to the fourth tally region, this region shows hardly any improvement over the SCR. Again, the most likely reason for this is that the 187 group core-averaged spectrum does not result in a materially better picture of the within group flux and as a result does not produce cross sections that are any better than those produced with a 30 group core-averaged weighting function. This then begs the questions of how many groups are necessary to resolve even a few resonances and how expensive will it be computationally to get this resolution with a low variance. The answers to these questions are unknown at this time. In Fig. 19 we see the difference in the TXSAMC and MCNP RRD's for the fifth tally region displayed graphically.

TABLE 32
MCNP reaction rates and reaction rate comparison in SCRA tally region 5

| Energy Group | MCNP RRD (cm ⁻³) | | | | | MCNP Standard Deviation | | | | | Partial Percent Error (TXSAMC-MCNP)/MCNP | | | | |
|--------------|------------------------------|----------|----------|----------|----------|-------------------------|---------|--------|---------|--------|--|--------|--------|---------|--------|
| | fission | nusigf | n2n | abs-fis | total | fission | nusigf | n2n | abs-fis | total | fission | nusigf | n2n | abs-fis | total |
| 1 | 0.00E+00 | 0.00E+00 | 0.00E+00 | 0.00E+00 | 0.00E+00 | N/A | N/A | N/A | N/A | N/A | N/A | N/A | N/A | N/A | N/A |
| 2 | 0.00E+00 | 0.00E+00 | 0.00E+00 | 0.00E+00 | 0.00E+00 | N/A | N/A | N/A | N/A | N/A | N/A | N/A | N/A | N/A | N/A |
| 3 | 0.00E+00 | 0.00E+00 | 0.00E+00 | 0.00E+00 | 0.00E+00 | N/A | N/A | N/A | N/A | N/A | N/A | N/A | N/A | N/A | N/A |
| 4 | 0.00E+00 | 0.00E+00 | 0.00E+00 | 0.00E+00 | 0.00E+00 | N/A | N/A | N/A | N/A | N/A | N/A | N/A | N/A | N/A | N/A |
| 5 | 0.00E+00 | 0.00E+00 | 0.00E+00 | 0.00E+00 | 0.00E+00 | N/A | N/A | N/A | N/A | N/A | N/A | N/A | N/A | N/A | N/A |
| 6 | 0.00E+00 | 0.00E+00 | 0.00E+00 | 0.00E+00 | 0.00E+00 | N/A | N/A | N/A | N/A | N/A | N/A | N/A | N/A | N/A | N/A |
| 7 | 0.00E+00 | 0.00E+00 | 0.00E+00 | 0.00E+00 | 0.00E+00 | N/A | N/A | N/A | N/A | N/A | N/A | N/A | N/A | N/A | N/A |
| 8 | 4.33E-12 | 1.05E-11 | 0.00E+00 | 4.66E-12 | 1.34E-11 | 100.00% | 100.00% | N/A | 99.97% | 93.89% | 0.00% | 0.00% | N/A | 0.00% | 0.00% |
| 9 | 8.47E-11 | 2.06E-10 | 0.00E+00 | 3.50E-11 | 3.41E-10 | 37.43% | 37.43% | N/A | 36.71% | 30.44% | 0.00% | 0.00% | N/A | 0.00% | 0.00% |
| 10 | 1.94E-09 | 4.72E-09 | 0.00E+00 | 1.10E-09 | 1.02E-08 | 8.74% | 8.74% | N/A | 8.53% | 7.20% | 0.00% | 0.00% | N/A | 0.00% | 0.00% |
| 11 | 9.89E-09 | 2.41E-08 | 0.00E+00 | 5.32E-09 | 1.16E-07 | 3.50% | 3.50% | N/A | 3.43% | 2.40% | 0.00% | 0.00% | N/A | 0.00% | -0.02% |
| 12 | 4.03E-08 | 9.81E-08 | 0.00E+00 | 1.61E-08 | 4.48E-07 | 1.42% | 1.42% | N/A | 1.38% | 1.05% | -0.01% | 0.00% | N/A | -0.02% | -0.01% |
| 13 | 1.93E-07 | 4.69E-07 | 0.00E+00 | 7.12E-08 | 2.48E-06 | 0.58% | 0.58% | N/A | 0.58% | 0.46% | -0.02% | -0.02% | N/A | -0.05% | -0.02% |
| 14 | 5.75E-07 | 1.39E-06 | 0.00E+00 | 1.94E-07 | 9.14E-06 | 0.30% | 0.30% | N/A | 0.30% | 0.24% | -0.04% | -0.04% | N/A | -0.10% | -0.07% |
| 15 | 1.33E-06 | 3.24E-06 | 0.00E+00 | 3.63E-07 | 2.35E-05 | 0.19% | 0.19% | N/A | 0.19% | 0.15% | -0.09% | -0.08% | N/A | -0.17% | -0.10% |
| 16 | 9.16E-07 | 2.25E-06 | 0.00E+00 | 1.97E-07 | 1.76E-05 | 0.20% | 0.20% | N/A | 0.20% | 0.16% | -0.06% | -0.06% | N/A | -0.09% | -0.08% |
| 17 | 8.30E-07 | 2.05E-06 | 0.00E+00 | 1.46E-07 | 2.00E-05 | 0.21% | 0.21% | N/A | 0.21% | 0.17% | -0.05% | -0.05% | N/A | -0.07% | -0.50% |
| 18 | 1.08E-06 | 2.70E-06 | 0.00E+00 | 1.49E-07 | 2.15E-05 | 0.19% | 0.19% | N/A | 0.19% | 0.14% | -0.08% | -0.08% | N/A | -0.08% | -0.20% |
| 19 | 8.50E-07 | 2.16E-06 | 0.00E+00 | 8.59E-08 | 1.55E-05 | 0.22% | 0.22% | N/A | 0.22% | 0.17% | -0.06% | -0.06% | N/A | -0.04% | -0.14% |
| 20 | 5.04E-07 | 1.31E-06 | 0.00E+00 | 3.64E-08 | 6.47E-06 | 0.28% | 0.28% | N/A | 0.27% | 0.22% | -0.03% | -0.03% | N/A | -0.02% | -0.03% |
| 21 | 4.64E-07 | 1.23E-06 | 0.00E+00 | 2.41E-08 | 5.50E-06 | 0.30% | 0.30% | N/A | 0.30% | 0.24% | -0.04% | -0.04% | N/A | -0.01% | -0.03% |
| 22 | 4.66E-07 | 1.26E-06 | 0.00E+00 | 1.61E-08 | 5.01E-06 | 0.31% | 0.31% | N/A | 0.30% | 0.24% | -0.06% | -0.06% | N/A | -0.02% | -0.03% |
| 23 | 3.00E-07 | 8.36E-07 | 0.00E+00 | 6.75E-09 | 4.04E-06 | 0.37% | 0.37% | N/A | 0.36% | 0.31% | -0.03% | -0.03% | N/A | 0.00% | -0.04% |
| 24 | 2.98E-07 | 8.89E-07 | 2.21E-09 | 4.31E-08 | 3.95E-06 | 0.36% | 0.36% | 1.20% | 0.46% | 0.30% | -0.03% | -0.04% | -0.03% | -0.19% | -0.03% |
| 25 | 6.33E-08 | 2.13E-07 | 1.54E-08 | 1.47E-08 | 5.19E-07 | 0.89% | 0.89% | 0.92% | 0.85% | 0.71% | 0.00% | 0.00% | -0.15% | -1.07% | 0.00% |
| 26 | 2.39E-08 | 8.71E-08 | 9.49E-09 | 5.76E-09 | 1.52E-07 | 1.59% | 1.59% | 1.56% | 1.31% | 1.29% | 0.00% | -0.01% | -0.38% | -0.42% | 0.00% |
| 27 | 4.47E-09 | 1.76E-08 | 2.58E-09 | 1.90E-09 | 2.92E-08 | 3.60% | 3.60% | 3.34% | 2.84% | 2.94% | 0.00% | 0.00% | -0.15% | -0.14% | 0.00% |
| 28 | 8.20E-10 | 3.44E-09 | 4.17E-10 | 3.07E-10 | 5.18E-09 | 8.52% | 8.54% | 7.56% | 6.40% | 6.95% | 0.00% | 0.00% | 0.04% | -0.02% | 0.00% |
| 29 | 2.82E-10 | 1.24E-09 | 1.04E-10 | 9.23E-11 | 1.67E-09 | 14.43% | 14.44% | 11.27% | 10.70% | 11.63% | 0.00% | 0.00% | 0.01% | -0.01% | 0.00% |
| 30 | 9.26E-11 | 4.29E-10 | 2.72E-11 | 2.40E-11 | 5.24E-10 | 22.67% | 22.69% | 15.47% | 17.02% | 18.77% | 0.00% | 0.00% | 0.00% | 0.00% | 0.00% |
| Total | 7.95E-06 | 2.02E-05 | 3.02E-08 | 1.38E-06 | 1.36E-04 | 0.09% | 0.09% | 0.77% | 0.11% | 0.07% | -0.60% | -0.60% | -0.66% | -2.50% | -1.30% |

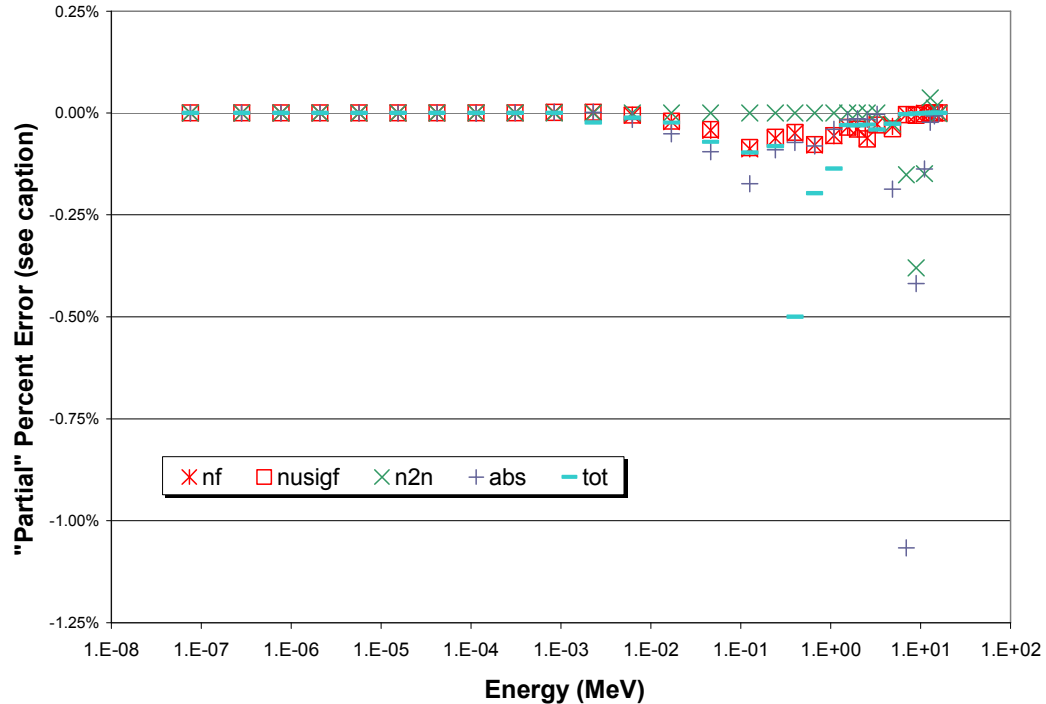


Fig. 19. "Partial" percent errors for reaction-rate densities in SCRA tally region 5. Each "partial" error is plotted at the midpoint energy of its group. The percent error in a given reaction rate is the sum of the 30 partial percent errors.

Overall, it appears that in fuel containing regions, the approach used in the SCRA was not measurably better than that used in the SCR and took significantly more computer time. However, in the coolant channel and control rod regions, which contain much more sodium, it does appear that there was value in using a 187 group weighting function since there was a significant reduction in error around the place that is most easily mapped (the 2.8 keV resonance). This suggests that there is benefit in the TXSAMC process in using weighting functions that can resolve at least some of the resonances in order to reduce error. However, given the computational cost, the net value of this approach may be very small.

HEX-COMPLEX REACTOR

This reactor is modeled as a regular hexagonal lattice with 23 pin-cells along the x-axis and like the SCR, it has non-fuel pin-cells and a reactor vessel. While this reactor is more complex and realistic in its layout and features than the HSR, it is by no means a high-fidelity model of an actual reactor. Like the SCR, it is missing many of the components that are usually modeled in a reactor such as a shield, coolant inlets and outlets or the power conversion system. It does, however, do a reasonable job of modeling some of the complexities associated with real reactor designs. The reactor vessel is a cylindrical shell of 316L stainless steel that is 35 cm long and 1.5 cm thick. Like the other three test cases, the coolant is liquid sodium at 450 K and the pins retain the same radial dimensions and temperatures. The fuel pins in this reactor are enriched to 90%, have a pin length of 30 cm and a fuel length of 29.8 cm. The higher enrichment results in a similar criticality ($k_{\text{eff}} \sim 1.10$) when compared to the HSR due to the tremendous increase in leakage in the system. This system also has three coolant channels and three control rod locations. The control rods are half the diameter of a fuel pin but the same length and are composed of an AgInCd core surrounded by a SS316L sleeve. The basic dimensions, materials and temperatures for the Hex-Complex Reactor (HCR) are described in Table 33. The HCR layout can be seen in Fig. 20.

TABLE 33
Description of materials, geometry and temperatures in HCR

| | |
|--------------------------------------|-----------------------|
| Reactor Label | HCR |
| Lattice Type | Hexagonal |
| Rows Along Diagonal | 23 |
| Pitch | 2.1 cm |
| Vessel Length | 35 cm |
| Vessel Thickness | 1.5 cm |
| Vessel Material | 316L Stainless Steel |
| Vessel Temperature | 400 K |
| Vessel Density | 5.5 g/cc |
| Coolant Material | Sodium |
| Coolant Temperature | 450 K |
| Coolant Density | 2.0 g/cc |
| Pin Length | 30.0 cm |
| Pin Diameter | 2.0 cm |
| Cladding Thickness | 0.1 cm |
| Cladding Material | Natural Zirconium |
| Cladding Temperature | 600 K |
| Cladding Density | 2.7 g/cc |
| Fuel Length | 29.8 cm |
| Fuel Diameter | 1.8 cm |
| Fuel Material | Uranium Dioxide |
| Enrichment | 90% |
| Fuel Temperature | 800 K |
| Fuel Density | 10.5 g/cc |
| Number of Control Rods | 3 |
| Control Rod Length | 30.0 cm |
| Control Rod Diameter | 1.0 cm |
| Control Rod Clad Thickness | 0.1 cm |
| Control Rod Clad Material | 316L Stainless Steel |
| Control Rod Clad Temperature | 400 K |
| Control Rod Clad Density | 5.5 g/cc |
| Control Rod Meat Length | 29.8 cm |
| Control Rod Meat Diameter | 0.8 cm |
| Control Rod Meat Material | Silver-Indium-Cadmium |
| Control Rod Meat Temperature | 500 K |
| Control Rod Meat Density | 8.5 g/cc |
| Number of Coolant Channels | 3 |
| Number of kcode cycles | 610 |
| Number of inactive cycles | 10 |
| Number of particles per cycle | 5000 |
| Number of histories | 3000000 |
| keff | 1.10227 |

In order to better test the ability of TXSAMC to produce properly shielded cross sections for a particular region in the reactor, the lattice was broken into five tally regions. The first region is composed of fuel pin-cells and is marked by the yellow fuel rods in Fig. 20. This region represents all fuel pins not adjacent to heterogeneities such as a coolant channel or control rod location. The second tally region is the three control rod positions which are marked by red on the reactor layout. The third region is the three coolant channels which are the light blue hexes in the interior of the core. The fourth region is composed of the six nearest pin-cells surrounding each control rod (eighteen total cells) and is marked in purple on the reactor layout. The final region is composed of the six nearest pin-cells surrounding the coolant channels (eighteen total cells) and is marked in brown on the reactor layout. For each of these regions, TXSAMC was used to create homogenized cross sections for the cells.

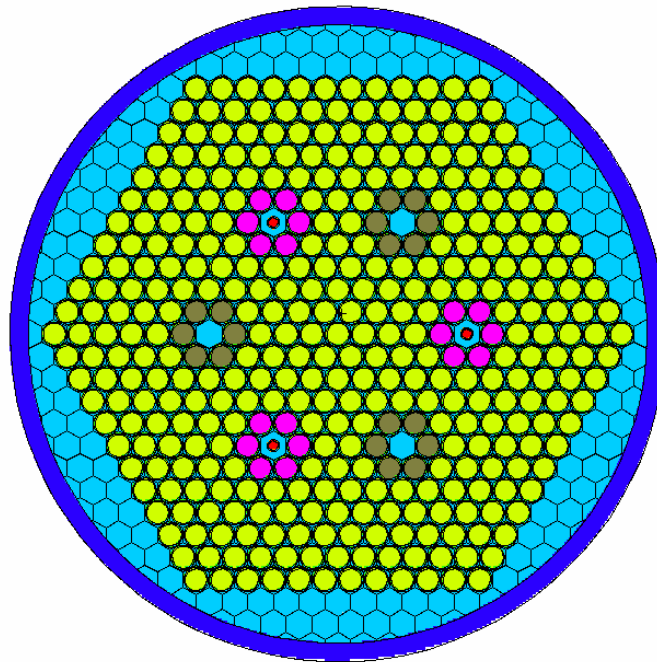


Fig. 20. HCR layout in x-y plane.

Yellow denotes tally region 1, red denotes tally region 2, light blue within core denotes tally region 3, purple denotes tally region 4 and brown denotes tally region 5. Dark blue denotes the reactor vessel.

The weighting function that is used in the NJOY module of TXSAMC is based on a core-averaged scalar flux. The multiplying scalar flux used to produce the TXSAMC RRD's is the cell-averaged scalar flux for the pin-cells within the specified tally region. The normalization of this scalar flux is over the combined cell volumes of the entire region. Since the TXSAMC-produced cross sections assume a one dimensional representation of the pin-cell, the MCNP-tallied RRD's are adjusted to reflect this. For example, in the fuel pin-cells the MCNP RRD for each component (meat, clad, coolant) is multiplied by the cross-sectional area in the x-y plane of that component and divided by the total pin-cell cross-sectional area. The net effect of this

adjustment is small as long as the pin length and vessel length are similar (i.e. not a lot of extra coolant) since the TXSAMC cross sections are produced by appropriately volume-normalized RZFLUX files and the MCNP RRD is also volume-normalized.

The first tally region is composed of all fuel pin-cells not immediately adjacent to the coolant channels or control rods. In Tables 34 we show the MCNP-tallied scalar flux for the pin-cell, its relative standard deviation, the TXSAMC-generated cross sections and the TXSAMC-generated reaction rate densities for the first tally region. Table 35 shows the MCNP-tallied reaction rate densities, their standard deviations and the partial percent error between the TXSAMC-generated reaction rates and the MCNP-tallied reaction rates for the first tally region.

TABLE 34
MCNP scalar flux, TXSAMC cross sections and reaction rates in HCR tally region 1

| Energy Group | Scalar Flux (n/cm ² /hps) | Rel. Error (1 σ) | TXSAMC SIGMA (cm ⁻¹) | | | | | TXSAMC RRD (cm ⁻³) | | | | | |
|--------------|--------------------------------------|--------------------------|----------------------------------|----------|----------|----------|----------|--------------------------------|----------|----------|----------|----------|----------|
| | | | fission | nusigf | n2n | abs-fis | total | fission | nusigf | n2n | abs-fis | total | |
| 1 | 0.00E+00 | 0.00% | 3.34E+00 | 8.13E+00 | 0.00E+00 | 5.75E-01 | 4.31E+00 | 0.00E+00 | 0.00E+00 | 0.00E+00 | 0.00E+00 | 0.00E+00 | 0.00E+00 |
| 2 | 0.00E+00 | 0.00% | 2.38E+00 | 5.81E+00 | 0.00E+00 | 5.01E-01 | 3.27E+00 | 0.00E+00 | 0.00E+00 | 0.00E+00 | 0.00E+00 | 0.00E+00 | 0.00E+00 |
| 3 | 0.00E+00 | 0.00% | 9.81E-01 | 2.39E+00 | 0.00E+00 | 1.36E-01 | 1.49E+00 | 0.00E+00 | 0.00E+00 | 0.00E+00 | 0.00E+00 | 0.00E+00 | 0.00E+00 |
| 4 | 0.00E+00 | 0.00% | 2.45E-01 | 5.96E-01 | 0.00E+00 | 9.00E-02 | 6.95E-01 | 0.00E+00 | 0.00E+00 | 0.00E+00 | 0.00E+00 | 0.00E+00 | 0.00E+00 |
| 5 | 0.00E+00 | 0.00% | 1.21E-01 | 2.96E-01 | 0.00E+00 | 1.67E-01 | 6.24E-01 | 0.00E+00 | 0.00E+00 | 0.00E+00 | 0.00E+00 | 0.00E+00 | 0.00E+00 |
| 6 | 1.14E-11 | 72.47% | 1.92E-04 | 4.67E-04 | 0.00E+00 | 7.77E-04 | 1.41E-01 | 2.18E-15 | 5.30E-15 | 0.00E+00 | 8.84E-15 | 1.61E-12 | |
| 7 | 1.83E-11 | 56.88% | 4.19E-01 | 1.02E+00 | 0.00E+00 | 2.13E-01 | 9.92E-01 | 7.66E-12 | 1.86E-11 | 0.00E+00 | 3.88E-12 | 1.81E-11 | |
| 8 | 2.35E-10 | 29.57% | 2.42E-01 | 5.89E-01 | 0.00E+00 | 1.45E-01 | 7.55E-01 | 5.68E-11 | 1.38E-10 | 0.00E+00 | 3.39E-11 | 1.77E-10 | |
| 9 | 1.62E-09 | 17.22% | 1.86E-01 | 4.53E-01 | 0.00E+00 | 8.36E-02 | 6.43E-01 | 3.03E-10 | 7.36E-10 | 0.00E+00 | 1.36E-10 | 1.04E-09 | |
| 10 | 1.55E-08 | 4.95% | 1.21E-01 | 2.95E-01 | 0.00E+00 | 6.52E-02 | 5.55E-01 | 1.88E-09 | 4.59E-09 | 0.00E+00 | 1.01E-09 | 8.63E-09 | |
| 11 | 1.03E-07 | 2.01% | 7.64E-02 | 1.86E-01 | 0.00E+00 | 3.57E-02 | 8.50E-01 | 7.89E-09 | 1.92E-08 | 0.00E+00 | 3.69E-09 | 8.77E-08 | |
| 12 | 7.58E-07 | 0.88% | 5.03E-02 | 1.22E-01 | 0.00E+00 | 1.99E-02 | 4.83E-01 | 3.81E-08 | 9.28E-08 | 0.00E+00 | 1.51E-08 | 3.66E-07 | |
| 13 | 5.13E-06 | 0.38% | 3.62E-02 | 8.79E-02 | 0.00E+00 | 1.33E-02 | 4.29E-01 | 1.86E-07 | 4.51E-07 | 0.00E+00 | 6.83E-08 | 2.20E-06 | |
| 14 | 2.15E-05 | 0.19% | 2.76E-02 | 6.69E-02 | 0.00E+00 | 9.26E-03 | 4.03E-01 | 5.94E-07 | 1.44E-06 | 0.00E+00 | 1.99E-07 | 8.68E-06 | |
| 15 | 6.63E-05 | 0.11% | 2.20E-02 | 5.35E-02 | 0.00E+00 | 5.98E-03 | 3.61E-01 | 1.46E-06 | 3.55E-06 | 0.00E+00 | 3.96E-07 | 2.39E-05 | |
| 16 | 5.54E-05 | 0.11% | 1.91E-02 | 4.69E-02 | 0.00E+00 | 4.10E-03 | 3.36E-01 | 1.06E-06 | 2.60E-06 | 0.00E+00 | 2.27E-07 | 1.86E-05 | |
| 17 | 5.45E-05 | 0.11% | 1.76E-02 | 4.34E-02 | 0.00E+00 | 3.06E-03 | 3.95E-01 | 9.59E-07 | 2.37E-06 | 0.00E+00 | 1.67E-07 | 2.15E-05 | |
| 18 | 8.09E-05 | 0.10% | 1.65E-02 | 4.11E-02 | 0.00E+00 | 2.25E-03 | 2.87E-01 | 1.33E-06 | 3.32E-06 | 0.00E+00 | 1.82E-07 | 2.32E-05 | |
| 19 | 5.91E-05 | 0.11% | 1.74E-02 | 4.42E-02 | 0.00E+00 | 1.76E-03 | 2.91E-01 | 1.03E-06 | 2.61E-06 | 0.00E+00 | 1.04E-07 | 1.72E-05 | |
| 20 | 3.27E-05 | 0.16% | 1.87E-02 | 4.86E-02 | 0.00E+00 | 1.35E-03 | 2.19E-01 | 6.12E-07 | 1.59E-06 | 0.00E+00 | 4.39E-08 | 7.15E-06 | |
| 21 | 2.92E-05 | 0.17% | 1.95E-02 | 5.15E-02 | 0.00E+00 | 1.01E-03 | 2.09E-01 | 5.69E-07 | 1.50E-06 | 0.00E+00 | 2.95E-08 | 6.08E-06 | |
| 22 | 3.05E-05 | 0.17% | 1.93E-02 | 5.23E-02 | 0.00E+00 | 6.84E-04 | 1.87E-01 | 5.89E-07 | 1.59E-06 | 0.00E+00 | 2.03E-08 | 5.70E-06 | |
| 23 | 2.06E-05 | 0.20% | 1.84E-02 | 5.13E-02 | 0.00E+00 | 4.12E-04 | 2.31E-01 | 3.77E-07 | 1.05E-06 | 0.00E+00 | 8.46E-09 | 4.74E-06 | |
| 24 | 2.19E-05 | 0.21% | 1.72E-02 | 5.13E-02 | 1.24E-04 | 2.34E-03 | 2.13E-01 | 3.76E-07 | 1.12E-06 | 2.72E-09 | 5.13E-08 | 4.65E-06 | |
| 25 | 3.57E-06 | 0.51% | 2.26E-02 | 7.63E-02 | 5.55E-03 | 0.00E+00 | 1.72E-01 | 8.08E-08 | 2.72E-07 | 1.98E-08 | 0.00E+00 | 6.12E-07 | |
| 26 | 1.05E-06 | 0.91% | 2.79E-02 | 1.01E-01 | 1.10E-02 | 0.00E+00 | 1.65E-01 | 2.92E-08 | 1.06E-07 | 1.16E-08 | 0.00E+00 | 1.73E-07 | |
| 27 | 2.06E-07 | 2.04% | 2.75E-02 | 1.08E-01 | 1.59E-02 | 0.00E+00 | 1.68E-01 | 5.65E-09 | 2.23E-08 | 3.26E-09 | 0.00E+00 | 3.45E-08 | |
| 28 | 3.49E-08 | 4.96% | 2.91E-02 | 1.22E-01 | 1.49E-02 | 0.00E+00 | 1.71E-01 | 1.01E-09 | 4.26E-09 | 5.21E-10 | 0.00E+00 | 5.98E-09 | |
| 29 | 1.25E-08 | 8.11% | 3.26E-02 | 1.44E-01 | 1.16E-02 | 0.00E+00 | 1.76E-01 | 4.08E-10 | 1.80E-09 | 1.45E-10 | 0.00E+00 | 2.20E-09 | |
| 30 | 4.13E-09 | 14.15% | 3.25E-02 | 1.50E-01 | 9.79E-03 | 0.00E+00 | 1.75E-01 | 1.35E-10 | 6.21E-10 | 4.05E-11 | 0.00E+00 | 7.23E-10 | |
| Total | 4.83E-04 | 0.04% | 8.59E+00 | 2.12E+01 | 6.89E-02 | 2.08E+00 | 1.94E+01 | 9.30E-06 | 2.37E-05 | 3.81E-08 | 1.52E-06 | 1.45E-04 | |

TABLE 35
MCNP reaction rates and reaction rate comparison in HCR tally region 1

| Energy Group | MCNP RRD (cm ⁻³) | | | | | MCNP Standard Deviation | | | | | Partial Percent Error (TXSAMC-MCNP)/MCNP | | | | |
|--------------|------------------------------|----------|----------|----------|----------|-------------------------|--------|-------|---------|--------|--|--------|--------|---------|--------|
| | fission | nusigf | n2n | abs | total | fission | nusigf | n2n | abs-fis | total | fission | nusigf | n2n | abs-fis | total |
| 1 | 0.00E+00 | 0.00E+00 | 0.00E+00 | 0.00E+00 | 0.00E+00 | N/A | N/A | N/A | N/A | N/A | N/A | N/A | N/A | N/A | N/A |
| 2 | 0.00E+00 | 0.00E+00 | 0.00E+00 | 0.00E+00 | 0.00E+00 | N/A | N/A | N/A | N/A | N/A | N/A | N/A | N/A | N/A | N/A |
| 3 | 0.00E+00 | 0.00E+00 | 0.00E+00 | 0.00E+00 | 0.00E+00 | N/A | N/A | N/A | N/A | N/A | N/A | N/A | N/A | N/A | N/A |
| 4 | 0.00E+00 | 0.00E+00 | 0.00E+00 | 0.00E+00 | 0.00E+00 | N/A | N/A | N/A | N/A | N/A | N/A | N/A | N/A | N/A | N/A |
| 5 | 0.00E+00 | 0.00E+00 | 0.00E+00 | 0.00E+00 | 0.00E+00 | N/A | N/A | N/A | N/A | N/A | N/A | N/A | N/A | N/A | N/A |
| 6 | 7.77E-12 | 1.89E-11 | 0.00E+00 | 1.34E-11 | 2.78E-11 | 72.56% | 72.56% | N/A | 84.26% | 79.33% | 0.00% | 0.00% | N/A | 0.00% | 0.00% |
| 7 | 1.61E-11 | 3.92E-11 | 0.00E+00 | 4.23E-12 | 2.92E-11 | 45.72% | 45.72% | N/A | 48.31% | 44.90% | 0.00% | 0.00% | N/A | 0.00% | 0.00% |
| 8 | 8.50E-11 | 2.07E-10 | 0.00E+00 | 5.27E-11 | 2.38E-10 | 32.67% | 32.67% | N/A | 30.49% | 27.30% | 0.00% | 0.00% | N/A | 0.00% | 0.00% |
| 9 | 2.95E-10 | 7.18E-10 | 0.00E+00 | 1.26E-10 | 1.02E-09 | 16.17% | 16.17% | N/A | 16.38% | 15.69% | 0.00% | 0.00% | N/A | 0.00% | 0.00% |
| 10 | 1.88E-09 | 4.57E-09 | 0.00E+00 | 1.03E-09 | 8.78E-09 | 5.21% | 5.21% | N/A | 5.25% | 4.59% | 0.00% | 0.00% | N/A | 0.00% | 0.00% |
| 11 | 8.33E-09 | 2.03E-08 | 0.00E+00 | 4.37E-09 | 7.90E-08 | 2.10% | 2.10% | N/A | 2.11% | 1.45% | 0.00% | 0.00% | N/A | -0.04% | 0.01% |
| 12 | 3.81E-08 | 9.27E-08 | 0.00E+00 | 1.52E-08 | 3.73E-07 | 0.91% | 0.91% | N/A | 0.89% | 0.74% | 0.00% | 0.00% | N/A | -0.01% | 0.00% |
| 13 | 1.87E-07 | 4.55E-07 | 0.00E+00 | 6.90E-08 | 2.22E-06 | 0.39% | 0.39% | N/A | 0.39% | 0.33% | -0.02% | -0.02% | N/A | -0.04% | -0.01% |
| 14 | 6.01E-07 | 1.46E-06 | 0.00E+00 | 2.02E-07 | 8.79E-06 | 0.20% | 0.20% | N/A | 0.20% | 0.17% | -0.08% | -0.08% | N/A | -0.19% | -0.07% |
| 15 | 1.47E-06 | 3.59E-06 | 0.00E+00 | 4.01E-07 | 2.42E-05 | 0.11% | 0.11% | N/A | 0.11% | 0.09% | -0.17% | -0.16% | N/A | -0.32% | -0.16% |
| 16 | 1.07E-06 | 2.62E-06 | 0.00E+00 | 2.29E-07 | 1.88E-05 | 0.11% | 0.11% | N/A | 0.11% | 0.09% | -0.09% | -0.09% | N/A | -0.11% | -0.12% |
| 17 | 9.69E-07 | 2.39E-06 | 0.00E+00 | 1.70E-07 | 2.18E-05 | 0.11% | 0.11% | N/A | 0.11% | 0.10% | -0.10% | -0.10% | N/A | -0.18% | -0.21% |
| 18 | 1.35E-06 | 3.36E-06 | 0.00E+00 | 1.85E-07 | 2.35E-05 | 0.10% | 0.10% | N/A | 0.10% | 0.08% | -0.14% | -0.14% | N/A | -0.15% | -0.24% |
| 19 | 1.04E-06 | 2.64E-06 | 0.00E+00 | 1.05E-07 | 1.72E-05 | 0.11% | 0.11% | N/A | 0.11% | 0.09% | -0.10% | -0.10% | N/A | -0.05% | -0.03% |
| 20 | 6.17E-07 | 1.60E-06 | 0.00E+00 | 4.44E-08 | 7.22E-06 | 0.16% | 0.16% | N/A | 0.16% | 0.14% | -0.05% | -0.05% | N/A | -0.03% | -0.05% |
| 21 | 5.73E-07 | 1.52E-06 | 0.00E+00 | 2.98E-08 | 6.14E-06 | 0.17% | 0.17% | N/A | 0.16% | 0.14% | -0.05% | -0.05% | N/A | -0.02% | -0.04% |
| 22 | 5.95E-07 | 1.61E-06 | 0.00E+00 | 2.06E-08 | 5.75E-06 | 0.17% | 0.17% | N/A | 0.17% | 0.14% | -0.06% | -0.07% | N/A | -0.02% | -0.03% |
| 23 | 3.82E-07 | 1.07E-06 | 0.00E+00 | 8.58E-09 | 4.79E-06 | 0.20% | 0.20% | N/A | 0.20% | 0.19% | -0.05% | -0.05% | N/A | -0.01% | -0.04% |
| 24 | 3.81E-07 | 1.13E-06 | 2.83E-09 | 5.45E-08 | 4.70E-06 | 0.21% | 0.21% | 0.68% | 0.27% | 0.19% | -0.04% | -0.05% | -0.31% | -0.20% | -0.03% |
| 25 | 8.10E-08 | 2.73E-07 | 1.97E-08 | 1.77E-08 | 6.18E-07 | 0.52% | 0.52% | 0.54% | 0.52% | 0.44% | 0.00% | 0.00% | 0.16% | -1.13% | 0.00% |
| 26 | 2.95E-08 | 1.07E-07 | 1.17E-08 | 6.22E-09 | 1.75E-07 | 0.91% | 0.91% | 0.90% | 0.82% | 0.78% | 0.00% | 0.00% | -0.20% | -0.40% | 0.00% |
| 27 | 5.70E-09 | 2.24E-08 | 3.29E-09 | 2.11E-09 | 3.48E-08 | 2.06% | 2.06% | 1.90% | 1.80% | 1.78% | 0.00% | 0.00% | -0.07% | -0.14% | 0.00% |
| 28 | 1.02E-09 | 4.26E-09 | 5.24E-10 | 3.23E-10 | 6.01E-09 | 4.96% | 4.96% | 4.43% | 4.15% | 4.29% | 0.00% | 0.00% | -0.01% | -0.02% | 0.00% |
| 29 | 4.05E-10 | 1.79E-09 | 1.44E-10 | 1.08E-10 | 2.20E-09 | 8.28% | 8.28% | 6.58% | 6.82% | 7.18% | 0.00% | 0.00% | 0.00% | -0.01% | 0.00% |
| 30 | 1.39E-10 | 6.50E-10 | 3.84E-11 | 2.93E-11 | 7.39E-10 | 14.10% | 14.13% | 9.74% | 11.33% | 12.31% | 0.00% | 0.00% | 0.01% | 0.00% | 0.00% |
| Total | 9.39E-06 | 2.40E-05 | 3.82E-08 | 1.57E-06 | 1.46E-04 | 0.04% | 0.04% | 0.44% | 0.06% | 0.03% | -0.97% | -0.97% | -0.42% | -3.06% | -1.04% |

From the first table, we observe the fast nature of the system with no tallied scalar flux in the first five groups. In the second table, we also observe an overall error of ~1% for all five reaction rates measured in this survey which is greater than was observed in the HSR test case. This is not surprising since the HCR is a more complex system that does not fit as easily into the TRANSX module of TXSAMC. That is, it is not an infinite lattice and there is significant leakage from the system. The error for this first tally region is also significantly smaller than that seen in a similar region in the SCR. It is unclear at this time why this is the case although it has been speculated that it

is related to the reduced fuel/coolant ratio in hex cells or a more accurate calculation of the background cross sections in TRANSX.

It is probable that this amount of error would be acceptable for design purposes but if not, a potential solution would be to divide this one region into smaller regions to better reflect the differences in flux each region sees. Since a pin near the center of a real reactor (as opposed to the infinite lattices of the HSR and SSR) sees a different level (and potentially energy shape) of neutron flux than a pin near the edge, there could be significant differences in the amount of shielding in each region. By dividing the core into smaller pieces, the relative fidelity of the shielding process is increased since one can now shield pin cells in a manner more reflective of reality. We would still expect to see greater errors than in the HSR and SSR test cases since there are still significant deviations from an infinite lattice but some of the error should be alleviated. This hypothesis appears to bear out in tally regions four and five for this reactor. Another possibility for reducing error in strongly heterogeneous systems would be to modify TXSAMC such that NJOY would employ regional, not core-averaged, spectral weight functions.

Although there are a number of groups where the difference between the TXSAMC- and MCNP-produced RRD is large, most of these groups have very low reaction rates so the RRD-weighted difference is very small. In some ways this is actually beneficial since most of the error lies in places that do not contribute much to the total reaction rates. This makes TXSAMC potentially more useful since it is most

accurate for the most common (and important) reactions and the energy groups where most of the reactions occur.

In Fig. 21 we see the difference in the TXSAMC and MCNP RRD's for the first tally region displayed graphically. The very low errors in the low energy range are quite obvious in this plot as well as the general accuracy of the cross sections at mid-to-high energy range groups which are more important for determining the overall RRD for the cell. It is apparent from the plot that the error in this region is smaller than for its sister region in the SCR.

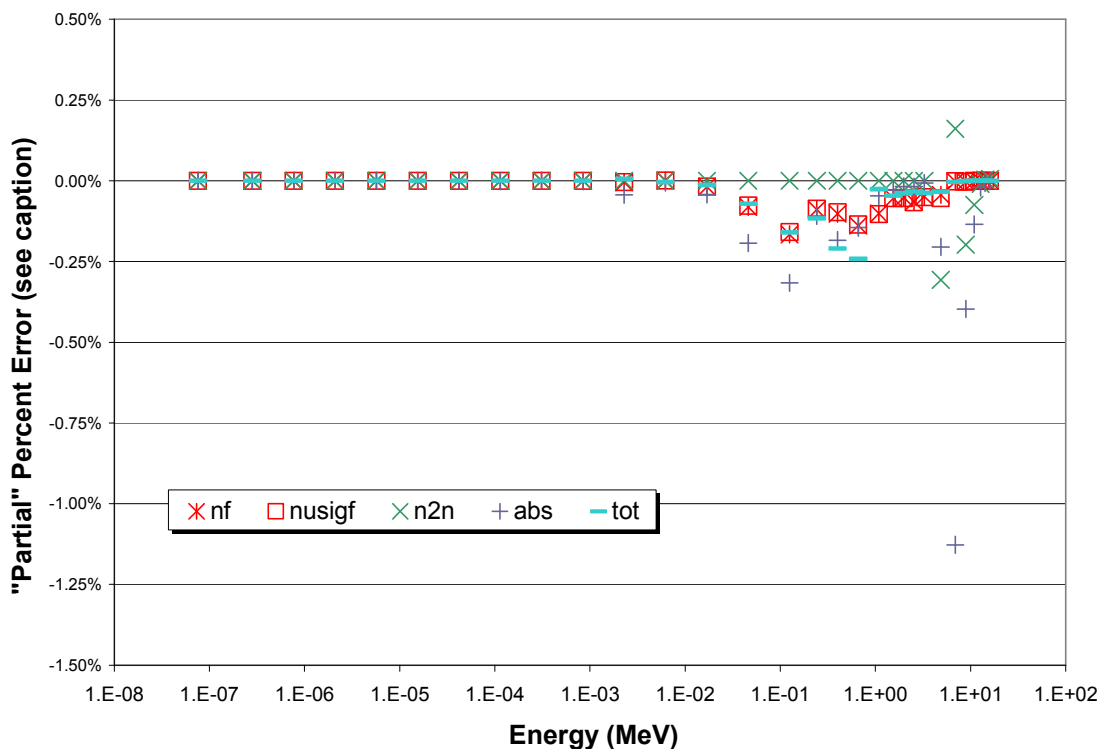


Fig. 21. "Partial" percent errors for reaction-rate densities in HCR tally region 1. Each "partial" error is plotted at the midpoint energy of its group. The percent error in a given reaction rate is the sum of the 30 partial percent errors.

The second tally region is made up of the control rod pin-cells which consist of an AgInCd cylinder in a SS316L sleeve surrounded by coolant. In Table 36 we show the MCNP-tallied scalar flux for the pin-cell, its relative standard deviation, the TXSAMC-generated cross sections and the TXSAMC-generated reaction rate densities for the second tally region. Table 37 shows the MCNP-tallied reaction rate densities, their standard deviations and the partial percent error between the TXSAMC-generated reaction rates and the MCNP-tallied reaction rates for the second tally region.

TABLE 36
MCNP scalar flux, TXSAMC cross sections and reaction rates in HCR tally region 2

| Energy Group | Scalar Flux (n/cm ² /nps) | Rel. Error (1 σ) | TXSAMC SIGMA (cm ⁻¹) | | | | | TXSAMC RRD (cm ⁻³) | | | | | |
|--------------|--------------------------------------|--------------------------|----------------------------------|----------|----------|----------|----------|--------------------------------|----------|----------|----------|----------|----------|
| | | | fission | nusigf | n2n | abs-fis | total | fission | nusigf | n2n | abs-fis | total | |
| 1 | 0.00E+00 | 0.00% | 0.00E+00 | 0.00E+00 | 0.00E+00 | 1.82E+00 | 2.05E+00 | 0.00E+00 | 0.00E+00 | 0.00E+00 | 0.00E+00 | 0.00E+00 | 0.00E+00 |
| 2 | 0.00E+00 | 0.00% | 0.00E+00 | 0.00E+00 | 0.00E+00 | 8.31E-01 | 1.05E+00 | 0.00E+00 | 0.00E+00 | 0.00E+00 | 0.00E+00 | 0.00E+00 | 0.00E+00 |
| 3 | 0.00E+00 | 0.00% | 0.00E+00 | 0.00E+00 | 0.00E+00 | 2.84E-01 | 4.99E-01 | 0.00E+00 | 0.00E+00 | 0.00E+00 | 0.00E+00 | 0.00E+00 | 0.00E+00 |
| 4 | 0.00E+00 | 0.00% | 0.00E+00 | 0.00E+00 | 0.00E+00 | 4.11E-01 | 6.44E-01 | 0.00E+00 | 0.00E+00 | 0.00E+00 | 0.00E+00 | 0.00E+00 | 0.00E+00 |
| 5 | 0.00E+00 | 0.00% | 0.00E+00 | 0.00E+00 | 0.00E+00 | 1.25E-01 | 3.68E-01 | 0.00E+00 | 0.00E+00 | 0.00E+00 | 0.00E+00 | 0.00E+00 | 0.00E+00 |
| 6 | 0.00E+00 | 0.00% | 0.00E+00 | 0.00E+00 | 0.00E+00 | 4.23E-02 | 2.64E-01 | 0.00E+00 | 0.00E+00 | 0.00E+00 | 0.00E+00 | 0.00E+00 | 0.00E+00 |
| 7 | 0.00E+00 | 0.00% | 0.00E+00 | 0.00E+00 | 0.00E+00 | 6.32E-02 | 2.87E-01 | 0.00E+00 | 0.00E+00 | 0.00E+00 | 0.00E+00 | 0.00E+00 | 0.00E+00 |
| 8 | 0.00E+00 | 0.00% | 0.00E+00 | 0.00E+00 | 0.00E+00 | 7.46E-02 | 3.37E-01 | 0.00E+00 | 0.00E+00 | 0.00E+00 | 0.00E+00 | 0.00E+00 | 0.00E+00 |
| 9 | 1.22E-09 | 100.00% | 0.00E+00 | 0.00E+00 | 0.00E+00 | 7.18E-02 | 3.47E-01 | 0.00E+00 | 0.00E+00 | 0.00E+00 | 8.79E-11 | 4.24E-10 | |
| 10 | 1.19E-08 | 27.58% | 0.00E+00 | 0.00E+00 | 0.00E+00 | 1.59E-02 | 2.66E-01 | 0.00E+00 | 0.00E+00 | 0.00E+00 | 1.89E-10 | 3.16E-09 | |
| 11 | 1.76E-07 | 9.73% | 0.00E+00 | 0.00E+00 | 0.00E+00 | 1.29E-02 | 1.32E+00 | 0.00E+00 | 0.00E+00 | 0.00E+00 | 2.27E-09 | 2.34E-07 | |
| 12 | 1.06E-06 | 3.73% | 0.00E+00 | 0.00E+00 | 0.00E+00 | 1.11E-02 | 4.53E-01 | 0.00E+00 | 0.00E+00 | 0.00E+00 | 1.18E-08 | 4.80E-07 | |
| 13 | 7.26E-06 | 1.41% | 0.00E+00 | 0.00E+00 | 0.00E+00 | 7.81E-03 | 2.70E-01 | 0.00E+00 | 0.00E+00 | 0.00E+00 | 5.66E-08 | 1.96E-06 | |
| 14 | 3.01E-05 | 0.71% | 0.00E+00 | 0.00E+00 | 0.00E+00 | 5.22E-03 | 2.79E-01 | 0.00E+00 | 0.00E+00 | 0.00E+00 | 1.57E-07 | 8.40E-06 | |
| 15 | 9.25E-05 | 0.43% | 0.00E+00 | 0.00E+00 | 0.00E+00 | 3.28E-03 | 2.20E-01 | 0.00E+00 | 0.00E+00 | 0.00E+00 | 3.03E-07 | 2.04E-05 | |
| 16 | 7.62E-05 | 0.48% | 0.00E+00 | 0.00E+00 | 0.00E+00 | 2.31E-03 | 2.39E-01 | 0.00E+00 | 0.00E+00 | 0.00E+00 | 1.76E-07 | 1.82E-05 | |
| 17 | 7.57E-05 | 0.51% | 0.00E+00 | 0.00E+00 | 0.00E+00 | 1.64E-03 | 2.14E-01 | 0.00E+00 | 0.00E+00 | 0.00E+00 | 1.24E-07 | 1.62E-05 | |
| 18 | 1.08E-04 | 0.43% | 0.00E+00 | 0.00E+00 | 0.00E+00 | 1.21E-03 | 2.63E-01 | 0.00E+00 | 0.00E+00 | 0.00E+00 | 1.31E-07 | 2.84E-05 | |
| 19 | 7.82E-05 | 0.52% | 0.00E+00 | 0.00E+00 | 0.00E+00 | 9.26E-04 | 2.11E-01 | 0.00E+00 | 0.00E+00 | 0.00E+00 | 7.24E-08 | 1.65E-05 | |
| 20 | 4.30E-05 | 0.69% | 0.00E+00 | 0.00E+00 | 0.00E+00 | 7.73E-04 | 1.66E-01 | 0.00E+00 | 0.00E+00 | 0.00E+00 | 3.33E-08 | 7.15E-06 | |
| 21 | 3.80E-05 | 0.75% | 0.00E+00 | 0.00E+00 | 0.00E+00 | 6.79E-04 | 1.68E-01 | 0.00E+00 | 0.00E+00 | 0.00E+00 | 2.58E-08 | 6.40E-06 | |
| 22 | 3.81E-05 | 0.74% | 0.00E+00 | 0.00E+00 | 0.00E+00 | 5.93E-04 | 1.65E-01 | 0.00E+00 | 0.00E+00 | 0.00E+00 | 2.26E-08 | 6.30E-06 | |
| 23 | 2.61E-05 | 0.90% | 0.00E+00 | 0.00E+00 | 0.00E+00 | 5.21E-04 | 1.41E-01 | 0.00E+00 | 0.00E+00 | 0.00E+00 | 1.36E-08 | 3.67E-06 | |
| 24 | 2.70E-05 | 0.88% | 0.00E+00 | 0.00E+00 | 0.00E+00 | 6.24E-04 | 1.32E-01 | 0.00E+00 | 0.00E+00 | 0.00E+00 | 1.69E-08 | 3.56E-06 | |
| 25 | 4.31E-06 | 2.17% | 0.00E+00 | 0.00E+00 | 8.14E-08 | 2.37E-03 | 1.20E-01 | 0.00E+00 | 0.00E+00 | 3.51E-13 | 1.02E-08 | 5.17E-07 | |
| 26 | 1.29E-06 | 4.01% | 0.00E+00 | 0.00E+00 | 8.60E-05 | 4.95E-03 | 1.17E-01 | 0.00E+00 | 0.00E+00 | 1.11E-10 | 6.38E-09 | 1.51E-07 | |
| 27 | 2.49E-07 | 8.71% | 0.00E+00 | 0.00E+00 | 3.27E-03 | 6.00E-03 | 1.13E-01 | 0.00E+00 | 0.00E+00 | 8.15E-10 | 1.49E-09 | 2.81E-08 | |
| 28 | 3.97E-08 | 21.02% | 0.00E+00 | 0.00E+00 | 1.32E-02 | 0.00E+00 | 1.24E-01 | 0.00E+00 | 0.00E+00 | 5.22E-10 | 0.00E+00 | 4.93E-09 | |
| 29 | 1.56E-08 | 33.01% | 0.00E+00 | 0.00E+00 | 1.52E-02 | 0.00E+00 | 1.19E-01 | 0.00E+00 | 0.00E+00 | 2.36E-10 | 0.00E+00 | 1.86E-09 | |
| 30 | 1.12E-08 | 44.88% | 0.00E+00 | 0.00E+00 | 1.43E-02 | 0.00E+00 | 1.09E-01 | 0.00E+00 | 0.00E+00 | 1.60E-10 | 0.00E+00 | 1.22E-09 | |
| Total | 6.47E-04 | 0.19% | 0.00E+00 | 0.00E+00 | 4.60E-02 | 3.80E+00 | 1.11E+01 | 0.00E+00 | 0.00E+00 | 1.84E-09 | 1.16E-06 | 1.38E-04 | |

TABLE 37
MCNP reaction rates and reaction rate comparison in HCR tally region 2

| Energy Group | MCNP RRD (cm ⁻³) | | | | | MCNP Standard Deviation | | | | | Partial Percent Error (TXSAMC-MCNP)/MCNP | | | | |
|--------------|------------------------------|----------|----------|----------|----------|-------------------------|--------|--------|---------|---------|--|--------|--------|---------|--------|
| | fission | nusigf | n2n | abs-fis | total | fission | nusigf | n2n | abs-fis | total | fission | nusigf | n2n | abs-fis | total |
| 1 | 0.00E+00 | 0.00E+00 | 0.00E+00 | 0.00E+00 | 0.00E+00 | N/A | N/A | N/A | N/A | N/A | N/A | N/A | N/A | N/A | N/A |
| 2 | 0.00E+00 | 0.00E+00 | 0.00E+00 | 0.00E+00 | 0.00E+00 | N/A | N/A | N/A | N/A | N/A | N/A | N/A | N/A | N/A | N/A |
| 3 | 0.00E+00 | 0.00E+00 | 0.00E+00 | 0.00E+00 | 0.00E+00 | N/A | N/A | N/A | N/A | N/A | N/A | N/A | N/A | N/A | N/A |
| 4 | 0.00E+00 | 0.00E+00 | 0.00E+00 | 0.00E+00 | 0.00E+00 | N/A | N/A | N/A | N/A | N/A | N/A | N/A | N/A | N/A | N/A |
| 5 | 0.00E+00 | 0.00E+00 | 0.00E+00 | 0.00E+00 | 0.00E+00 | N/A | N/A | N/A | N/A | N/A | N/A | N/A | N/A | N/A | N/A |
| 6 | 0.00E+00 | 0.00E+00 | 0.00E+00 | 0.00E+00 | 0.00E+00 | N/A | N/A | N/A | N/A | N/A | N/A | N/A | N/A | N/A | N/A |
| 7 | 0.00E+00 | 0.00E+00 | 0.00E+00 | 0.00E+00 | 0.00E+00 | N/A | N/A | N/A | N/A | N/A | N/A | N/A | N/A | N/A | N/A |
| 8 | 0.00E+00 | 0.00E+00 | 0.00E+00 | 0.00E+00 | 0.00E+00 | N/A | N/A | N/A | N/A | N/A | N/A | N/A | N/A | N/A | N/A |
| 9 | 0.00E+00 | 0.00E+00 | 0.00E+00 | 3.50E-13 | 1.92E-10 | N/A | N/A | N/A | 100.00% | 100.00% | N/A | N/A | N/A | 0.01% | 0.00% |
| 10 | 0.00E+00 | 0.00E+00 | 0.00E+00 | 2.04E-11 | 2.52E-09 | N/A | N/A | N/A | 77.40% | 22.95% | N/A | N/A | N/A | 0.01% | 0.00% |
| 11 | 0.00E+00 | 0.00E+00 | 0.00E+00 | 2.20E-09 | 2.13E-07 | N/A | N/A | N/A | 21.78% | 9.27% | N/A | N/A | N/A | 0.01% | 0.01% |
| 12 | 0.00E+00 | 0.00E+00 | 0.00E+00 | 1.17E-08 | 5.01E-07 | N/A | N/A | N/A | 6.26% | 3.06% | N/A | N/A | N/A | 0.00% | -0.02% |
| 13 | 0.00E+00 | 0.00E+00 | 0.00E+00 | 5.64E-08 | 1.96E-06 | N/A | N/A | N/A | 2.32% | 1.09% | N/A | N/A | N/A | 0.03% | 0.00% |
| 14 | 0.00E+00 | 0.00E+00 | 0.00E+00 | 1.57E-07 | 8.47E-06 | N/A | N/A | N/A | 1.15% | 0.57% | N/A | N/A | N/A | -0.02% | -0.05% |
| 15 | 0.00E+00 | 0.00E+00 | 0.00E+00 | 3.04E-07 | 2.05E-05 | N/A | N/A | N/A | 0.69% | 0.34% | N/A | N/A | N/A | -0.06% | -0.09% |
| 16 | 0.00E+00 | 0.00E+00 | 0.00E+00 | 1.75E-07 | 1.82E-05 | N/A | N/A | N/A | 0.78% | 0.39% | N/A | N/A | N/A | 0.04% | -0.01% |
| 17 | 0.00E+00 | 0.00E+00 | 0.00E+00 | 1.25E-07 | 1.61E-05 | N/A | N/A | N/A | 0.83% | 0.41% | N/A | N/A | N/A | -0.14% | 0.08% |
| 18 | 0.00E+00 | 0.00E+00 | 0.00E+00 | 1.30E-07 | 2.87E-05 | N/A | N/A | N/A | 0.70% | 0.37% | N/A | N/A | N/A | 0.08% | -0.18% |
| 19 | 0.00E+00 | 0.00E+00 | 0.00E+00 | 7.19E-08 | 1.66E-05 | N/A | N/A | N/A | 0.87% | 0.42% | N/A | N/A | N/A | 0.05% | -0.04% |
| 20 | 0.00E+00 | 0.00E+00 | 0.00E+00 | 3.35E-08 | 7.17E-06 | N/A | N/A | N/A | 1.15% | 0.55% | N/A | N/A | N/A | -0.02% | -0.01% |
| 21 | 0.00E+00 | 0.00E+00 | 0.00E+00 | 2.57E-08 | 6.42E-06 | N/A | N/A | N/A | 1.22% | 0.60% | N/A | N/A | N/A | 0.01% | -0.01% |
| 22 | 0.00E+00 | 0.00E+00 | 0.00E+00 | 2.28E-08 | 6.31E-06 | N/A | N/A | N/A | 1.12% | 0.58% | N/A | N/A | N/A | -0.02% | -0.01% |
| 23 | 0.00E+00 | 0.00E+00 | 0.00E+00 | 1.37E-08 | 3.66E-06 | N/A | N/A | N/A | 1.20% | 0.70% | N/A | N/A | N/A | -0.01% | 0.01% |
| 24 | 0.00E+00 | 0.00E+00 | 0.00E+00 | 1.67E-08 | 3.54E-06 | N/A | N/A | N/A | 0.92% | 0.69% | N/A | N/A | N/A | 0.01% | 0.01% |
| 25 | 0.00E+00 | 0.00E+00 | 4.10E-13 | 1.01E-08 | 5.30E-07 | N/A | N/A | 13.74% | 1.84% | 1.68% | N/A | N/A | 0.00% | 0.01% | -0.01% |
| 26 | 0.00E+00 | 0.00E+00 | 8.91E-11 | 6.54E-09 | 1.51E-07 | N/A | N/A | 11.59% | 3.58% | 3.15% | N/A | N/A | 1.51% | -0.01% | 0.00% |
| 27 | 0.00E+00 | 0.00E+00 | 8.25E-10 | 2.21E-09 | 2.95E-08 | N/A | N/A | 15.19% | 7.77% | 6.91% | N/A | N/A | -0.72% | -0.06% | 0.00% |
| 28 | 0.00E+00 | 0.00E+00 | 2.48E-10 | 4.04E-10 | 4.09E-09 | N/A | N/A | 36.36% | 19.73% | 17.45% | N/A | N/A | 19.02% | -0.03% | 0.00% |
| 29 | 0.00E+00 | 0.00E+00 | 1.14E-10 | 1.46E-10 | 1.54E-09 | N/A | N/A | 54.87% | 30.70% | 28.62% | N/A | N/A | 8.48% | -0.01% | 0.00% |
| 30 | 0.00E+00 | 0.00E+00 | 1.67E-10 | 9.67E-11 | 1.22E-09 | N/A | N/A | 43.02% | 41.77% | 35.89% | N/A | N/A | -0.46% | -0.01% | 0.00% |
| Total | 0.00E+00 | 0.00E+00 | 1.44E-09 | 1.17E-06 | 1.39E-04 | N/A | N/A | 12.59% | 0.34% | 0.15% | N/A | N/A | 27.82% | -0.16% | -0.33% |

Since this region is composed of non-fissionable materials, there is obviously no fission or nusigf RRD. The total and absorption RRD's show good agreement with the MCNP-tallied RRD's but the (n,2n) RRD shows significant disagreement with as much as 20% error in an energy group. Compared to the SCR, the partial percent error in RRD's is very similar. For this tally region, we do not see the reduction in partial percent error compared to the SCR we saw for the first tally region.

In Fig. 22 we see the difference in the TXSAMC and MCNP RRD's for the second tally region displayed graphically. The very low errors in the low energy range are quite obvious in this plot as well as the general accuracy of the cross sections in the

middle energy range. At very high energies we see the significant error in the (n,2n) reaction rate.

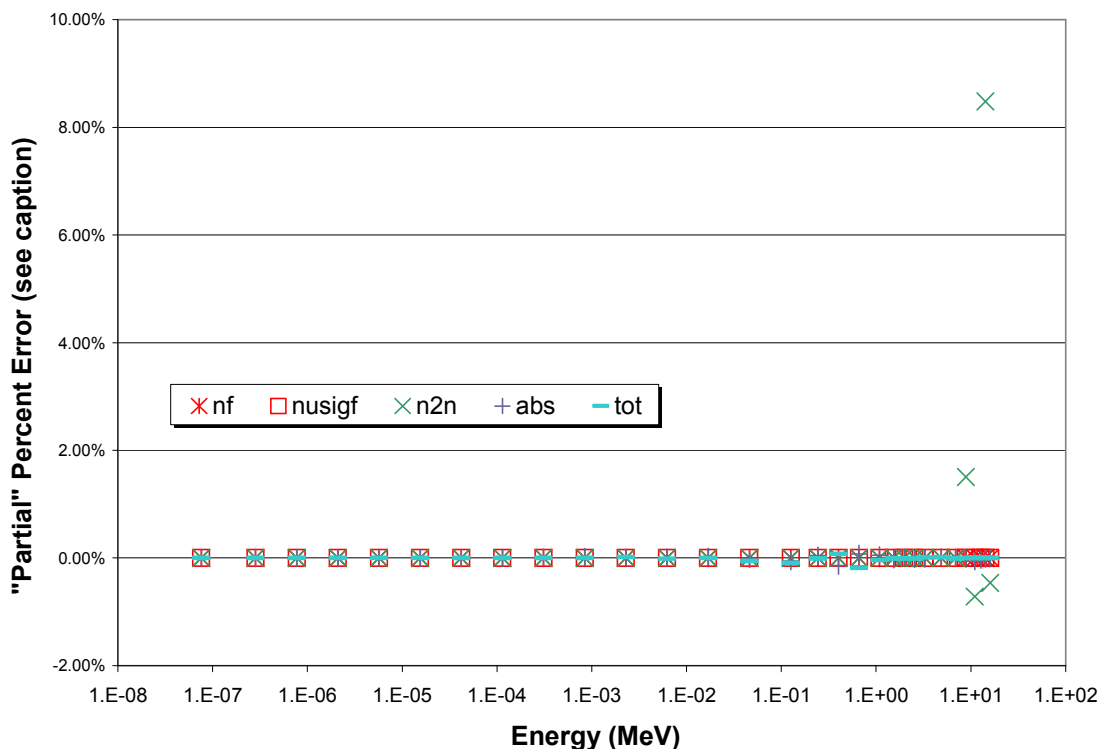


Fig. 22. "Partial" percent errors for reaction-rate densities in HCR tally region 2. Each "partial" error is plotted at the midpoint energy of its group. The percent error in a given reaction rate is the sum of the 30 partial percent errors.

The third tally region is composed of coolant channels filled with liquid sodium. In Table 38 we show the MCNP-tallied scalar flux for the pin-cell, its relative standard deviation, the TXSAMC-generated cross sections and the TXSAMC-generated reaction rate densities for the third tally region. Table 39 shows the MCNP-tallied reaction rate densities, their standard deviations and the partial percent error between the TXSAMC-

generated reaction rates and the MCNP-tallied reaction rates for the third tally region. It should be noted that as a result of the homogenous nature of these cells, there is no heterogeneity option applied in the TRANSX module of TXSAMC and no mixing (since it is all one nuclide).

TABLE 38
MCNP scalar flux, TXSAMC cross sections and reaction rates in HCR tally region 3

| Energy Group | Scalar Flux (n/cm ² /hps) | Rel. Error (1 σ) | TXSAMC SIGMA (cm ⁻¹) | | | | | TXSAMC RRD (cm ⁻³) | | | | |
|-----------------|---|-----------------------------|----------------------------------|----------|----------|----------|----------|--------------------------------|--------|----------|----------|----------|
| | | | fission | nusigf | n2n | abs-fis | total | fission | nusigf | n2n | abs-fis | total |
| 1 | 0.00E+00 | 0.00% | 0.00E+00 | 0.00E+00 | 0.00E+00 | 1.34E-02 | 1.87E-01 | N/A | N/A | N/A | N/A | N/A |
| 2 | 0.00E+00 | 0.00% | 0.00E+00 | 0.00E+00 | 0.00E+00 | 8.73E-03 | 1.80E-01 | N/A | N/A | N/A | N/A | N/A |
| 3 | 0.00E+00 | 0.00% | 0.00E+00 | 0.00E+00 | 0.00E+00 | 5.38E-03 | 1.74E-01 | N/A | N/A | N/A | N/A | N/A |
| 4 | 0.00E+00 | 0.00% | 0.00E+00 | 0.00E+00 | 0.00E+00 | 3.27E-03 | 1.70E-01 | N/A | N/A | N/A | N/A | N/A |
| 5 | 0.00E+00 | 0.00% | 0.00E+00 | 0.00E+00 | 0.00E+00 | 1.70E-03 | 1.67E-01 | N/A | N/A | N/A | N/A | N/A |
| 6 | 0.00E+00 | 0.00% | 0.00E+00 | 0.00E+00 | 0.00E+00 | 1.05E-03 | 1.65E-01 | N/A | N/A | N/A | N/A | N/A |
| 7 | 0.00E+00 | 0.00% | 0.00E+00 | 0.00E+00 | 0.00E+00 | 6.93E-04 | 1.65E-01 | N/A | N/A | N/A | N/A | N/A |
| 8 | 0.00E+00 | 0.00% | 0.00E+00 | 0.00E+00 | 0.00E+00 | 4.50E-04 | 1.65E-01 | N/A | N/A | N/A | N/A | N/A |
| 9 | 0.00E+00 | 0.00% | 0.00E+00 | 0.00E+00 | 0.00E+00 | 3.17E-04 | 1.68E-01 | N/A | N/A | N/A | N/A | N/A |
| 10 | 1.88E-08 | 27.64% | 0.00E+00 | 0.00E+00 | 0.00E+00 | 3.31E-04 | 1.92E-01 | N/A | N/A | N/A | 6.24E-12 | 3.61E-09 |
| 11 | 1.70E-07 | 9.41% | 0.00E+00 | 0.00E+00 | 0.00E+00 | 5.29E-03 | 5.57E+00 | N/A | N/A | N/A | 8.96E-10 | 9.45E-07 |
| 12 | 1.03E-06 | 3.66% | 0.00E+00 | 0.00E+00 | 0.00E+00 | 1.28E-04 | 4.73E-01 | N/A | N/A | N/A | 1.33E-10 | 4.89E-07 |
| 13 | 7.22E-06 | 1.45% | 0.00E+00 | 0.00E+00 | 0.00E+00 | 2.42E-06 | 2.31E-01 | N/A | N/A | N/A | 1.75E-11 | 1.67E-06 |
| 14 | 3.01E-05 | 0.72% | 0.00E+00 | 0.00E+00 | 0.00E+00 | 9.73E-05 | 2.72E-01 | N/A | N/A | N/A | 2.93E-09 | 8.20E-06 |
| 15 | 9.23E-05 | 0.43% | 0.00E+00 | 0.00E+00 | 0.00E+00 | 3.44E-05 | 1.81E-01 | N/A | N/A | N/A | 3.17E-09 | 1.67E-05 |
| 16 | 7.55E-05 | 0.48% | 0.00E+00 | 0.00E+00 | 0.00E+00 | 5.28E-05 | 2.21E-01 | N/A | N/A | N/A | 3.99E-09 | 1.66E-05 |
| 17 | 7.45E-05 | 0.51% | 0.00E+00 | 0.00E+00 | 0.00E+00 | 2.28E-05 | 1.84E-01 | N/A | N/A | N/A | 1.70E-09 | 1.37E-05 |
| 18 | 1.08E-04 | 0.44% | 0.00E+00 | 0.00E+00 | 0.00E+00 | 1.68E-05 | 2.67E-01 | N/A | N/A | N/A | 1.82E-09 | 2.88E-05 |
| 19 | 7.79E-05 | 0.53% | 0.00E+00 | 0.00E+00 | 0.00E+00 | 1.20E-05 | 1.98E-01 | N/A | N/A | N/A | 9.36E-10 | 1.55E-05 |
| 20 | 4.27E-05 | 0.70% | 0.00E+00 | 0.00E+00 | 0.00E+00 | 1.08E-05 | 1.42E-01 | N/A | N/A | N/A | 4.60E-10 | 6.06E-06 |
| 21 | 3.83E-05 | 0.74% | 0.00E+00 | 0.00E+00 | 0.00E+00 | 1.01E-05 | 1.49E-01 | N/A | N/A | N/A | 3.87E-10 | 5.71E-06 |
| 22 | 3.88E-05 | 0.74% | 0.00E+00 | 0.00E+00 | 0.00E+00 | 9.46E-06 | 1.48E-01 | N/A | N/A | N/A | 3.67E-10 | 5.75E-06 |
| 23 | 2.58E-05 | 0.90% | 0.00E+00 | 0.00E+00 | 0.00E+00 | 8.87E-06 | 1.20E-01 | N/A | N/A | N/A | 2.29E-10 | 3.10E-06 |
| 24 | 2.76E-05 | 0.89% | 0.00E+00 | 0.00E+00 | 0.00E+00 | 1.92E-04 | 1.09E-01 | N/A | N/A | N/A | 5.31E-09 | 3.01E-06 |
| 25 | 4.34E-06 | 2.20% | 0.00E+00 | 0.00E+00 | 0.00E+00 | 2.32E-03 | 9.46E-02 | N/A | N/A | N/A | 1.00E-08 | 4.10E-07 |
| 26 | 1.27E-06 | 3.98% | 0.00E+00 | 0.00E+00 | 0.00E+00 | 5.70E-03 | 8.67E-02 | N/A | N/A | N/A | 7.26E-09 | 1.10E-07 |
| 27 | 2.70E-07 | 8.61% | 0.00E+00 | 0.00E+00 | 0.00E+00 | 1.08E-02 | 8.62E-02 | N/A | N/A | N/A | 2.91E-09 | 2.32E-08 |
| 28 | 3.80E-08 | 21.92% | 0.00E+00 | 0.00E+00 | 5.25E-05 | 1.15E-02 | 8.85E-02 | N/A | N/A | 2.00E-12 | 4.38E-10 | 3.37E-09 |
| 29 | 1.93E-08 | 27.47% | 0.00E+00 | 0.00E+00 | 1.52E-03 | 8.88E-03 | 9.01E-02 | N/A | N/A | 2.94E-11 | 1.71E-10 | 1.74E-09 |
| 30 | 7.17E-09 | 54.93% | 0.00E+00 | 0.00E+00 | 4.52E-03 | 5.14E-03 | 9.20E-02 | N/A | N/A | 3.24E-11 | 3.68E-11 | 6.59E-10 |
| Total | 6.46E-04 | 0.19% | 0.00E+00 | 0.00E+00 | 6.10E-03 | 8.55E-02 | 1.05E+01 | N/A | N/A | 6.38E-11 | 4.32E-08 | 1.27E-04 |

TABLE 39
MCNP reaction rates and reaction rate comparison in HCR tally region 3

| Energy Group | MCNP RRD (cm ⁻³) | | | | | MCNP Standard Deviation | | | | | Partial Percent Error (TXSAMC-MCNP)/MCNP | | | | |
|-----------------|------------------------------|----------|----------|----------|----------|-------------------------|--------|--------|---------|--------|--|--------|--------|---------|-------|
| | fission | nusigf | n2n | abs-fis | total | fission | nusigf | n2n | abs-fis | total | fission | nusigf | n2n | abs-fis | total |
| 1 | 0.00E+00 | 0.00E+00 | 0.00E+00 | 0.00E+00 | 0.00E+00 | 0.00% | 0.00% | 0.00% | 0.00% | 0.00% | N/A | N/A | N/A | N/A | N/A |
| 2 | 0.00E+00 | 0.00E+00 | 0.00E+00 | 0.00E+00 | 0.00E+00 | 0.00% | 0.00% | 0.00% | 0.00% | 0.00% | N/A | N/A | N/A | N/A | N/A |
| 3 | 0.00E+00 | 0.00E+00 | 0.00E+00 | 0.00E+00 | 0.00E+00 | 0.00% | 0.00% | 0.00% | 0.00% | 0.00% | N/A | N/A | N/A | N/A | N/A |
| 4 | 0.00E+00 | 0.00E+00 | 0.00E+00 | 0.00E+00 | 0.00E+00 | 0.00% | 0.00% | 0.00% | 0.00% | 0.00% | N/A | N/A | N/A | N/A | N/A |
| 5 | 0.00E+00 | 0.00E+00 | 0.00E+00 | 0.00E+00 | 0.00E+00 | 0.00% | 0.00% | 0.00% | 0.00% | 0.00% | N/A | N/A | N/A | N/A | N/A |
| 6 | 0.00E+00 | 0.00E+00 | 0.00E+00 | 0.00E+00 | 0.00E+00 | 0.00% | 0.00% | 0.00% | 0.00% | 0.00% | N/A | N/A | N/A | N/A | N/A |
| 7 | 0.00E+00 | 0.00E+00 | 0.00E+00 | 0.00E+00 | 0.00E+00 | 0.00% | 0.00% | 0.00% | 0.00% | 0.00% | N/A | N/A | N/A | N/A | N/A |
| 8 | 0.00E+00 | 0.00E+00 | 0.00E+00 | 0.00E+00 | 0.00E+00 | 0.00% | 0.00% | 0.00% | 0.00% | 0.00% | N/A | N/A | N/A | N/A | N/A |
| 9 | 0.00E+00 | 0.00E+00 | 0.00E+00 | 0.00E+00 | 0.00E+00 | 0.00% | 0.00% | 0.00% | 0.00% | 0.00% | N/A | N/A | N/A | N/A | N/A |
| 10 | 0.00E+00 | 0.00E+00 | 0.00E+00 | 6.44E-12 | 3.70E-09 | 0.00% | 0.00% | 0.00% | 27.38% | 27.43% | N/A | N/A | N/A | 0.00% | 0.00% |
| 11 | 0.00E+00 | 0.00E+00 | 0.00E+00 | 2.75E-10 | 2.28E-07 | 0.00% | 0.00% | 0.00% | 10.09% | 10.74% | N/A | N/A | N/A | 1.52% | 0.58% |
| 12 | 0.00E+00 | 0.00E+00 | 0.00E+00 | 1.19E-10 | 4.45E-07 | 0.00% | 0.00% | 0.00% | 16.27% | 4.14% | N/A | N/A | N/A | 0.03% | 0.04% |
| 13 | 0.00E+00 | 0.00E+00 | 0.00E+00 | 1.72E-11 | 1.67E-06 | 0.00% | 0.00% | 0.00% | 1.75% | 1.46% | N/A | N/A | N/A | 0.00% | 0.00% |
| 14 | 0.00E+00 | 0.00E+00 | 0.00E+00 | 1.78E-09 | 7.20E-06 | 0.00% | 0.00% | 0.00% | 9.33% | 0.76% | N/A | N/A | N/A | 2.80% | 0.82% |
| 15 | 0.00E+00 | 0.00E+00 | 0.00E+00 | 2.85E-09 | 1.67E-05 | 0.00% | 0.00% | 0.00% | 7.12% | 0.43% | N/A | N/A | N/A | 0.79% | 0.01% |
| 16 | 0.00E+00 | 0.00E+00 | 0.00E+00 | 3.56E-09 | 1.58E-05 | 0.00% | 0.00% | 0.00% | 2.52% | 0.51% | N/A | N/A | N/A | 1.05% | 0.69% |
| 17 | 0.00E+00 | 0.00E+00 | 0.00E+00 | 1.59E-09 | 1.33E-05 | 0.00% | 0.00% | 0.00% | 2.59% | 0.52% | N/A | N/A | N/A | 0.27% | 0.34% |
| 18 | 0.00E+00 | 0.00E+00 | 0.00E+00 | 1.81E-09 | 2.78E-05 | 0.00% | 0.00% | 0.00% | 0.44% | 0.46% | N/A | N/A | N/A | 0.02% | 0.83% |
| 19 | 0.00E+00 | 0.00E+00 | 0.00E+00 | 9.35E-10 | 1.53E-05 | 0.00% | 0.00% | 0.00% | 0.53% | 0.53% | N/A | N/A | N/A | 0.00% | 0.10% |
| 20 | 0.00E+00 | 0.00E+00 | 0.00E+00 | 4.60E-10 | 6.01E-06 | 0.00% | 0.00% | 0.00% | 0.70% | 0.70% | N/A | N/A | N/A | 0.00% | 0.04% |
| 21 | 0.00E+00 | 0.00E+00 | 0.00E+00 | 3.87E-10 | 5.69E-06 | 0.00% | 0.00% | 0.00% | 0.74% | 0.75% | N/A | N/A | N/A | 0.00% | 0.01% |
| 22 | 0.00E+00 | 0.00E+00 | 0.00E+00 | 3.67E-10 | 5.75E-06 | 0.00% | 0.00% | 0.00% | 0.74% | 0.74% | N/A | N/A | N/A | 0.00% | 0.00% |
| 23 | 0.00E+00 | 0.00E+00 | 0.00E+00 | 2.29E-10 | 3.07E-06 | 0.00% | 0.00% | 0.00% | 0.90% | 0.91% | N/A | N/A | N/A | 0.00% | 0.02% |
| 24 | 0.00E+00 | 0.00E+00 | 0.00E+00 | 5.43E-09 | 3.00E-06 | 0.00% | 0.00% | 0.00% | 1.87% | 0.89% | N/A | N/A | N/A | -0.30% | 0.01% |
| 25 | 0.00E+00 | 0.00E+00 | 0.00E+00 | 1.01E-08 | 4.10E-07 | 0.00% | 0.00% | 0.00% | 2.32% | 2.21% | N/A | N/A | N/A | -0.04% | 0.00% |
| 26 | 0.00E+00 | 0.00E+00 | 0.00E+00 | 7.39E-09 | 1.10E-07 | 0.00% | 0.00% | 0.00% | 4.14% | 3.98% | N/A | N/A | N/A | -0.31% | 0.00% |
| 27 | 0.00E+00 | 0.00E+00 | 0.00E+00 | 2.91E-09 | 2.32E-08 | 0.00% | 0.00% | 0.00% | 8.60% | 8.61% | N/A | N/A | N/A | 0.00% | 0.00% |
| 28 | 0.00E+00 | 0.00E+00 | 2.25E-12 | 4.43E-10 | 3.36E-09 | 0.00% | 0.00% | 46.83% | 21.89% | 21.93% | N/A | N/A | -0.35% | -0.01% | 0.00% |
| 29 | 0.00E+00 | 0.00E+00 | 2.88E-11 | 2.01E-10 | 1.74E-09 | 0.00% | 0.00% | 32.73% | 27.44% | 27.48% | N/A | N/A | 0.91% | -0.07% | 0.00% |
| 30 | 0.00E+00 | 0.00E+00 | 3.92E-11 | 6.93E-11 | 6.63E-10 | 0.00% | 0.00% | 56.79% | 54.94% | 54.99% | N/A | N/A | -9.69% | -0.08% | 0.00% |
| Total | 0.00E+00 | 0.00E+00 | 7.02E-11 | 4.09E-08 | 1.23E-04 | 0.00% | 0.00% | 34.46% | 1.38% | 0.20% | N/A | N/A | -9.14% | 5.68% | 3.50% |

As expected, this region of non-fissionable material had no fission or fission neutron emission reactions and a fairly small number of (n,2n) reactions. It is readily apparent that this region has a greater error in the overall reaction rates than other regions in the HCR. Part of the error may be attributable to the large resonance in group 11 however there is significant error in many higher energy groups that contributes a great deal of error as well. The sodium resonance can be seen in Fig. 10. Fortunately, the overall error is a still manageable 5-10%.

In Fig. 23 we see the difference in the TXSAMC and MCNP RRD's for the third tally region displayed graphically. The very low errors in the low energy range are quite obvious in this plot as well as the modest error at the sodium resonance. At very high

energies we see significant error in the (n,2n) reaction rate. It is important to note that away from the resonance and the upper thresholds, the error is actually quite low.

Unfortunately, the overall error is still not as good as any of the other tally regions.

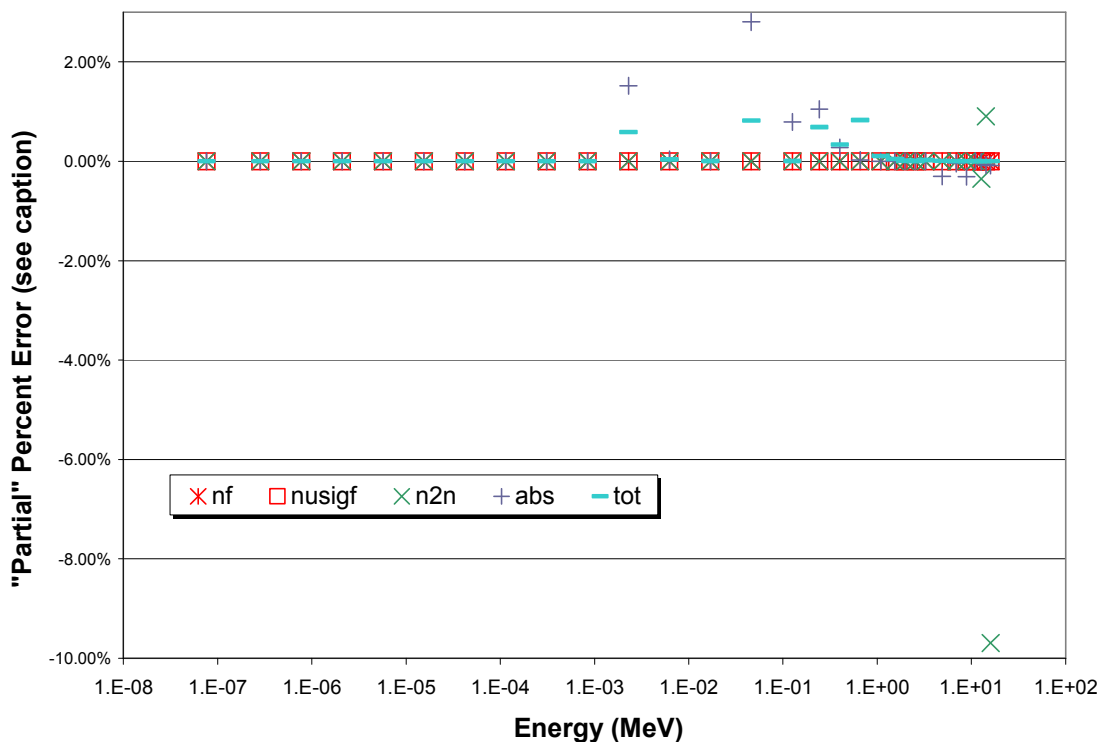


Fig. 23. "Partial" percent errors for reaction-rate densities in HCR tally region 3. Each "partial" error is plotted at the midpoint energy of its group. The percent error in a given reaction rate is the sum of the 30 partial percent errors.

The fourth tally region is composed of the six nearest fuel pin-cells to each control rod location for a total of eighteen cells. In Table 40 we show the MCNP-tallied scalar flux for the pin-cell, its relative standard deviation, the TXSAMC-generated cross sections and the TXSAMC-generated reaction rate densities for the fourth tally region.

Table 41 shows the MCNP-tallied reaction rate densities, their standard deviations and the partial percent error between the TXSAMC-generated reaction rates and the MCNP-tallied reaction rates for the fourth tally region. The hope with modeling this region was to obtain a more accurate picture of the cross sections in this region of depressed flux due to the presence of the control rod. It should be noted that the presence of a control rod in a fast system has less of an effect than it might in a thermal system since much of the absorbing power of the rod is in thermal regions. This means that while there is some flux depression it is not as pronounced as it is in a light water reactor, for example.

TABLE 40
MCNP scalar flux, TXSAMC cross sections and reaction rates in HCR tally region 4

| Energy Group | Scalar Flux (n/cm ² /hps) | Rel. Error (1 σ) | TXSAMC SIGMA (cm ⁻¹) | | | | | TXSAMC RRD (cm ⁻³) | | | | |
|--------------|--------------------------------------|--------------------------|----------------------------------|----------|----------|----------|----------|--------------------------------|----------|----------|----------|----------|
| | | | fission | nusigf | n2n | abs-fis | total | fission | nusigf | n2n | abs-fis | total |
| 1 | 0.00E+00 | 0.00% | 3.34E+00 | 8.13E+00 | 0.00E+00 | 5.75E-01 | 4.31E+00 | 0.00E+00 | 0.00E+00 | 0.00E+00 | 0.00E+00 | 0.00E+00 |
| 2 | 0.00E+00 | 0.00% | 2.38E+00 | 5.81E+00 | 0.00E+00 | 5.01E-01 | 3.27E+00 | 0.00E+00 | 0.00E+00 | 0.00E+00 | 0.00E+00 | 0.00E+00 |
| 3 | 0.00E+00 | 0.00% | 9.81E-01 | 2.39E+00 | 0.00E+00 | 1.36E-01 | 1.49E+00 | 0.00E+00 | 0.00E+00 | 0.00E+00 | 0.00E+00 | 0.00E+00 |
| 4 | 0.00E+00 | 0.00% | 2.45E-01 | 5.96E-01 | 0.00E+00 | 9.00E-02 | 6.95E-01 | 0.00E+00 | 0.00E+00 | 0.00E+00 | 0.00E+00 | 0.00E+00 |
| 5 | 0.00E+00 | 0.00% | 1.21E-01 | 2.96E-01 | 0.00E+00 | 1.67E-01 | 6.24E-01 | 0.00E+00 | 0.00E+00 | 0.00E+00 | 0.00E+00 | 0.00E+00 |
| 6 | 1.68E-10 | 100.00% | 3.13E-01 | 7.61E-01 | 0.00E+00 | 2.71E-01 | 9.51E-01 | 5.26E-11 | 1.28E-10 | 0.00E+00 | 4.56E-11 | 1.60E-10 |
| 7 | 0.00E+00 | 0.00% | 4.24E-01 | 1.03E+00 | 0.00E+00 | 2.15E-01 | 1.00E+00 | 0.00E+00 | 0.00E+00 | 0.00E+00 | 0.00E+00 | 0.00E+00 |
| 8 | 1.43E-10 | 100.00% | 2.44E-01 | 5.93E-01 | 0.00E+00 | 1.46E-01 | 7.60E-01 | 3.49E-11 | 8.48E-11 | 0.00E+00 | 2.08E-11 | 1.09E-10 |
| 9 | 1.74E-09 | 47.54% | 1.94E-01 | 4.73E-01 | 0.00E+00 | 8.71E-02 | 6.64E-01 | 3.37E-10 | 8.21E-10 | 0.00E+00 | 1.51E-10 | 1.15E-09 |
| 10 | 1.27E-08 | 14.10% | 1.22E-01 | 2.98E-01 | 0.00E+00 | 6.57E-02 | 5.60E-01 | 1.55E-09 | 3.78E-09 | 0.00E+00 | 8.34E-10 | 7.11E-09 |
| 11 | 1.37E-07 | 5.64% | 7.59E-02 | 1.85E-01 | 0.00E+00 | 3.55E-02 | 8.43E-01 | 1.04E-08 | 2.53E-08 | 0.00E+00 | 4.86E-09 | 1.15E-07 |
| 12 | 1.01E-06 | 2.14% | 5.03E-02 | 1.22E-01 | 0.00E+00 | 1.99E-02 | 4.83E-01 | 5.08E-08 | 1.24E-07 | 0.00E+00 | 2.01E-08 | 4.88E-07 |
| 13 | 6.97E-06 | 0.85% | 3.62E-02 | 8.80E-02 | 0.00E+00 | 1.33E-02 | 4.29E-01 | 2.52E-07 | 6.13E-07 | 0.00E+00 | 9.30E-08 | 2.99E-06 |
| 14 | 2.98E-05 | 0.43% | 2.76E-02 | 6.68E-02 | 0.00E+00 | 9.26E-03 | 4.03E-01 | 8.22E-07 | 1.99E-06 | 0.00E+00 | 2.76E-07 | 1.20E-05 |
| 15 | 9.13E-05 | 0.26% | 2.20E-02 | 5.36E-02 | 0.00E+00 | 5.98E-03 | 3.61E-01 | 2.01E-06 | 4.89E-06 | 0.00E+00 | 5.46E-07 | 3.30E-05 |
| 16 | 7.65E-05 | 0.27% | 1.91E-02 | 4.69E-02 | 0.00E+00 | 4.10E-03 | 3.36E-01 | 1.46E-06 | 3.59E-06 | 0.00E+00 | 3.14E-07 | 2.57E-05 |
| 17 | 7.46E-05 | 0.28% | 1.76E-02 | 4.34E-02 | 0.00E+00 | 3.06E-03 | 3.95E-01 | 1.31E-06 | 3.24E-06 | 0.00E+00 | 2.28E-07 | 2.94E-05 |
| 18 | 1.10E-04 | 0.24% | 1.65E-02 | 4.11E-02 | 0.00E+00 | 2.26E-03 | 2.87E-01 | 1.82E-06 | 4.53E-06 | 0.00E+00 | 2.49E-07 | 3.16E-05 |
| 19 | 8.06E-05 | 0.28% | 1.74E-02 | 4.42E-02 | 0.00E+00 | 1.77E-03 | 2.91E-01 | 1.40E-06 | 3.56E-06 | 0.00E+00 | 1.42E-07 | 2.34E-05 |
| 20 | 4.42E-05 | 0.37% | 1.87E-02 | 4.86E-02 | 0.00E+00 | 1.35E-03 | 2.19E-01 | 8.28E-07 | 2.15E-06 | 0.00E+00 | 5.94E-08 | 9.67E-06 |
| 21 | 3.93E-05 | 0.40% | 1.95E-02 | 5.15E-02 | 0.00E+00 | 1.01E-03 | 2.08E-01 | 7.65E-07 | 2.02E-06 | 0.00E+00 | 3.97E-08 | 8.19E-06 |
| 22 | 4.10E-05 | 0.40% | 1.93E-02 | 5.23E-02 | 0.00E+00 | 6.65E-04 | 1.87E-01 | 7.93E-07 | 2.15E-06 | 0.00E+00 | 2.73E-08 | 7.67E-06 |
| 23 | 2.79E-05 | 0.48% | 1.84E-02 | 5.13E-02 | 0.00E+00 | 4.12E-04 | 2.31E-01 | 5.13E-07 | 1.43E-06 | 0.00E+00 | 1.15E-08 | 6.44E-06 |
| 24 | 2.96E-05 | 0.47% | 1.72E-02 | 5.13E-02 | 1.24E-04 | 2.34E-03 | 2.13E-01 | 5.09E-07 | 1.52E-06 | 3.68E-09 | 6.93E-08 | 6.29E-06 |
| 25 | 4.73E-06 | 1.16% | 2.26E-02 | 7.63E-02 | 5.55E-03 | 0.00E+00 | 1.72E-01 | 1.07E-07 | 3.61E-07 | 2.62E-08 | 0.00E+00 | 8.11E-07 |
| 26 | 1.36E-06 | 2.09% | 2.79E-02 | 1.02E-01 | 1.10E-02 | 0.00E+00 | 1.65E-01 | 3.81E-08 | 1.38E-07 | 1.51E-08 | 0.00E+00 | 2.26E-07 |
| 27 | 2.71E-07 | 4.68% | 2.73E-02 | 1.07E-01 | 1.58E-02 | 0.00E+00 | 1.67E-01 | 7.40E-09 | 2.92E-08 | 4.28E-09 | 0.00E+00 | 4.53E-08 |
| 28 | 4.35E-08 | 11.64% | 2.92E-02 | 1.22E-01 | 1.50E-02 | 0.00E+00 | 1.72E-01 | 1.27E-09 | 5.32E-09 | 6.51E-10 | 0.00E+00 | 7.46E-09 |
| 29 | 1.39E-08 | 19.73% | 3.09E-02 | 1.36E-01 | 1.14E-02 | 0.00E+00 | 1.71E-01 | 4.30E-10 | 1.90E-09 | 1.59E-10 | 0.00E+00 | 2.38E-09 |
| 30 | 8.27E-09 | 25.68% | 3.28E-02 | 1.52E-01 | 9.69E-03 | 0.00E+00 | 1.76E-01 | 2.72E-10 | 1.25E-09 | 8.01E-11 | 0.00E+00 | 1.46E-09 |
| Total | 6.59E-04 | 0.11% | 8.91E+00 | 2.20E+01 | 6.86E-02 | 2.35E+00 | 2.02E+01 | 1.27E-05 | 3.24E-05 | 5.01E-08 | 2.08E-06 | 1.98E-04 |

TABLE 41
MCNP reaction rates and reaction rate comparison in HCR tally region 4

| Energy Group | MCNP RRD (cm ⁻³) | | | | | MCNP Standard Deviation | | | | | Partial Percent Error (TXSAMC-MCNP)/MCNP | | | | |
|--------------|------------------------------|----------|----------|----------|----------|-------------------------|---------|--------|---------|--------|--|--------|--------|---------|--------|
| | fission | nusigf | n2n | abs-fis | total | fission | nusigf | n2n | abs-fis | total | fission | nusigf | n2n | abs-fis | total |
| 1 | 0.00E+00 | 0.00E+00 | 0.00E+00 | 0.00E+00 | 0.00E+00 | N/A | N/A | N/A | N/A | N/A | N/A | N/A | N/A | N/A | N/A |
| 2 | 0.00E+00 | 0.00E+00 | 0.00E+00 | 0.00E+00 | 0.00E+00 | N/A | N/A | N/A | N/A | N/A | N/A | N/A | N/A | N/A | N/A |
| 3 | 0.00E+00 | 0.00E+00 | 0.00E+00 | 0.00E+00 | 0.00E+00 | N/A | N/A | N/A | N/A | N/A | N/A | N/A | N/A | N/A | N/A |
| 4 | 0.00E+00 | 0.00E+00 | 0.00E+00 | 0.00E+00 | 0.00E+00 | N/A | N/A | N/A | N/A | N/A | N/A | N/A | N/A | N/A | N/A |
| 5 | 0.00E+00 | 0.00E+00 | 0.00E+00 | 0.00E+00 | 0.00E+00 | N/A | N/A | N/A | N/A | N/A | N/A | N/A | N/A | N/A | N/A |
| 6 | 7.32E-11 | 1.78E-10 | 0.00E+00 | 5.78E-11 | 1.72E-10 | 100.00% | 100.00% | N/A | 99.87% | 92.39% | 0.00% | 0.00% | N/A | 0.00% | 0.00% |
| 7 | 0.00E+00 | 0.00E+00 | 0.00E+00 | 0.00E+00 | 0.00E+00 | N/A | N/A | N/A | N/A | N/A | N/A | N/A | N/A | N/A | N/A |
| 8 | 2.87E-11 | 6.99E-11 | 0.00E+00 | 1.23E-11 | 9.78E-11 | 100.00% | 100.00% | N/A | 99.92% | 94.57% | 0.00% | 0.00% | N/A | 0.00% | 0.00% |
| 9 | 3.49E-10 | 8.49E-10 | 0.00E+00 | 2.09E-10 | 1.21E-09 | 49.52% | 49.52% | N/A | 50.40% | 45.16% | 0.00% | 0.00% | N/A | 0.00% | 0.00% |
| 10 | 1.70E-09 | 4.13E-09 | 0.00E+00 | 9.25E-10 | 7.73E-09 | 14.92% | 14.92% | N/A | 15.78% | 13.89% | 0.00% | 0.00% | N/A | 0.00% | 0.00% |
| 11 | 1.11E-08 | 2.70E-08 | 0.00E+00 | 5.86E-09 | 1.05E-07 | 6.42% | 6.42% | N/A | 6.21% | 4.35% | -0.01% | -0.01% | N/A | -0.05% | 0.00% |
| 12 | 5.05E-08 | 1.23E-07 | 0.00E+00 | 2.02E-08 | 4.95E-07 | 2.31% | 2.31% | N/A | 2.25% | 1.86% | 0.00% | 0.00% | N/A | 0.00% | 0.00% |
| 13 | 2.54E-07 | 6.18E-07 | 0.00E+00 | 9.37E-08 | 3.02E-06 | 0.90% | 0.90% | N/A | 0.89% | 0.76% | -0.01% | -0.01% | N/A | -0.03% | -0.01% |
| 14 | 8.32E-07 | 2.02E-06 | 0.00E+00 | 2.80E-07 | 1.22E-05 | 0.45% | 0.45% | N/A | 0.45% | 0.38% | -0.08% | -0.07% | N/A | -0.18% | -0.07% |
| 15 | 2.02E-06 | 4.94E-06 | 0.00E+00 | 5.52E-07 | 3.33E-05 | 0.27% | 0.27% | N/A | 0.27% | 0.23% | -0.14% | -0.14% | N/A | -0.27% | -0.15% |
| 16 | 1.47E-06 | 3.62E-06 | 0.00E+00 | 3.16E-07 | 2.59E-05 | 0.28% | 0.28% | N/A | 0.28% | 0.24% | -0.10% | -0.10% | N/A | -0.12% | -0.12% |
| 17 | 1.33E-06 | 3.27E-06 | 0.00E+00 | 2.32E-07 | 2.99E-05 | 0.29% | 0.29% | N/A | 0.29% | 0.26% | -0.11% | -0.10% | N/A | -0.19% | -0.21% |
| 18 | 1.83E-06 | 4.57E-06 | 0.00E+00 | 2.52E-07 | 3.21E-05 | 0.25% | 0.25% | N/A | 0.26% | 0.20% | -0.13% | -0.13% | N/A | -0.14% | -0.24% |
| 19 | 1.42E-06 | 3.60E-06 | 0.00E+00 | 1.43E-07 | 2.35E-05 | 0.30% | 0.30% | N/A | 0.29% | 0.25% | -0.10% | -0.10% | N/A | -0.05% | -0.04% |
| 20 | 8.33E-07 | 2.16E-06 | 0.00E+00 | 5.99E-08 | 9.76E-06 | 0.40% | 0.40% | N/A | 0.39% | 0.34% | -0.04% | -0.04% | N/A | -0.02% | -0.04% |
| 21 | 7.73E-07 | 2.04E-06 | 0.00E+00 | 4.01E-08 | 8.27E-06 | 0.42% | 0.42% | N/A | 0.42% | 0.36% | -0.06% | -0.07% | N/A | -0.02% | -0.04% |
| 22 | 8.01E-07 | 2.17E-06 | 0.00E+00 | 2.77E-08 | 7.74E-06 | 0.42% | 0.42% | N/A | 0.41% | 0.35% | -0.06% | -0.07% | N/A | -0.02% | -0.03% |
| 23 | 5.20E-07 | 1.45E-06 | 0.00E+00 | 1.17E-08 | 6.52E-06 | 0.50% | 0.50% | N/A | 0.49% | 0.45% | -0.05% | -0.05% | N/A | -0.01% | -0.04% |
| 24 | 5.16E-07 | 1.54E-06 | 3.83E-09 | 7.39E-08 | 6.37E-06 | 0.50% | 0.50% | 1.64% | 0.63% | 0.44% | -0.06% | -0.07% | -0.30% | -0.21% | -0.04% |
| 25 | 1.08E-07 | 3.64E-07 | 2.64E-08 | 2.34E-08 | 8.22E-07 | 1.23% | 1.23% | 1.28% | 1.26% | 1.05% | -0.01% | -0.01% | -0.25% | -1.09% | -0.01% |
| 26 | 3.84E-08 | 1.40E-07 | 1.52E-08 | 8.13E-09 | 2.28E-07 | 2.19% | 2.19% | 2.16% | 1.98% | 1.88% | 0.00% | 0.00% | -0.24% | -0.38% | 0.00% |
| 27 | 7.63E-09 | 3.00E-08 | 4.39E-09 | 2.79E-09 | 4.63E-08 | 4.94% | 4.94% | 4.57% | 4.31% | 4.28% | 0.00% | 0.00% | -0.22% | -0.13% | 0.00% |
| 28 | 1.33E-09 | 5.60E-09 | 6.64E-10 | 4.11E-10 | 7.70E-09 | 12.27% | 12.28% | 10.96% | 10.38% | 10.76% | 0.00% | 0.00% | -0.02% | -0.02% | 0.00% |
| 29 | 4.48E-10 | 1.97E-09 | 1.65E-10 | 1.22E-10 | 2.45E-09 | 21.31% | 21.24% | 17.74% | 17.79% | 18.52% | 0.00% | 0.00% | -0.01% | -0.01% | 0.00% |
| 30 | 2.83E-10 | 1.31E-09 | 8.31E-11 | 5.97E-11 | 1.49E-09 | 27.18% | 27.13% | 20.27% | 22.89% | 23.92% | 0.00% | 0.00% | -0.01% | 0.00% | 0.00% |
| Total | 1.28E-05 | 3.27E-05 | 5.07E-08 | 2.14E-06 | 2.00E-04 | 0.11% | 0.11% | 1.04% | 0.14% | 0.10% | -0.96% | -0.96% | -1.06% | -2.95% | -1.04% |

From the second table, it appears that this goal was not achieved. The error in the RRD's is approximately the same as in the first tally region. This is different than the SCR where a reduction in error was observed after segmenting. This may mean that this technique is not as effective for hexagonal lattice reactors, that we have segmented the reactor poorly, etc. At this time, it is not possible to directly determine the reasons for this lack of reduction in error. The partial percent errors observed here are also about the same as seen in the fourth tally region in the SCR. Overall the TXSAMC-produced cross sections reproduce the reaction rates very well. The total percent error for the fourth tally region is very reasonable at levels around one percent for each reaction.

In Fig. 24 we see the difference in the TXSAMC and MCNP RRD's for the fourth tally region displayed graphically. The very low errors in the low energy range are quite obvious in this plot. Unlike the previous three tally regions, there is very little error at the high energies. In fact, for much of the energy spectrum, the error is near zero. It is also apparent that the error in this tally region is significantly less than that for the first three tally regions.

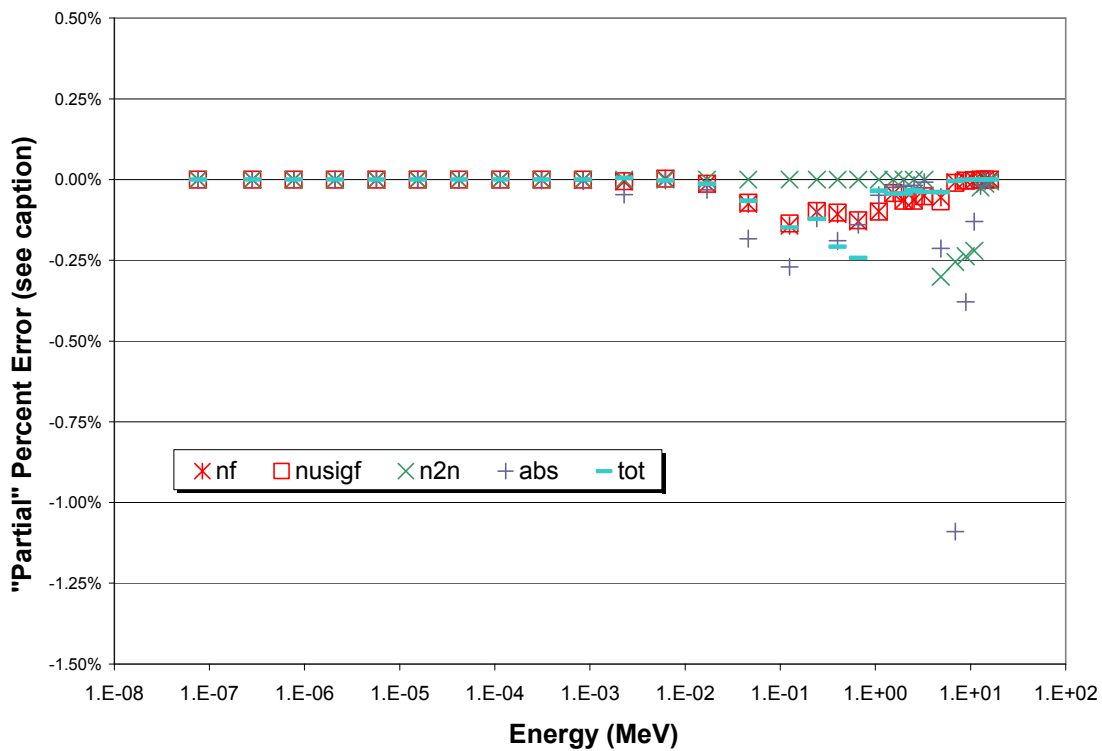


Fig. 24. "Partial" percent errors for reaction-rate densities in HCR tally region 4. Each "partial" error is plotted at the midpoint energy of its group. The percent error in a given reaction rate is the sum of the 30 partial percent errors.

The fifth tally region is composed of the six nearest fuel pin-cells to each coolant channel location for a total of eighteen cells. In Table 42 we show the MCNP-tallied scalar flux for the pin-cell, its relative standard deviation, the TXSAMC-generated cross sections and the TXSAMC-generated reaction rate densities for the fifth tally region.

Table 43 shows the MCNP-tallied reaction rate densities, their standard deviations and the partial percent error between the TXSAMC-generated reaction rates and the MCNP-tallied reaction rates for the fifth tally region.

TABLE 42
MCNP scalar flux, TXSAMC cross sections and reaction rates in HCR tally region 5

| Energy Group | Scalar Flux (n/cm ² /nps) | Rel. Error (1 σ) | TXSAMC SIGMA (cm ⁻¹) | | | | | TXSAMC RRD (cm ⁻³) | | | | |
|--------------|--------------------------------------|--------------------------|----------------------------------|----------|----------|----------|----------|--------------------------------|----------|----------|----------|----------|
| | | | fission | nusigf | n2n | abs-fis | total | fission | nusigf | n2n | abs-fis | total |
| 1 | 0.00E+00 | 0.00% | 3.34E+00 | 8.13E+00 | 0.00E+00 | 5.75E-01 | 4.31E+00 | 0.00E+00 | 0.00E+00 | 0.00E+00 | 0.00E+00 | 0.00E+00 |
| 2 | 0.00E+00 | 0.00% | 2.38E+00 | 5.81E+00 | 0.00E+00 | 5.01E-01 | 3.27E+00 | 0.00E+00 | 0.00E+00 | 0.00E+00 | 0.00E+00 | 0.00E+00 |
| 3 | 0.00E+00 | 0.00% | 9.81E-01 | 2.39E+00 | 0.00E+00 | 1.36E-01 | 1.49E+00 | 0.00E+00 | 0.00E+00 | 0.00E+00 | 0.00E+00 | 0.00E+00 |
| 4 | 0.00E+00 | 0.00% | 2.45E-01 | 5.96E-01 | 0.00E+00 | 9.00E-02 | 6.95E-01 | 0.00E+00 | 0.00E+00 | 0.00E+00 | 0.00E+00 | 0.00E+00 |
| 5 | 0.00E+00 | 0.00% | 1.21E-01 | 2.96E-01 | 0.00E+00 | 1.67E-01 | 6.24E-01 | 0.00E+00 | 0.00E+00 | 0.00E+00 | 0.00E+00 | 0.00E+00 |
| 6 | 1.19E-10 | 100.00% | 3.13E-01 | 7.61E-01 | 0.00E+00 | 2.71E-01 | 9.51E-01 | 3.72E-11 | 9.05E-11 | 0.00E+00 | 3.23E-11 | 1.13E-10 |
| 7 | 0.00E+00 | 0.00% | 4.24E-01 | 1.03E+00 | 0.00E+00 | 2.15E-01 | 1.00E+00 | 0.00E+00 | 0.00E+00 | 0.00E+00 | 0.00E+00 | 0.00E+00 |
| 8 | 0.00E+00 | 0.00% | 1.78E-01 | 4.34E-01 | 0.00E+00 | 1.07E-01 | 5.97E-01 | 0.00E+00 | 0.00E+00 | 0.00E+00 | 0.00E+00 | 0.00E+00 |
| 9 | 1.55E-09 | 47.58% | 1.41E-01 | 3.43E-01 | 0.00E+00 | 6.37E-02 | 5.24E-01 | 2.19E-10 | 5.32E-10 | 0.00E+00 | 9.87E-11 | 8.14E-10 |
| 10 | 1.53E-08 | 16.25% | 1.26E-01 | 3.06E-01 | 0.00E+00 | 6.75E-02 | 5.69E-01 | 1.92E-09 | 4.67E-09 | 0.00E+00 | 1.03E-09 | 8.70E-09 |
| 11 | 1.40E-07 | 5.62% | 7.53E-02 | 1.83E-01 | 0.00E+00 | 3.52E-02 | 8.58E-01 | 1.06E-08 | 2.57E-08 | 0.00E+00 | 4.94E-09 | 1.20E-07 |
| 12 | 9.83E-07 | 2.16% | 5.03E-02 | 1.22E-01 | 0.00E+00 | 1.99E-02 | 4.83E-01 | 4.94E-08 | 1.20E-07 | 0.00E+00 | 1.96E-08 | 4.75E-07 |
| 13 | 6.97E-06 | 0.85% | 3.62E-02 | 8.79E-02 | 0.00E+00 | 1.33E-02 | 4.29E-01 | 2.52E-07 | 6.13E-07 | 0.00E+00 | 9.29E-08 | 2.99E-06 |
| 14 | 2.97E-05 | 0.43% | 2.76E-02 | 6.69E-02 | 0.00E+00 | 9.26E-03 | 4.03E-01 | 8.20E-07 | 1.99E-06 | 0.00E+00 | 2.75E-07 | 1.20E-05 |
| 15 | 9.14E-05 | 0.26% | 2.20E-02 | 5.35E-02 | 0.00E+00 | 5.98E-03 | 3.61E-01 | 2.01E-06 | 4.89E-06 | 0.00E+00 | 5.46E-07 | 3.30E-05 |
| 16 | 7.60E-05 | 0.27% | 1.91E-02 | 4.70E-02 | 0.00E+00 | 4.11E-03 | 3.36E-01 | 1.45E-06 | 3.57E-06 | 0.00E+00 | 3.12E-07 | 2.55E-05 |
| 17 | 7.44E-05 | 0.28% | 1.76E-02 | 4.34E-02 | 0.00E+00 | 3.06E-03 | 3.95E-01 | 1.31E-06 | 3.23E-06 | 0.00E+00 | 2.28E-07 | 2.94E-05 |
| 18 | 1.10E-04 | 0.24% | 1.65E-02 | 4.11E-02 | 0.00E+00 | 2.25E-03 | 2.87E-01 | 1.81E-06 | 4.52E-06 | 0.00E+00 | 2.48E-07 | 3.16E-05 |
| 19 | 8.04E-05 | 0.28% | 1.74E-02 | 4.42E-02 | 0.00E+00 | 1.77E-03 | 2.91E-01 | 1.40E-06 | 3.56E-06 | 0.00E+00 | 1.42E-07 | 2.34E-05 |
| 20 | 4.40E-05 | 0.37% | 1.87E-02 | 4.86E-02 | 0.00E+00 | 1.35E-03 | 2.19E-01 | 8.24E-07 | 2.13E-06 | 0.00E+00 | 5.91E-08 | 9.62E-06 |
| 21 | 3.93E-05 | 0.40% | 1.95E-02 | 5.15E-02 | 0.00E+00 | 1.01E-03 | 2.08E-01 | 7.66E-07 | 2.03E-06 | 0.00E+00 | 3.97E-08 | 8.20E-06 |
| 22 | 4.10E-05 | 0.40% | 1.93E-02 | 5.22E-02 | 0.00E+00 | 6.64E-04 | 1.87E-01 | 7.91E-07 | 2.14E-06 | 0.00E+00 | 2.72E-08 | 7.66E-06 |
| 23 | 2.77E-05 | 0.48% | 1.84E-02 | 5.13E-02 | 0.00E+00 | 4.12E-04 | 2.31E-01 | 5.08E-07 | 1.42E-06 | 0.00E+00 | 1.14E-08 | 6.38E-06 |
| 24 | 2.94E-05 | 0.47% | 1.72E-02 | 5.13E-02 | 1.24E-04 | 2.34E-03 | 2.13E-01 | 5.06E-07 | 1.51E-06 | 3.65E-09 | 6.89E-08 | 6.25E-06 |
| 25 | 4.75E-06 | 1.15% | 2.27E-02 | 7.64E-02 | 5.56E-03 | 0.00E+00 | 1.72E-01 | 1.08E-07 | 3.63E-07 | 2.64E-08 | 0.00E+00 | 8.15E-07 |
| 26 | 1.39E-06 | 2.11% | 2.80E-02 | 1.02E-01 | 1.11E-02 | 0.00E+00 | 1.66E-01 | 3.89E-08 | 1.42E-07 | 1.54E-08 | 0.00E+00 | 2.30E-07 |
| 27 | 2.87E-07 | 4.63% | 2.74E-02 | 1.08E-01 | 1.59E-02 | 0.00E+00 | 1.67E-01 | 7.86E-09 | 3.10E-08 | 4.55E-09 | 0.00E+00 | 4.80E-08 |
| 28 | 4.51E-08 | 11.12% | 2.87E-02 | 1.20E-01 | 1.46E-02 | 0.00E+00 | 1.70E-01 | 1.29E-09 | 5.42E-09 | 6.57E-10 | 0.00E+00 | 7.68E-09 |
| 29 | 1.36E-08 | 20.26% | 3.14E-02 | 1.39E-01 | 1.15E-02 | 0.00E+00 | 1.73E-01 | 4.27E-10 | 1.89E-09 | 1.57E-10 | 0.00E+00 | 2.35E-09 |
| 30 | 5.87E-09 | 36.14% | 3.42E-02 | 1.58E-01 | 9.60E-03 | 0.00E+00 | 1.80E-01 | 2.01E-10 | 9.28E-10 | 5.64E-11 | 0.00E+00 | 1.06E-09 |
| Total | 6.58E-04 | 0.11% | 8.80E+00 | 2.17E+01 | 6.83E-02 | 2.29E+00 | 2.00E+01 | 1.27E-05 | 3.23E-05 | 5.09E-08 | 2.08E-06 | 1.98E-04 |

TABLE 43
MCNP reaction rates and reaction rate comparison in HCR tally region 5

| Energy Group | MCNP RRD (cm ⁻³) | | | | | MCNP Standard Deviation | | | | | Partial Percent Error (TXSAMC-MCNP)/MCNP | | | | |
|-----------------|------------------------------|----------|----------|----------|----------|-------------------------|---------|--------|---------|---------|--|--------|--------|---------|--------|
| | fission | nusigf | n2n | abs-fis | total | fission | nusigf | n2n | abs-fis | total | fission | nusigf | n2n | abs-fis | total |
| 1 | 0.00E+00 | 0.00E+00 | 0.00E+00 | 0.00E+00 | 0.00E+00 | N/A | N/A | N/A | N/A | N/A | N/A | N/A | N/A | N/A | N/A |
| 2 | 0.00E+00 | 0.00E+00 | 0.00E+00 | 0.00E+00 | 0.00E+00 | N/A | N/A | N/A | N/A | N/A | N/A | N/A | N/A | N/A | N/A |
| 3 | 0.00E+00 | 0.00E+00 | 0.00E+00 | 0.00E+00 | 0.00E+00 | N/A | N/A | N/A | N/A | N/A | N/A | N/A | N/A | N/A | N/A |
| 4 | 0.00E+00 | 0.00E+00 | 0.00E+00 | 0.00E+00 | 0.00E+00 | N/A | N/A | N/A | N/A | N/A | N/A | N/A | N/A | N/A | N/A |
| 5 | 0.00E+00 | 0.00E+00 | 0.00E+00 | 0.00E+00 | 0.00E+00 | N/A | N/A | N/A | N/A | N/A | N/A | N/A | N/A | N/A | N/A |
| 6 | 5.95E-11 | 1.45E-10 | 0.00E+00 | 2.01E-11 | 1.28E-10 | 100.00% | 100.00% | N/A | 100.00% | 100.00% | 0.00% | 0.00% | N/A | 0.00% | 0.00% |
| 7 | 0.00E+00 | 0.00E+00 | 0.00E+00 | 0.00E+00 | 0.00E+00 | N/A | N/A | N/A | N/A | N/A | N/A | N/A | N/A | N/A | N/A |
| 8 | 0.00E+00 | 0.00E+00 | 0.00E+00 | 0.00E+00 | 0.00E+00 | N/A | N/A | N/A | N/A | N/A | N/A | N/A | N/A | N/A | N/A |
| 9 | 2.74E-10 | 6.68E-10 | 0.00E+00 | 1.44E-10 | 9.84E-10 | 50.65% | 50.65% | N/A | 47.76% | 46.79% | 0.00% | 0.00% | N/A | 0.00% | 0.00% |
| 10 | 1.73E-09 | 4.21E-09 | 0.00E+00 | 9.18E-10 | 8.33E-09 | 17.21% | 17.21% | N/A | 18.55% | 15.85% | 0.00% | 0.00% | N/A | 0.01% | 0.00% |
| 11 | 1.16E-08 | 2.81E-08 | 0.00E+00 | 6.18E-09 | 1.08E-07 | 6.37% | 6.37% | N/A | 6.17% | 4.42% | -0.01% | -0.01% | N/A | -0.06% | 0.01% |
| 12 | 4.92E-08 | 1.20E-07 | 0.00E+00 | 1.97E-08 | 4.82E-07 | 2.32% | 2.32% | N/A | 2.26% | 1.87% | 0.00% | 0.00% | N/A | -0.01% | 0.00% |
| 13 | 2.55E-07 | 6.19E-07 | 0.00E+00 | 9.39E-08 | 3.02E-06 | 0.90% | 0.90% | N/A | 0.89% | 0.76% | -0.02% | -0.02% | N/A | -0.04% | -0.01% |
| 14 | 8.29E-07 | 2.01E-06 | 0.00E+00 | 2.79E-07 | 1.21E-05 | 0.45% | 0.45% | N/A | 0.45% | 0.38% | -0.07% | -0.07% | N/A | -0.18% | -0.07% |
| 15 | 2.03E-06 | 4.94E-06 | 0.00E+00 | 5.52E-07 | 3.33E-05 | 0.27% | 0.27% | N/A | 0.27% | 0.23% | -0.16% | -0.15% | N/A | -0.30% | -0.16% |
| 16 | 1.46E-06 | 3.59E-06 | 0.00E+00 | 3.14E-07 | 2.58E-05 | 0.28% | 0.28% | N/A | 0.28% | 0.24% | -0.07% | -0.07% | N/A | -0.09% | -0.11% |
| 17 | 1.32E-06 | 3.26E-06 | 0.00E+00 | 2.31E-07 | 2.98E-05 | 0.29% | 0.29% | N/A | 0.29% | 0.26% | -0.10% | -0.10% | N/A | -0.18% | -0.22% |
| 18 | 1.83E-06 | 4.57E-06 | 0.00E+00 | 2.51E-07 | 3.20E-05 | 0.26% | 0.26% | N/A | 0.26% | 0.21% | -0.14% | -0.13% | N/A | -0.14% | -0.24% |
| 19 | 1.41E-06 | 3.58E-06 | 0.00E+00 | 1.43E-07 | 2.35E-05 | 0.30% | 0.30% | N/A | 0.29% | 0.25% | -0.08% | -0.08% | N/A | -0.04% | -0.02% |
| 20 | 8.31E-07 | 2.15E-06 | 0.00E+00 | 5.98E-08 | 9.72E-06 | 0.40% | 0.40% | N/A | 0.39% | 0.34% | -0.06% | -0.06% | N/A | -0.03% | -0.05% |
| 21 | 7.74E-07 | 2.05E-06 | 0.00E+00 | 4.02E-08 | 8.29E-06 | 0.42% | 0.42% | N/A | 0.42% | 0.36% | -0.06% | -0.06% | N/A | -0.02% | -0.04% |
| 22 | 8.01E-07 | 2.17E-06 | 0.00E+00 | 2.77E-08 | 7.74E-06 | 0.42% | 0.42% | N/A | 0.41% | 0.35% | -0.08% | -0.08% | N/A | -0.02% | -0.04% |
| 23 | 5.15E-07 | 1.44E-06 | 0.00E+00 | 1.16E-08 | 6.46E-06 | 0.50% | 0.50% | N/A | 0.49% | 0.45% | -0.05% | -0.05% | N/A | -0.01% | -0.04% |
| 24 | 5.12E-07 | 1.53E-06 | 3.87E-09 | 7.33E-08 | 6.32E-06 | 0.50% | 0.50% | 1.64% | 0.64% | 0.44% | -0.04% | -0.06% | -0.43% | -0.20% | -0.03% |
| 25 | 1.08E-07 | 3.64E-07 | 2.65E-08 | 2.35E-08 | 8.23E-07 | 1.23% | 1.23% | 1.28% | 1.26% | 1.05% | 0.00% | -0.01% | -0.15% | -1.10% | 0.00% |
| 26 | 3.95E-08 | 1.44E-07 | 1.57E-08 | 8.40E-09 | 2.33E-07 | 2.22% | 2.22% | 2.19% | 2.03% | 1.91% | 0.00% | -0.01% | -0.58% | -0.39% | 0.00% |
| 27 | 7.94E-09 | 3.13E-08 | 4.58E-09 | 2.96E-09 | 4.85E-08 | 4.92% | 4.92% | 4.54% | 4.27% | 4.24% | 0.00% | 0.00% | -0.07% | -0.14% | 0.00% |
| 28 | 1.34E-09 | 5.62E-09 | 6.78E-10 | 4.20E-10 | 7.83E-09 | 11.54% | 11.56% | 10.23% | 9.64% | 10.02% | 0.00% | 0.00% | -0.04% | -0.02% | 0.00% |
| 29 | 4.17E-10 | 1.85E-09 | 1.55E-10 | 1.14E-10 | 2.33E-09 | 21.79% | 21.90% | 16.12% | 17.87% | 18.59% | 0.00% | 0.00% | 0.00% | -0.01% | 0.00% |
| 30 | 1.92E-10 | 8.93E-10 | 5.92E-11 | 4.08E-11 | 1.03E-09 | 36.40% | 36.47% | 25.94% | 29.55% | 31.48% | 0.00% | 0.00% | -0.01% | 0.00% | 0.00% |
| Total | 1.28E-05 | 3.26E-05 | 5.15E-08 | 2.14E-06 | 2.00E-04 | 0.11% | 0.11% | 1.05% | 0.14% | 0.10% | -0.94% | -0.94% | -1.26% | -2.96% | -1.03% |

Similar to the fourth tally region, this region shows a difference between the TXSAMC and MCNP RRD's that is very near to that calculated for the first tally region. The overall error is very manageable at around one percent for all but the absorption RRD. Although there are a number of groups where the difference between the TXSAMC- and MCNP-produced RRD is large, most of these groups have very low reaction rates so the RRD-weighted difference is very small. Again, one of the benefits to this statistical weighting approach (through the MCNP derived scalar flux) is that some of the regions/energy groups with the worst error contribute least to the overall reaction rate so, to a certain extent, the high errors in certain energy groups are unimportant.

In Fig. 25 we see the difference in the TXSAMC and MCNP RRD's for the fifth tally region displayed graphically. The very low errors in the low energy range are quite obvious in this plot as well as some error near the sodium resonance. At very high energies we see modest error in the (n,2n) and fission/nusigf reaction rates. It is important to note that away from the resonance and the upper thresholds, the error is quite low. In fact, for much of the energy spectrum, the error is near zero. It is also apparent that the error in this tally region is significantly less than that for the first three tally regions.

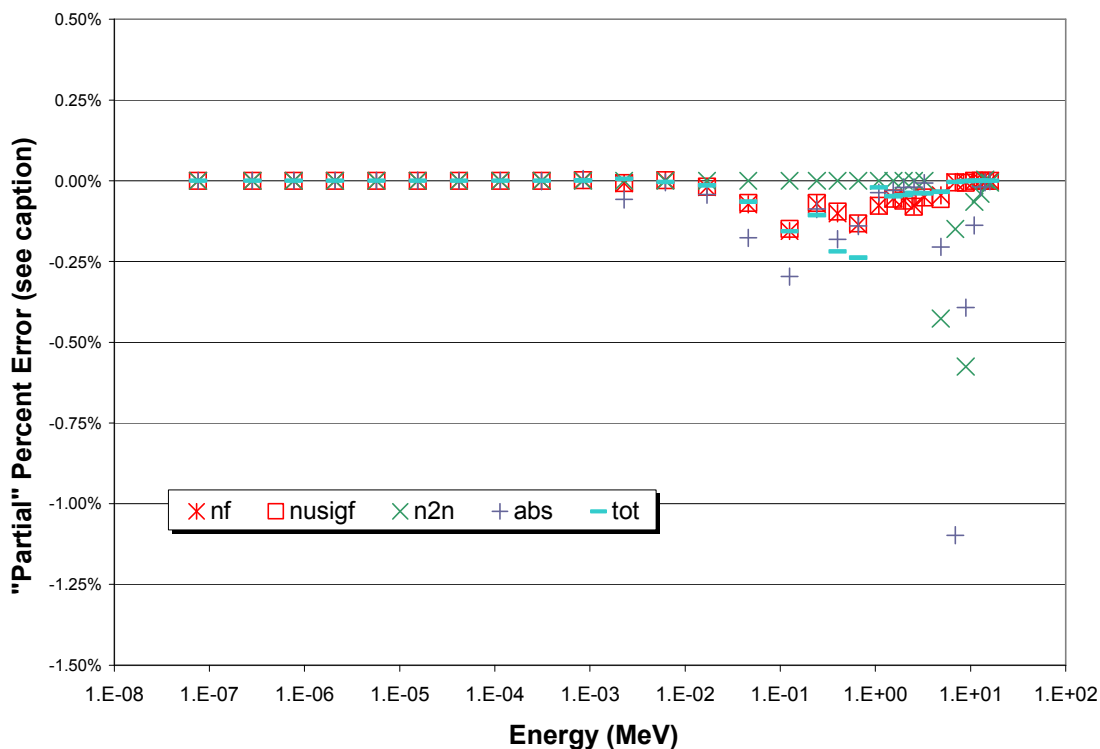


Fig. 25. "Partial" percent errors for reaction-rate densities in HCR tally region 5. Each "partial" error is plotted at the midpoint energy of its group. The percent error in a given reaction rate is the sum of the 30 partial percent errors.

Overall, it appears that the various tally regions in the HCR are reasonably well represented by the homogenized cross sections generated for each region. Unlike the SCR and not as expected, the smaller fuel tally regions (four and five) had similar partial percent errors to the core wide tally region (region one). It is unclear exactly why this is the case but it does suggest that more work needs to be done to determine how to segment the reactor for the best results. It is possible that a different set of regions would have the same reduction in error effect as in the SCR or it may be that there is a limit on the minimum error for a hexagonal lattice type reactor. Again, TXSAMC appears to work fairly well for the hexagonal lattice reactor problem with heterogeneities and the cross sections should be quite useful for a range of applications.

CHAPTER V

SUMMARY AND CONCLUSIONS

In this thesis, we have presented a tool called TXSAMC that produces shielded and homogenized multigroup cross sections for small fast reactor systems. The motivation for this tool comes from a desire to investigate small fast reactor systems that are difficult to analyze with existing tools. Investigation of these systems usually requires the use of deterministic codes to characterize the time-dependent reactor behavior and to link the reactor neutronics with thermal-hydraulics and/or other physics codes. Deterministic codes require an accurate set of multigroup cross section libraries. These systems usually have not been explored sufficiently for the needed libraries to already exist and since multigroup cross sections are highly problem-specific, new libraries must be generated for each system that is investigated. The current process for generating these libraries is tedious. TXSAMC offers a shorter and potentially more accurate route for generating these libraries.

TXSAMC links three different external codes together to create properly shielded and homogenized libraries. The code sets up an MCNP model of the reactor under investigation and calculates the zone-averaged scalar flux in various tally regions selected by the user as well as a core-averaged scalar flux. The core-averaged scalar flux is used to provide a weighting function for NJOY's GROUPT module. The zone-averaged scalar flux data is used to write RZFLUX files which are used in TRANSX. The code runs NJOY to produce energy-self-shielded multigroup cross sections that are tabulated by nuclide, temperature and background cross section in a MATXS formatted

library. This MATXS formatted library is read by TRANSX which, in conjunction with the RZFLUX files, performs spatial and mixture shielding on the cross sections and homogenizes them. The result is a macroscopic cross section that accurately represents the cell within the reactor from which the RZFLUX file was written. The cross sections produced by this process have been tested in five different sample problems and have been shown to be reasonably accurate. For cells containing fuel pins, the typical error in the overall fission, ν_{sigf} , $(n,2n)$, absorption and total RRD's is only a few percent and in many cases is less than one percent. It appears that the error is less for hexagonal lattices than for square lattices. This may be caused by TRANSX calculating background cross sections more accurately for hex lattices or it may be due to the greater fuel/coolant ratio in a hex cell. There is a significant amount of error associated with the threshold reactions like $(n,2n)$ in the sodium coolant in these test problems. The greatest error in any place is found in the coolant channels. For the square lattice test problems, there was a reduction in error when smaller tally regions were selected. This reduction was not observed for hexagonal lattice reactors. From a limited test, it appears that using a weight function in GROUPT with more points than the final cross section may have a limited benefit. This benefit was primarily noted in cells/regions where there is a great deal of sodium. It is suspected that this is due to a better mapping of the 2.8 keV resonance. Overall, the cross sections produced by TXSAMC performed very well.

Currently, TXSAMC is limited in a number of ways, many of which we expect to rectify in the future. The system is currently limited to only two reactor types and a maximum lattice size of 25x25. The MCNP model is not as accurate as it might be; a

number of features that are common to real reactors are not included in the model (including a reflector, a fission gas plenum, a downcomer, etc.). It may be necessary to add new scattering models to the reactor if epithermal or thermal systems are going to be investigated. We envision these problems being resolved in the future. The code is also currently limited to Windows based systems. Future modifications to make the code usable on Linux/UNIX systems are planned. One of the major advantages to porting to these systems would be the ability to use parallelized MCNP on a Linux cluster. This would significantly speed up the MCNP portion of the process and allow for better statistics in threshold and resonance regions. Another possible improvement would be to use regional spectra instead of a core-averaged spectrum in the GROUPT module. This might allow us to perform the energy-self-shielding better.

Other future work could involve investigating the use of finer group structures to calculate the core-averaged scalar flux that is used for the weighting function in GROUPT. We would retain the same group structure output on MATXS but the within-group shape of the flux would potentially be known better. This area of work would be greatly enabled if parallelized MCNP could be used since finer group structures will require many more histories to achieve the same statistics within each group that we have now. We feel that this new weight function could make a significant improvement in the error around major resonances and thresholds depending on how it is applied in GROUPT. There is some question about using a finer weight function since it may effectively double-shield the cross sections produced by equation (5).

Another major improvement that is being looked at is to find a way to use MCNP to tally the higher Legendre moments of the flux. Currently all of the shielding and homogenization is done by using the P0 scalar flux. This is probably adequate right now but a better treatment of the anisotropic scattering in the higher moments is probably needed. One way this might be achieved could be through functional expansion tallies, where each particle tallied in an area contributes to a functional shape rather than a histogram¹². This method has not been expanded to cover the full range needed to calculate all of the moments but it does show the potential to do so. It also might be useful to add a smoothing function to the weighting function used in GROUPT for coarser spectra (i.e. one that is not fine enough to resolve the resonances). When some groups have no tallied particles and other nearby groups have a few tallied particles, there can be artificial “dips” of four orders of magnitude or more due to the way TXSAMC “corrects” zeros in the weighting function. The addition of a smoothing function would level some of this out and perhaps produce a slightly more accurate weighting function in these areas. Another possible area for future work would be to improve the way that the coolant channels are modeled in TRANSX, perhaps modeling it as cylinder of coolant in a ring of fuel, to better account for the spatial shielding effects within this region.

Finally, we should note that the results in this thesis only benchmark the five reaction rates discussed. It was not within the scope of the thesis to benchmark the accuracy of the scattering matrices/moments produced by TXSAMC or the vast number of possible reactions. Although we have done some work in this area as part of a

previous project that suggests the matrices produced are adequate, future work with deterministic codes or a much more complicated MCNP scheme would be needed to completely validate the accuracy of the produced scattering matrices/moments. It would be relatively straightforward to benchmark almost any other reaction although some of the results in this thesis suggest the difficulty of validating cross sections for very low probability or threshold reactions.

It should also be noted that there are a number of improvements that could be made in the actual programming technique. These include but are not limited to modifying the section of the code that reads the MCTAL file to use formatted reads with implied DO loops and not using a scratch file to convert the universe number on the input file from character to integer and vice versa. There are also some additions that need to be made to make sure that output cross section files from TRANSX for each tally region do not overwrite each other. This has been done for ACEM formatted output but not other output types.

While there remain tasks to be accomplished, it seems reasonable to conclude that the TXSAMC code has achieved its goals of demonstrating an easy-to-use process for generating shielded and homogenized cross sections for small fast reactor systems. The level of error in the cross sections seems reasonable and the process is reasonably flexible.

REFERENCES

1. J. J. DUDERSTADT and L. J. HAMILTON, *Nuclear Reactor Analysis*, John Wiley and Sons, Inc., New York (1976).
2. W. M. STACEY, *Nuclear Reactor Physics*, John Wiley and Sons, Inc., New York (2001).
3. KOREA ATOMIC ENERGY RESEARCH INSTITUTE, “Table of Nuclides”, Nuclear Data Evaluation Lab (2000), available at <http://atom.kaeri.re.kr/index.html>.
4. DEPARTMENT OF ENERGY, “DOE – Global Nuclear Energy Partnership”, DOE (2006), available at <http://www.gnep.energy.gov>.
5. B. T. REARDEN, T. A. PARISH and W. S. CHARLTON, “Generation of Two-Group Cross Sections for WG-MOX Fuel Using MCNP”, *Trans. American Nuclear Society*, **77**, 323-324 (1997).
6. E. L. REDMOND, “Multigroup Cross Section Generation Via Monte Carlo Methods”, PhD Dissertation, Massachusetts Institute of Technology, Cambridge, MA (1997).
7. T. E. BOOTH, F. B. BROWN, J. S. BULL, L. J. COX, R. A. FORSTER, J. T. GOORLEY, H. G. HUGHES, R. D. MOSTELLER, R. E. PRAEL, E. C. SELCOW, A. SOOD, J. E. SWEEZY, R. F. BARRETT, S. E. POST and T. L. ROBERTS, “MCNP -- A General Monte Carlo N-Particle Transport Code, Version 5 Volume I: Overview and Theory”, LANL/LA-UR-03-1987, Los Alamos National Laboratory (2003).
8. T. E. BOOTH, F. B. BROWN, J. S. BULL, L. J. COX, R. A. FORSTER, J. T. GOORLEY, H. G. HUGHES, R. D. MOSTELLER, R. E. PRAEL, E. C. SELCOW, A. SOOD, J. E. SWEEZY, R. F. BARRETT, S. E. POST and T. L. ROBERTS, “MCNP -- A General Monte Carlo N-Particle Transport Code, Version 5 Volume II: User’s Guide”, LANL/LA-CP-03-0245, Los Alamos National Laboratory (2003).
9. R. E. MACFARLANE and D. W. MUIR, “The NJOY Nuclear Data Processing System, Version 91”, LANL/LA-12740-M, Los Alamos National Laboratory (1994).
10. R. E. MACFARLANE, “TRANSX 2: A Code for Interfacing MATXS Cross-Section Libraries to Nuclear Transport Codes”, LANL/LA-12312-MS, Los Alamos National Laboratory (1992).

11. R.D. O'DELL, "Standard Interface Files for Reactor Physics Codes, Version IV", LANL/LA-6941-MS, Los Alamos National Laboratory (1977).
12. D. P. GRIESHEIMER, "Functional Expansion Tallies for Monte Carlo Simulations", PhD Dissertation, University of Michigan, Ann Arbor (2005).

APPENDIX A

DETAILED DESCRIPTION OF TXSAMC CODE

This section describes the general flow of the processing in TXSAMC. Most of the hard-core data processing in TXSAMC is done by the underlying codes so much of the responsibility of TXSAMC is simply producing the right input files and interfacing between each code. The remainder of this section describes this process in general terms; the source code is included in Appendix B for those who wish to investigate further.

TXSAMC begins with the declaration of over one hundred variables and arrays that control every aspect of the process. All of the integer and real variables are declared in double precision. For the integer variables, this is probably unnecessary, but on modern machines the cost is negligible. All of the arrays are declared allocatable. This allows flexibility to read in different numbers of variables from problem to problem without having to employ the very large container arrays often used in older codes (NJOY and TRANSX both use this style). After the types of all of the variables have been declared, TXSAMC attempts to open the input file "input.txt". If it cannot find the file, the program terminates. It then opens the "matxsrinput" and "mcin" files. The former will control the processing of the GENDF files into a MATXS formatted file and the latter is the input file for MCNP (again, MCNP4C, MCNP5 or MCNPX can all be used so we refer to these generically as "MCNP"). It then attempts to open the "wtfxn.txt" and "gstruc.txt" files. The former describes the weighting flux used in GROUPT and the latter describes the group structure used in GROUPT. If TXSAMC is run as designed, "wtfxn.txt" will be overwritten with results from MCNP. The program

then opens the first of several scratch files. The scratch files are not intended to be kept long term and are simply used within the code for various functions. Finally, we assign a numerical value to π of 3.14159 for simplicity.

After the variables have all been declared, the code begins reading through the input file. After reading the general options section at the beginning of the file, it has enough information to locate the executables for MCNP, NJOY, TRANSX and MERG_GENDF and it assigns these locations to a variable. One of the major items that we decided was important in TXSAMC was creating a code that reported on what task it was doing and what errors it encountered. Part of this goal was achieved by statements throughout the code that output to the execution shell the current task. The first of these is a report of “Reading the global input file”. The other notifications like this will not be discussed in this report since they are generally self-explanatory.

TXSAMC then reads the section that describes the MCNP options off of the input file. It allocates arrays as it reads in the variables that provide the array dimensions. It also opens a scratch file so that it can read a variable in one type (character), write it out to the scratch file and read it in again in another type (integer). This seems like an awkward solution to this problem and there is a potentially easier method to do this task but it did not occur to the author at the time. Before reading in the tally map, the code calculates the MCNP lattice dimensions. The MCNP model of the reactor is built in a fashion where a square or hexagonal lattice completely fills the vessel space. This lattice is necessarily larger than the actual lattice of fuel pins since the core doesn't completely

fill the vessel space. As part of this lattice calculation, the inner and outer radii of the vessel are also calculated.

When it reaches the time to read in the tally map, the code has the option (if the “mapwrite” variable is equal to one) to write out a “blank” tally map of the appropriate size for the reactor with a “1” in positions inside the core and a “0” in the remaining lattice positions. This allows the user to save the time it would take to enter by hand the tally map and only change the numbers in particular locations of interest (coolant channels, control rods, etc.). This blank map is written to a scratch file and the code exits. The user can then copy and paste this map from the scratch file to the “input.txt” file. If the code does not write the blank map, it reads in the user specified tally map. One future area of work for the code is to have TXSAMC automatically select the tally regions instead of using a user-specified map. It should be noted that the code does not currently have the capability to mix cell types in the same tally region.

TXSAMC then reads the NJOY options off of the input file. This section is significantly more straight-forward than the reading of the MCNP options section. The code does check to see if the group structure and number of groups are consistent for the built-in NJOY structures. Finally, the code reads in the options for the TRANSX section of the code.

At this point, the code begins making various calculations needed to write the MCNP input file “mcin” from the given data. For both lattice types, the code calculates the base fuel pin radius, the fuel meat radius, the fuel meat length, the volume of the cell, the volume of the pin, the volume of fuel and the volume of the moderator. When

calculating the fuel length, the cladding has the same axial thickness as it does in the radial direction and there is no fission gas plenum. The code makes the same calculations of length and volume for other cell-types such as control rods and coolant channels. The code also calculates the cross-sectional area of each region in the cell for use in TRANSX. The code then creates the array that will be written to the MCNP input deck and describes which universe each cell in the lattice will be filled with. The reactor vessel is filled with universe one which is made up of coolant. The base fuel pins are in universe two and control rods are in universe three. Other cell types are in universe four through nine. The code assigns these universe numbers based on the x-y coordinates it read off of the input file. The last thing it does before writing “mcin” is to call the Suffr subroutine which assigns ZAID suffixes for each material based on the temperature. The code assumes the existence of a continuous energy cross section library with temperatures ranging from 300-1500 K, incremented by 100 K, where a suffix of “.30c” corresponds to 300 K, “.40c” corresponds to 400 K and so forth.

With all of these calculations complete, TXSAMC begins writing the MCNP input file. It writes the cell cards for the reactor vessel followed by the array that describes where each universe is positioned in the lattice. It should be noted that this lattice is effectively “upside-down” from the perspective of the user due to the way MCNP will read in the input file. It then writes the cell cards for the base fuel pin. Following this, it cycles through each of the other universes in the problem to write the cell cards for those universes. This finishes the writing of the cell cards.

The code then writes the surface cards for the reactor vessel and the basic pin-cell. The surfaces are oriented such that the long axis of the reactor lies along the z-axis. For the square lattice, the basic pin-cell is four planes perpendicular to the x-y plane in the shape of a square. For the hexagonal lattice, the basic pin-cell is six planes perpendicular to the x-y plane in the shape of a hexagon. Both of these cells are capped in the z-axis by the inside wall of the reactor vessel. The surface cards for the basic fuel pin are then written. Following this, the code cycles through each of the other cell-types and writes the surface cards for each region within that cell. It should be noted that for cells where there are more than two regions within the pin (clad and meat), all of the internal regions have the same length. This finishes the surface card writing.

The process then calls the Matter subroutine to write the material cards for the MCNP input file. As mentioned earlier, the code only has six materials pre-programmed but more can easily be added by modifying the Matter subroutine (and also the Mixer subroutine which is called to write the TRANSX input). TXSAMC then writes the data cards for MCNP. It begins with writing the problem mode (assumed to be neutron only) and, based on the input, it writes the KCODE and KSRC cards.

It follows this with one of the more critical sections of the entire code: the tallies. The code creates one scalar flux (F4) tally for each tally region, with a bin for each region within the cell-type covered by that tally region. For example, in a fuel pin, there would be three bins. Each bin within the tally is normalized by the volume of the region represented by that bin; this is done by writing an "sd" card containing the volumes immediately after the "f" tally card. After these portions of the tallies are written, the

Energizer subroutine is called which segments the tally by the appropriate energy bins. The energy bins are identical to the group structure specified for the NJOY section of TXSAMC. Finally, there is one single F4 tally over the entire core region which is also segmented by energy. The result of this tally is used as the weighting function in GROUPT. The code finishes the “mcin” file by writing a PRDMP card. This card requests the output of the MCNP routine to be written to an MCTAL formatted file⁵⁻⁶. This is an ASCII formatted file that is easy to read for external codes since it has a fixed format.

The code then sends a series of commands to the DOS shell on the system that deletes any existing MCNP output files and executes the code using “mcin” as the input file. The output will be the files “mcino”, “mcinm”, “mcinr” and “mcins”. The “mcinm” file is the MCTAL file that will be read by TXSAMC. The code reads the MCTAL file to determine how many tally regions were written to it and then begins a loop over that number of tally regions. For each tally region, it reads the number of bins, the energy structure, the tally results and the relative standard deviation for each tally. The code then uses the last tally region on the MCTAL file (the core averaged scalar flux) to write a new “wtfxn.txt” for the NJOY section of the code. The values on the MCTAL file are integrals over the tally region but NJOY requires point values so each tally is divided by the width of the bin, converted into units of eV (MCNP output is in MeV) and assigned to the midpoint of the bin to create the weighting function. Because the NJOY weighting function cannot have any non-positive values, any values of zero on the MCNP tally are “corrected” by changing them to a positive value that is four orders of magnitude smaller

than the smallest positive value on the tally. The header of the “wtfxn.txt” file includes a specification of the number of points in the weighting function and the interpolation scheme to be used in GROUPT. By default, a log-log interpolation is used although four other schemes are possible.

The code then uses the remaining data it read off of the “mcinm” file to create the various RZFLUX files needed for each tally region. The code specifies values for the header on the file. The code specifies the values for the twenty control variables on the RZFLUX file (see the TRANSX or CCCC-IV manuals for more information on the formatting of this file). Only one of these control variables is actually relevant to TRANSX and that is the number of neutron groups. Following these specifications, the code writes the header and control variables to an RZFLUX file (the files are titled “rzflux9#” where the # sign is the number of the tally region from the original tally map). The code then writes the scalar flux in each group for each bin to the RZFLUX file. It should be noted that the bins must run inside to out within the cell in order to be read correctly by TRANSX. The values on the file also run in reverse energy order (high to low) relative to the MCNP tallies. It should be noted that in order to read this RZFLUX file in the format it is written, the TRANSX source code had to be modified to read the RZFLUX file as an ASCII formatted file rather than an unformatted binary file. These changes are small and are detailed in Appendix C.

With the RZFLUX files written, TXSAMC sends some commands to the shell to clear out any NJOY output files in the working directory. It then begins writing the NJOY input file for each nuclide. Using the data read from the NJOY options section of

the global input file, TXSAMC writes the RECONR, BROADR, HEATR and PURR input sections. If the THERMR option is selected, it also writes the input for this section. If not, it uses a MODER section as filler. Currently, within the THERMR section, the code only uses free gas scattering models. Future modifications might include the ability to use special scattering models like ZrH or H₂O. TXSAMC then writes a GROUPE input section for each temperature. Within the GROUPE section, “wtfxn.txt” is opened and written into the NJOY input file. The code also selects which cross sections to call based on the cross section type for that nuclide (specified on “input.txt”).

After finishing writing the NJOY input, TXSAMC sends commands to the DOS shell to copy the necessary ENDF tape to the local working directory and run each input file through NJOY. The outputs are renamed so that they are not overwritten during the successive NJOY runs. The output GENDF file for each nuclide is renamed to the nuclide name and “.gendf” is appended to it. The output text file for each NJOY run is renamed to the nuclide name and “.out” is appended to it. Following the execution of NJOY for each nuclide, all of the GENDF files are combined into one ALL.G file through the MERG_GENDF utility (see Appendix D for a listing). The code then writes the MATXSU input section onto the “matxsuinput” file and executes NJOY again. The output tape from this is renamed “matxs”. This concludes the NJOY section of TXSAMC.

The code then begins preparing and writing the TRANSX input files for each tally region. Each input file is sequentially labeled “pincell8#.inp” where the # is replaced by the number of the tally region. The code calculates the number of regions

within the cell for each tally region and then checks for correspondence between the heterogeneity option and the lattice type. The code then writes the problem title and tally region as a header to the TRANSX input file. It follows this by writing the control variables that it read from “input.txt” on the next two lines. It then writes the number of the output mixture (begins with 101 and increments upward for each tally region). After this it cycles through the possible cell types and writes the region and mixture descriptions for that cell type (more detail can be found about the TRANSX input file structure in the TRANSX 2 manual). The mixture descriptions are written by calling the Mixer subroutine.

With the TRANSX input files complete, the code begins passing commands to the shell to execute the code and rename the output files. At this writing, not all of the possible output formats have been coded for proper renaming so it may be possible to overwrite files from prior runs. With the TRANSX runs complete, TXSAMC is complete and the system has produced a series of shielded and homogenized cross section files, one per tally region.


```

!inac
!rrdflag
!mcnpngs
!mcnpnng
!-----Tally Map-----
!talflaf mapwrite
!tally map goes here
!
!-----NJOY Input Block-----
!niso
!iso_name(i) matid(i) za(i) xstype(i) tape(i) ireg(i)
!ntemp
!temps(i) suffs(i) gtape(i)
!ngs
!nng
!pgs
!npg
!wtfxn
!nleg
!nsig
!sigzer(i)
!thermopt
!npart
!ntype
!-----TRANSX Input Block-----
!iout
!iprob
!iset
!iform
!itrc
!icoll
!initf
!ngroup
!nl
!nup
!nthg
!nmix
!ned
!neds
!ihet
!hed
!eds(i)
!-----RZFLUX Data-----
!power
!nu

!Inactive cycles
!Tally reaction rates? (0=no,1=yes)
!MCNP core-averaged scalar flux group structure
!MCNP core-averaged scalar flux # of neutron groups

!Tally Map flag (0=off,1=on), Mapwriter (0=off,1=on)

!Number of isotopes
!ISO_NAME MATID ZA XSTYPE TAPE IREG
!Number of Temperatures
!Temperature, suffix and group tape #
!Neutron group structure
!Number of neutron groups
!Photon group structure
!Number of photon groups
!Flux weighting function
!Number of Legendre orders
!Number of sigma zeroes
!Sigma zeroes (1E8 == Infinite dilution)
!THERMR option (0=off,1=on)
!Number of particles with a group structure for MATXSR
!Number of data types for MATXSR (not including ntherm)

!IOUT (Output Format)
!IPROB (0=Direct/1=Adjoint)
!ISET (Particle Set) (usually 1)
!IFORM (1=Matwise/2=Groupwise)
!ITRC (Transport Correction)
!ICOLL (Collapse 0=No/NFINE=Yes)
!INITF (Initial Flux) (only use 0 or 4)
!NGROUP (Number of groups)
!NL (Number of Legendre tables)
!NUP (Number of upscatter groups)
!NTHG (Number of thermal groups)
!NMIX (# of output mixes) This should be 1 almost always
!NED
!NEDS
!IHET (usually 3 or 4)
!HED (list of edits)
!Edit specifications

!Power level in kW (used for normalization purposes)
!nu (used for normalization purposes)

```

PROGRAM txsame

USE DFLIB !Allows use of the systemqq command

```

INTEGER*8 :: i,j,k,m,p,q,r,funit,bplen,ctr,ctr2,ctr3,ctr4,ctr5,ctr7,ctr6
INTEGER*8 :: niso,ntemp,nsig,nng,npg,wtfxn,nleg,pgs,ngs,thermopt
INTEGER*8 :: tlen,slen,npart,ntype,nlen,nlat,sunit,mcnpngs,mcnpnng
INTEGER*8 :: ltype,nrows,nmat,exec,exmat,noct,ntreg
INTEGER*8 :: ingerr,iwterr,inperr,materr,junk3,ppc,inac,ac
INTEGER*8 :: maxmat,maxpos,talflag,jlen,finflag,mapwrite
INTEGER*8 :: iout,iprob,iset,iform,itrc,icoll,initf,ngroup
INTEGER*8 :: nl,nthg,nmix,nreg,nmixs,ned,neds,ihet,ntabl
INTEGER*8 :: tunit,octindex,mctalerr,ndex,tfc,ntal,go,hetchange
INTEGER*8 :: nmixline,nocount,ivers,rrdflag
REAL*8 :: pitch,clength,tc,dpin,rpin,flength,rfuel,modvol,pinvol
REAL*8 :: cellvol,hexside,pi,cvol,mvol,fvol,totfuelvol
REAL*8 :: enri,rvout,rvin,b1,nps,minmctal,power,neurate,nu

```

```

REAL*8 :: fuelvol,cladvol,junk5,junk6
CHARACTER(LEN=4) :: id
CHARACTER(LEN=6) :: junk,hname
CHARACTER(LEN=8) :: xsdir
CHARACTER(LEN=40) :: title,hed
CHARACTER(LEN=48) :: bpath
CHARACTER(LEN=60) :: endf_path,tlist,siglist,notlist
CHARACTER(LEN=80) :: njoy_exe,merg_exe,transx_exe,mcnp_exe
CHARACTER(LEN=120) :: junk2,blankmap,command6,command7

INTEGER*8,ALLOCATABLE :: za(:),ireg(:),xstype(:),ntpins(:),ncelloc(:)
INTEGER*8,ALLOCATABLE :: unum2(:),nbins(:),tregtype(:),ia(:)
INTEGER*8,ALLOCATABLE :: nrad(:),latx(:,:),laty(:,:),talmap2(:,:)
REAL*8,ALLOCATABLE :: mctemp(:),mcdens(:),otrad(:,:),otdens(:,:)
REAL*8,ALLOCATABLE :: mctal(:,:),estruc(:),mcrelerr(:,:),fvals(:,:),estruc2(:)
REAL*8,ALLOCATABLE :: otvol(:,:),ottemp(:,:),otenri(:),zgf(:,:),midpts(:)
REAL*8,ALLOCATABLE :: midpts2(:)
CHARACTER(LEN=1),ALLOCATABLE :: slat(:,:),unum(:),talmap(:,:)
CHARACTER(LEN=2),ALLOCATABLE :: mcsuff(:),otsuff(:,:),fnumber(:)
CHARACTER(LEN=2),ALLOCATABLE :: gtape(:)
CHARACTER(LEN=4),ALLOCATABLE :: matid(:)
CHARACTER(LEN=5),ALLOCATABLE :: iso_name(:),matname(:),ftype(:)
CHARACTER(LEN=6),ALLOCATABLE :: tape(:),temps(:),sigzger(:),suffs(:),mcmat(:)
CHARACTER(LEN=6),ALLOCATABLE :: huse(:),otmat(:,:)
CHARACTER(LEN=8),ALLOCATABLE :: rzname(:)
CHARACTER(LEN=25),ALLOCATABLE :: eds(:)
CHARACTER(LEN=30),ALLOCATABLE :: fname(:)
CHARACTER(LEN=70),ALLOCATABLE :: latlist(:)
CHARACTER(LEN=80),ALLOCATABLE :: command1(:),command2(:),command3(:)
CHARACTER(LEN=80),ALLOCATABLE :: command4(:,:)
CHARACTER(LEN=125),ALLOCATABLE :: command5(:,:),tline(:)

!Open global input file
OPEN(unit=25,file='input.txt',status='OLD',iostat=inperr)
IF (inperr==29) THEN
    WRITE(*,*) "FATAL ERROR: 'input.txt' not found"
    WRITE(*,*) "Program Exiting"
    GOTO 1001
ENDIF
!Open MATXSr input file
OPEN(unit=26,file='matxsrinput',status='REPLACE')
!Open MCNPX input file
OPEN(unit=35,file='mcin',status='REPLACE')
!Open files containing user-specified weight functions and group structures
OPEN(unit=36,file='wtfxn.txt',status='OLD',iostat=iwtterr)
IF (iwtterr==29) THEN
    WRITE(*,*) "WARNING: 'wtfxn.txt' not found"
    WRITE(*,*) "Program will only be able to use default NJOY weighting functions"
ENDIF
OPEN(unit=38,file='gstruc.txt',status='OLD',iostat=ingerr)
IF (ingerr==29) THEN
    WRITE(*,*) "WARNING: 'gstruc.txt' not found"
    WRITE(*,*) "Program will only be able to use default NJOY group structures"
ENDIF
OPEN(unit=34,file='scratch',status='REPLACE')
!Don't use a file number greater than 44 without modifying funit variable

pi=3.14159

!-----
!----Read the global input file for general options-----
!-----

WRITE(*,*) "-----"
WRITE(*,*) "Reading the global input file"
WRITE(*,*) "-----"

```

```

!Read the execute variable
!0=off,1=on,2=njoy only,3=mcnp only,4=transx only
READ(25,*) exec

!Read the problem title card
READ(25,112) title

!Read the basepath that determines the location of executables
READ(25,*) bpath
bplen=LEN(trim(bpath))
endf_path=bpath(1:bplen)//'\ENDFB6_ZAID'
njoy_exe=bpath(1:bplen)//'\NJOY99_112\NJOY.EXE'
merg_exe=bpath(1:bplen)//'\MERC_GENDF\Debug\MERG_GENDF.EXE'
mcnp_exe=bpath(1:bplen)//'\MCNPX\MCNPX.EXE'
transx_exe=bpath(1:bplen)//'\TRANSX\CODE\Debug\TRANSX.EXE'

!-----
!----Read the global input file for MCNP options-----
!-----

WRITE(*,*) "Reading the MCNP options"

READ(25,*)

!Read the MCNP options
READ(25,*) xsdir
READ(25,*) ltype
READ(25,*) nrows
READ(25,*) pitch
READ(25,*) clength
READ(25,*) tc
READ(25,*) dpin
READ(25,*) tv
READ(25,*) vlength
READ(25,*) exmat
!Read fuel section of the input file
ALLOCATE(mcmat(exmat),mcdens(exmat),mctemp(exmat),mcsuff(exmat))
DO i=1,exmat
  READ(25,*) mcmat(i),mcdens(i),mctemp(i)
ENDDO
READ(25,*) enri
READ(25,*) noct
maxmat=5      !Maximum number of materials/radii in a pincell
maxpos=20    !Maximum number of lattice positions for an alternate pincell
OPEN(unit=33,file='scratch3',status='REPLACE')
IF (noct.ne.0) THEN
  ALLOCATE(unum(noct),nrad(noct),ncelloc(noct),otenri(noct),unum2(noct))
  ALLOCATE(otrad(noct,maxmat),otmat(noct,maxmat),otdens(noct,maxmat))
  ALLOCATE(ottemp(noct,maxmat),otsuff(noct,maxmat))
  ALLOCATE(latx(noct,maxpos),laty(noct,maxpos),otvol(noct,maxmat))
  DO i=1,noct
    READ(25,*) unum(i)
    WRITE(33,126) unum(i)
    BACKSPACE(33)
    READ(33,*) unum2(i)
    READ(25,*) nrad(i)
    IF (nrad(i).ne.0) THEN
      DO j=1,nrad(i)
        READ(25,*) otrad(i,j)
      ENDDO
      DO j=1,nrad(i)
        READ(25,*) otmat(i,j),otdens(i,j),ottemp(i,j)
      ENDDO
    ENDF
    READ(25,*) ncelloc(i)

```

```

DO j=1,ncelloc(i)
  READ(25,*) latx(i,j),laty(i,j)
ENDDO
IF (unum(i).ne."1".and.unum(i).ne."3") THEN
  READ(25,*) otenri(i)
ENDIF
ENDDO
ENDIF
READ(25,*) nntreg          !Indicated number of different tally regions
READ(25,*) ppc             !Particles per kcode cycle
READ(25,*) ac              !Number of active cycles
READ(25,*) inac           !Number of inactive cycles
READ(25,*) rrdflag        !(this feature doesn't work)
READ(25,*) mcnpngs        !Neutron group structure for C(E)
READ(25,*) mcnpng         !Number of neutron groups
READ(25,*)
READ(25,*) talflag,mapwrite
IF (talflag.eq.1) THEN
  IF (ltype.eq.1) THEN
    rvin=(nrows*pitch*sqrt(2.)+2.0)/2      !Inner vessel radius
    rvout=rvin+tv                          !Outer vessel radius
    nlat=ceiling((rvin-pitch)/pitch)       !Number of lattice positions
  ELSEIF (ltype.eq.2) THEN
    rvin=REAL((nrows+1)/2)*pitch          !Inner vessel radius
    rvout=rvin+tv                          !Outer vessel radius
    nlat=(nrows+5)/2                       !Number of lattice positions
  ELSEIF (ltype.eq.3) THEN
    rvin=(nrows*pitch)/2.+1.
    nlat=(nrows+1)/2
  ELSEIF (ltype.eq.4) THEN
    rvin=(nrows+1)/2.*pitch/2*tan(pi/3)
    nlat=(nrows+1)/2
  ENDIF
  !Write a "blank" tally map file and exit so it can be inserted into the input file
  IF (mapwrite.eq.1) THEN
    OPEN(unit=39,file='scratch2',status='REPLACE')
    DO j=nlat,-nlat,-1
      blankmap='0'
      DO i=-nlat+1,nlat
        If (ltype.eq.1.or.ltype.eq.3) THEN
          IF (i.ge.(-(nrows-1)/2).and.i.le.((nrows-1)/2).and. &
            j.ge.(-(nrows-1)/2).and.j.le.((nrows-1)/2)) THEN
            WRITE(39,126) blankmap(1:len(trim(blankmap)))/" 1"
          ELSE
            WRITE(39,126) blankmap(1:len(trim(blankmap)))/" 0"
          ENDIF
        ELSEIF (ltype.eq.2.or.ltype.eq.4) THEN
          IF (i.ge.(-(nrows-1)/2).and.i.le.((nrows-1)/2).and. &
            j.ge.(-(nrows-1)/2).and.j.le.((nrows-1)/2)) THEN
            IF (j.ge.0.and.(i+j).gt.((nrows-1)/2)) THEN
              WRITE(39,126) blankmap(1:len(trim(blankmap)))/" 1"
            ELSEIF (j.le.0.and.(i-j).gt.((nrows-1)/2)) THEN
              WRITE(39,126) blankmap(1:len(trim(blankmap)))/" 0"
            ELSE
              WRITE(39,126) blankmap(1:len(trim(blankmap)))/" 1"
            ENDIF
          ELSE
            WRITE(39,126) blankmap(1:len(trim(blankmap)))/" 0"
          ENDIF
        ENDIF
      ENDIF
    ENDIF
    BACKSPACE(39)
    READ(39,113) blankmap
    BACKSPACE(39)
  ENDDO
  READ(39,*)
ENDDO

```

```

        CLOSE(unit=39)
        WRITE(*,*) "Exiting to write a blank tally map, look in scratch2 file"
        GOTO 1001
    ENDF
    ALLOCATE(tline(-nlat:nlat))
    DO j=-nlat,-nlat,-1
        READ(25,113) tline(j)
    ENDDO
    ALLOCATE(talmap(-nlat:nlat,-nlat:nlat),talmap2(-nlat:nlat,-nlat:nlat))
    DO j=-nlat,nlat,1
        !y direction
        junk3=1
        DO i=-nlat,nlat !x direction
            talmap(i,j)=tline(j)(junk3:junk3)
            WRITE(34,126) talmap(i,j)
            BACKSPACE(34)
            READ(34,*) talmap2(i,j)
            junk3=junk3+2
        ENDDO
    ENDDO
ELSEIF (talflag.eq.0) THEN
    !Add in the calcs here to select pin regions automatically
    !This option is not functional at this juncture
    IF (ltype.eq.1) THEN
        rvin=(nrows*pitch*sqrt(2.)+2.0)/2
        rvout=rvin+tv
        nlat=ceiling((rvin-pitch/2)/pitch)
        !Inner vessel radius
        !Outer vessel radius
        !Number of lattice positions
    ELSEIF (ltype.eq.2) THEN
        rvin=REAL((nrows+1)/2)*pitch
        rvout=rvin+tv
        nlat=(nrows+1)/2
        !Inner vessel radius
        !Outer vessel radius
        !Number of lattice positions
    ENDIF
ENDIF

!-----
!----Read the global input file for NJOY options-----
!-----

WRITE(*,*) "Reading NJOY options"

READ(25,*)
READ(25,*) niso
ALLOCATE(iso_name(niso),matid(niso),za(niso),xstype(niso),tape(niso),ireg(niso))
ALLOCATE(command1(niso),command2(niso),command3(niso))
DO i=1,niso
    READ(25,*) iso_name(i),matid(i),za(i),xstype(i),tape(i),ireg(i)
ENDDO

READ(25,*) ntemp
ALLOCATE(temps(ntemp),suffs(ntemp),gtape(ntemp))
DO i=1,ntemp
    READ(25,*) temps(i),suffs(i),gtape(i)
ENDDO

ALLOCATE(command4(niso,ntemp),command5(niso,ntemp))

tlist=""
DO i=1,ntemp
    tlen=len(trim(tlist))
    tlist=tlist(1:tlen)//" "//temps(i)
ENDDO

READ(25,*) ngs
READ(25,*) nng
READ(25,*) pgs
READ(25,*) npg
READ(25,*) wtfxn

```

```

READ(25,*) nleg
READ(25,*) nsig
ALLOCATE(sigzer(nsig))
DO i=1,nsig
  READ(25,*) sigzer(i)
ENDDO

siglist=""
DO i=1,nsig
  slen=len(trim(siglist))
  siglist=siglist(1:slen)//' '//sigzer(i)
ENDDO

!Turn THERMR off or on
READ(25,*) thermopt

!Read MATXS particle options
READ(25,*) npart
READ(25,*) ntype

!Check for consistency of group structure
IF (ngs.eq.3.and.nng.ne.30) THEN
  WRITE(*,*) "FATAL ERROR: Number of neutron groups is inconsistent"// &
    "with neutron group structure"
  WRITE(*,*) "Program Exiting"
  GOTO 1001
ELSEIF (ngs.eq.9.and.nng.ne.69) THEN
  WRITE(*,*) "FATAL ERROR: Number of neutron groups is inconsistent"// &
    "with neutron group structure"
  WRITE(*,*) "Program Exiting"
  GOTO 1001
ELSEIF (ngs.eq.10.and.nng.ne.187) THEN
  WRITE(*,*) "FATAL ERROR: Number of neutron groups is inconsistent"// &
    "with neutron group structure"
  WRITE(*,*) "Program Exiting"
  GOTO 1001
ELSEIF (ngs.eq.13.and.nng.ne.80) THEN
  WRITE(*,*) "FATAL ERROR: Number of neutron groups is inconsistent"// &
    "with neutron group structure"
  WRITE(*,*) "Program Exiting"
  GOTO 1001
ELSEIF (ngs.eq.2.and.nng.ne.240) THEN
  WRITE(*,*) "FATAL ERROR: Number of neutron groups is inconsistent"// &
    "with neutron group structure"
  WRITE(*,*) "Program Exiting"
  GOTO 1001
ELSEIF (ngs.eq.11.and.nng.ne.70) THEN
  WRITE(*,*) "FATAL ERROR: Number of neutron groups is inconsistent"// &
    "with neutron group structure"
  WRITE(*,*) "Program Exiting"
  GOTO 1001
ENDIF

!-----
!---Read the global input file for TRANSX options-----
!-----

WRITE(*,*) "Reading TRANSX options"

READ(25,*)
READ(25,*) iout
READ(25,*) iprob
READ(25,*) iset
READ(25,*) iform
READ(25,*) itrc
READ(25,*) icoll

```

```

READ(25,*) initf
READ(25,*) ngroup
READ(25,*) nl
READ(25,*) nup
READ(25,*) nthg
READ(25,*) nmix
READ(25,*) ned
READ(25,*) neds
ALLOCATE(eds(neds))
READ(25,*) ihet
READ(25,301) hed
DO i=1,neds
    READ(25,301) eds(i)
ENDDO
IF (initf.eq.4) THEN
    READ(25,*)
    READ(25,*) power
    READ(25,*) nu
ENDIF

301 FORMAT(a25)

!-----
!----Calculations for MCNP Input-----
!-----

!Assign suffixes to temps
DO i=1,exmat
    call Suffr(mctemp(i),mcsuff(i))
ENDDO

IF (noct.ne.0) THEN
    DO i=1,noct
        DO j=1,nrad(i)
            call Suffr(ottemp(i,j),otsuff(i,j))
        ENDDO
    ENDDO
ENDIF

rpin=dpin/2.
rfuel=rpin-tc
flength=length-2*tc
!Calculate lattice/pin/assembly dimensions
!Square Lattice=Type 1, Hex(Triangular) Lattice=Type 2
If (ltype.eq.1.or.ltype.eq.3) THEN
    cellvol=(vlength-2*tv)*pitch**2
    pinvol=pi*rpin**2*length
    fuelvol=length*rfuel**2*pi
    cladvol=pinvol-fuelvol
    modvol=cellvol-pinvol
    !Calculate area "volumes" for TRANSX
    fvol=pi*rfuel**2
    mvol=pitch**2-rpin**2*pi
    cvol=pi*rpin**2-pi*rfuel**2
    ALLOCATE(slat(-nlat:nlat,-nlat:nlat),latlist(-nlat:nlat))
    !Note that this setup only works for odd numbered matrices (3x3,5x5 etc.)
    DO i=-nlat,nlat
        DO j=-nlat,nlat
            slat(i,j)="1"
        ENDDO
    ENDDO
    DO i=-(nrows-1)/2,(nrows-1)/2
        DO j=-(nrows-1)/2,(nrows-1)/2
            slat(i,j)="2"
        ENDDO
    ENDDO

```



```

IF (noct.ne.0) THEN
  DO i=1,noct
    DO j=1,ncelloc(i)
      slat(latx(i,j),laty(i,j))=unum(i)
    ENDDO
  ENDDO
ENDIF
latlist=""
DO j=-nlat,nlat
  DO i=-nlat,nlat
    latlen=len(trim(latlist(j)))
    latlist(j)=latlist(j)(1:latlen) //' '//slat(i,j)
  ENDDO
ENDDO
IF (noct.ne.0) THEN
  DO i=1,noct
    IF (nrad(i).ne.0) THEN
      DO j=1,nrad(i)+1
        IF (j.eq.1) THEN
          otvol(i,j)=cellvol-otrad(i,j)**2*pi*clength
        ELSEIF (j.eq.2) THEN
          otvol(i,j)=otrad(i,j-1)**2*pi*clength-otrad(i,j)**2*pi*flength
        ELSEIF (j.ne.nrad(i)+1) THEN
          otvol(i,j)=otrad(i,j-1)**2*pi*flength-otrad(i,j)**2*pi*flength
        ELSE
          otvol(i,j)=otrad(i,j-1)**2*pi*flength
        ENDIF
      ENDDO
    ENDIF
  ENDDO
ENDIF
ELSEIF (ltype.eq.2.or.ltype.eq.4) THEN
  hexside=pitch*tan(pi/6.)
  cellvol=(3*sqrt(3.))/2*hexside**2*(vlength-2*tv)
  pinvol=pi*rpin**2*clength
  fuelvol=flength*rfuel**2*pi
  cladvol=pinvol-fuelvol
  modvol=cellvol-pinvol
  !Calculate area "volumes" for TRANSX
  fvol=pi*rfuel**2 !Fuel volume
  mvol=(3*sqrt(3.))/2*hexside**2-pi*rpin**2 !Moderator volume
  cvol=pi*rpin**2-pi*rfuel**2 !Clad volume
  ALLOCATE(slat(-nlat:nlat,-nlat:nlat),latlist(-nlat:nlat))
  DO i=-nlat,nlat
    DO j=-nlat,nlat
      slat(i,j)="1"
    ENDDO
  ENDDO
  DO i=-(nrows-1)/2,(nrows-1)/2
    DO j=-(nrows-1)/2,(nrows-1)/2
      IF (j.ge.0.and.(i+j).gt.(nrows-1)/2) THEN
        slat(i,j)="1"
      ELSEIF (j.le.0.and.(-i+j).gt.(nrows-1)/2) THEN
        slat(i,j)="1"
      ELSE
        slat(i,j)="2"
      ENDIF
    ENDDO
  ENDDO
  IF (noct.ne.0) THEN
    DO i=1,noct
      DO j=1,ncelloc(i)
        slat(latx(i,j),laty(i,j))=unum(i)
      ENDDO
    ENDDO
  ENDIF

```

```

latlist=""
DO j=-nlat,nlat
    DO i=-nlat,nlat
        latlen=len(trim(latlist(j)))
        latlist(j)=latlist(j)(1:latlen)//' '//slat(i,j)
    ENDDO
ENDDO
IF (noct.ne.0) THEN
    DO i=1,noct
        IF (nrad(i).ne.0) THEN
            DO j=1,nrad(i)+1
                IF (j.eq.1) THEN
                    otvol(i,j)=cellvol-otrad(i,j)**2*pi*clength
                ELSEIF (j.eq.2) THEN
                    otvol(i,j)=otrad(i,j-1)**2*pi*clength-otrad(i,j)**2*pi*flength
                ELSEIF (j.ne.nrad(i)+1) THEN
                    otvol(i,j)=otrad(i,j-1)**2*pi*flength-otrad(i,j)**2*pi*flength
                ELSE
                    otvol(i,j)=otrad(i,j-1)**2*pi*flength
                ENDIF
            ENDDO
        ENDIF
    ENDDO
ENDIF
ENDIF
IF (ltype.eq.3) THEN
    cellvol=(flength+.2)*pitch**2
    pinvol=pi*rpin**2*flength
    fuelvol=pi*rfuel**2*flength
    cladvol=pinvol-fuelvol
    modvol=cellvol-pinvol
ELSEIF (ltype.eq.4) THEN
    cellvol=(flength+.2)*(3*sqrt(3.))/2*hexside**2
    pinvol=pi*rpin**2*flength
    fuelvol=pi*rfuel**2*flength
    cladvol=pinvol-fuelvol
    modvol=cellvol-pinvol
ENDIF

!-----
!-----Write MCNPX Input-----
!-----

!Write the cell cards
WRITE(35,126) title
WRITE(35,126) "c"
WRITE(35,126) "c Cell Cards"
IF (ltype.eq.1.or.ltype.eq.2) THEN
    WRITE(35,127) "1 101",mcdens(1)," -301 -302 303 (304:305:-306) imp:n=1"
    WRITE(35,128) "2 102",mcdens(2)," -304 -305 306 fill=1 imp:n=1"
ELSEIF (ltype.eq.3) THEN
    WRITE(35,155) "1 102",mcdens(2)," -301 302 -303 304 -305 306 fill=1 imp:n=1"
ELSEIF (ltype.eq.4) THEN
    WRITE(35,159) "1 102",mcdens(2)," -301 302 -303 304 -305 306 -307 308 &
        fill=1 imp:n=1"
ENDIF
IF (ltype.eq.1.or.ltype.eq.3) THEN
    WRITE(35,127) "3 102",mcdens(2)," -401 402 -403 404 lat=1 u=1 imp:n=1 "
ELSEIF(ltype.eq.2.or.ltype.eq.4) THEN
    WRITE(35,155) "3 102",mcdens(2)," -401 402 -403 404 -405 406 lat=2 u=1 imp:n=1 "
ENDIF
WRITE(35,130) " fill=-,nlat,":",nlat," ",-nlat,":",nlat," 0:0"
DO i=-nlat,nlat
    WRITE(35,131) " ",latlist(i)
ENDDO

```

```

!Fuel Clad
WRITE(35,132) "4 103",mcdens(3)," -501 -503 504 (502:505:-506) imp:n=1 u=2"
!Fuel Meat
WRITE(35,133) "5 104",mcdens(4)," -502 -505 506 imp:n=1 u=2"
!Coolant Flow around fuel
WRITE(35,134) "6 102",mcdens(2)," #4 #5 imp:n=1 u=2"

!Write cell cards for other pincell types
IF (noct.ne.0) THEN
  ctr2=exmat+1
  DO i=1,noct
    IF (unum(i).ne."1".and.unum(i).ne."2") THEN
      DO j=1,nrad(i)
        IF (ctr2.lt.10.and.j.eq.1) THEN
          WRITE(35,143) unum(i),j,"10",ctr2,otdens(i,j)," -5"//unum(i),j,&
            " -5"//unum(i),nrad(i)+1," 5"//unum(i),nrad(i)+2,&
            " (5"//unum(i),j+1,"-5"//unum(i),nrad(i)+3,"-5"&
            //unum(i),nrad(i)+4,") imp:n=1 u=",unum(i)
        ELSEIF (ctr2.lt.10.and.j.ne.nrad(i).and.j.ne.1) THEN
          WRITE(35,144) unum(i),j,"10",ctr2,otdens(i,j)," -5"//unum(i),j,&
            " 5"//unum(i),j+1," -5"//unum(i),nrad(i)+3," 5"&
            //unum(i),nrad(i)+4," imp:n=1 u=",unum(i)
        ELSEIF (ctr2.lt.10.and.j.eq.nrad(i)) THEN
          WRITE(35,145) unum(i),j,"10",ctr2,otdens(i,j)," -5"//unum(i),j,&
            " -5"//unum(i),nrad(i)+3," 5"//unum(i),nrad(i)+4,&
            " imp:n=1 u=",unum(i)
        ELSEIF (ctr2.ge.10.and.j.eq.1) THEN
          WRITE(35,146) unum(i),j,"1",ctr2,otdens(i,j)," -5"//unum(i),j,&
            " 5"//unum(i),j+1," -5"//unum(i),nrad(i)+1," 5"&
            //unum(i),nrad(i)+2," 5"//unum(i),nrad(i)+3," -5"&
            //unum(i),nrad(i)+4," imp:n=1 u=",unum(i)
        ELSEIF (ctr2.lt.10.and.j.ne.nrad(i).and.j.ne.1) THEN
          WRITE(35,147) unum(i),j,"1",ctr2,otdens(i,j)," -5"//unum(i),j,&
            " 5"//unum(i),j+1," -5"//unum(i),nrad(i)+3," 5"&
            //unum(i),nrad(i)+4," imp:n=1 u=",unum(i)
        ELSEIF (ctr2.ge.10.and.j.eq.nrad(i)) THEN
          WRITE(35,148) unum(i),j,"1",ctr2,otdens(i,j)," -5"//unum(i),j,&
            " -5"//unum(i),nrad(i)+3," 5"//unum(i),nrad(i)+4,&
            " imp:n=1 u=",unum(i)
        ENDIF
        ctr2=ctr2+1
      ENDDO
      WRITE(34,149) unum(i),0," 102",mcdens(2)
      DO j=1,nrad(i)
        BACKSPACE (34)
        READ(34,113) junk2
        nlen=len(trim(junk2))
        WRITE(34,150) junk2(1:nlen)//" #"/unum(i),j
      ENDDO
      BACKSPACE(34)
      READ(34,113) junk2
      nlen=len(trim(junk2))
      WRITE(35,126) junk2(1:nlen)//" imp:n=1 u="//unum(i)
    ENDIF
  ENDDO
ENDIF
ENDIF
IF (ltype.eq.1.or.ltype.eq.2) THEN
  WRITE(35,126) "100 0 #1 #2 imp:n=0"
ELSEIF (ltype.eq.3.or.ltype.eq.4) THEN
  WRITE(35,126) "100 0 #1 imp:n=0"
ENDIF
!Write the surface cards
WRITE(35,126) ""
WRITE(35,126) "c"
WRITE(35,126) "c Surface Cards"
IF (ltype.eq.1.or.ltype.eq.2) THEN

```

```

1300-310 for vessel definition
WRITE(35,126) "c Reactor Vessel"
WRITE(35,129) "301 cz",rvout
WRITE(35,129) "302 pz",vlength/2.
WRITE(35,129) "303 pz",-vlength/2.
WRITE(35,129) "304 cz",rvin
WRITE(35,129) "305 pz",vlength/2.-tv
WRITE(35,129) "306 pz",-vlength/2.+tv
ELSEIF (ltype.eq.3) THEN
WRITE(35,126) "c reflecting reactor boundary"
WRITE(35,129) "*301 pz",flength/2.+1
WRITE(35,129) "*302 pz",-flength/2.-1
WRITE(35,129) "*303 px",rvin
WRITE(35,129) "*304 px",-rvin
WRITE(35,129) "*305 py",rvin
WRITE(35,129) "*306 py",-rvin
ELSEIF (ltype.eq.4) THEN
WRITE(35,126) "c reflecting reactor boundary"
WRITE(35,129) "*301 pz",flength/2.+1
WRITE(35,129) "*302 pz",-flength/2.-1
WRITE(35,129) "*303 py",rvin
WRITE(35,129) "*304 py",-rvin
WRITE(35,156) "*305 p 1.7320508076 1 0",2*rvin
WRITE(35,156) "*306 p 1.7320508076 1 0",-2*rvin
WRITE(35,156) "*307 p 1.7320508076 -1 0",2*rvin
WRITE(35,156) "*308 p 1.7320508076 -1 0",-2*rvin
ENDIF
IF (ltype.eq.1.or.ltype.eq.3) THEN
!400-410 for cell definitions
WRITE(35,126) "c Pin Cell"
WRITE(35,129) "401 px",pitch/2.
WRITE(35,129) "402 px",-pitch/2.
WRITE(35,129) "403 py",pitch/2.
WRITE(35,129) "404 py",-pitch/2.
ELSEIF (ltype.eq.2.or.ltype.eq.4) THEN
!400-410 for cell definitions
WRITE(35,126) "c Pin Cell"
WRITE(35,129) "401 px",pitch/2.
WRITE(35,129) "402 px",-pitch/2.
WRITE(35,156) "403 p 1 1.7320508076 0",pitch
WRITE(35,156) "404 p 1 1.7320508076 0",-pitch
WRITE(35,156) "405 p -1 1.7320508076 0",pitch
WRITE(35,156) "406 p -1 1.7320508076 0",-pitch
ENDIF
!500-510 for pin definitions
IF (ltype.eq.1.or.ltype.eq.2) THEN
WRITE(35,126) "c Pin"
WRITE(35,129) "501 cz",rpin
WRITE(35,129) "502 cz",rfuel
WRITE(35,129) "503 pz",clength/2.
WRITE(35,129) "504 pz",-clength/2.
WRITE(35,129) "505 pz",flength/2.
WRITE(35,129) "506 pz",-flength/2.
ELSEIF (ltype.eq.3.or.ltype.eq.4) THEN
WRITE(35,126) "c Pin"
WRITE(35,129) "501 cz",rpin
WRITE(35,129) "502 cz",rfuel
WRITE(35,129) "503 pz",flength/2.
WRITE(35,129) "504 pz",-flength/2.
WRITE(35,129) "505 pz",flength/2.
WRITE(35,129) "506 pz",-flength/2.
ENDIF
!Write surface cards for other universe types
IF (noct.ne.0) THEN
DO i=1,noct
IF (unum(i).eq."3") THEN

```

```

!Control Rod cells
!530-539 for control rod definitions
WRITE(35,126) "c Control Rod/Safety Rod Universe 3"

ELSEIF (unum(i).eq."1") THEN
!Coolant channel cells
!Shouldn't need to add anything here
ELSEIF (unum(i).ge."4") THEN
!Other fuel cells
!540-599 for u=4-9
WRITE(35,126) "c Fuel Rods Universe "//unum(i)
ENDIF
IF (unum(i).ne."1".and.unum(i).ne."2") THEN
DO j=1,nrad(i)
WRITE(35,142) "5//unum(i),j," cz",otrad(i,j)
ENDDO
WRITE(35,142) "5//unum(i),nrad(i)+1," pz",clength/2.
WRITE(35,142) "5//unum(i),nrad(i)+2," pz",-clength/2.
WRITE(35,142) "5//unum(i),nrad(i)+3," pz",flength/2.
WRITE(35,142) "5//unum(i),nrad(i)+4," pz",-flength/2.
ENDIF
ENDDO
ENDIF
WRITE(35,126) ""
!Write material cards
WRITE(35,126) "c Material Cards"
DO i=1,exmat
Call Matter(i,mcmat(i),mcdens(i),mcsuff(i),enri,materr)
GOTO (1001,1004) materr
1004 Continue
ENDDO
ctr=exmat+1
DO i=1,noct
DO j=1,nrad(i)
Call Matter(ctr,otmat(i,j),otdens(i,j),otsuff(i,j),enri,materr)
ctr=ctr+1
GOTO (1001,1005) materr
1005 Continue
ENDDO
ENDDO
!Write data cards
WRITE(35,126) "c Data Cards"
WRITE(35,126) "mode:n"
WRITE(35,141) "kcode ",ppc," 1.0 ",inac,ac+inac
nps=REAL(ppc*ac)
WRITE(35,126) "ksrc 0 0 0"
!Write tally cards
!Tally energy-dependent scalar flux
ALLOCATE(tregtype(ntreg))
DO k=1,ntreg
sunit=k+70
OPEN(unit=sunit,file=sunit,status='REPLACE')
WRITE(sunit,140) "f",k,"4:n"
ctr5=1
ctr4=1 !First write counter
1101 CONTINUE
ctr3=0 !Position counter
DO j=-nlat,nlat
DO i=-nlat,nlat
ctr3=ctr3+1
IF (talmap2(i,j).eq.k) THEN
IF (slat(i,j).eq."2") THEN !Fuel type tallies
tregtype(k)=2
IF (ctr4.eq.1.and.ctr5.eq.1) THEN
BACKSPACE(sunit)
READ(sunit,113) junk2

```

```

        jlen=len(trim(junk2))
        BACKSPACE(sunit)
        WRITE(sunit,126) junk2(1:jlen)/" (5<("
        ctr4=ctr4+1
        finflag=1
    ELSEIF (ctr4.eq.2.and.ctr5.eq.2) THEN
        WRITE(sunit,126) " (4<("
        finflag=1
        ctr4=ctr4+1
    ELSEIF (ctr4.eq.3.and.ctr5.eq.3) THEN
        WRITE(sunit,126) " (6<("
        finflag=2
        ctr4=ctr4+1
    ENDIF
    WRITE(sunit,151) " 3[" ,ctr3,"]"
ELSEIF (slat(i,j).eq."1") THEN !Coolant Channel tallies
    tregtype(k)=1
    IF (ctr4.eq.1.and.ctr5.eq.1) THEN
        BACKSPACE(sunit)
        READ(sunit,113) junk2
        jlen=len(trim(junk2))
        BACKSPACE(sunit)
        WRITE(sunit,126) junk2(1:jlen)/" (3<("
        ctr4=ctr4+1
        finflag=2
    ENDIF
    WRITE(sunit,151) " 3[" ,ctr3,"]"
ENDIF
IF (slat(i,j).ne."1".and.slat(i,j).ne."2") THEN !Other cell types
    DO m=1,noct
        IF (unum(m).eq.slat(i,j)) THEN
            octindex=m
        ENDIF
    ENDDO
    tregtype(k)=unum2(octindex)
    DO m=1,nrad(octindex)+1
        IF (ctr4.eq.m.and.ctr5.eq.m) THEN
            BACKSPACE(sunit)
            READ(sunit,113) junk2
            jlen=len(trim(junk2))
            BACKSPACE(sunit)
            WRITE(sunit,154) junk2(1:jlen)/"
            ("//unum(octindex),&
            (nrad(octindex))+1-m,"<("
            ctr4=ctr4+1
            IF (m.eq.(nrad(octindex)+1)) THEN
                finflag=2
            ELSE
                finflag=1
            ENDIF
        ENDIF
    ENDDO
    WRITE(sunit,151) " 3[" ,ctr3,"]"
    ENDIF
ENDIF
!Finish off a tally bin
IF (i.eq.nlat.and.j.eq.nlat) THEN
    BACKSPACE(sunit)
    READ(sunit,113) junk2
    jlen=len(trim(junk2))
    BACKSPACE(sunit)
    WRITE(sunit,126) junk2(1:jlen)/"
ENDIF
ENDDO
ENDDO

```

```

ctr5=ctr5+1
GOTO (1101,1102) finflag
1102 CONTINUE
!Write the f cards to mcin
WRITE(35,(a,i3)) "c Tallies for universe number",tregtype(k)
REWIND(sunit)
DO m=1,50000
    READ(sunit,113,END=1103) junk2
    WRITE(35,113) junk2
ENDDO
1103 CONTINUE
!Write the volume cards.
!Note that the volume is for one cell, not the aggregate, since only
!relative magnitude matters
If (tregtype(k).eq.2) THEN
    WRITE(35,157) "sd",k,"4 ",fuelvol,cladvol,modvol
ELSEIF (tregtype(k).eq.1) THEN
    WRITE(35,157) "sd",k,"4 ",cellvol
ELSEIF (tregtype(k).gt.2) THEN
    WRITE(35,158) "sd",k,"4 ",(otvol(octindex,j),j=nrad(octindex)+1,1,-1)
ENDIF
!Write the energy distribution card
Call Energizer(k,ngs)
ENDDO
!General whole core tally
WRITE (35,153) "f104:n (3<(3[",-(nrows-1)/2,";",(nrows-1)/2,-(nrows-1)/2,";"&
(nrows-1)/2,"0:0])"
WRITE (35,126) "sd104 1"
Call Energizer(10,mcnpngs)
!Write the MCTAL file
WRITE(35,126) "prtmp 0 0 1"
!Consider adding a CUT card for the "simple" problems
IF (ltype.eq.3.or.ltype.eq.4) THEN
    WRITE (35,126) "CUT:n 500"
ENDIF

!MCNP Format Statements
!Reserve 126-200 for these format statements
126 FORMAT(a)
127 FORMAT(a7,f7.2,a37)
128 FORMAT(a7,f7.2,a29)
129 FORMAT(a7,X,f8.4)
130 FORMAT(a16,i3,a1,i2,a1,i3,a1,i2,a4)
131 FORMAT(a7,a)
132 FORMAT(a7,f7.2,a41)
133 FORMAT(a7,f7.2,a26)
134 FORMAT(a7,f7.2,a18)
135 FORMAT(a9,f4.1,a14,f4.1,a31)
136 FORMAT(a12,a2,a18,a2,a17,a2,a11)
137 FORMAT(a1,i3,a8,a2,a18,a2,a17,a2,a11)
138 FORMAT(a9,f4.1,a14,f4.1,a11,f4.1,a1)
139 FORMAT(a1,i3,a8,a2,a3,f6.4,a8,a2,a3,f6.4,a8,a2,a9)
140 FORMAT(a1,i1,a)
141 FORMAT(a7,i4,a5,i3,X,i5)
142 FORMAT(a2,i1,a4,X,f8.4)
143 FORMAT(a1,i1,2X,a2,i1,f7.2,a4,i1,a4,i1,a3,i1,a4,i1,a3,i1,a4,i1,a2,a1)
144 FORMAT(a1,i1,2X,a2,i1,f7.2,a4,i1,a3,i1,a4,i1,a3,i1,a11,a1)
145 FORMAT(a1,i1,2X,a2,i1,f7.2,a4,i1,a4,i1,a3,i1,a11,a1)
146 FORMAT(a1,i1,2X,a1,i2,f7.2,a4,i1,a3,i1,a4,i1,a3,i1,a3,i1,a4,i1,a11,a1)
147 FORMAT(a1,i1,2X,a1,i2,f7.2,a4,i1,a3,i1,a4,i1,a3,i1,a11,a1)
148 FORMAT(a1,i1,2X,a1,i2,f7.2,a4,i1,a4,i1,a3,i1,a11,a1)
149 FORMAT(a1,i1,a5,f7.2)
150 FORMAT(a,i1)
151 FORMAT(a,i4,a1)
152 FORMAT(a2,i1,a6,i2,a1)
153 FORMAT(a13,i3,a1,i3,X,i3,a1,i3,X,a6)

```



```

!Read the energy structure
IF (i.eq.1) THEN
  ALLOCATE(estruc(nng),estruc2(mcpnng))
ENDIF
IF (i.ne.ntal) THEN
DO j=1,nng-mod(nng,6),6
  READ(37,*) estruc(j),estruc(j+1),estruc(j+2),estruc(j+3),estruc(j+4),estruc(j+5)
ENDDO
IF (mod(nng,6).eq.0) THEN
ELSEIF (mod(nng,6).eq.1) THEN
  READ(37,*) estruc(nng)
ELSEIF (mod(nng,6).eq.2) THEN
  READ(37,*) estruc(nng-1),estruc(nng)
ELSEIF (mod(nng,6).eq.3) THEN
  READ(37,*) estruc(nng-2),estruc(nng-1),estruc(nng)
ELSEIF (mod(nng,6).eq.4) THEN
  READ(37,*) estruc(nng-3),estruc(nng-2),estruc(nng-1),estruc(nng)
ELSEIF (mod(nng,6).eq.5) THEN
  READ(37,*) estruc(nng-4),estruc(nng-3),estruc(nng-2),estruc(nng-1),estruc(nng)
ENDIF
READ(37,*)
READ(37,*)

!Read tallied data for RZFLUX
ndex=nbins(i)*(nng+1)
DO j=1,ndex-mod(ndex,4),4
  READ(37,*) mctal(i,j),mcrelerr(i,j),mctal(i,j+1),mcrelerr(i,j+1),mctal(i,j+2),&
  mcrelerr(i,j+2),mctal(i,j+3),mcrelerr(i,j+3)
ENDDO
IF (mod(ndex,4).eq.0) THEN
ELSEIF (mod(ndex,4).eq.1) THEN
  READ(37,*) mctal(i,ndex),mcrelerr(i,ndex)
ELSEIF (mod(ndex,4).eq.2) THEN
  READ(37,*) mctal(i,ndex-1),mcrelerr(i,ndex-1),mctal(i,ndex),mcrelerr(i,ndex)
ELSEIF (mod(ndex,4).eq.3) THEN
  READ(37,*) mctal(i,ndex-2),mcrelerr(i,ndex-2),mctal(i,ndex-1),&
  mcrelerr(i,ndex-1),mctal(i,ndex),mcrelerr(i,ndex)
ENDIF

!Read TFC data
READ(37,402) tfc
DO j=1,tfc
  READ(37,*)
ENDDO

ELSE
DO j=1,mcpnng-mod(mcpnng,6),6
  READ(37,*) estruc2(j),estruc2(j+1),estruc2(j+2),estruc2(j+3),estruc2(j+4),estruc2(j+5)
ENDDO
IF (mod(mcpnng,6).eq.0) THEN
ELSEIF (mod(mcpnng,6).eq.1) THEN
  READ(37,*) estruc2(mcpnng)
ELSEIF (mod(mcpnng,6).eq.2) THEN
  READ(37,*) estruc2(mcpnng-1),estruc2(mcpnng)
ELSEIF (mod(mcpnng,6).eq.3) THEN
  READ(37,*) estruc2(mcpnng-2),estruc2(mcpnng-1),estruc2(mcpnng)
ELSEIF (mod(nng,6).eq.4) THEN
  READ(37,*) estruc2(mcpnng-3),estruc2(mcpnng-2),estruc2(mcpnng-1),estruc2(mcpnng)
ELSEIF (mod(mcpnng,6).eq.5) THEN
  READ(37,*) estruc2(mcpnng-4),estruc2(mcpnng-3),estruc2(mcpnng-2),estruc2(mcpnng-
1),estruc2(mcpnng)
ENDIF
READ(37,*)
READ(37,*)

```

```

!Read tallied data
ndex=nbins(i)*(mcnpnng+1)
DO j=1,ndex-mod(ndex,4),4
    READ(37,*) mctal(i,j),mcrelerr(i,j),mctal(i,j+1),mcrelerr(i,j+1),mctal(i,j+2),&
        mcrelerr(i,j+2),mctal(i,j+3),mcrelerr(i,j+3)
ENDDO
IF (mod(ndex,4).eq.0) THEN
ELSEIF (mod(ndex,4).eq.1) THEN
    READ(37,*) mctal(i,ndex),mcrelerr(i,ndex)
ELSEIF (mod(ndex,4).eq.2) THEN
    READ(37,*) mctal(i,ndex-1),mcrelerr(i,ndex-1),mctal(i,ndex),mcrelerr(i,ndex)
ELSEIF (mod(ndex,4).eq.3) THEN
    READ(37,*) mctal(i,ndex-2),mcrelerr(i,ndex-2),mctal(i,ndex-1),&
        mcrelerr(i,ndex-1),mctal(i,ndex),mcrelerr(i,ndex)
ENDIF

!Read TFC data
READ(37,402) tfc
DO j=1,tfc
    READ(37,*)
ENDDO
ENDIF
ENDDO

!Calculate and write out MCNP tallies
IF(wtfxn.eq.1.and.iwtterr.eq.29) THEN
    GOTO 1302
ELSEIF(wtfxn.eq.1.and.iwtterr.ne.29) THEN
    !WRITE(*,*) "wtfxn.txt exists and IWT=1. Overwrite with MCNP results? 1=Yes,2=No"
    !READ(*,*) go
    go=1
    IF (go.eq.2) THEN
        WRITE(*,*) "WARNING: NJOY section will not work with IWT=1 and no wtfxn.txt"
    ENDIF
    GOTO (1302,1301) go
ENDIF
1302 Continue

WRITE(*,*) "-----"
WRITE(*,*) "Writing wtfxn.txt for use in NJOY"
WRITE(*,*) "-----"

!Adjust tally values
DO j=1,ntal-1

    !Find minimum value in the array
    minmctal=1E6
    DO i=1,nbins(j)*(nng+1)
        IF (mctal(j,i).ne.0) THEN
            IF (mctal(j,i).lt.minmctal) THEN
                minmctal=mctal(j,i)
            ENDIF
        ENDIF
    ENDDO

    !Correct zeros in the tally bins with very small numbers
    DO i=1,nbins(j)*(nng+1)
        IF (mctal(j,i).eq.0) THEN
            mctal(j,i)=1E-4*minmctal
        ENDIF
    ENDDO
ENDDO

!Find minimum value in the array
minmctal=1E6

```

```

DO i=1,nbins(ntl)*(mcnpnng+1)
  IF (mctal(ntl,i).ne.0) THEN
    IF (mctal(ntl,i).lt.minmctal) THEN
      minmctal=mctal(ntl,i)
    ENDIF
  ENDIF
ENDDO

!Correct zeros in the tally bins with very small numbers
DO i=1,nbins(ntl)*(mcnpnng+1)
  IF (mctal(ntl,i).eq.0) THEN
    mctal(ntl,i)=1E-4*minmctal
  ENDIF
ENDDO

!Calculate the midpts in eV
ALLOCATE(midpts(nng),midpts2(mcnpnng))
WRITE(*,*) "Calculating midpoints of the energy structure"
DO i=1,nng
  IF (i.ne.1) THEN
    midpts(i)=(estruc(i)+estruc(i-1))/2*1E6
  ELSE
    midpts(i)=(estruc(i)-0)/2*1E6
  ENDIF
ENDDO

DO i=1,mcnpnng
  IF (i.ne.1) THEN
    midpts2(i)=(estruc2(i)+estruc2(i-1))/2*1E6
  ELSE
    midpts2(i)=(estruc2(i)-0)/2*1E6
  ENDIF
ENDDO

!Calculate the point flux values (n/cm^2)
!It'd be smart to add a smoothing function here.
WRITE(*,*) "Calculating the point flux values for each tally"
ctr6=1
DO i=1,ntl
  IF (i.ne.ntl) THEN
    DO j=1,nbins(i)*(nng+1)
      IF (ctr6.eq.nng+1) THEN
        ctr6=1
        GOTO 1303
      ENDIF
      IF (ctr6.eq.1) THEN
        fvals(i,j)=mctal(i,j)*nps/1E6/(estruc(ctr6)-0)
      ELSE
        fvals(i,j)=mctal(i,j)*nps/1E6/(estruc(ctr6)-estruc(ctr6-1))
      ENDIF
      ctr6=ctr6+1
    ENDDO
  ELSE
    DO j=1,nbins(i)*(mcnpnng+1)
      IF (ctr6.eq.mcnpnng+1) THEN
        ctr6=1
        GOTO 1313
      ENDIF
      IF (ctr6.eq.1) THEN
        fvals(i,j)=mctal(i,j)*nps/1E6/(estruc2(ctr6)-0)
      ELSE
        fvals(i,j)=mctal(i,j)*nps/1E6/(estruc2(ctr6)-estruc2(ctr6-1))
      ENDIF
      ctr6=ctr6+1
    ENDDO
  ENDIF
ENDDO

```

```

                                1313 Continue
                                ENDDO
                                ENDIF
                                ENDDO

!Write wtfxn.txt from the MCNP output
OPEN(unit=36,file='wtfxn.txt',status='REPLACE',iostat=iwterr)
WRITE(36,403) "0.0 0.0 0 0 1",mcnpnng,mcnpnng, " 5"
DO i=1,mcnpnng
    WRITE(36,409) midpts2(i),fvals(ntl,i)
ENDDO
WRITE(36,126) "/"
REWIND(36)

WRITE(*,*) "-----"
WRITE(*,*) "Writing RZFLUX files for TRANSX"
WRITE(*,*) "-----"

!Thermal power in W
power=power*1000
!Calculate volume for this power
DO i=1,noct
    nocount=nocount+ncelloc(i)
ENDDO

!Normalizing volume for the power although it doesn't matter
totfuelvol=REAL(nrows**2-nocount)*flength*rfuel**2*pi

!Neutron emission rate
neutrate=power/1.602E-13/200*nu

!Write the RZFLUX file
ALLOCATE(rzname(ntl-1))
hname='rzflux'
ALLOCATE(huse(2))
huse(1)='matthe'
huse(2)='whiatt'
ALLOCATE(ia(20))

!RZFLUX file parameters
ia(1)=50
ia(2)=INT(power)
ia(3)=INT(totfuelvol)
ia(4)=1
ia(5)=1
ia(6)=1
ia(7)=1000
ia(8)=900
ia(9)=50
ia(10)=25
ia(11)=15
ia(12)=10
ia(13)=1
ia(14)=1
ia(15)=1
ia(16)=1
ia(17)=1
ia(19)=nng
ia(20)=1000

DO i=1,ntl-1
    ia(18)=nbins(i)
    rzunit=90+i
    ivers=i
    WRITE(34,*) rzunit
    BACKSPACE(34)

```

```

READ(34,*) junk2
rzname(i)='rzflux//junk2(1:len(trim(junk2)))
OPEN(unit=rzunit,file=rzname(i),status='REPLACE')
!Note this file is written as 'formatted' even though
!a CCCC-IV file is normally an unformatted binary
!RZFLUX Header
WRITE(rzunit,*) (REAL(j),j=1,3),ivers
WRITE(rzunit,*) (ia(j),j=1,20)
ctr6=1
ctr7=1

!Calculate group averaged flux
ALLOCATE(zgf(nng,nbins(i)))
DO j=1,nbins(i)*(nng+1)
    IF (ctr6.eq.nng+1) THEN
        ctr6=1
        ctr7=ctr7+1
        GOTO 1304
    ENDIF
    zgf(ctr6,ctr7)=mctal(i,j)*neurate
    ctr6=ctr6+1
    1304 Continue
ENDDO

!Write group averaged flux in order of decreasing energy
!At the moment this is the assumed order
WRITE(rzunit,*) ((zgf(k,j),k=nng,1,-1),j=1,nbins(i))
DEALLOCATE(zgf)
CLOSE(rzunit)
ENDDO
ENDIF
1301 CONTINUE

400 FORMAT(4X,I6)
401 FORMAT(2X,I8)
402 FORMAT(3X,I5)
403 FORMAT(a,X,i3,X,i3,a2)
404 FORMAT(a,i3)
405 FORMAT(a,X,f10.3,X,f10.4,X,a)
406 FORMAT(3a8,i3)
407 FORMAT(a,i3,i4,X,a)
408 FORMAT(ES13.7,X,ES13.7,X,ES13.7) !This is not used.
409 FORMAT(ES11.4,X,ES11.4)

!-----
!-----Clear out working directory-----
!-----

IF (exec.eq.1.or.exec.eq.2) THEN
    result=SYSTEMQQ('DEL tape*')
    result=SYSTEMQQ('DEL ALL.G')
    result=SYSTEMQQ('DEL *.gendf')
    result=SYSTEMQQ('DEL *.out')
    result=SYSTEMQQ('DEL matxs')
ENDIF

!-----
!-----Write NJOY Input-----
!-----

DO i=1,niso
    funit=45+i
    OPEN(unit=funit,file=iso_name(i),status='replace')

    !Write the RECONR section
    WRITE(funit,*) "reconr"

```

```

WRITE(funit,*) "20 21"
WRITE(funit,*) """,iso_name(i),"from ",endf_path,""/"
WRITE(funit,*) matid(i), " 2 0"
WRITE(funit,*) "0.001 0.0/"
WRITE(funit,*) """,iso_name(i),"from ",endf_path,""/"
WRITE(funit,105) ""processed with njoy99.112 ",njoy_exe,""/"
WRITE(funit,*) "0/"

!Write the BROADR section
WRITE(funit,*) "broadr"
WRITE(funit,*) "20 21 22"
WRITE(funit,106) matid(i),ntemp,"0 0 0.0/"
WRITE(funit,*) "0.001/"
WRITE(funit,*) tlist
WRITE(funit,*) "0/"

!Write HEATR section
WRITE(funit,*) "heatr"
WRITE(funit,*) "20 22 23 /"
WRITE(funit,107) matid(i),"6 0",ntemp,"0 0 /"
WRITE(funit,*) "302 303 304 318 443 444"

!Write PURR section
WRITE(funit,*) "purrr"
WRITE(funit,*) "20 23 32"
WRITE(funit,108) matid(i),ntemp,nsig,"20 4 0/"
WRITE(funit,*) tlist
WRITE(funit,*) siglist
WRITE(funit,*) "0/"

!Write THERMR section
IF (thermopt.eq.0) THEN !THERMR off
    WRITE(funit,*) "moder"
    WRITE(funit,*) "32 33"
ELSEIF (thermopt.eq.1) THEN !THERMR on
    !We should probably consider adding a flag to do special
    !types of thermal treatments like H2O or ZrH
    WRITE(funit,*) "thermr"
    WRITE(funit,*) "0 32 33"
    WRITE(funit,109) "0",matid(i),"8",ntemp,"1 0 1 221 1"
    WRITE(funit,*) tlist
    WRITE(funit,*) "1.0E-3 4.5/"
ENDIF

!Write GROUPT sections (one for each temp)
DO j=1,ntemp
    WRITE(funit,*) "grouprr"
    WRITE(funit,110) "20 33 0",gtape(j),"0"
    WRITE(funit,111) matid(i),ngs,pgs,wtfxn,nleg,"1",nsig,"1"
    WRITE(funit,*) """,iso_name(i),"from ",endf_path,""/"
    WRITE(funit,*) temps(j)
    WRITE(funit,*) siglist
    !Read in and write group structure if necessary
    IF (ngs==1) THEN
        IF (inger==29) THEN
            WRITE(*,*) "FATAL ERROR: ngs=1 and 'gstruc.txt' does not exist"
            WRITE(*,*) "TXSAMC Exiting"
            GOTO 1001
        ENDIF
        DO k=1,100000
            IF (k.eq.1) THEN
                READ(38,113) junk2
                WRITE(funit,114) junk2(1:len(trim(junk2)))
            ELSE
                READ(38,115,END=1002) junk5,junk6
                WRITE(funit,115) junk5,junk6
            ENDIF
        END DO
    ENDIF
END DO

```

```

                ENDIF
            ENDDO
            1002 CONTINUE
            REWIND(37)
        ENDIF
        !Read in and write weighting function if necessary
        IF (wtfxn==1) THEN
            IF (iwtfr==29) THEN
                WRITE(*,*) "FATAL ERROR: wtfxn=1 and 'wtfxn.txt' does not exist"
                WRITE(*,*) "TXSAMC Exiting"
                GOTO 1001
            ENDIF
            DO k=1,100000
                READ(36,113,END=1003) junk2
                WRITE(funit,114) junk2
            ENDDO
            1003 CONTINUE
            REWIND(36)
        ENDIF
        !Write XS calls for each isotope/temp
        IF (thermopt.eq.0) THEN !THERMR off
            IF(xstype(i)==1.or.xstype(i)==2.or.xstype(i)==5) THEN
                WRITE(funit,*) "3/"
                WRITE(funit,*) "3 251 'MUBAR'"
                WRITE(funit,*) "3 252 'XI'"
                WRITE(funit,*) "3 259 '1/V'"
                WRITE(funit,*) "6/"
                WRITE(funit,*) "0/"
                WRITE(funit,*) "0/"
            ELSEIF(xstype(i)==3) THEN
                WRITE(funit,*) "3/"
                WRITE(funit,*) "3 251 'MUBAR'"
                WRITE(funit,*) "3 252 'XI'"
                WRITE(funit,*) "3 259 '1/V'"
                WRITE(funit,*) "3 452 'TOTNU'"
                WRITE(funit,*) "3 455 'DELAYNU'"
                WRITE(funit,*) "5 455 'CHID'"
                WRITE(funit,*) "6/"
                WRITE(funit,*) "0/"
                WRITE(funit,*) "0/"
            ELSEIF(xstype(i)==4) THEN
                WRITE(funit,*) "3/"
                WRITE(funit,*) "3 251 'MUBAR'"
                WRITE(funit,*) "3 252 'XI'"
                WRITE(funit,*) "3 259 '1/V'"
                WRITE(funit,*) "3 452 'TOTNU'"
                WRITE(funit,*) "6/"
                WRITE(funit,*) "0/"
                WRITE(funit,*) "0/"
            ENDIF
        ELSEIF(thermopt.eq.1) THEN !THERMR On
            IF(xstype(i)==1.or.xstype(i)==2.or.xstype(i)==5) THEN
                WRITE(funit,*) "3/"
                WRITE(funit,*) "3 221 'FREE'"
                WRITE(funit,*) "3 251 'MUBAR'"
                WRITE(funit,*) "3 252 'XI'"
                WRITE(funit,*) "3 259 '1/V'"
                WRITE(funit,*) "6/"
                WRITE(funit,*) "6 221 'FREE'"
                WRITE(funit,*) "0/"
                WRITE(funit,*) "0/"
            ELSEIF(xstype(i)==3) THEN
                WRITE(funit,*) "3/"
                WRITE(funit,*) "3 221 'FREE'"
                WRITE(funit,*) "3 251 'MUBAR'"
                WRITE(funit,*) "3 252 'XI'"
            ENDIF
        ENDIF
    ENDIF
END

```

```

WRITE(funit,*) "3 259 '1/V'"
WRITE(funit,*) "3 452 'TOTNU'"
WRITE(funit,*) "3 455 'DELAYNU'"
WRITE(funit,*) "5 455 'CHID'"
WRITE(funit,*) "6/"
WRITE(funit,*) "6 221 'FREE'"
WRITE(funit,*) "0/"
WRITE(funit,*) "0/"
ELSEIF(xstype(i)==4) THEN
WRITE(funit,*) "3/"
WRITE(funit,*) "3 221 'FREE'"
WRITE(funit,*) "3 251 'MUBAR'"
WRITE(funit,*) "3 252 'XI'"
WRITE(funit,*) "3 259 '1/V'"
WRITE(funit,*) "3 452 'TOTNU'"
WRITE(funit,*) "6/"
WRITE(funit,*) "6 221 'FREE'"
WRITE(funit,*) "0/"
WRITE(funit,*) "0/"
ENDIF
ENDIF
ENDDO
WRITE(funit,*) "stop"
WRITE(funit,*) "xnjoy"
CLOSE(unit=funit)
ENDDO

!NJOY Format Statements
105 FORMAT(X,a27,a67,a2)
106 FORMAT(X,a4,I2,a9)
107 FORMAT(X,a4,a4,X,I2,a6)
108 FORMAT(X,a4,X,I2,X,I2,X,a8)
109 FORMAT(a2,X,a4,X,a2,X,I2,X,a12)
110 FORMAT(a8,a3,a2)
111 FORMAT(X,a4,I3,I3,I3,a2,I3,a2)
112 FORMAT(a40)
113 FORMAT(a120)
114 FORMAT(X,a120)
115 FORMAT(X,ES11.4,X,ES11.4)
!Reserve up to 115 for this section

!-----
!-----Run NJOY to create .GENDF files-----
!-----

IF (exec.eq.1.or.exec.eq.2) THEN
DO i=1,niso
command1(i)='copy '//endf_path(1:len(trim(endf_path)))/'^'&
//tape(i)/' tape20'
WRITE(*,*) '-----'
WRITE(*,*) 'Running NJOY for isotope ',iso_name(i)
WRITE(*,*) 'Temperatures == ',tlist(1:len(trim(tlist))),' K'
WRITE(*,*) 'Sigma Zeroes == ',siglist
WRITE(*,*(a,i3)) 'Weight Function IWT == ',wtfxn
WRITE(*,*(a,i3)) 'Number of Neutron Groups == ',nng
WRITE(*,*) '-----'
command2(i)=njoy_exe(1:len(trim(njoy_exe)))/' < '//iso_name(i)
command3(i)='ren output '//iso_name(i)(1:len(trim(iso_name(i))))/'.out'
result=SYSTEMQQ(command1(i))
result=SYSTEMQQ(command2(i))
result=SYSTEMQQ(command3(i))
DO j=1,ntemp
command4(i,j)='ren tape//gtape(j)/' '^'&
iso_name(i)(1:len(trim(iso_name(i))))/ '&
temps(j)(1:len(trim(temps(j))))/'.gendf
result=SYSTEMQQ(command4(i,j))
ENDDO

```



```

        ENDDO
ENDIF

!Clean up the tapes
IF (exec.eq.1.or.exec.eq.2) THEN
    result=SYSTEMQQ('DEL tape*')
    result=SYSTEMQQ('DEL matxsroutput')
ENDIF

!Merge the .gendf files together
IF (exec.eq.1.or.exec.eq.2) THEN
    WRITE (*,*) '-----'
    WRITE (*,*) 'Running MERG_GENDF.exe'
    WRITE (*,*) '-----'
    DO i=1,niso
        DO j=1,ntemp
            command5(i,j)=merg_exe/' '//iso_name(i)(1:len(trim(iso_name(i))))&
                //temps(j)(1:len(trim(temps(j))))/'_gendf/' ALL.G 0'
            result=SYSTEMQQ(command5(i,j))
        ENDDO
    ENDDO
ENDIF

!Finish off All.G file
IF (exec.eq.1.or.exec.eq.2) THEN
    result=SYSTEMQQ('ECHO', '&', '-1 0 0 >> ALL.G')
    result=SYSTEMQQ('copy ALL.g tape24')
ENDIF

!-----
!-----Run NJOY to create MATXS file-----
!-----
IF (thermopt.eq.1) THEN
    ntype=ntype+1
ENDIF
!Write matxsrinput file
WRITE(26,*) "matxsr"
WRITE(26,*) " 24 0 -40/"
WRITE(26,*) "1 'TXSAMC Generated'"
WRITE(26,116) npart,ntype,"2 ",niso
WRITE(26,117) "",nng,"X",npg," LIBRARY, ",tlist(1:len(trim(tlist))),&
    "K, IWT=",wtfxn,"/"
WRITE(26,118) "Generated for ",title(1:len(trim(title))),"/"
!Add 'nfree' call to this
IF (npart.eq.1.and.ntype.eq.2.and.thermopt.eq.1) THEN
    WRITE(26,*) "n"
    WRITE(26,119) nng
    WRITE(26,*) "nscat' 'ntherm'"
    WRITE(26,*) "1 1"
    WRITE(26,*) "1 1"
ELSEIF(npart.eq.1.and.ntype.eq.1.and.thermopt.eq.0) THEN
    WRITE(26,*) "n"
    WRITE(26,119) nng
    WRITE(26,*) "nscat'"
    WRITE(26,*) "1"
    WRITE(26,*) "1"
ELSEIF (npart.eq.2.and.ntype.eq.3.and.thermopt.eq.1) THEN
    WRITE(26,*) "n' 'g'"
    WRITE(26,119) nng,npg
    WRITE(26,*) "nscat' 'ng' 'mtherm'"
    WRITE(26,*) "1 1 1"
    WRITE(26,*) "1 2 1"
ELSEIF (npart.eq.2.and.ntype.eq.2.and.thermopt.eq.0) THEN
    WRITE(26,*) "n' 'g'"
    WRITE(26,119) nng,npg

```

```

        WRITE(26,*) "nscat 'ng'"
        WRITE(26,*) "1 1"
        WRITE(26,*) "1 2"
ELSEIF (npart.eq.2.and.ntype.eq.4.and.thermopt.eq.1) THEN
        WRITE(26,*) "n' 'g'"
        WRITE(26,119) nng,npng
        WRITE(26,*) "nscat 'ng' 'gscat' 'ntherm'"
        WRITE(26,*) "1 1 2 1"
        WRITE(26,*) "1 2 2 1"
ELSEIF (npart.eq.2.and.ntype.eq.3.and.thermopt.eq.0) THEN
        WRITE(26,*) "n' 'g'"
        WRITE(26,119) nng,npng
        WRITE(26,*) "nscat 'ng' 'gscat'"
        WRITE(26,*) "1 1 2"
        WRITE(26,*) "1 2 2"
ENDIF
DO i=1,niso
        WRITE(26,*) iso_name(i), " ",matid(i), " 0"
ENDDO
WRITE(26,*) "stop"
WRITE(26,*) "xnjoy"

IF (exec.eq.1.or.exec.eq.2) THEN
        !Run NJOY for MATXS
        WRITE(*,*) "-----"
        WRITE(*,*) "Running MATXSR"
        WRITE(*,*) "-----"
        result=SYSTEMQQ(njoy_exe/'< matxsrinput')
        !Copy tape40 to matxs
        result=SYSTEMQQ('ren tape40 matxs')
        !Copy output from NJOY
        result=SYSTEMQQ('ren output matxsoutput')
ENDIF

!MATXSR Format Statements
116 FORMAT(I2,I2,a3,I3)
117 FORMAT(a2,I3,a1,I2,a10,a,a7,i2,a)
118 FORMAT(a,a,a)
119 FORMAT(I3,X,I3)
!Reserve up to 125 for these format statements

!-----
!-----Write TRANSX input(s)-----
!-----

ALLOCATE(fname(ntreg),fnumber(ntreg))

IF (initf.ne.0.and.mctalerr.eq.29) THEN
        WRITE(*,*) "FATAL ERROR: MCTAL file was not written and data from it was called for"
        WRITE(*,*) "Program Exiting"
        GOTO 1001
ENDIF

WRITE(*,*) "-----"
WRITE(*,*) "Writing TRANSX input files"
WRITE(*,*) "-----"

!Loop over each TRANSX input file
DO i=1,ntreg
        nmixs=0
        !Set region and heterogeneity characteristics
        IF (tregtype(i).eq.1) THEN
                nreg=1
        ELSEIF (tregtype(i).eq.2) THEN
                nreg=3

```

```

        b1=1.35
ELSEIF (tregtype(i).ge.3) THEN
    IF (noct.ne.0) THEN
        DO j=1,noct
            IF (unum2(j).eq.tregtype(i)) THEN
                nreg=nrad(j)+1
                b1=1.35
                octindex=j
            ENDIF
        ENDDO
    ENDIF
ENDIF
ENDIF

IF (Itype.eq.1.and.(ihet.ne.4.and.ihet.ne.1.and.ihet.ne.0)) THEN
    WRITE(*,*) "WARNING: You have specified the wrong heterogeneity"//&
        " option for this lattice type"
    WRITE(*,*) "Change IHET to appropriate value? 1=Yes,2=No"
    READ(*,*) hetchange
    IF (hetchange.eq.1) THEN
        ihet=4
    ENDIF
ELSEIF (Itype.eq.2.and.(ihet.ne.3.and.ihet.ne.1.and.ihet.ne.0)) THEN
    WRITE(*,*) "WARNING: You have specified the wrong heterogeneity"//&
        " option for this lattice type"
    WRITE(*,*) "Change IHET to appropriate value? 1=Yes,2=No"
    READ(*,*) hetchange
    IF (hetchange.eq.1) THEN
        ihet=3
    ENDIF
ENDIF

!Write the input file
tunit=80+i
WRITE(33,207) tunit
BACKSPACE(33)
READ(33,*) fnumber(i)
fname(i)="pincell"//fnumber(i)//".inp"
OPEN(unit=tunit,file=fname(i),status="REPLACE")
WRITE(tunit,201) title(1:len(trim(title))//"-- Tally Region ==",i
WRITE(tunit,202) 0,iout,iprob,iset,iform,1,0,itrc,icoll,initf
ntabl=ngroup+ned+3+nup
WRITE(tunit,203) ngroup,nl,ntabl,nup,nthg,nmix,nreg,nmixs,ned,neds
WRITE(tunit,204) 100+i

!Write the region and mixture specifications for each input file
IF (tregtype(i).eq.1) THEN
    !We ignore self-shielding for coolant channels
    WRITE(tunit,208) "mod ",mctemp(2)," "
    Call Mixer(tunit,1,mcmat(2),-mcdens(2),enri/100.,materr,nmixline)
    GOTO (1001,1008) materr
    1008 Continue
    nmixs=nmixline+nmixs
ELSEIF (tregtype(i).eq.2) THEN
    !Fuel cells
    IF (ihet.eq.0) THEN
        WRITE(tunit,208) "fuel",mctemp(4)," "
        WRITE(tunit,208) "clad",mctemp(3)," "
        WRITE(tunit,208) "mod ",mctemp(2)," "
    ELSEIF (ihet.gt.1) THEN
        WRITE(tunit,205) "fuel",mctemp(4),fvol,ihet,b1,b1," "
        WRITE(tunit,206) "clad",mctemp(3),cvol,-ihet," "
        WRITE(tunit,206) "mod ",mctemp(2),mvol,-ihet," "
    ELSEIF (ihet.eq.1) THEN
        !Calculate your own chord length. This feature doesn't work
    ENDIF
    DO k=1,nreg
        Call Mixer(tunit,k,mcmat(nreg-k+2),-mcdens(nreg-k+2),enri/100.,&
            materr,nmixline)

```

```

        GOTO (1001,1006) materr
        1006 Continue
        nmixs=nmixline+nmixs
    ENDDO
ELSEIF (tregtype(i).ge.3) THEN          !Control rod and other fuel cells
    IF (ihet.eq.0) THEN
        DO j=nreg,2,-1
            WRITE(tunit,209) "ring",nreg+1-j,otemp(octindex,j-1),"/"
        ENDDO
        WRITE(tunit,209) "modr",nreg,mctemp(2),"/"
    ELSEIF (ihet.gt.1) THEN
        DO j=nreg,1,-1
            IF (j.eq.nreg) THEN
                ringvol=pi*otrad(octindex,nreg-1)**2
                WRITE(tunit,210) "ring1",otemp(octindex,nreg-1),ringvol,&
                    ihet,b1,b1,"/"
            ELSEIF(j.ne.1) THEN
                ringvol=pi*otrad(octindex,j-1)**2-pi*otrad(octindex,j)**2
                WRITE(tunit,211) "ring",nreg+1-j,otemp(octindex,j-1),ringvol,&
                    -ihet,"/"
            ELSEIF(j.eq.1) THEN
                IF (ltype.eq.1) THEN
                    ringvol=pitch**2-pi*otrad(octindex,j)**2
                ELSEIF (ltype.eq.2) THEN
                    ringvol=(3*sqrt(3.))/2*hexside-pi*otrad(octindex,j)**2
                ENDIF
                WRITE(tunit,211) "modr",nreg,mctemp(2),ringvol,-ihet,"/"
            ENDIF
        ENDDO
    ELSEIF (ihet.eq.1) THEN
        !Calculate your own chord length. This feaature doesn't work
    ENDIF
    DO k=1,nreg-1
        Call Mixer(tunit,k,otmat(octindex,nreg-k),-otdens(octindex,nreg-k),&
            otenri(octindex)/100.,materr,nmixline)
        GOTO (1001,1007) materr
        1007 Continue
        nmixs=nmixline+nmixs
    ENDDO
    Call Mixer(tunit,nreg,mcmat(2),-mcdens(2),enri/100.,materr,nmixline)
    nmixs=nmixline+nmixs
ENDIF
WRITE(tunit,126) hed
DO k=1,neds
    WRITE(tunit,126) eds(k)
ENDDO
WRITE(tunit,126) "stop"
!This is where I'll need to replace nmixs
OPEN(unit=32,file="scratch4",status='REPLACE')

REWIND(tunit)
DO m=1,50000
    READ(tunit,113,END=1009) junk2
    IF (m.eq.3) THEN
        WRITE(32,203) ngroup,nl,ntabl,nup,nthg,nmix,nreg,nmixs,ned,neds
    ELSE
        WRITE(32,113) junk2
    ENDIF
ENDDO
1009 Continue
REWIND(32)
REWIND(tunit)
DO m=1,50000
    READ(32,113,END=1010) junk2
    WRITE(tunit,113) junk2
ENDDO

```

```

1010 Continue
REWIND(32)
ENDDO

!TRANSX Format Statements
201 FORMAT(a,i1)
202 FORMAT(i1,7i2,i4,i2)
203 FORMAT(i3,i2,i4,i3,i3,i3,i4,i3,i3)
204 FORMAT(i3)
205 FORMAT(a4,X,f7.2,f8.4,i3,f7.3,f7.3,a1)
206 FORMAT(a4,X,f7.2,f8.4,i3,a1)
207 FORMAT(i2)
208 FORMAT(a4,X,f7.2,a1)
209 FORMAT(a4,i1,X,f7.3,a1)
210 FORMAT(a5,X,f7.2,f8.4,i3,f7.3,f7.3,a1)
211 FORMAT(a4,i1,X,f7.2,f8.4,i3,a1)

!-----
!-----Run TRANSX-----
!-----

IF (exec.eq.1.or.exec.eq.4) THEN
  WRITE(*,*) "-----"
  WRITE(*,*) "Running TRANSX.exe"
  WRITE(*,*) "-----"
  DO i=1,ntreg
    result=SYSTEMQQ('copy '//tzname(i)//' rzflux')
    command6=transx_exe(1:len(trim(transx_exe))//'" <"/"&
      fname(i)(1:len(trim(fname(i))))//'" >pincell"/"&
      fnumber(i)//".out"
    result=SYSTEMQQ(command6)
    WRITE(*,(a,i2,a)) "TRANSX run ",i," completed"
    IF (iout.eq.9) THEN
      result=SYSTEMQQ('del acemg//fnumber(i)')
      result=SYSTEMQQ('del xsdir//fnumber(i)')
      result=SYSTEMQQ('ren acemg acemg//fnumber(i)')
      result=SYSTEMQQ('ren xsdir xsdir//fnumber(i)')
    ELSEIF (iout.eq.8) THEN
      !Work here
    ELSE
      WRITE(*,*) "WARNING: The output format you have chosen has"/"&
        " not been coded for renaming in TXSAMC"
      WRITE(*,(a,i2)) "Input the command to rename the xsfile "/"&
        "for tally region",ntreg
      READ(*,113) junk2
      result=SYSTEMQQ(junk2)
    ENDIF
  ENDDO
ENDIF

ENDIF

1001 CONTINUE

END

!This is a subroutine that assigns suffixes to temperatures
subroutine Suffr(temp,xsnum)
  CHARACTER(LEN=2) :: xsnum
  REAL*8 :: temp
  if (temp.lt.350) xsnum='30'
  if (temp.ge.350.and.temp.lt.450) xsnum='40'
  if (temp.ge.450.and.temp.lt.550) xsnum='50'
  if (temp.ge.550.and.temp.lt.650) xsnum='60'
  if (temp.ge.650.and.temp.lt.750) xsnum='70'
  if (temp.ge.750.and.temp.lt.850) xsnum='80'
  if (temp.ge.850.and.temp.lt.950) xsnum='90'
  if (temp.ge.950.and.temp.lt.1050) xsnum='10'

```

```

if (temp.ge.1050.and.temp.lt.1150) xsnum='11'
if (temp.ge.1150.and.temp.lt.1250) xsnum='12'
if (temp.ge.1250.and.temp.lt.1350) xsnum='13'
if (temp.ge.1350.and.temp.lt.1450) xsnum='14'
if (temp.ge.1450.and.temp.lt.1550) xsnum='15'
if (temp.ge.1550) xsnum='16'
end subroutine

```

!Alternate subroutine if one has a xs library with more temperature options

```

subroutine Suffr2(temp,xsnum)
  CHARACTER(LEN=2) :: xsnum
  REAL*8 :: temp
  if (temp.lt.375) xsnum='30'
  if (temp.ge.375.and.temp.lt.425) xsnum='40'
  if (temp.ge.425.and.temp.lt.475) xsnum='45'
  if (temp.ge.475.and.temp.lt.525) xsnum='50'
  if (temp.ge.525.and.temp.lt.575) xsnum='55'
  if (temp.ge.575.and.temp.lt.625) xsnum='59'
  if (temp.ge.625.and.temp.lt.675) xsnum='65'
  if (temp.ge.675.and.temp.lt.725) xsnum='70'
  if (temp.ge.725.and.temp.lt.775) xsnum='75'
  if (temp.ge.775.and.temp.lt.825) xsnum='80'
  if (temp.ge.825.and.temp.lt.875) xsnum='85'
  if (temp.ge.875.and.temp.lt.925) xsnum='90'
  if (temp.ge.925.and.temp.lt.975) xsnum='95'
  if (temp.ge.975.and.temp.lt.1050) xsnum='10'
  if (temp.ge.1050.and.temp.lt.1150) xsnum='11'
  if (temp.ge.1150.and.temp.lt.1250) xsnum='12'
  if (temp.ge.1250.and.temp.lt.1350) xsnum='13'
  if (temp.ge.1350.and.temp.lt.1450) xsnum='14'
  if (temp.ge.1450.and.temp.lt.1550) xsnum='15'
  if (temp.ge.1550) xsnum='16'
end subroutine

```

!This subroutine writes the energy group structure for MCNP tallies

```

subroutine Energizer(talnum,neutgs)
  INTEGER*8 :: talnum,neutgs,flag

```

```

IF (talnum.lt.10) THEN
  ASSIGN 140 TO flag
ELSEIF (talnum.ge.10) THEN
  ASSIGN 141 TO flag
ENDIF

```

```

IF (neutgs.eq.3) THEN
  !LANL 30 Group Structure
  WRITE(35,flag) "e",talnum,"4 1.52E-7 4.14E-7 1.13E-6 3.06E-6 8.32E-6 2.26E-5 6.14E-5 "
  WRITE(35,126) " 1.67E-4 4.54E-4 1.235E-3 3.35E-3 9.12E-3 2.48E-2 6.76E-2"
  WRITE(35,126) " 1.84E-1 3.03E-1 5.0E-1 8.23E-1 1.353 1.738 2.232 2.865"
  WRITE(35,126) " 3.68 6.07 7.79 1.0E01 1.2E01 1.35E01 1.5E01 1.7E01"
  ELSEIF (neutgs.eq.9) THEN
  !EPRI 69 Group Structure
  WRITE(35,flag) "e",talnum,"4 0.000000005 0.000000001 0.000000015 0.00000002 "&
  // " 0.000000025"
  WRITE(35,126) " 0.00000003 0.000000035 0.000000042 0.00000005 0.000000058 "
  WRITE(35,126) " 0.000000067 0.00000008 0.0000001 0.00000014 0.00000018 "
  WRITE(35,126) " 0.00000022 0.00000025 0.00000028 0.0000003 0.00000032 "
  WRITE(35,126) " 0.00000035 0.0000004 0.0000005 0.000000625 0.00000078 "
  WRITE(35,126) " 0.00000085 0.00000091 0.00000095 0.000000972 0.000000996 "
  WRITE(35,126) " 0.0000102 0.00001045 0.00001071 0.00001097 0.00001123 "
  WRITE(35,126) " 0.0000115 0.000013 0.000015 0.000021 0.000026 "
  WRITE(35,126) " 0.000033 0.00004 0.00009877 0.00015968 0.000277 "
  WRITE(35,126) " 0.00048052 0.00075501 0.00148728 0.00367262 0.00906898 "
  WRITE(35,126) " 0.014251 0.0223945 0.0035191 0.00553 0.009118 "
  WRITE(35,126) " 0.01503 0.02478 0.04085 0.06734 0.111 "
  WRITE(35,126) " 0.183 0.3025 0.5 0.821 1.353 "

```

```

WRITE(35,126) " 2.231 3.679 6.0655 10 "
ELSEIF (neutgs.eq.10) THEN
!LANL 187 Group Structure
WRITE(35,flag) "e",talnum,"4 2.5399E-10 7.6022E-10 2.2769E-9 0.0000000063247"//&
" 0.000000012396 "
WRITE(35,126) " 0.000000020492 0.0000000255 0.000000030612 0.0000000355"//&
" 0.000000042755"
WRITE(35,126) " 0.00000005 0.000000056922 0.000000067 0.000000081968"//&
" 0.00000011157 "
WRITE(35,126) " 0.00000014572 0.0000001523 0.00000018443 0.00000022769"//&
" 0.00000025103 "
WRITE(35,126) " 0.00000027052 0.00000029074 0.00000030112 0.00000032063"//&
" 0.00000035767 "
WRITE(35,126) " 0.00000041499 0.00000050323 0.00000062506 0.00000078208"//&
" 0.00000083368 "
WRITE(35,126) " 0.00000087642 0.00000091 0.00000095065 0.000000971"//&
" 0.000000992 "
WRITE(35,126) " 0.0000010137 0.0000010427 0.0000010525 0.0000010623"//&
" 0.0000010722 "
WRITE(35,126) " 0.0000010987 0.0000011254 0.0000011664 0.0000013079"//&
" 0.0000014574 "
WRITE(35,126) " 0.0000015949 0.0000017261 0.00000185539 0.00000210243"//&
" 0.00000238237 "
WRITE(35,126) " 0.00000269958 0.00000305902 0.00000346633 0.00000392786"//&
" 0.00000445085 "
WRITE(35,126) " 0.00000504348 0.00000571501 0.00000647595 0.000006868"//&
" 0.00000733822 "
WRITE(35,126) " 0.00000831529 0.00000942245 0.000010677 0.0000120987 0.0000137096"
WRITE(35,126) " 0.000015535 0.0000176035 0.0000199473 0.0000226033 0.0000256129 "
WRITE(35,126) " 0.0000290232 0.0000328876 0.0000372665 0.0000422285 0.0000478512 "
WRITE(35,126) " 0.0000542225 0.0000614421 0.000069623 0.0000788932 0.0000893978 "
WRITE(35,126) " 0.000101301 0.000114789 0.000130073 0.000147392 0.000167017 "
WRITE(35,126) " 0.000189255 0.000214454 0.000243008 0.000275364 0.000312029 "
WRITE(35,126) " 0.000353575 0.000400653 0.000453999 0.000514449 0.000582947 "
WRITE(35,126) " 0.000660565 0.000748518 0.000848182 0.000961117 0.00108909 "
WRITE(35,126) " 0.0012341 0.00139842 0.00158461 0.0017956 0.00203468 "
WRITE(35,126) " 0.0023056 0.00261259 0.00296045 0.00335463 0.00380129 "
WRITE(35,126) " 0.00430743 0.00488095 0.00553084 0.00626727 0.00710174 "
WRITE(35,126) " 0.00804733 0.00911882 0.010333 0.0117088 0.0132678 "
WRITE(35,126) " 0.0150344 0.0170362 0.0193045 0.0218749 0.0247875 "
WRITE(35,126) " 0.026058 0.0280879 0.0318278 0.0360656 0.0408677 "
WRITE(35,126) " 0.0463092 0.0524752 0.0594622 0.0673795 0.0763509 "
WRITE(35,126) " 0.086517 0.0980366 0.11109 0.125881 0.142642 "
WRITE(35,126) " 0.161635 0.183156 0.207543 0.235177 0.266491 "
WRITE(35,126) " 0.301974 0.342181 0.387742 0.439369 0.497871 "
WRITE(35,126) " 0.564161 0.639279 0.724398 0.82085 0.930145 "
WRITE(35,126) " 1.05399 1.19433 1.35335 1.53355 1.73774 "
WRITE(35,126) " 1.96912 2.2313 2.5284 2.86505 3.24652 "
WRITE(35,126) " 3.67879 4.16862 4.72367 5.35261 6.06531 "
WRITE(35,126) " 6.87289 7.78801 8.82497 10 11 "
WRITE(35,126) " 12 13 13.5 13.75 13.94 "
WRITE(35,126) " 14.2 14.42 14.64 15 16 "
WRITE(35,126) " 17 20 "
ELSEIF (neutgs.eq.11) THEN
!LANL 70 Group Structure
WRITE(35,flag) "e",talnum,"4 61.4421E-6 101.301E-6 130.073E-6 167.017E-6 "
WRITE(35,126) " 214.454E-6 275.365E-6 353.575E-6 453.999E-6 582.947E-6 748.518E-6"
WRITE(35,126) " 961.117E-6 1089.09E-6 1234.1E-6 1398.42E-6 1584.61E-6 1795.6E-6 "
WRITE(35,126) " 0.00203468 0.0023056 0.00261259 0.00296045 0.00335463 0.00380129 "
WRITE(35,126) " 0.00430743 0.00488095 0.00553084 0.00626727 0.00710174 0.00804733"
WRITE(35,126) " 0.00911882 0.0103333 0.0117088 0.0132678 0.0150344 0.0170362 "
WRITE(35,126) " 0.0193045 0.0218749 0.0247875 0.0280879 0.0318278 0.0408677 "
WRITE(35,126) " 0.0524752 0.0673795 0.0865170 0.1110900 0.1426420 0.1831560 "
WRITE(35,126) " 0.2351780 0.3019740 0.3877420 0.4393690 0.4978710 0.5641610 "
WRITE(35,126) " 0.6392790 0.7243980 0.8208500 0.9301450 1.0539900 "
WRITE(35,126) " 1.1943300 1.3533500 1.7377400 2.2313000 2.8650500 "

```

```

WRITE(35,126) " 3.6787900 4.7236700 6.0653100 7.7880100 10.000000 12.840300 "
WRITE(35,126) " 16.487200 20.000000 "
ELSEIF (neutgs.eq.1) THEN
!User input Group Structure
!Think about how to read this in off of gstruc.txt
WRITE(*,*) "I haven't coded this option yet"
ENDIF

126 FORMAT(a)
140 FORMAT(a1,i1,a)
141 FORMAT(a1,i2,a)
end subroutine

!This subroutine writes the material cards for the MCNP input
subroutine Matter(mnum,mat,dens,suff,enri,ergo)
CHARACTER(LEN=6) :: mat
CHARACTER(LEN=2) :: suff
INTEGER*8 :: mnum,ergo
REAL*8 :: enri,dens

ergo=2
!Add materials as needed
!The comment lines are unnecessary except as descriptors
IF (mat.eq."SS316L") THEN
WRITE(35,135) "c SS316L(",-dens,") Stainless, ",-dens,"g/cc, 2%Mo, 16%Cr,"//&
" 72%Fe, 10%Ni"
WRITE(35,137) "m",100+mnum," 42000.",suff,"c -0.0200 24050.",suff,"c -0.0070"//&
" 24052.",suff,"c -0.1341 "
WRITE(35,136) " 24053.",suff,"c -0.0152 24054.",suff,"c -0.0037 26054.",&
suff,"c -0.0418 "
WRITE(35,136) " 26056.",suff,"c -0.6604 26057.",suff,"c -0.0158 26058.",&
suff,"c -0.0020 "
WRITE(35,136) " 28058.",suff,"c -0.0683 28060.",suff,"c -0.0261 28061.",&
suff,"c -0.0011 "
WRITE(35,136) " 28062.",suff,"c -0.0036 28064.",suff,"c -0.0009 "
ELSEIF (mat.eq."Na ") THEN
WRITE(35,135) "c Na (",-dens,") Liquid Na, ",-dens,"g/cc, 100% Na " //&
" "
WRITE(35,137) "m",100+mnum," 11023.",suff,"c 1.0000 "
ELSEIF (mat.eq."Zirc ") THEN
WRITE(35,135) "c Zirc (",-dens,") ZrNat Clad, ",-dens,"g/cc, 100% Zr " //&
" "
WRITE(35,137) "m",100+mnum," 40000.",suff,"c 1.0000 "
ELSEIF (mat.eq."UO2 ") THEN
WRITE(35,138) "c UO2 (",-dens,") UO2 Fuel, ",-dens,"g/cc, Enri=",enri,"% "
WRITE(35,139) "m",100+mnum," 92235.",suff,"c ",enri/100.," 92238.",suff,"c ",&
1-enri/100.," 8016.",suff,"c 2.0000"
ELSEIF (mat.eq."Alum ") THEN
WRITE(35,135) "c Alum (",-dens,") Alum Clad, ",-dens,"g/cc, 100% Al27 " //&
" "
WRITE(35,137) "m",100+mnum," 13027.",suff,"c 1.0000 "
ELSEIF (mat.eq."AgInCd") THEN
WRITE(35,135) "c AgInCd(",-dens,") AgInCd CR, ",-dens,"g/cc, 80%Ag 15%In " //&
" 5%Cd "
WRITE(35,137) "m",100+mnum," 47107.",suff,"c -0.4147 47109.",suff,"c -0.3853"//&
" 49000.",suff,"c -0.1500 "
WRITE(35,136) " 48000.",suff,"c -0.0500 "
ELSE
WRITE(*,*) "FATAL ERROR: Material not defined for MCNP"
ergo=1
ENDIF

135 FORMAT(a9,f4.1,a14,f4.1,a31)
136 FORMAT(a12,a2,a18,a2,a17,a2,a11)
137 FORMAT(a1,i3,a8,a2,a18,a2,a17,a2,a11)
138 FORMAT(a9,f4.1,a14,f4.1,a11,f4.1,a1)

```



```
139 FORMAT(a1,i3,a8,a2,a3,f6.4,a8,a2,a3,f6.4,a8,a2,a9)
```

```
end subroutine
```

```
!This subroutine writes the mix specifications for the TRANSX input
```

```
subroutine Mixer(tunit,reg,mat,dens,enri,ergo,nmixl)
```

```
INTEGER*8 :: reg,ergo,tunit,nmixl
```

```
CHARACTER(LEN=6) :: mat
```

```
REAL*8 :: dens,enri,avog,barn,muo2
```

```
avog=6.022E23
```

```
barn=1E-24
```

```
ergo=2
```

```
!This variable controls the number of mix specs written to card 2 of TRANSX input
```

```
nmixl=1
```

```
IF (mat.eq."SS316L") THEN
```

```
WRITE(tunit,101) "1 ",reg,"MONAT ",.02*(dens*avog*barn)/95.94,"/"
```

```
WRITE(tunit,101) "1 ",reg,"CR50 ",.007*(dens*avog*barn)/49.946049,"/"
```

```
WRITE(tunit,101) "1 ",reg,"CR52 ",.1341*(dens*avog*barn)/51.940512,"/"
```

```
WRITE(tunit,101) "1 ",reg,"CR53 ",.0152*(dens*avog*barn)/52.940653,"/"
```

```
WRITE(tunit,101) "1 ",reg,"CR54 ",.0037*(dens*avog*barn)/53.938885,"/"
```

```
WRITE(tunit,101) "1 ",reg,"FE54 ",.0418*(dens*avog*barn)/53.939613,"/"
```

```
WRITE(tunit,101) "1 ",reg,"FE56 ",.6604*(dens*avog*barn)/55.934941,"/"
```

```
WRITE(tunit,101) "1 ",reg,"FE57 ",.0158*(dens*avog*barn)/56.935398,"/"
```

```
WRITE(tunit,101) "1 ",reg,"FE58 ",.002*(dens*avog*barn)/57.933280,"/"
```

```
WRITE(tunit,101) "1 ",reg,"NI58 ",.0683*(dens*avog*barn)/57.935348,"/"
```

```
WRITE(tunit,101) "1 ",reg,"NI60 ",.0261*(dens*avog*barn)/59.930790,"/"
```

```
WRITE(tunit,101) "1 ",reg,"NI61 ",.0011*(dens*avog*barn)/60.931060,"/"
```

```
WRITE(tunit,101) "1 ",reg,"NI62 ",.0036*(dens*avog*barn)/61.928348,"/"
```

```
WRITE(tunit,101) "1 ",reg,"NI64 ",.0009*(dens*avog*barn)/63.927969,"/"
```

```
nmixl=14
```

```
ELSEIF (mat.eq."Na ") THEN
```

```
WRITE(tunit,101) "1 ",reg,"NA23 ",(dens*avog*barn)/22.989770,"/"
```

```
ELSEIF (mat.eq."Zirc ") THEN
```

```
WRITE(tunit,101) "1 ",reg,"ZRNAT ",(dens*avog*barn)/91.224,"/"
```

```
ELSEIF (mat.eq."Alum ") THEN
```

```
WRITE(tunit,101) "1 ",reg,"AL27 ",(dens*avog*barn)/26.981538,"/"
```

```
ELSEIF (mat.eq."UO2 ") THEN
```

```
muo2=enri*235.043922+(1-enri)*238.050785+2*15.994914622
```

```
WRITE(tunit,101) "1 ",reg,"U235 ",enri*(dens*avog*barn)/muo2,"/"
```

```
WRITE(tunit,101) "1 ",reg,"U238 ",(1-enri)*(dens*avog*barn)/muo2,"/"
```

```
WRITE(tunit,101) "1 ",reg,"O16 ",2*(dens*avog*barn)/muo2,"/"
```

```
nmixl=3
```

```
ELSEIF (mat.eq."AgInCd") THEN
```

```
WRITE(tunit,101) "1 ",reg,"AG107 ",.4147*(dens*avog*barn)/106.90509,"/"
```

```
WRITE(tunit,101) "1 ",reg,"AG109 ",.3853*(dens*avog*barn)/108.904756,"/"
```

```
WRITE(tunit,101) "1 ",reg,"INNAT ",.1500*(dens*avog*barn)/114.818,"/"
```

```
WRITE(tunit,101) "1 ",reg,"CDNAT ",.0500*(dens*avog*barn)/112.411,"/"
```

```
nmixl=4
```

```
ELSE
```

```
WRITE(*,*) "FATAL ERROR: Material not defined for TRANSX"
```

```
ergo=1
```

```
ENDIF
```

```
101 FORMAT(a3,i3,X,a6,X,f9.6,a1)
```

```
end subroutine
```

APPENDIX C

TRANSX MODIFICATIONS

The section of code below is taken from a modified `trx.f90` source file from TRANSX. To run TXSAMC, this block of code must replace lines 533-573 of the standard `trx.f90` source file. There are only three lines changed in this section and all are marked with the “MTH Change” comment directly above them.

```

!--initialize flux interface file (if any)
nflx=0
if (initf.ge.2) then
  write(sflux,'(a6)') hflux
  !MTH Change all to formatted reads
  call seek(sflux.0,nflx,6)
  nwds=1+3*mult
  jrec=1
  call find(nflx,jrec)
  !MTH Change all to formatted reads
  read(nflx,*) (ha(11h+i-1),i=1,3),ia(11+3*mult)
  iver=ia(11+3*mult)
  write(nsysto,'(/&
    &' input flux file'//&
    &' -----'//&
    &' file id ',3a8,' vers ',i3)'&
    ha(11h),ha(11h+1),ha(11h+2),iver
  nwds=8
  if (initf.eq.2) nwds=9
  if (initf.eq.4) nwds=20
  jrec=jrec+1
  call find(nflx,jrec)
  !MTH Change
  read(nflx,*) (ia(11+i-1),i=1,nwds)
  if (initf.lt.4.and.ia(11+1).ne.nfine)&
    call error('inconsistent flux file')
  if (initf.eq.4.and.ia(11+18).ne.nfine)&
    call error('inconsistent flux file')
  if (initf.eq.2.and.ia(11+8).ne.1)&
    call error('inconsistent flux file')
  if (initf.lt.4.and.ia(11+4).ne.1)&
    call error('inconsistent flux file')
  nrfl=ia(11+2)
  if (initf.eq.4) nrfl=ia(11+17)
  n2nd=0
  if (initf.lt.4.and.ia(11).gt.1) n2nd=ia(11+3)
  nfl=1
  nblk=0
  if (initf.eq.2) nblk=ia(11+8)
  if (initf.eq.3) then
    nfl=ia(11+5)
    if (nfl.gt.1) inflo=1
  endif
endif
endif

```

Fig. C.1. TRANSX modifications.

APPENDIX D

MERG_GENDF LISTING

This section shows the MERG_GENDF program as written by Tom Marcille. It is a simple utility that strips GENDF files to combine them into a single GENDF file. It should be noted that after combining all of the required files, the user must append the ending tape signal to the GENDF file which consists of a “-1 0 0”, beginning in column 68.

⌘ This program simply strips the GENDF file in ARG1 of the beginning of tape and end of tape C markers and adds it to the file specified by ARG2

```

PROGRAM MERG_GENDF
USE DFLIB
character*(80) ARG1, ARG2
character*(80) LINEIN,BOT,EOT
logical SKIP_BOT
character*(1) WRITE_EOT
DATA
1 bot /'1 0 0 0'/.eot /'-1 0 0'/
call getarg(1,ARG1)
call getarg(2,ARG2)
call getarg(3,WRITE_EOT)

open(UNIT=7,FILE=ARG1,STATUS='OLD',ACCESS='SEQUENTIAL')
inquire(FILE=ARG2,EXIST=SKIP_BOT)
open(UNIT=8,FILE=ARG2,STATUS='UNKNOWN',ACCESS='APPEND')
if (SKIP_BOT.EQ..FALSE.) write(8,"(69X A11)")BOT
L1: do
  read (7,"(A80)")LINEIN
  if( LINEIN(70:80).EQ.bot) then
    write(*,*) 'Starting new tape...'
  else
    if (LINEIN(69:75).EQ.eot) then
      EXIT L1
    else
      write(8,"(A80)") LINEIN
    endif
  endif
enddo L1
close(7)
if (WRITE_EOT.EQ."1") write(8,"(68X A12)") EOT//
close(8)
END

```

Fig. D.1. MERG_GENDF program listing.

VITA

Name

Matthew Torgerson Hiatt

Address

Texas A&M Department of Nuclear Engineering
3133 TAMU
College Station, TX 77843

E-mail

mthduratec@hotmail.com

Education

2007 M.S. Nuclear Engineering, Texas A&M University
2006 B.S. Nuclear Engineering, Texas A&M University – Summa Cum
Laude

Employment

Los Alamos National Laboratory – Internship
Supervisor: Tom Marcille/Dave Poston
June 2006 – August 2006

Los Alamos National Laboratory - Internship
Supervisor: Dave Poston
June 2005 – August 2005

Publications

Evaluation of Metal-Fueled Surface Reactor Concepts
Poston, D.I.; Marcille, T.F.; Kapernick, R.J.; Hiatt, M.T.
Space Tech. and Applications Intl. Forum. Albuquerque, NM, February
11-15, 2007

Design of a 25-kWe Surface Reactor System Based on SNAP Reactor
Technologies
Dixon, D.D.; Hiatt, M.T.; Poston, D.I.; R.J. Kapernick
Space Tech. and Applications Intl. Forum. Albuquerque, NM, February
12-16, 2006

Large Plastic Scintillation Detectors for the Nuclear Materials
Identification System
Neal, J.S.; Mihalcz, J.T.; Hiatt, M.T.; and Edwards, J.D.
Inst. of Nuclear Materials Mgmt. Annual Meeting, Orlando, FL, July 18-
22, 2004